# Nitrogen and Sulfur Cycling During Wastewater Treatment

by

Jeseth Delgado Vela

A dissertation submitted in partial fulfillment
of the requirements for the degree of
Doctor of Philosophy
(Environmental Engineering)
in the University of Michigan
2018

Doctoral Committee:

Associate Professor Gregory J. Dick, Co-Chair
Professor Nancy G. Love, Co-Chair
Dr. Charles B. Bott, Hampton Roads Sanitation District
Professor Glen Daigger
Dr. Kelly J. Gordon, Black and Veatch
Assistant Professor Hui Jiang

2018

jesethdv@umich.edu

ORCID 0000-0001-6171-4400

# DEDICATION

Para mis abuelos Dr. Jaime Delgado Herrera, Luz Maria Saldivar Ramirez, Beatriz Acosta Torres, y Javier Vela Fuerte por valorar la educación. Sus sacrificios son la fundación para mis éxitos.

To my grandparents Dr. Jaime Delgado Herrera, Luz Maria Saldivar Ramirez, Beatriz Acosta Torres, and Javier Vela Fuerte for holding education paramount. My success builds upon their hard work and sacrifices.

## ACKNOWLEDGMENTS

This dissertation research is supported by the Water Environment Research Foundation (Project ENER4R12) and the National Science Foundation (grant no. 1438560). I feel fortunate to have received several fellowships that gave me the flexibility to define my research agenda. These include the National Science Foundation Graduate Research Fellowship Program, the University of Michigan Rackham Merit Fellowship, the University of Michigan Predoctoral Fellowship, and the Ford Foundation Dissertation Fellowship. In particular, the Burroughs Wellcome Fund Integrated Training in Microbial Systems program allowed me to expand my horizons and conduct research I wouldn't have thought possible a few years ago.

I would like to acknowledge my co-advisors Dr. Nancy G. Love and Dr. Gregory J. Dick. Both of you have given me incredible mentorship and encouragement. Thank you for letting me explore my curiosity, for the lessons in science, leadership, and communication, and for always looking out for my best interests. I would like to thank my committee members, Dr. Charles B. Bott, Dr. Glen Daigger. Dr. Kelly J. Gordon, and Dr. Hui Jiang for your encouragement, guidance, and insights.

I would not have been able to conduct this research without the help of many wonderful and thoughtful scientists. Dr. Judith Klatt, Dr. Laura Bristow, and Dr. Hannah Marchant contributed significantly to Chapters 4 and 5. I would like to thank past and present members of the "Downstream" team: Nigel Beaton, Zerihun A. Bekele, Andrea McFarland, and Brett Wagner and undergraduate researchers Adriana Arcelay, Brittany Brown, Nora Kusako Herrero, and Yan Du. Thank you for your willingness to talk through issues and lend a helping hand. The research conducted by my colleagues in the Environmental Biotechnology and Geomicrobiology group has served as an inspiration. I am grateful and humbled to be a part of these groups, thank you all for being a sounding board. I would especially like to acknowledge the friendship, patience, and support of my writing group Dr. Lauren Stadler, Dr. Adam Smith, and Dr. Tara Webster, and of Heather Goetsch, Chia-Chen Wu, Dr. Nadine Kotlarz, Sara Troutman, and Nicole Rockey. I am

also grateful for the staff in the Department of Civil and Environmental Engineering, in particular Tom Yavaraski for always keeping an eye on my analytical runs, Rick Bruch for his assistance building the reactor, and Mike Lazarz for always keeping track of my (many) packages and gas cylinders.

My parents immigrated to the U.S. and obtained doctorates in a foreign language at a great personal sacrifice. These sacrifices have helped keep me grounded. Thank you for all you did to make my life easier and for your support. I want to thank my mom for instilling a passion for engineering by showing me the problems associated with a lack of sanitation. I want to thank my dad for always encouraging me to be curious, supporting a love of reading, and teaching me about fractals and computer programming. I want to thank my brother for his love and encouragement, and for pushing me to be a well-rounded person by teaching me about history, art, and culture. Lastly, I want to thank my husband Ibrahim. His love, patience, sense of humor, and excellent beer-brewing and cooking skills have made these years wonderful.

# TABLE OF CONTENTS

# LIST OF TABLES

# LIST OF FIGURES

## LIST OF APPENDICES

## ABSTRACT

Amid the challenges of climate change, aging infrastructure, and urbanization environmental engineers must develop resource efficient water and wastewater treatment. As the population in coastal communities continues to increase and effluent nitrogen regulations become more stringent, innovation in our wastewater treatment infrastructure can help promote resource efficient nitrogen removal. Sea level rise due to global climate change causes seawater intrusion to wastewater collection systems and increases sulfate concentrations in wastewater. When the wastewater collection system is anaerobic, sulfate is biologically converted to sulfide. Sulfide is an electron donor for denitrification, reducing the need for supplemental carbon addition for nitrogen removal. This dissertation presents advancements in our understanding of how sulfur can affect nitrogen cycling during wastewater treatment.

The effects of hydrogen sulfide on nitrogen cycling were evaluated in three wastewater treatment systems: two full-scale treatment processes that employ different redox environments, thereby supporting distinct microbial communities, and one lab-scale bioreactor. Studies using microbial communities from the full-scale treatment processes showed that nitrite oxidizing bacteria (NOB) were more sensitive to sulfide than ammonia oxidizing bacteria (AOB). Inhibiting nitrite oxidizing bacteria promotes resource efficient treatment because it can reduce the aeration demands of treatment and support nitrite-based denitrifying metabolisms. However, the extent of inhibition was distinct in the two treatment plants, demonstrating that the effect of sulfide is community specific.

Given the potential benefits of sulfide for both denitrification and for inhibiting NOB, the effect of sulfide was tested in a mixed-redox membrane aerated biofilm reactor (MABR). A MABR biofilm is counter-diffusional, meaning the electron donor and electron acceptor diffuse into the biofilm in opposite directions. Accordingly, sulfide is amended in the anoxic bulk liquid, which curtails aerobic oxidation and allows for sulfide oxidation using nitrite or nitrate that was formed in the inner regions of the biofilm as an electron acceptor. Incubation experiments with heavy nitrogen revealed that, consistent with the full-scale systems, sulfide could inhibit NOB but had

no impact on the rates of ammonia oxidation. During routine reactor monitoring, inhibition of NOB was not apparent, most likely due to the rapid conversion of nitrite to ammonia. Higher effluent ammonia concentrations observed during operation were attributed to inhibition of AOB instead of nitrite reduction to ammonia. Biofilm modeling was used to elucidate dissimilatory nitrite or nitrate reduction to ammonia (DNRA). Simulation results show that DNRA with sulfide as the electron donor could increase effluent ammonium. The genetic potential for nitrite reduction to ammonia was found in a unique population of denitrifying anaerobic methane oxidizers. These organisms are beneficial in the treatment of effluents from mainstream anaerobic processes as they curtail an important greenhouse gas emission while denitrifying. On the other hand, results show that sulfide inhibits nitrous oxide reduction, leading to higher emissions of nitrous oxide, a greenhouse gas with a global warming potential 300 times higher than carbon dioxide. Overall, studies in the mixed-redox counter-diffusional biofilm enhanced our understanding of how sulfide affects microbial community interactions.

The results of this dissertation show that hydrogen sulfide could have beneficial impacts on nitrogen cycling in engineered systems. The effect of hydrogen sulfide is complex because microbial communities are adaptable and sulfide induces feedback effects which change overall microbial community interactions. Ultimately, this knowledge can spur the development of technologies that use hydrogen sulfide to develop resource efficient wastewater treatment technologies.

# CHAPTER 1.

## INTRODUCTION

Water and wastewater treatment plants are traditionally slow to adopt new technologies (Kiparsky et al., 2016; Parker, 2011), but current trends in the industry are moving towards the rapid development and adoption of resource efficient technologies. Aside from managing the energy and chemical resources needed to treat water, the practice of resource efficiency evaluates the resources available in wastewater and reduces the environmental and societal demands for treatment (Larsen, 2011). The global stressors of water scarcity, rapid urbanization, and global climate change are spurring utilities to rethink resource management, and advances in research accelerate technology adoption. For example, water scarcity in Big Spring, Texas led to the rapid adoption of direct potable water reuse (Weissmann, 2014). Understanding how technologies function can reveal opportunities to develop resource efficient water and wastewater treatment processes. Furthermore, close collaborations between utilities and universities (Water Environment Federation, 2018) and connections between utilities (e.g. Water Research Foundation's LIFT Test Bed Network (Mihelcic et al., 2017)) can enhance technology development and adoption. Stimulated by needs identified through a utility (Hampton Roads Sanitation District in Virginia) and university (University of Michigan) partnership, this dissertation presents advancements in our understanding of how sulfur can affect nitrogen cycling during wastewater treatment. Ultimately, this knowledge can spur the development of technologies that use sulfur to improve the resource efficiency of wastewater treatment.

Since the implementation of the Clean Water Act in 1972, the goals of wastewater management have shifted from being primarily focused on carbon removal to meeting increasingly stringent nutrient (nitrogen and phosphorus) criteria. While dual nutrient management in both freshwater and coastal ecosystems is important (Paerl et al., 2016), nitrogen is the limiting nutrient in ocean and estuary ecosystems where more than 40% of the global population currently lives (Martínez et al., 2007). In the U.S., coastal populations are four times more densely urbanized than the rest of the country and population density is projected to increase (National Oceanic and Atmospheric

Administration, 2013). Therefore, there is a need to develop efficient nitrogen management strategies in these urbanizing coastal communities. Projected sea level rise caused by global climate change presents additional challenges for wastewater infrastructure due to seawater intrusion into collection systems. Consequently, new nitrogen removal technologies in coastal regions need to address the challenges of urbanization and climate change.

The densely populated coastal regions of the country have unique opportunities for adopting new technologies for wastewater treatment that reduce the energy, greenhouse gas, and space requirements for treatment. For example, coastal communities that are freshwater limited may consider adopting seawater for toilet flushing. Since 1958, Hong Kong has used seawater for toilet flushing and has reduced freshwater demands by almost a quarter (Chen et al., 2012). Life cycle analysis revealed that communities should be within 30 km of a coast and have an effective population density exceeding 3,000 persons/km$^2$ for seawater for toilet flushing to be environmentally sustainable (Liu et al., 2016). Thus, seawater for toilet flushing is beneficial in coastal megacities worldwide and examples from the U.S. include New York City (11,000 persons/km$^2$), San Francisco (6,700 persons/km$^2$), and Los Angeles (3,100 persons/km$^2$) (U.S. Census Bureau, 2010). As was the case with direct potable water reuse in Big Spring, Texas, water scarcity in Southern California may accelerate adoption of seawater for toilet flushing. In addition to the advantages of adopting seawater for toilet flushing for reducing freshwater demands, it is important to consider the ensuing wastewater salinity and its effect on the biological nitrogen removal process.

Another example of a technology that could be adopted for the treatment of wastewater in densely urbanized coastal communities is mainstream anaerobic treatment. There have been recent advances in anaerobic treatment that favor its adoption even at low temperatures (Smith et al., 2013). Though mainstream anaerobic treatment is still evolving, it is an attractive option compared with conventional treatment technologies due to its space efficiency, low solids production, and potential for energy recovery (McCarty et al., 2011). Life-cycle analysis showed that mainstream anaerobic treatment (in the form of anaerobic membrane bioreactors) is more sustainable when high strength wastewaters are treated (Smith et al., 2014). Therefore, mainstream anaerobic treatment is particularly attractive in the densely populated regions of the country such as cities along coasts. Both mainstream anaerobic treatment and seawater for toilet flushing are promising

technologies for reducing the resources required for the urban water cycle because these technologies reduce freshwater demands and lower the energy requirements of treatment, however neither of these strategies address nitrogen emissions.

A consequence of seawater intrusion into sewers, seawater for toilet flushing, and mainstream anaerobic treatment is that sulfur will play a more prominent role in the treatment plant. Several considerations indicate that sulfur is likely to influence individual steps in the nitrogen cycle, but the specific impacts of sulfur on overall nitrogen cycling during wastewater treatment are poorly understood and require further research. One such consideration is during the first step of nitrogen removal where oxic environments are used to support nitrifying organisms. Ammonia oxidizing bacteria (AOB) convert the ammonia present in wastewater to nitrite, and nitrite oxidizing bacteria (NOB) oxidize nitrite to nitrate. Nitrifying organisms are inhibited by hydrogen sulfide (Bejarano Ortiz et al., 2013; Sears et al., 2004) and NOB are inhibited at lower concentrations of sulfide than AOB (Bejarano-Ortiz et al., 2015; Erguder et al., 2008; Kouba et al., 2017). Inhibiting NOB is advantageous in the wastewater treatment as it can result in lower energy demands from aeration, lower electron donor requirements for denitrification, and can provide substrate for anammox bacteria, which are beneficial due to their low growth yield.

Sulfide can also affect denitrification, which occurs when electron donors are used in anoxic environments to reduce the nitrite or nitrate to dinitrogen gas. Combined, nitrification and denitrification convert the ammonia from the liquid stream to an inert gas, eliminating the harmful impact of nitrogen on the receiving water stream. Hydrogen sulfide inhibits the nitrous oxide reductase within denitrifying organisms which leads to the emissions of nitrous oxide (Fajardo et al., 2014; Manconi et al., 2006; Pan et al., 2013; Senga et al., 2006; Sorensen et al., 1980). This has implications for the overall environmental impacts of treatment because nitrous oxide is a powerful greenhouse gas. In contrast, hydrogen sulfide can have positive effects on denitrification as it can serve as an electron donor that supports nitrogen removal. This can reduce resource requirements for treatment because external electron donors such as methanol are often used to meet stringent effluent nitrogen regulations, which increases the life cycle costs associated with wastewater treatment (Foley et al., 2010). A better understanding of how sulfur impacts nitrogen cycling in existing and emerging wastewater treatment systems can inform operational strategies to reduce the resource demands required for treatment.

## 1.1 Overview of Dissertation

The objective of this dissertation is to understand how sulfur affects nitrogen cycling during wastewater treatment. Chapter 2 provides background on the sources and speciation of sulfur in wastewater treatment plants and the known effects sulfur has on nitrogen transformations that are relevant to wastewater treatment. An advantage of hydrogen sulfide is that it may differentially inhibit AOB and NOB. In Chapter 3, batch experiments were used to investigate nitrification inhibition using biomass from two different full-scale systems with distinct nitrifying communities. By linking microbial community characteristics to process rates, this research showed that different taxa of NOB have distinct propensities for sulfide inhibition. The results highlight that links between treatment process data and microbial community characteristics are needed to generalize results and improve process models.

To explore the effect of sulfur when multiple redox environments are available, a membrane aerated biofilm reactor (MABR) is studied in Chapters 4 and 5. In this reactor configuration membranes are used to aerate a biofilm that provides oxic and anoxic zones, which allows for studying interactions and cross-feeding relationships between aerobic and anaerobic microbial populations. Furthermore, a MABR biofilm is counter-diffusional, meaning the electron donor and electron acceptor diffuse into the biofilm in opposite directions. Accordingly, sulfide is amended in the anoxic bulk liquid, which curtails aerobic oxidation and allows for sulfide oxidation using nitrite or nitrate as an electron acceptor. Additionally, a counter-diffusional biofilm supports distinct metabolic interactions compared with co-diffusional biofilms and allows for independent control of electron donor and acceptor. Chapter 4 presents how sulfide impacted the functional potential within the microbial community using both whole community shotgun DNA sequencing and incubation experiments with heavy nitrogen ($^{15}N$). Consistent with Chapter 3, NOB were inhibited during short-term incubation experiments and were more easily inhibited by sulfide than ammonia oxidizing bacteria (AOB). However, inhibition of NOB was not detected during the long-term stepwise increases of influent sulfide; the evidence suggests this is because nitrite was rapidly consumed, in part by dissimilatory nitrite reduction to ammonia (DNRA). In addition, Chapter 4 showed that the MABR hosted a unique species of denitrifying anaerobic methane oxidizing bacteria, which may have been enriched by a combination of nitrite accumulation and a shift in redox.

The knowledge of the functional potential that was developed in Chapter 4 is then applied in Chapter 5, which explores the impact of long-term stepwise increases in sulfide on nitrogen cycling. The results from Chapter 5 show that in the lab-scale MABR, sulfide induced higher effluent ammonia concentrations. Since Chapter 4 showed that the potential rate of reduction of nitrite to ammonia exceeded potential ammonia oxidation rates, Chapter 5 presents a stochiometric analysis showing that, in combination with inhibition of nitrification, DNRA likely contributed to the higher effluent ammonia concentrations. Lastly, biofilm modeling was used to evaluate the conditions that support sulfide-based denitrification over nitrite reduction to ammonia. The simulated increases in effluent ammonium was only up to 1%, indicating that sulfide may not have been the electron donor for DNRA. This analysis is valuable to understanding how sulfur can be used to support efficient nitrogen removal in the MABR, an emerging and rapidly developing technology with reduced energy demands for aeration. In Chapter 6, the impact of these findings and areas of future research are presented.

## 1.2 References


Bejarano-Ortiz, D.I., Huerta-Ochoa, S., Thalasso, F., Cuervo-López, F. de M., Texier, A.C., 2015. Kinetic Constants for Biological Ammonium and Nitrite Oxidation Processes Under Sulfide Inhibition. Appl. Biochem. Biotechnol. 177, 1665–1675. doi:10.1007/s12010-015-1844-3

Bejarano Ortiz, D.I., Thalasso, F., Cuervo López, F.D.M., Texier, A.C., 2013. Inhibitory effect of sulfide on the nitrifying respiratory process. J. Chem. Technol. Biotechnol. 88, 1344–1349. doi:10.1002/jctb.3982

Chen, G.H., Chui, H.K., Wong, C.L., Tang, D.T.W., Lu, H., 2012. An Innovative Triple Water Supply System and a Novel SANI® Process to Alleviate Water Shortage and Pollution Problem for Water-scarce Coastal Areas in China. J. Water Sustain. 2, 121–129. doi:10.11912/jws.2.2.121-129

Erguder, T.H., Boon, N., Vlaeminck, S.E., Verstraete, W., 2008. Partial nitrification achieved by pulse sulfide doses in a sequential batch reactor. Environ. Sci. Technol. 42, 8715–8720. doi:10.1021/es801391u

Fajardo, C., Mora, M., Fernández, I., Mosquera-Corral, A., Campos, J.L., Méndez, R., 2014. Cross effect of temperature, pH and free ammonia on autotrophic denitrification process with sulphide as electron donor. Chemosphere 97, 10–5. doi:10.1016/j.chemosphere.2013.10.028

Foley, J., de Haas, D., Hartley, K., Lant, P., 2010. Comprehensive life cycle inventories of alternative wastewater treatment systems. Water Res. 44, 1654–1666. doi:10.1016/j.watres.2009.11.031

Kiparsky, M., Thompson, B.H., Binz, C., Sedlak, D.L., Tummers, L., Truffer, B., 2016. Barriers to Innovation in Urban Wastewater Utilities: Attitudes of Managers in California. Environ. Manage. 57, 1204–1216. doi:10.1007/s00267-016-0685-3

Kouba, V., Proksova, E., Wiesinger, H., Vejmelkova, D., Bartacek, J., 2017. Good servant, bad master: sulfide and dissolved methane influence on partial nitritation of sewage. Water Sci. Technol. wst2017490. doi:10.2166/wst.2017.490

Larsen, T.A., 2011. Redesigning wastewater infrastructure to improve resource efficiency. Water Sci. Technol. 63, 2535–2541. doi:10.2166/wst.2011.502

Liu, X., Dai, J., Wu, D., Jiang, F., Chen, G., Chui, H.K., van Loosdrecht, M.C.M., 2016. Sustainable Application of a Novel Water Cycle Using Seawater for Toilet Flushing. Engineering 2, 460–469. doi:10.1016/J.ENG.2016.04.013

Manconi, I., van der Maas, P., Lens, P., 2006. Effect of copper dosing on sulfide inhibited reduction of nitric and nitrous oxide. Nitric Oxide - Biol. Chem. 15, 400–407. doi:10.1016/j.niox.2006.04.262

Martínez, M.L., Intralawan, A., Vázquez, G., Pérez-Maqueo, O., Sutton, P., Landgrave, R., 2007. The coasts of our world: Ecological, economic and social importance. Ecol. Econ. 63, 254–272. doi:10.1016/j.ecolecon.2006.10.022

McCarty, P.L., Bae, J., Kim, J., 2011. Domestic wastewater treatment as a net energy producer--can this be achieved? Environ. Sci. Technol. 45, 7100–6. doi:10.1021/es2014264

Mihelcic, J.R., Ren, Z.J., Cornejo, P.K., Fisher, A., Simon, A.J., Snyder, S.W., Zhang, Q., Rosso, D., Huggins, T.M., Cooper, W., Moeller, J., Rose, B., Schottel, B.L., Turgeon, J., 2017. Accelerating Innovation that Enhances Resource Recovery in the Wastewater Sector: Advancing a National Testbed Network. Environ. Sci. Technol. 51, 7749–7758. doi:10.1021/acs.est.6b05917

National Oceanic and Atmospheric Administration, 2013. National Coastal Population Report, population trends from 1970 to 2020.

Paerl, H.W., Scott, J.T., McCarthy, M.J., Newell, S.E., Gardner, W.S., Havens, K.E., Hoffman, D.K., Wilhelm, S.W., Wurtsbaugh, W.A., 2016. It Takes Two to Tango: When and Where Dual Nutrient (N & P) Reductions Are Needed to Protect Lakes and Downstream Ecosystems. Environ. Sci. Technol. 50, 10805–10813. doi:10.1021/acs.est.6b02575

Pan, Y., Ye, L., Yuan, Z., 2013. Effect of H2S on N2O reduction and accumulation during denitrification by methanol utilizing denitrifiers. Environ. Sci. Technol. 47, 8408–8415. doi:10.1021/es401632r

Parker, D.S., 2011. Introduction of New Process Technology into the Wastewater Treatment Sector. Water Environ. Res. 83, 483–497. doi:10.2175/106143009X12465435983015

Sears, K., Alleman, J.E., Barnard, J.L., Oleszkiewicz, J. a., 2004. Impacts of reduced sulfur components on active and resting ammonia oxidizers. J. Ind. Microbiol. Biotechnol. 31, 369–378. doi:10.1007/s10295-004-0157-2

Senga, Y., Mochida, K., Fukumori, R., Okamoto, N., Seike, Y., 2006. N2O accumulation in

estuarine and coastal sediments: The influence of H2S on dissimilatory nitrate reduction. Estuar. Coast. Shelf Sci. 67, 231–238. doi:10.1016/j.ecss.2005.11.021

Smith, A.L., Skerlos, S.J., Raskin, L., 2013. Psychrophilic anaerobic membrane bioreactor treatment of domestic wastewater. Water Res. 47, 1655–1665. doi:10.1016/j.watres.2012.12.028

Smith, A.L., Stadler, L.B., Cao, L., Love, N.G., Raskin, L., Skerlos, S.J., 2014. Navigating Wastewater Energy Recovery Strategies: A Life Cycle Comparison of Anaerobic Membrane Bioreactor and Conventional Treatment Systems with Anaerobic Digestion. Environ. Sci. Technol. doi:10.1021/es5006169

Sorensen, J., Tiedje, J.M., Firestone, R.B., 1980. Inhibition by Sulfide of Nitric and Nitrous-Oxide Reduction by Denitrifying Pseudomonas-Fluorescens. Appl. Environ. Microbiol. 39, 105–108.

U.S. Census Bureau, 2010. American Fact Finder [WWW Document]. Popul. Hous. Units, Area, Density 2010. URL https://factfinder.census.gov/faces/tableservices/jsf/pages/productview.xhtml?src=bkmk (accessed 12.4.18).

Water Environment Federation, 2018. University-Utility Collaborative Partnerships.

Weissmann, D., 2014. Texas town closes the toilet-to-tap loop: Is this our future water supply. NPR Marketpl.

# CHAPTER 2.

# BACKGROUND

## 2.1 Introduction

Our ability to predict the relationship between the sulfur and nitrogen cycles in a wastewater treatment plant is limited because sulfur is not regularly monitored in wastewater treatment plants. Existing research and knowledge suggests that sulfur can be present in different forms in wastewater treatment plants and can affect nitrogen removal. For example, when sulfur is present as hydrogen sulfide it can inhibit nitrifying (Bejarano Ortiz et al., 2013; Erguder et al., 2008; Vojtech Kouba et al., 2017) and denitrifying (Sorensen et al., 1980) bacteria, and can serve as an electron donor for denitrification. Unraveling the ways that sulfur can benefit wastewater treatment is complex because of the many competing microbial populations and interactions involved in both sulfur and nitrogen cycling. While the potential interactions are complex, investigating these interactions will help us understand how to harness sulfur to improve treatment.

## 2.2 Sulfur in Domestic Wastewater Treatment Plants

The speciation of sulfur depends on the redox environment and the activity of microorganisms. Sulfur can be in soluble, precipitated, and intracellular forms and is present as sulfide, sulfite, thiosulfate, elemental sulfur, and sulfate (in order of increasing oxidation state). Elemental sulfur is solid and is often an intermediary of other sulfur oxidation processes (B. S. Moraes et al., 2012; Sahinkaya et al., 2011). Sulfite and thiosulfate on the other hand are rarely detected in conventional treatment processes and have instead been proposed as external electron donors for denitrification (Chung et al., 2014; Sabba et al., 2016). Sulfur can also precipitate with other compounds; for instance, iron-sulfur precipitates are common in wastewater treatment processes (Nielsen et al., 2005). Intracellularly, sulfur can be stored as sulfur globules and be used by microorganisms experiencing starvation conditions (Dahl and Prange, 2006). Although sulfur can take various forms during wastewater treatment, sulfur mass balances across treatment plants and information on sulfur speciation are scarce in the peer-reviewed literature. Nevertheless, we can develop

hypotheses for the locations of sulfur-rich streams within a treatment plant by drawing upon existing literature and our knowledge of biological and abiotic sulfur reactions.

The concentrations and forms of sulfur in wastewater treatment plants vary and are shown in Figure 2-1. The most dominant forms of sulfur in conventional treatment processes are hydrogen sulfide and sulfate, though some sulfur intermediates have been reported (Fisher et al., 2017). Under anaerobic conditions in the presence of an electron donor, sulfate reducing bacteria convert sulfate to hydrogen sulfide. Since both biotic and abiotic processes can rapidly oxidize sulfide in the presence of air, sulfide is typically not measurable in aerobic regions of a biological treatment process. The form of hydrogen sulfide present at treatment plants is dictated by pH since sulfide is a weak acid ($pK_a$=7.0); therefore, while the ionized ($HS^-$) form is dominant, both ionized and unionized ($H_2S$) forms are present. Equilibrium reactions with the gas phase are also important to consider because $H_2S$ is only slightly soluble in water (Henry's constant of $1x10^{-3}$ mol $H_2S/m^3$-Pa at 25°C (Sander, 2015)). Since the form of sulfur depends on the redox environment, different regions of the wastewater treatment plant will have different forms of sulfur present.

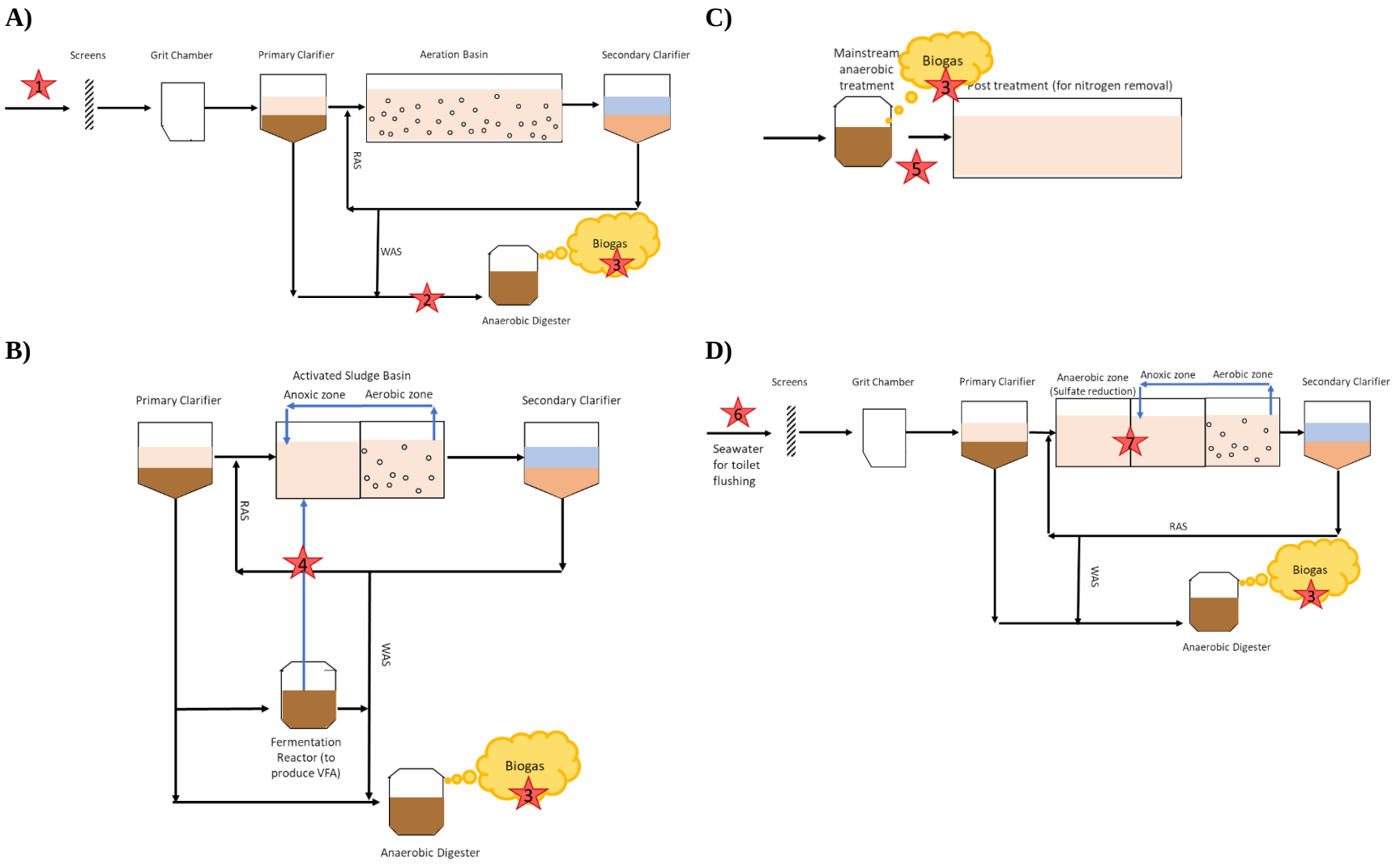


**Figure 2-1.** Potential locations and concentrations of sulfur in A) conventional activated sludge; B) fermentation reactor (VFA: volatile fatty acid); C) ,ainstream anaerobic treatment; D) seawater for toilet flushing with a SANI Process. Stars indicate sulfur sources: 1) baseline is 10-20 mg $SO_4^{2-}$/L as S (Tchobanoglous et al., 2003) but can be as high as 200 mg $SO_4^{2-}$/L as S (Lens et al., 1998); 2) 10-20 mg $SO_4^{2-}$/L as S (Düppenbecker and Cornel, 2016); 3) 0.1-500 $ppm_v$ $H_2S$ (Noyola et al., 2006); 4) estimates of 10-20 mg sulfide/L as S and 4-5 mg $SO_4^{2-}$/L as S, based on thickened WAS and primary sludge (Fisher et al., 2017); 5) 1-95 mg sulfide/L as S (Delgado Vela et al., 2015); 6) 200 mg $SO_4^{2-}$/L as S (Wang et al., 2009); 7) 100 mg sulfide/L as S (Lu et al., 2012).

The concentration of sulfur in a wastewater treatment plant is variable and depends on the influent characteristics. Processes that influence influent sulfur include industrial inputs, seawater intrusion, and drinking water treatment process (e.g. if coagulation uses aluminum or ferric sulfate). In conventional treatment processes (Figure 2-1A), baseline influent concentrations of sulfate are between 10-20 mg/L as S (Tchobanoglous et al., 2003), but concentrations as high as 200 mg/L as S have been reported (Lens et al., 1998). Depending on the characteristics of the collection system, some portion of the sulfate present in the sewer system can be converted to hydrogen sulfide by sulfate reducing bacteria. This process can lead to corrosion in sewer pipes or in the headworks of the treatment plant. In addition, sulfate reducing bacteria in anaerobic digestion processes are considered nuisance organisms because they compete with methanogenic bacteria for carbon, and at pH's relevant for anaerobic processes (6.8-7.4), $H_2S$ will diminish the quality of the biogas.

With the advent of new types of treatment processes, there is the potential for the adoption of technologies that will increase the concentrations of sulfur in a wastewater treatment plant. For example, when anaerobic digestion is used for wastewater treatment, researchers have proposed using the $H_2S$ present in the biogas as an electron donor for denitrification by recycling it into the anoxic regions of treatment plants (Bayrakdar et al., 2015). Besides anaerobic digestion as a sidestream treatment technology, anaerobic digestion in the mainstream, which generates sulfide-rich streams, is increasingly being considered (Figure 2-1C) (McCarty et al., 2011). In addition, sidestream fermentation processes used to generate carbon for nitrogen removal (Canziani et al., 1995) represent an additional potential source of hydrogen sulfide (Figure 2-1B), though typical concentrations of sulfur in this stream could not be found in the peer-reviewed literature. Lastly, the use of seawater for toilet flushing has been proposed to reduce freshwater demands in coastal environments (Chen et al., 2012). This will increase sulfur concentrations in the wastewater treatment plant significantly (Figure 2-1D) and it is particularly attractive in coastal, urbanized, and water stressed regions of the world (X. Liu et al., 2016). The use of seawater for toilet flushing in Hong Kong has spurred the development of a new process that harnesses sulfur for wastewater treatment, called the SANI® process (Wang et al., 2009). Sea level rise due to global climate change will also continue to be an important consideration and increases the potential for seawater

infiltration into the wastewater collection system. Given these emerging sources of sulfur in wastewater treatment systems, additional research on sulfur cycling during wastewater treatment is needed.

### *2.2.1 Abiotic and biotic sulfur reactions*

Sulfide can be oxidized through both biotic and abiotic processes. In clean water without any impurities, abiotic sulfide oxidation is slow and depends on pH and temperature (Chen and Morris, 1972; Luther et al., 2011). However, in the presence of metals or organic matter abiotic oxidation of hydrogen sulfide is rapidly accelerated (Nielsen et al., 2003; Vazquez et al., 1989). This makes it difficult to quantify the abiotic and biotic contribution of sulfide oxidation in wastewater systems. While studies of pure cultures have suggested that biotic sulfur oxidation is significantly faster than abiotic sulfide oxidation (Luther et al., 2011), attempts to quantify the relative importance of abiotic and biotic factors in real wastewater environments have found both factors are important (Nielsen et al., 2006; Wilmot et al., 1988).

The process of reducing sulfate to sulfide is catalyzed by sulfate reducing bacteria, a diverse and metabolically flexible bacterial group (Hao et al., 2014; Muyzer and Stams, 2008). For instance, anaerobic methane oxidizers can use sulfate as an electron acceptor and produce disulfide (Milucka et al., 2012). In the context of wastewater treatment, the activity of sulfate reducing bacteria has largely been studied in the anaerobic digestion process (e.g. (Harada, 1994; Oude Elferink et al., 1994)) and wastewater collection systems (e.g. (Zhang et al., 2009, 2008)). Sulfate reducers can also be active in the mainstream of domestic wastewater treatment systems (Lens et al., 1995), especially biofilm systems that support multiple redox environments (Santegoeds et al., 1998). One hypothesis is that sulfate reducers in these multi-redox environments survive by having a cross-feeding relationship with sulfide oxidizing bacteria; when carbon and dissolved oxygen are available, sulfur can cycle between sulfate and hydrogen sulfide and support these metabolisms (Lens et al., 1995). The role that sulfate reducers play in carbon removal during conventional wastewater treatment is not well understood but may be significant even in the presence of relatively low amounts of sulfate due to potential cross-feeding with sulfide oxidizing bacteria.

## 2.3 Nitrogen in Domestic Wastewater Treatment Plants

Compared with sulfur, nitrogen cycling in wastewater is better understood because the release of excessive nitrogen into water bodies can cause oxygen depletion and algal blooms that can be harmful to aquatic life and human health. In U.S. freshwaters, excessive nutrients are estimated to result in economic loses of 2.2 billion dollars annually (Dodds et al., 2008). In recent years, toxins released by these algal blooms have impaired freshwater drinking water sources and caused temporary shut downs of drinking water treatment plants (Tanber, 2014). Increasingly, the combined effect of both nitrogen and phosphorus is important for toxin production (Paerl et al., 2016), and in some instances, the form of nitrogen is important for toxin production (Chaffin et al., 2018). In considering these detrimental human health and environmental effects, wastewater treatment plants are central to nitrogen management strategies because they represent point-sources of nitrogen to the environment.

Nitrogen comes into the wastewater treatment plant as ammonium and organic nitrogen. Organic nitrogen is degraded into ammonium via ammonification, but a portion is soluble and inert (approximately 1.5 mg/L as N (Grady et al., 2011)) and contributes to effluent total nitrogen concentrations. The typical influent ammonium concentrations are between 20 and 75 mg/L as N (Tchobanoglous et al., 2003). Nitrogen concentrations are less variable than sulfur concentrations and depend on the strength of the influent wastewater. Ammonium can be oxidized biologically to nitrite or nitrate. If nitrogen removal is required, nitrite or nitrate are then reduced to dinitrogen gas. The form of nitrogen present in wastewater treatment plant schemes is more carefully monitored since it is an important pollutant; however, improving nitrogen removal during wastewater treatment continues to be an active area of research.

Conventionally, removing nitrogen from wastewater is an energy intensive and costly process. With our growing understanding of the negative impacts of nutrients onto water bodies and a general trend towards urbanizing populations, we can expect effluent nitrogen in wastewater treatment plants to be more strictly regulated in the future. Therefore, we need to better understand how to manage nitrogen in wastewater without greatly increasing energy demands or the environmental footprint of the process. A better understanding of how to control the microbial

processes that are underpinning the removal of nitrogen from wastewater may lead to improvements in the sustainability of nitrogen removal.

### *2.3.1 Microbiological processes for nitrogen removal*

Environmental engineers seek ways to control microbial communities to improve the sustainability of wastewater treatment; however, this is difficult because our understanding of which microbes are involved in nitrogen cycling and how they are functioning is rapidly changing (reviewed by Kuypers et al. (2018)). For example, there is interest in controlling the first step of nitrogen removal, nitrification, in which ammonia is oxidized to nitrite or nitrate. Ammonia oxidizing bacteria and archaea oxidize ammonia to nitrite, and nitrite oxidizing bacteria oxidize nitrite to nitrate. A nitritation process, in which the oxidation of nitrite to nitrate is prevented, reduces the need for the energy-intensive aeration process (Rosso et al., 2008). Furthermore, nitritation is especially advantageous when the wastewater is electron donor limited because compared with nitrate reduction, reducing nitrite to nitrogen gas requires lower quantities of electron donor, so inducing a nitritation process can reduce the need for external electron donor (Daigger, 2014). However, maintaining a nitritation process in low strength wastewater is challenging and although various methods have been proposed (Blackburne et al., 2008; Ganigué et al., 2007; Gilbert et al., 2014; Regmi et al., 2014; Shannon et al., 2015; Vadivelu et al., 2006; Van Kempen et al., 2001; Villaverde et al., 1997), there is still not a consensus on the most effective strategy.

Maintaining a nitritation process was further complicated in 2015 when it was discovered that one organism can oxidize completely ammonia to nitrate, termed comammox bacteria (Daims et al., 2015; van Kessel et al., 2015). Annavajhala et al. (2018) recently showed that comammox bacteria are prevalent in wastewater treatment environments, but our understanding of whether comammox bacteria are detrimental to nitritation processes is unknown. There is some evidence that comammox can reduce nitrate to nitrite, therefore they may be advantageous to have in systems that depend on denitrification via nitrite (Daims et al., 2016). The conditions that select for comammox-mediated nitritation, nitrate reduction, or full nitrification are unknown, therefore we do not yet know how to control comammox bacteria to perform processes that improve treatment.

Nitrite or nitrate can be reduced to dinitrogen gas, a process termed denitrification. Conventionally the organic carbon that is present in wastewater is used as an electron donor for denitrification but often when stringent nitrogen requirements must be met an external electron donor such as methanol is used, which represents a high life cycle cost (Foley et al., 2010). However, there are a variety of additional potential electron donors that are present in wastewater and can be used for denitrification (Delgado Vela et al., 2015). For example, if nitrite is present, ammonia can be used as an electron donor by anammox bacteria (Mulder et al., 1995). Both nitrite and nitrate can be used as electron acceptors when methane is used as an electron donor (Ettwig et al., 2010; Haroon et al., 2013; Luesken et al., 2011). Lastly, reduced sulfur compounds can be used as electron donors for denitrification (reviewed by (Shao et al., 2010)). Understanding how to harness these alternative electron donors may reduce the need for external carbon addition and improve the sustainability of nitrogen removal.

In addition to denitrification processes, nitrite and nitrate can be reduced to ammonia, a process termed dissimilatory nitrate or nitrite reduction to ammonia (DNRA). A variety of electron donors can be used but typically simple organics are used as electron donors. This process is widespread among bacteria (Rütting et al., 2011) and has been identified in sulfate reducers (Dalsgaard and Bah, 1994; Keith and Herbert, 1983) and anammox bacteria (Kartal et al., 2007; Winkler et al., 2012). It is thought that DNRA occurs when the concentration of electron donor is high relative to nitrate and denitrification will occur when nitrate or nitrite concentrations are high relative to electron donor. However, DNRA and denitrification can co-occur (van den Berg et al., 2016) and under these conditions it is difficult to unravel which community members are engaging in DNRA or denitrification. Given the complexity of nitrogen cycling bacteria, controlling the communities that form in wastewater treatment is challenging to achieve.

### *2.3.2 Nitrous oxide emissions during wastewater treatment*

An important consideration in evaluating the nitrogen removal processes is the emission of nitrous oxide ($N_2O$), a gas with a global warming potential approximately 300 times more potent than carbon dioxide (Kampschreur et al., 2009; U.S. Environmental Protection Agency, 2010); nitrous oxide emissions are heavily influenced by the microbial community structure and function (Bakken and Frostegård, 2017). $N_2O$ is emitted during heterotrophic denitrification (Lu and

Chandran, 2010; Rassamee et al., 2011; Tallec et al., 2008) and autotrophic nitrification processes (Tallec et al., 2006; Zheng et al., 1994). Ammonia oxidizing bacteria (AOB) typically emit $N_2O$ in a process termed nitrifier denitrification in which AOB reduce nitrite to nitric oxide and then to $N_2O$ (Kim et al., 2010; Yu et al., 2010). In addition, hydroxylamine, an intermediate of ammonia oxidation by nitrifying organisms, can be chemically reduced to nitric oxide, which is then biologically reduced to $N_2O$ (Wunderlin et al., 2012). In a wastewater treatment communities, it appears that both heterotrophic and autotrophic processes contribute to nitrous oxide emissions (Ishii et al., 2014; Ma et al., 2017; Mampaey et al., 2015).

$N_2O$ emissions from wastewater treatment processes are also influenced by the reactor configuration and operation, but there is uncertainty on how to operate reactors to reduce the emission of $N_2O$. For instance, rapid cycling between oxic and anoxic conditions (i.e. intermittent aeration) has been shown to both increase (Rassamee et al., 2011) and decrease (Domingo-Félez et al., 2014; Su et al., 2017) $N_2O$ emissions. In addition, dissolved oxygen levels also affect $N_2O$ emissions (Rassamee et al., 2011; Tallec et al., 2008). In a biofilm reactor, there are distinct sources and sinks of $N_2O$ compared to suspended cultures. $N_2O$ emissions from biofilms depend on biofilm thickness, diffusional characteristics, and substrate concentrations (Kinh et al., 2017b, 2017a; Sabba et al., 2017). Given the uncertainty surrounding $N_2O$ emissions from wastewater we are still far from understanding how to design and operate wastewater treatment plants to reduce emissions. In emerging treatment processes we need an improved understanding of biological sources and sinks.

## 2.4 Links Between Sulfur and Nitrogen Cycles During Wastewater Treatment

As emerging technologies such as mainstream anaerobic treatment or seawater for toilet flushing are adopted, there is a growing need to understand how the sulfur and nitrogen cycles are linked in wastewater treatment plants. In marine oxygen minimum zones, a cryptic sulfur cycle was described in which tight coupling of sulfate reducers and sulfide-based denitrifiers conduct nitrogen removal without measurable changes in sulfate and sulfide concentrations (Canfield et al., 2010). Wastewater treatment plants also support analogous microaerobic environments in which a cryptic sulfur cycle is possible.

Despite the promise of harnessing sulfur for nitrogen removal, sulfide inhibition of important microorganisms represents an additional challenge. Sulfide can inhibit nitrifying bacteria (Joye and Hollibaugh, 1995). Interestingly, there is evidence that sulfide inhibits ammonia oxidizing and nitrite oxidizing bacteria to different extents and may help induce nitritation processes (Erguder et al., 2008; V. Kouba et al., 2017). Although sulfide is inhibitory for anammox bacteria (Jin et al., 2013), studies have found active anammox bacteria in the presence of sulfide (Arshad et al., 2017; Guo et al., 2016; Jones et al., 2017; Rios-Del Toro and Cervantes, 2016; Russ et al., 2014). The growth of anammox in the presence of sulfide may be because sulfide-based denitrifiers reduce the concentrations of sulfide to below inhibitory levels. An additional advantage is that sulfide-based denitrifiers will also reduce the nitrate that is produced anabolically by anammox. In addition to sulfide inhibition of anammox, some studies have found sulfide inhibits $N_2O$ reduction to $N_2$ (Fajardo et al., 2014; Manconi et al., 2006; Pan et al., 2013; Senga et al., 2006; Sorensen et al., 1980), which leads to higher nitrous oxide emissions. However this isn't a consistent finding (Yang et al., 2016b) and modeling results show that this depends on reactor operation (Y. Liu et al., 2016). In summary, sulfide has complex effects on microbial communities due to inhibition that could be both detrimental, such as higher $N_2O$ emissions, or beneficial, such as NOB inhibition to support a nitritation process.

Sulfide is not only an electron donor for denitrification, sulfide can also induce nitrate reduction to ammonia (DNRA)(Brunet and Garcia-Gil, 1996). At higher sulfide/N ratios, nitrate gets reduced to ammonia, while at lower sulfide/N ratios denitrification occurs (Dolejs et al., 2014; Yin et al., 2015). DNRA has been shown to be beneficial to anammox in wetland communities(Wang et al., 2018), and DNRA induced by sulfide has also been shown (Jones et al., 2017). In wastewater environments, we do not know if sulfide-induced DNRA that would improve the anammox process would occur.

There has been growing interest in using sulfur as an alternative electron donor for denitrification. Of note is the SANI® process that harnesses the high sulfate concentrations of wastewater in Hong Kong due to seawater toilet flushing (Wang et al., 2009). In this system the activity of sulfate reducers and sulfide based denitrifiers are separated into two unit processes: an anaerobic zone where sulfate reduction occurs, and an anoxic process that denitrifies the recycled nitrate from the

aerobic zone. A pilot-scale demonstration exhibited low sludge production using this process (Wu et al., 2016). Other applications of sulfide-based denitrification include anoxic granular processes (Yang et al., 2016a) that exhibited low nitrous oxide emissions (Yang et al., 2016b) and simultaneous nitrification/denitrification reactors (B.S. Moraes et al., 2012). Elemental sulfur has also been used as a consumable biofilm carrier for denitrification reactors (Wang et al., 2016). The interest in sulfur-based denitrification is growing and given the complex metabolisms that are associated with both sulfur and nitrogen cycling, there is a need to understand the reactor configurations where the use of sulfur is realistic.

## 2.5 The Membrane Aerated Biofilm Reactor

One reactor configuration that could be advantageous for harnessing the sulfur and nitrogen cycles is a membrane aerated biofilm reactor (MABR). In a MABR, membranes are used to aerate a biofilm and support multiple redox environments thereby providing an environment for the growth of both aerobic and anaerobic metabolisms (Downing and Nerenberg, 2008; Gilmore et al., 2013; Martin and Nerenberg, 2012). Membrane aeration prevents bubbles from forming and the stripping of hydrogen sulfide. Furthermore, sulfide is added into the anoxic bulk liquid so rapid aerobic oxidation is prevented. MABRs also uniquely maintain a counter-diffusional biofilm in which the electron donor and electron acceptor diffuse into the biofilm in opposite directions and can be independently controlled (Figure 2-2). This counter-diffusional biofilm allows for sulfide to be maximum in the anoxic bulk liquid, preserving its availability as a potential electron donor for denitrification. Conversely, the aerobic nitrifying bacteria are in the innermost regions of the biofilm and can be protected from sulfide inhibition.

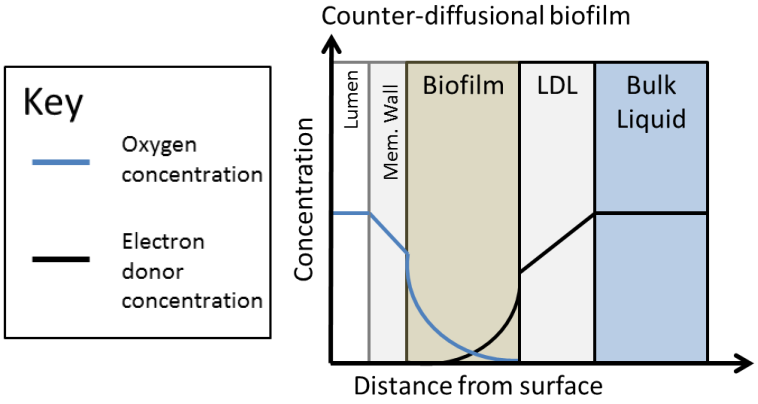


**Figure 2-2.** Conceptual schematic of a counter-diffusional biofilm. LDL= Liquid diffusion layer

These unique characteristics of an MABR biofilm make it suitable for evaluating interactions of sulfur and nitrogen cycling microorganisms.

Interest in the MABR is growing (Heffernan et al., 2017; Houweling et al., 2017) because it achieves energy efficient aeration. MABRs can be operated with the membranes either closed or opened at one end. Typically open-ended configurations are used and one study showed oxygen transfer efficiencies of 20-35% (Gilmore et al., 2009) compared with 5-15% for the fine bubble diffusers typically used in aeration basins (Tchobanoglous et al., 2003). When operated with a closed end, oxygen transfer efficiencies can be close to 100%, however gas back diffusion is possible. The adoption of MABRs is due to its potential aeration energy efficiency, however, operational strategies to select for desirable populations such as nitritation processes in an MABR can further improve the process and have not been developed.

Most previous studies of MABRs have been lab-scale demonstrations of high strength wastewater (Gilmore et al., 2013; Pellicer-Nàcher et al., 2010; Terada et al., 2003) and few have evaluated nitrogen removal of low strength wastewater (Downing and Nerenberg, 2008). An additional advantage of MABRs is that they have low $N_2O$ emissions relative to co-diffusional biofilms (Kinh et al., 2017b, 2017a). Researchers have shown some degree of nitritation using both sequential (i.e. periods of no air being fed through lumen of membrane) (Pellicer-Nàcher et al., 2014, 2010) or continuous (Gilmore et al., 2013; Terada et al., 2003) aeration. Although nitrogen removal, sulfur oxidation (Sahinkaya et al., 2011), and methane oxidation (Casey et al., 2004) have been studied separately in an MABR, no laboratory based studies have looked at both of these aspects at once (Chen et al., 2016). Overall, the unique configuration of the MABR provides a platform for discovery, especially when considering the complex metabolisms involved in microbial cycling of nitrogen and sulfur.

## 2.6 References

Annavajhala, M.K., Kapoor, V., Santo-Domingo, J., Chandran, K., 2018. Comammox Functionality Identified in Diverse Engineered Biological Wastewater Treatment Systems. Environ. Sci. Technol. Lett. acs.estlett.7b00577. doi:10.1021/acs.estlett.7b00577

Arshad, A., Martins, P.D., Frank, J., Jetten, M.S.M., Op den Camp, H.J.M., Welte, C.U., 2017. Mimicking microbial interactions under nitrate-reducing conditions in an anoxic bioreactor:

enrichment of novel Nitrospirae bacteria distantly related to Thermodesulfovibrio. Environ. Microbiol. 00, 1–41. doi:10.1111/1462-2920.

Bakken, L.R., Frostegård, Å., 2017. Sources and sinks for N2O, can microbiologist help to mitigate N2O emissions? Environ. Microbiol. 19, 4801–4805. doi:10.1111/1462-2920.13978

Bayrakdar, A., Tilahun, E., Calli, B., 2015. Biogas desulfurization using autotrophic denitrification process. Appl. Microbiol. Biotechnol. doi:10.1007/s00253-015-7017-z

Bejarano Ortiz, D.I., Thalasso, F., Cuervo López, F.D.M., Texier, A.C., 2013. Inhibitory effect of sulfide on the nitrifying respiratory process. J. Chem. Technol. Biotechnol. 88, 1344–1349. doi:10.1002/jctb.3982

Blackburne, R., Yuan, Z., Keller, J., 2008. Partial nitrification to nitrite using low dissolved oxygen concentration as the main selection factor. Biodegradation 19, 303–312. doi:10.1007/s10532-007-9136-4

Brunet, R.C., Garcia-Gil, L.J., 1996. Sulfide-induced dissimilatory nitrate reduction to ammonia in anaerobic freshwater sediments. FEMS Microbiol. Ecol. 21, 131–138. doi:10.1016/0168-6496(96)00051-7

Canfield, D.E., Stewart, F.J., Thamdrup, B., Brabandere, L. De, Delong, E.F., Revsbech, N.P., Ulloa, O., De Brabandere, L., Dalsgaard, T., Delong, E.F., Revsbech, N.P., Ulloa, O., Brabandere, L. De, Delong, E.F., Revsbech, N.P., Ulloa, O., 2010. A cryptic sulfur cycle in oxygen-minimum-zone waters off the Chilean coast. Science 330, 1375–1378. doi:10.1126/science.1196889

Canziani, R., Pollice, A., Ragazzi, M., 1995. Feasibility of using primary-sludge mesophilic hydrolysis for biological removal of nitrogen and phosphorus from wastewater. Bioresour. Technol. 54, 255–260. doi:10.1016/0960-8524(95)00134-4

Casey, E., Susan, R., Glennon, B., Hamer, G., 2004. Characteristics of a Methanotrophic Culture in a Membrane-Aerated Biofilm Reactor Characteristics of a Methanotrophic Culture in a Membrane-Aerated Biofilm Reactor. Biotechnol. Prog. 1–10.

Chaffin, J.D., Davis, T.W., Smith, D.J., Baer, M.M., Dick, G.J., 2018. Interactions between nitrogen form, loading rate, and light intensity on Microcystis and Planktothrix growth and microcystin production. Harmful Algae 73, 84–97. doi:10.1016/j.hal.2018.02.001

Chen, G.H., Chui, H.K., Wong, C.L., Tang, D.T.W., Lu, H., 2012. An Innovative Triple Water Supply System and a Novel SANI® Process to Alleviate Water Shortage and Pollution Problem for Water-scarce Coastal Areas in China. J. Water Sustain. 2, 121–129. doi:10.11912/jws.2.2.121-129

Chen, K.Y., Morris, J.C., 1972. Kinetics of Oxidation of Aqueous Sulfide by O2. Environ. Sci. Technol. 6, 529–537. doi:10.1021/es60065a008

Chen, X., Liu, Y., Peng, L., Yuan, Z., Ni, B.-J., 2016. Model-Based Feasibility Assessment of Membrane Biofilm Reactor to Achieve Simultaneous Ammonium, Dissolved Methane, and Sulfide Removal from Anaerobic Digestion Liquor. Sci. Rep. 6, 25114. doi:10.1038/srep25114

Chung, J., Amin, K., Kim, S., Yoon, S., Kwon, K., Bae, W., 2014. Autotrophic denitrification of nitrate and nitrite using thiosulfate as an electron donor. Water Res. 58, 169–178. doi:10.1016/j.watres.2014.03.071

Dahl, C., Prange, A., 2006. Bacterial Sulfur Globules: Occurrence, Structure and Metabolism, in: Shively, J.M. (Ed.), Inclusions in Prokaryotes. Springer Berlin Heidelberg, Berlin, Heidelberg, pp. 21–51. doi:10.1007/3-540-33774-1_2

Daigger, G.T., 2014. Oxygen and Carbon Requirements for Biological Nitrogen Removal Processes Accomplishing Nitrification, Nitritation, and Anammox. Water Environ. Res. 86, 204–209. doi:10.2175/106143013X13807328849459

Daims, H., Lebedeva, E. V., Pjevac, P., Han, P., Herbold, C., Albertsen, M., Jehmlich, N., Palatinszky, M., Vierheilig, J., Bulaev, A., Kirkegaard, R.H., Bergen, M. von, Rattei, T., Bendinger, B., Nielsen, P.H., Wagner, M., 2015. Complete nitrification by Nitrospira bacteria. Nature. doi:10.1038/nature16461

Daims, H., Lücker, S., Wagner, M., 2016. A New Perspective on Microbes Formerly Known as Nitrite-Oxidizing Bacteria. Trends Microbiol. 24, 699–712. doi:10.1016/j.tim.2016.05.004

Dalsgaard, T., Bah, F., 1994. Nitrate reduction in a sulfate-reducing bacterium Desulfovibrio desulfuricans, isolated from rice paaddy soil: sulfate inhibition, and regulation. Appl. Environ. Microbiol. 60, 291–297.

Delgado Vela, J., Stadler, L.B., Martin, K.J., Raskin, L., Bott, C., Love, N.G., 2015. Prospects for Biological Nitrogen Removal from Anaerobic Effluents during Mainstream Wastewater Treatment. Environ. Sci. Technol. Lett. 2, 233–244. doi:10.1021/acs.estlett.5b00191

Dodds, W.K., Bouska, W.W., Eitzmann, J.L., Pilger, T.J., Pitts, K.L., Riley, A.J., Schloesser, J.T., Thornbrugh, D.J., 2008. Eutrophication of US freshwaters: analysis of potential economic damages. Environ. Sci. Technol. 43, 12–19.

Dolejs, P., Paclík, L., Maca, J., Pokorna, D., Zabranska, J., Bartacek, J., Paclik, L., Maca, J., Pokorna, D., Zabranska, J., Bartacek, J., Paclík, L., Maca, J., Pokorna, D., Zabranska, J., Bartacek, J., 2014. Effect of S/N ratio on sulfide removal by autotrophic denitrification. Appl. Microbiol. Biotechnol. 99, 2383–2392. doi:10.1007/s00253-014-6140-6

Domingo-Félez, C., Mutlu, A.G., Jensen, M.M., Smets, B.F., 2014. Aeration strategies to mitigate nitrous oxide emissions from single-stage nitritation/anammox reactors. Environ. Sci. Technol. 48, 8679–8687. doi:10.1021/es501819n

Downing, L.S., Nerenberg, R., 2008. Total nitrogen removal in a hybrid, membrane-aerated activated sludge process. Water Res. 42, 3697–3708. doi:10.1016/j.watres.2008.06.006

Düppenbecker, B., Cornel, P., 2016. Anaerobic treatment of sulfate-containing municipal wastewater with a fluidized bed reactor at 20°C. Water Sci. Technol. 73, 2446–2452. doi:10.2166/wst.2016.109

Erguder, T.H., Boon, N., Vlaeminck, S.E., Verstraete, W., 2008. Partial nitrification achieved by pulse sulfide doses in a sequential batch reactor. Environ. Sci. Technol. 42, 8715–8720. doi:10.1021/es801391u

Ettwig, K.F., Butler, M.K., Le Paslier, D., Pelletier, E., Mangenot, S., Kuypers, M.M.M., Schreiber, F., Dutilh, B.E., Zedelius, J., de Beer, D., Gloerich, J., Wessels, H.J.C.T., van Alen, T., Luesken, F., Wu, M.L., van de Pas-Schoonen, K.T., Op den Camp, H.J.M., Janssen-Megens, E.M., Francoijs, K.-J., Stunnenberg, H., Weissenbach, J., Jetten, M.S.M., Strous, M., 2010. Nitrite-driven anaerobic methane oxidation by oxygenic bacteria. Nature 464, 543–8. doi:10.1038/nature08883

Fajardo, C., Mora, M., Fernández, I., Mosquera-Corral, A., Campos, J.L., Méndez, R., 2014. Cross effect of temperature, pH and free ammonia on autotrophic denitrification process with sulphide as electron donor. Chemosphere 97, 10–5. doi:10.1016/j.chemosphere.2013.10.028

Fisher, R.M., Alvarez-Gaitan, J.P., Stuetz, R.M., Moore, S.J., 2017. Sulfur flows and biosolids processing: Using Material Flux Analysis (MFA) principles at wastewater treatment plants. J. Environ. Manage. 198, 153–162. doi:10.1016/j.jenvman.2017.04.056

Foley, J., de Haas, D., Hartley, K., Lant, P., 2010. Comprehensive life cycle inventories of alternative wastewater treatment systems. Water Res. 44, 1654–1666. doi:10.1016/j.watres.2009.11.031

Ganigué, R., López, H., Balaguer, M.D., Colprim, J., 2007. Partial ammonium oxidation to nitrite of high ammonium content urban landfill leachates. Water Res. 41, 3317–3326. doi:10.1016/j.watres.2007.04.027

Gilbert, E.M., Agrawal, S., Brunner, F.C., Schwartz, T., Horn, H., Lackner, S., 2014. Response of different Nitrospira sp. to anoxic periods depends on operational DO. Environ. Sci. Technol. doi:10.1021/es404992g

Gilmore, K.R., Little, J.C., Smets, B.F., Love, N.G., 2009. Oxygen Transfer Model for a Flow-Through Hollow-Fiber Membrane Biofilm Reactor. J. Environ. Eng. 135, 806–814.

doi:10.1061/(ASCE)EE.1943-7870.0000035

Gilmore, K.R., Terada, A., Smets, B.F., Love, N.G., Garland, J.L., 2013. Autotrophic Nitrogen Removal in a Membrane-Aerated Biofilm Reactor Under Continuous Aeration: A Demonstration. Environ. Eng. Sci. 30, 38–45. doi:10.1089/ees.2012.0222

Grady, C.P.L., Daigger, G.T., Love, N.G., Filipe, C.D.M., 2011. Biological Wastewater Treatment, 3rd ed. CRC Press, Boca Raton.

Guo, Q., Hu, H.-Y., Shi, Z.-J., Yang, C.-C., Li, P., Huang, M., Ni, W.-M., Shi, M.-L., Jin, R.-C., 2016. Towards simultaneously removing nitrogen and sulfur by a novel process: Anammox and autotrophic desulfurization–denitrification (AADD). Chem. Eng. J. 297, 207–216. doi:10.1016/j.cej.2016.03.138

Hao, T., Xiang, P., Mackey, H.R., Chi, K., Lu, H., Chui, H., van Loosdrecht, M.C.M., Chen, G.-H., 2014. A review of biological sulfate conversions in wastewater treatment. Water Res. 65, 1–21. doi:10.1016/j.watres.2014.06.043

Harada, H.U.S.M.K., 1994. Interaction Between Sulfate Reducing Bacteria and Methane Producing Bacteria In Uasb Reactors Fed With Low Strength Wastes Containing Different Levels Of Sulfate. Water Res. 28, 355–367. doi:10.1016/0043-1354(94)90273-9

Haroon, M.F., Hu, S., Shi, Y., Imelfort, M., Keller, J., Hugenholtz, P., Yuan, Z., Tyson, G.W., 2013. Anaerobic oxidation of methane coupled to nitrate reduction in a novel archaeal lineage. Nature 2–7. doi:10.1038/nature12375

Heffernan, A.B., Shrivastava, A., Toniolo, D., Semmens, M., Syron, E., 2017. Operation of a Large Scale Membrane Aerated Biofilm Reactor for the treatment of Municipal Wastewater. Proc. Water Environ. Fed. 285–297.

Houweling, D., Peeters, J., Cote, P., Long, Z., Adams, N., 2017. Proving Membrane Aerated Biofilm Reactor (MABR) Performance and Reliability: Results from Four Pilots and a Full-Scale Plant. Proc. Water Environ. Fed. 272–284.

Ishii, S., Song, Y., Rathnayake, L., Tumendelger, A., Satoh, H., Toyoda, S., Yoshida, N., Okabe, S., 2014. Identification of key nitrous oxide production pathways in aerobic partial nitrifying granules. Environ. Microbiol. 16, 3168–3180. doi:10.1111/1462-2920.12458

Jin, R.C., Yang, G.F., Zhang, Q.Q., Ma, C., Yu, J.J., Xing, B.S., 2013. The effect of sulfide inhibition on the ANAMMOX process. Water Res. 47, 1459–1469. doi:10.1016/j.watres.2012.12.018

Jones, Z.L., Jasper, J.T., Sedlak, D.L., Sharp, J.O., 2017. Sulfide Induced Dissimilatory Nitrate Reduction to Ammonium Supports Anaerobic Ammonium Oxidation (Anammox) in an

Open-Water Unit Process Wetland. Appl. Environ. Microbiol. 83, 1–14.

Joye, S.B., Hollibaugh, J.T., 1995. Influence of Sulfide Inhibition of Nitrification on Nitrogen Regeneration in Sediments. Science. 270, 623–625. doi:10.1126/science.270.5236.623

Kampschreur, M.J., Temmink, H., Kleerebezem, R., Jetten, M.S.M., van Loosdrecht, M.C.M., 2009. Nitrous oxide emission during wastewater treatment. Water Res. 43, 4093–103. doi:10.1016/j.watres.2009.03.001

Kartal, B., Kuypers, M.M.M., Lavik, G., Schalk, J., Op den Camp, H.J.M., Jetten, M.S.M., Strous, M., 2007. Anammox bacteria disguised as denitrifiers: nitrate reduction to dinitrogen gas via nitrite and ammonium. Environ. Microbiol. 9, 635–42. doi:10.1111/j.1462-2920.2006.01183.x

Keith, S.M., Herbert, R.A., 1983. Dissimilatory nitrate reduction by a strain of Desulfovibrio desulfuricans. FEMS Microbiol. Lett. 55–59.

Kim, S.W., Miyahara, M., Fushinobu, S., Wakagi, T., Shoun, H., 2010. Nitrous oxide emission from nitrifying activated sludge dependent on denitrification by ammonia-oxidizing bacteria. Bioresour. Technol. 101, 3958–3963. doi:10.1016/j.biortech.2010.01.030

Kinh, C.T., Riya, S., Hosomi, M., Terada, A., 2017a. Identification of hotspots for NO and N 2 O production and consumption in counter- and co-diffusion biofilms for simultaneous nitrification and denitrification. Bioresour. Technol. doi:10.1016/j.biortech.2017.08.051

Kinh, C.T., Suenaga, T., Hori, T., Riya, S., Hosomi, M., Smets, B.F., Terada, A., 2017b. Counter-diffusion biofilms have lower N 2 O emissions than co-diffusion biofilms during simultaneous nitrification and denitrification: Insights from depth-profile analysis. Water Res. doi:10.1016/j.watres.2017.07.058

Kouba, V., Proksova, E., Wiesinger, H., Vejmelkova, D., Bartacek, J., 2017. Good servant, bad master: sulfide and dissolved methane influence on partial nitritation of sewage. Water Sci. Technol. wst2017490. doi:10.2166/wst.2017.490

Kouba, V., Vejmelkova, D., Proksova, E., Wiesinger, H., Concha, M., Dolejs, P., Hejnic, J., Jenicek, P., Bartacek, J., 2017. High-Rate Partial Nitritation of Municipal Wastewater after Psychrophilic Anaerobic Pretreatment. Environ. Sci. Technol. acs.est.7b02078. doi:10.1021/acs.est.7b02078

Kuypers, M.M.M., Marchant, H.K., Kartal, B., 2018. The microbial nitrogen-cycling network. Nat. Rev. Microbiol. doi:10.1038/nrmicro.2018.9

Lens, P.N., De Poorter, M.P., Cronenberg, C.C., Verstraete, W.H., 1995. Sulfate reducing and methane producing bacteria in aerobic wastewater treatment systems. Water Res. 29, 871–

880. doi:10.1016/0043-1354(94)00195-D

Lens, P.N.L., Visser, A., Janssen, A.J.H., Hulshoff Pol, L.W., Lettinga, G., 1998. Biotechnological treatment of sulfate-rich wastewaters. Crit. Rev. Environ. Sci. Technol. 28, 41–88. doi:10.1080/10643389891254160

Liu, X., Dai, J., Wu, D., Jiang, F., Chen, G., Chui, H.K., van Loosdrecht, M.C.M., 2016. Sustainable Application of a Novel Water Cycle Using Seawater for Toilet Flushing. Engineering 2, 460–469. doi:10.1016/J.ENG.2016.04.013

Liu, Y., Peng, L., Ngo, H.H., Guo, W., Wang, D., Pan, Y., Sun, J., Ni, B.-J., 2016. Evaluation of Nitrous Oxide Emission from Sulfide- and Sulfur-Based Autotrophic Denitrification Processes. Environ. Sci. Technol. acs.est.6b02202. doi:10.1021/acs.est.6b02202

Lu, H., Chandran, K., 2010. Factors promoting emissions of nitrous oxide and nitric oxide from denitrifying sequencing batch reactors operated with methanol and ethanol as electron donors. Biotechnol. Bioeng. 106, 390–398. doi:10.1002/bit.22704

Lu, H., Ekama, G.A., Wu, D., Feng, J., van Loosdrecht, M.C.M., Chen, G.H., 2012. SANI ?? process realizes sustainable saline sewage treatment: Steady state model-based evaluation of the pilot-scale trial of the process. Water Res. 46, 475–490. doi:10.1016/j.watres.2011.11.031

Luesken, F. a, van Alen, T. a, van der Biezen, E., Frijters, C., Toonen, G., Kampman, C., Hendrickx, T.L.G., Zeeman, G., Temmink, H., Strous, M., Op den Camp, H.J.M., Jetten, M.S.M., 2011. Diversity and enrichment of nitrite-dependent anaerobic methane oxidizing bacteria from wastewater sludge. Appl. Microbiol. Biotechnol. 92, 845–54. doi:10.1007/s00253-011-3361-9

Luther, G.W., Findlay, A.J., MacDonald, D.J., Owings, S.M., Hanson, T.E., Beinart, R. a., Girguis, P.R., 2011. Thermodynamics and kinetics of sulfide oxidation by oxygen: A look at inorganically controlled reactions and biologically mediated processes in the environment. Front. Microbiol. 2, 1–9. doi:10.3389/fmicb.2011.00062

Ma, C., Jensen, M.M., Smets, B.F., Thamdrup, B., 2017. Pathways and controls of N2O production in nitritation-anammox biomass. Environ. Sci. Technol. acs.est.7b01225. doi:10.1021/acs.est.7b01225

Mampaey, K.E., De Kreuk, M.K., van Dongen, L.G.J.M., van Loosdrecht, M.C.M., Volcke, E.I.P., 2015. Identifying N2O formation and emissions from a full-scale partial nitritation reactor. Water Res. doi:10.1016/j.watres.2015.10.047

Manconi, I., van der Maas, P., Lens, P., 2006. Effect of copper dosing on sulfide inhibited reduction of nitric and nitrous oxide. Nitric Oxide - Biol. Chem. 15, 400–407. doi:10.1016/j.niox.2006.04.262

Martin, K.J., Nerenberg, R., 2012. The membrane biofilm reactor (MBfR) for water and wastewater treatment: principles, applications, and recent developments. Bioresour. Technol. 122, 83–94. doi:10.1016/j.biortech.2012.02.110

McCarty, P.L., Bae, J., Kim, J., 2011. Domestic wastewater treatment as a net energy producer--can this be achieved? Environ. Sci. Technol. 45, 7100–6. doi:10.1021/es2014264

Milucka, J., Ferdelman, T.G., Polerecky, L., Franzke, D., Wegener, G., Schmid, M., Lieberwirth, I., Wagner, M., Widdel, F., Kuypers, M.M.M., 2012. Zero-valent sulphur is a key intermediate in marine methane oxidation. Nature 491, 541–6. doi:10.1038/nature11656

Moraes, B.S., Orrú, J.G.T., Foresti, E., 2012. Nitrogen and sulfide removal from effluent of UASB reactor in a sequencing fed-batch biofilm reactor under intermittent aeration. J. Biotechnol. 164, 378–385. doi:10.1016/j.jbiotec.2012.06.032

Moraes, B.S., Souza, T.S.O., Foresti, E., 2012. Effect of sulfide concentration on autotrophic denitrification from nitrate and nitrite in vertical fixed-bed reactors. Process Biochem. 47, 1395–1401. doi:10.1016/j.procbio.2012.05.008

Mulder, A., van de Graaf, A.A., Robertson, L.A., Kuenen, J.G., 1995. Anaerobic ammonium oxidation discovered in a denitrifying fluidized bed reactor. FEMS Microbiol. Ecol. 16, 177–183. doi:10.1016/0168-6496(94)00081-7

Muyzer, G., Stams, A.J.M., 2008. The ecology and biotechnology of sulphate-reducing bacteria. Nat. Rev. - Microbiol. 6, 441–454. doi:10.1038/nrmicro1892

Nielsen, A.H., Lens, P., Vollertsen, J., Hvitved-Jacobsen, T., 2005. Sulfide-iron interactions in domestic wastewater from a gravity sewer. Water Res. 39, 2747–2755. doi:10.1016/j.watres.2005.04.048

Nielsen, A.H., Vollertsen, J., Hvitved-jacobsen, T., 2006. Kinetics and Stoichiometry of Aerobic Sulfide Oxidation in Wastewater from Sewers — Effects of pH and Temperature. Water Environ. Res. 78, 275–283.

Nielsen, A.H., Vollertsen, J., Hvitved-Jacobsen, T., 2003. Determination of kinetics and stoichiometry of chemical sulfide oxidation in wastewater of sewer networks. Environ. Sci. Technol. 37, 3853–3858. doi:10.1021/es034035l

Noyola, A., Morgan-Sagastume, J.M., López-Hernández, J.E., 2006. Treatment of biogas produced in anaerobic reactors for domestic wastewater: Odor control and energy/resource recovery. Rev. Environ. Sci. Biotechnol. 5, 93–114. doi:10.1007/s11157-005-2754-6

Oude Elferink, S.J.W.H., Visser, A., Hulshoff Pol, L.W., Stams, A.J.M., 1994. Sulfate reduction in methanogenic bioreactors. FEMS Microbiol. Rev. 15, 119–136. doi:10.1111/j.1574-

6976.1994.tb00130.x

Paerl, H.W., Scott, J.T., McCarthy, M.J., Newell, S.E., Gardner, W.S., Havens, K.E., Hoffman, D.K., Wilhelm, S.W., Wurtsbaugh, W.A., 2016. It Takes Two to Tango: When and Where Dual Nutrient (N & P) Reductions Are Needed to Protect Lakes and Downstream Ecosystems. Environ. Sci. Technol. 50, 10805–10813. doi:10.1021/acs.est.6b02575

Pan, Y., Ye, L., Yuan, Z., 2013. Effect of H2S on N2O reduction and accumulation during denitrification by methanol utilizing denitrifiers. Environ. Sci. Technol. 47, 8408–8415. doi:10.1021/es401632r

Pellicer-Nàcher, C., Franck, S., Gülay, A., Ruscalleda, M., Terada, A., Al-Soud, W.A., Hansen, M.A., Sørensen, S.J., Smets, B.F., 2014. Sequentially aerated membrane biofilm reactors for autotrophic nitrogen removal: microbial community composition and dynamics. Microb. Biotechnol. 7, 32–43. doi:10.1111/1751-7915.12079

Pellicer-Nàcher, C., Sun, S., Lackner, S., Terada, A., Schreiber, F., Zhou, Q., Smets, B.F., 2010. Sequential aeration of membrane-aerated biofilm reactors for high-rate autotrophic nitrogen removal: experimental demonstration. Environ. Sci. Technol. 44, 7628–34. doi:10.1021/es1013467

Rassamee, V., Sattayatewa, C., Pagilla, K., Chandran, K., 2011. Effect of oxic and anoxic conditions on nitrous oxide emissions from nitrification and denitrification processes. Biotechnol. Bioeng. 108, 2036–2045. doi:10.1002/bit.23147

Regmi, P., Miller, M.W., Holgate, B., Bunce, R., Park, H., Chandran, K., Wett, B., Murthy, S., Bott, C.B., 2014. Control of aeration, aerobic SRT and COD input for mainstream nitritation/denitritation. Water Res. 57, 162–71. doi:10.1016/j.watres.2014.03.035

Rios-Del Toro, E.E., Cervantes, F.J., 2016. Coupling between anammox and autotrophic denitrification for simultaneous removal of ammonium and sulfide by enriched marine sediments. Biodegradation. doi:10.1007/s10532-016-9759-4

Rosso, D., Larson, L.E., Stenstrom, M.K., 2008. Aeration of large-scale municipal wastewater treatment plants: state of the art. Water Sci. Technol. 57, 973–978.

Russ, L., Speth, D.R., Jetten, M.S.M.M., Op den Camp, H.J.M.M., Kartal, B., 2014. Interactions between anaerobic ammonium and sulfur-oxidizing bacteria in a laboratory scale model system. Environ. Microbiol. 16, 3487–3498. doi:10.1111/1462-2920.12487

Rütting, T., Boeckx, P., Müller, C., Klemedtsson, L., 2011. Assessment of the importance of dissimilatory nitrate reduction to ammonium for the terrestrial nitrogen cycle. Biogeosciences 8, 1779–1791. doi:10.5194/bg-8-1779-2011

Sabba, F., Devries, A., Vera, M., Druschel, G., Bott, C., Nerenberg, R., 2016. Potential use of sulfite as a supplemental electron donor for wastewater denitrification. Rev. Environ. Sci. Bio/Technology 15, 563–572. doi:10.1007/s11157-016-9413-y

Sabba, F., Picioreanu, C., Nerenberg, R., 2017. Mechanisms of nitrous oxide (N2O) formation and reduction in denitrifying biofilms. Biotechnol. Bioeng. 1–9. doi:10.1002/bit.26399

Sahinkaya, E., Hasar, H., Kaksonen, A.H., Rittmann, B.E., 2011. Performance of a sulfide-oxidizing, sulfur-producing membrane biofilm reactor treating sulfide-containing bioreactor effluent. Environ. Sci. Technol. 45, 4080–4087. doi:10.1021/es200140c

Sander, R., 2015. Compilation of Henry's law constants (version 4.0) for water as solvent. Atmos. Chem. Phys. 15, 4399–4981. doi:10.5194/acp-15-4399-2015

Santegoeds, C.M., Ferdelman, T.G., Beer, D. De, Planck, M., Microbiology, M., Bremen, D.-, 1998. Structural and Functional Dynamics of Sulfate-Reducing Populations in Bacterial Biofilms. Appl. Environ. Microbiol. 64, 3731–3739.

Senga, Y., Mochida, K., Fukumori, R., Okamoto, N., Seike, Y., 2006. N2O accumulation in estuarine and coastal sediments: The influence of H2S on dissimilatory nitrate reduction. Estuar. Coast. Shelf Sci. 67, 231–238. doi:10.1016/j.ecss.2005.11.021

Shannon, J.M., Hauser, L.W., Liu, X., Parkin, G.F., Mattes, T.E., Just, C.L., 2015. Partial nitritation ANAMMOX in submerged attached growth bioreactors with smart aeration at 20 °C. Environ. Sci. Process. Impacts 17, 81–9. doi:10.1039/c4em00481g

Shao, M.F., Zhang, T., Fang, H.H.P., 2010. Sulfur-driven autotrophic denitrification: Diversity, biochemistry, and engineering applications. Appl. Microbiol. Biotechnol. 88, 1027–1042. doi:10.1007/s00253-010-2847-1

Sorensen, J., Tiedje, J.M., Firestone, R.B., 1980. Inhibition by Sulfide of Nitric and Nitrous-Oxide Reduction by Denitrifying Pseudomonas-Fluorescens. Appl. Environ. Microbiol. 39, 105–108.

Su, Q., Ma, C., Domingo-Félez, C., Kiil, A.S., Thamdrup, B., Jensen, M.M., Smets, B.F., 2017. Low nitrous oxide production through nitrifier-denitrification in intermittent-feed high-rate nitritation reactors. Water Res. 123, 429–438. doi:10.1016/j.watres.2017.06.067

Tallec, G., Garnier, J., Billen, G., Gousailles, M., 2008. Nitrous oxide emissions from denitrifying activated sludge of urban wastewater treatment plants, under anoxia and low oxygenation. Bioresour. Technol. 99, 2200–2209. doi:10.1016/j.biortech.2007.05.025

Tallec, G., Garnier, J., Billen, G., Gousailles, M., 2006. Nitrous oxide emissions from secondary activated sludge in nitrifying conditions of urban wastewater treatment plants: effect of

oxygenation level. Water Res. 40, 2972–80. doi:10.1016/j.watres.2006.05.037

Tanber, G., 2014. Toxin leaves 500,000 in northwest Ohio without drinking water. Reuters.

Tchobanoglous, G., Burton, F.L., Stensel, H.., 2003. Wastewater Engineering: Treatment, Disposal and Reuse, Fourth Edi. ed. McGraw-Hill.

Terada, A., Hibiya, K., Nagai, J., Tsuneda, S., Hirata, A., 2003. Nitrogen removal characteristics and biofilm analysis of a membrane-aerated biofilm reactor applicable to high-strength nitrogenous wastewater treatment. J. Biosci. Bioeng. 95, 170–178. doi:10.1263/jbb.95.170

U.S. Environmental Protection Agency, ', 2010. Methane and Nitrous Oxide Emissions from Natural Sources.

Vadivelu, V.M., Keller, J., Yuan, Z., 2006. Effect of Free Ammonia and Free Nitrous Acid Concentration on the Anabolic and Catabolic Processes of an Enriched Nitrosomonas Culture. Biotechnol. Bioeng. 95. doi:10.1002/bit

van den Berg, E.M., Boleij, M., Kuenen, J.G., Kleerebezem, R., van Loosdrecht, M.C.M., 2016. DNRA and denitrification coexist over a broad range of acetate/N-NO3- ratios, in a chemostat enrichment culture. Front. Microbiol. 7, 1–12. doi:10.3389/fmicb.2016.01842

Van Kempen, R., Mulder, J.W., Uijterlinde, C. a., Loosdrecht, M.C.M., 2001. Overview: Full scale experience of the SHARON?? process for treatment of rejection water of digested sludge dewatering. Water Sci. Technol. 44, 145–152.

van Kessel, M.A.H.J., Speth, D.R., Albertsen, M., Nielsen, P.H., Huub, J.M., 2015. Complete nitrification by a single microorganism. Nature 528, 555–559. doi:10.1038/nature16459

Vazquez, F.G., Zhang, J., Millero, F.J., 1989. Effect of Metals on the Rate of Oxidation of H2S in Seawater. Geophys. Res. Lett. 16, 1363–1366.

Villaverde, S., García-Encina, P. a., Fdz-Polanco, F., 1997. Influence of pH over nitrifying biofilm activity in submerged biofilters. Water Res. 31, 1180–1186. doi:10.1016/S0043-1354(96)00376-4

Wang, J., Lu, H., Chen, G.H., Lau, G.N., Tsang, W.L., van Loosdrecht, M.C.M., 2009. A novel sulfate reduction, autotrophic denitrification, nitrification integrated (SANI) process for saline wastewater treatment. Water Res. 43, 2363–2372. doi:10.1016/j.watres.2009.02.037

Wang, S., Wang, W., Liu, L., Zhuang, L., Zhao, S., Su, Y., Li, Y., Wang, M., Wang, C., Xu, L., Zhu, G., 2018. Microbial nitrogen cycle hotspots in the plant-bed/ditch system of a constructed wetland with N2O mitigation. Environ. Sci. Technol. acs.est.7b04925. doi:10.1021/acs.est.7b04925

Wang, Y., Bott, C., Nerenberg, R., 2016. Sulfur-based denitrification: Effect of biofilm development on denitrification fluxes. Water Res. 100, 184–193. doi:10.1016/j.watres.2016.05.020

Wilmot, P.D., Cadee, K., Katinic, J.J., Kavanagh, B. V, 1988. Kinetics of Sulfide Oxidation by Dissolved Oxygen. J. (Water Pollut. Control Fed. 60, 1264–1270.

Winkler, M.K.H., Yang, J., Kleerebezem, R., Plaza, E., Trela, J., Hultman, B., van Loosdrecht, M.C.M., 2012. Nitrate reduction by organotrophic Anammox bacteria in a nitritation/anammox granular sludge and a moving bed biofilm reactor. Bioresour. Technol. 114, 217–223. doi:10.1016/j.biortech.2012.03.070

Wu, D., Ekama, G.A., Chui, H.K., Wang, B., Cui, Y.X., Hao, T.W., van Loosdrecht, M.C.M., Chen, G.H., 2016. Large-scale demonstration of the sulfate reduction autotrophic denitrification nitrification integrated (SANI®) process in saline sewage treatment. Water Res. 100, 496–507. doi:10.1016/j.watres.2016.05.052

Wunderlin, P., Mohn, J., Joss, A., Emmenegger, L., Siegrist, H., 2012. Mechanisms of N 2O production in biological wastewater treatment under nitrifying and denitrifying conditions. Water Res. 46, 1027–1037. doi:10.1016/j.watres.2011.11.080

Yang, W., Lu, H., Khanal, S.K., Zhao, Q., Meng, L., Chen, G.H., 2016a. Granulation of sulfur-oxidizing bacteria for autotrophic denitrification. Water Res. 104, 507–519. doi:10.1016/j.watres.2016.08.049

Yang, W., Zhao, Q., Lu, H., Ding, Z., Meng, L., Chen, G.-H., 2016b. Sulfide-driven autotrophic denitrification significantly reduces N2O emissions. Water Res. 90, 176–184. doi:10.1016/j.watres.2015.12.032

Yin, Z., Xie, L., Zhou, Q., 2015. Effects of sulfide on the integration of denitrification with anaerobic digestion. J. Biosci. Bioeng. 120, 426–431. doi:10.1016/j.jbiosc.2015.02.004

Yu, R., Kampschreur, M.J., van Loosdrecht, M.C.M., Chandran, K., 2010. Mechanisims and Specific Directionality of Autotrophic Nitrous Oxide and Nitric Oxide Generation during Transient Anoxia. Environ. Sci. Technol. 44, 1313–1319. doi:10.1021/es902794a

Zhang, L., De Schryver, P., De Gusseme, B., De Muynck, W., Boon, N., Verstraete, W., 2008. Chemical and biological technologies for hydrogen sulfide emission control in sewer systems: A review. Water Res. 42, 1–12. doi:10.1016/j.watres.2007.07.013

Zhang, L., Keller, J., Yuan, Z., 2009. Inhibition of sulfate-reducing and methanogenic activities of anaerobic sewer biofilms by ferric iron dosing. Water Res. 43, 4123–4132. doi:10.1016/j.watres.2009.06.013

Zheng, H., Hanaki, K., Matsuo, T., 1994. Production of nitrous oxide gas during nitrification of wastewater. Water Sci. Technol.

# CHAPTER 3.

## SULFIDE INHIBITION OF NITRITE OXIDATION IN ACTIVATED SLUDGE DEPENDS ON MICROBIAL COMMUNITY COMPOSITION

Reprinted with permission from: Jeseth Delgado Vela, Gregory J. Dick, Nancy G. Love, Sulfide inhibition of nitrite oxidation in activated sludge depends on microbial community composition, *Water Research*, **2018**, https://doi.org/10.1016/j.watres.2018.03.047. 

### 3.1 Abstract

Increasingly, technologies that use sulfide as an electron donor are being considered for nitrogen removal; however, our understanding of how sulfide affects microbial communities in nitrifying treatment processes is limited. In this study, we used batch experiments to quantify sulfide inhibition of both ammonium oxidizing bacteria (AOB) and nitrite oxidizing bacteria (NOB) using activated sludge from two full-scale treatment plants with distinct treatment processes. The batch experiments showed that NOB were more vulnerable to sulfide inhibition than AOB, and that inhibition constants ($K_I$) for NOB were distinct between the two treatment plants, which also had distinct nitrite oxidizing microbial communities. A Nitrospira-rich, less diverse NOB community was inhibited more by sulfide than a more diverse community rich in Nitrotoga and Nitrobacter. Therefore, sulfide-induced nitritation may be more successful in less diverse, Nitrospira-rich communities. Additionally, sulfide significantly influenced the activity of non-nitrifying microbial community members, as measured by 16S rRNA cDNA sequencing. Overall, these results indicate that sulfide has a strong impact on both nitrification and the activity of the underlying microbial communities, and that the response is community-specific.

### 3.2 Introduction

As our understanding of the environmental and human health impacts of eutrophication grows, increasingly stringent effluent nitrogen regulations are being implemented worldwide.

Conventional biological nitrogen removal consists of first converting the ammonium in wastewater to nitrate using nitrifying microorganisms, then converting the nitrate to nitrogen gas using denitrifying microorganisms. Amidst a move within the water industry toward resource efficiency, there is a growing interest in technologies that promote and maintain nitritation, the oxidation of ammonium to nitrite by ammonia oxidizing bacteria (AOB) while preventing further oxidation of nitrite to nitrate by nitrite oxidizing bacteria (NOB). Nitritation reduces aeration costs by 25% based on stoichiometry, offers an alternative to nitrate as an electron acceptor for denitrification, which reduces electron donor requirements, and can significantly reduce the overall energy cost of operating a treatment plant (Rosso et al., 2008). However, sustaining nitritation processes in low-strength wastewater systems is challenging, and while various methods have been proposed (Blackburne et al., 2008; Gilbert et al., 2014; Regmi et al., 2014; Shannon et al., 2015; Vadivelu et al., 2006; Villaverde et al., 1997), to date there is no consensus on the most effective strategy.

In addition to nitritation processes, there is growing interest in harnessing hydrogen sulfide as an alternative electron donor for nitrogen removal. Although toxic and corrosive, hydrogen sulfide can be used as an electron donor for denitrification in natural environments (e.g. Canfield et al., 2010) and during wastewater treatment (Lu et al., 2012; Sabba et al., 2016). Hydrogen sulfide is frequently produced biologically from sulfate in sewers (e.g., Zhang et al., 2008) and by anaerobic processes within treatment plants (e.g. Isa et al., 1986). The amount of hydrogen sulfide produced is a function of the sulfate content in wastewater, which is variable and depends on factors such as industrial wastewater discharges, drinking water source water, and the coagulant used for drinking water treatment. In coastal regions, sulfate concentrations in wastewater increase due to seawater infiltration into both groundwater reservoirs used as drinking water sources and wastewater collection systems, a phenomenon that will be magnified by global climate change, sea level rise, and projected population growth along coasts. These increases all lead to increased sulfide loads to wastewater treatment plants. The Sulfate Reduction, Autotrophic Denitrification and Nitrification Integrated (SANI®) process incorporates sulfur-driven denitrification to achieve nitrogen removal and is now deployed at the demonstration scale (Wang et al., 2009; Wu et al., 2016). The SANI® process takes advantage of increased wastewater sulfide concentrations that are present due to the practice of using seawater for toilet flushing. It has lower space requirements

(Wu et al., 2016), lower sludge production (Wu et al., 2016), and reduced nitrous oxide emissions (Yang et al., 2016) compared to conventional nitrification and heterotrophic denitrification. However, despite the progress with sulfur-driven denitrification, more research is needed to understand how sulfide impacts nitrification and, more specifically, nitritation.

Sulfide is a known inhibitor of nitrification and has specifically been shown to differentially inhibit ammonium oxidizing and nitrite oxidizing bacteria (Bejarano-Ortiz et al., 2015; Erguder et al., 2008; Kouba et al., 2017). However, estimates of inhibition constants vary significantly. In this study we associate the variability in experimentally determined sulfide inhibition with microbial community dynamics. Specifically, we evaluated the impact of sulfide on the kinetics of nitrite oxidation and ammonium oxidation independently using biomass from two full-scale treatment plants that use different treatment processes, and compared our kinetic observations with the differences we found in the underlying microbial community ecology. Our results suggest that sulfide may be a useful selective inhibitor of nitrite oxidizing bacteria (NOB) for treatment systems but this depends on the composition and diversity of the NOB communities.

## 3.3 Materials and Methods

### *3.3.1 Batch experimental design*

Eight-hour batch experiments were performed on freshly collected activated sludge April-June 2016 from two local wastewater treatment plants (WWTPs), an extended aeration process (Novi, Michigan, USA) and an A2O (Anaerobic-Anoxic-Aerobic, Ann Arbor, Michigan, USA) process, with process and performance characteristics shown in Table 3-1. Both treatment plants have experienced sulfide-induced corrosion in either the collection system, lift station or grit chamber. Activated sludge was collected from the aerobic tank in the same location at approximately the same time of day (± 1 hour) for each experiment. Batch experiments were conducted at five target sulfide concentrations for each WWTP; 2, 4, 8, 15, and 35 mg/L as S for the A2O process and 2, 5, 10, 15, and 35 mg/L as S for the extended aeration process. These concentrations are consistent with baseline sulfur levels typically found in domestic wastewater (6-17 mg/L as S (Burton et al., 2014)). Each batch experiment had ten flasks duplicate sulfide-free controls with ammonium, duplicate sulfide-free controls with nitrite, triplicate sulfide and ammonium-amended cultures, and

triplicate sulfide and nitrite-amended cultures. Flasks were covered with aluminium foil and maintained in the dark in a shaking water bath set to 25°C at a shaking speed which had been determined to maintain dissolved oxygen concentrations above 2 mg/L.

**Table 3-1.** Characteristics of wastewater treatment plants from which biomass was collected. *for aeration zone (oxic) phase of treatment. † average for April 2017

| **Process type** | Anaerobic-Anoxic-Oxic (A2O) | Extended Aeration |
|---|---|---|
| **Wastewater type** | Mostly municipal | Mostly municipal |
| **Solids Residence Time (days)** | 6.5 | 16 |
| **Dissolved Oxygen Concentration (mg/L)** | 2-4* | 4.75 |
| **Total Suspended Solids (mg/L)** | 2,000 | 2,500-3,600 |
| **Average daily flow (MGD)** | 18 | 3.5 |
| **Nitrification (% ammonia oxidized)†** | 100 | 100 |
| **$BOD_5$ removal (%)†** | 98 | 99 |

To initiate batch experiments, 1.2 L of activated sludge was washed using three centrifugation (7500 x g) and resuspension steps in a 0.12 M phosphate buffer (3.2 g/L $KH_2PO_4$, 13.7 g/L $Na_2HPO_4$, pH=7.5). Batch media was prepared ahead of time and left in an anaerobic chamber overnight. It was prepared using 1000x dilutions of four separate stock solutions in the following order: acidic trace metal, basic trace metal, chelating, and divalent cation. The acidic trace metal stock solution consisted of (per liter): $CoCl_2 \cdot 6H_2O$, 280 mg; $ZnSO_4 \cdot 7H_2O$, 340 mg; $H_3BO_3$, 37 mg; $MnCl_2 \cdot 4H_2O$, 110 mg; $AlCl_3 \cdot 6H_2O$, 28 mg; $NiCl_2 \cdot 6H_2O$, 140 mg; $CuCl_2 \cdot 2H_2O$, 100 mg. The basic trace metal stock solution consisted of (per liter): $(NH_4)_2MoO_4 \cdot 4H_2O$, 160 mg; $Na_2SeO_4$, 22 mg; $Na_2WO_4 \cdot 2H_2O$, 40 mg. The chelating stock solution consisted of 10 g/L NaEDTA, and the

divalent cation stock solution consisted of (per liter): $CaCl_2 \cdot 2H_2O$, 5.0 g; $MgCl_2 \cdot 6H_2O$, 33 g. Sufficient ammonium bicarbonate was added to the ammonium amended batches to achieve an initial concentration of 50 mg N/L, and sodium nitrite was added to the nitrite amended batches to achieve an initial concentration of 20 mg N/L. Nitrite-N concentrations and ammonium-N concentrations were chosen to be representative of mainstream wastewater treatment plants using nitritation processes. At the pH measured across all samples and experiments (average 7.71 ± 0.10), free nitrous acid concentrations were calculated to be $5 \times 10^{-7}$ mg $HNO_2$-N/L at most, well below inhibitory free nitrous acid concentrations for nitrite oxidizers (0.023 mg $HNO_2$-N/L) (Vadivelu et al., 2006). Similarly, the maximum free ammonia concentration was calculated to be 1.3 mg $NH_3$-N/L, which is below the inhibitory free ammonia concentration for ammonia oxidizers (10-100 mg $NH_3$-N/L) (Anthonisen et al., 1976). Sulfide was added to each flask individually using a 5 g S/L stock. The sulfide stock was made in the glove box using a sodium sulfide nonahydrate salt. Following sulfide addition, flasks were quickly moved from the anaerobic chamber to a fume hood. To reduce the available reaction time between sulfide and iron which can cause sulfide precipitation, iron was added separately from the other trace metals. Just prior (<2 minutes) to initiating batch experiments, iron (III) (stock concentration 6.5 g/L $FeCl_3 \cdot 6H_2O$) was added (100 µL) to each flask and followed immediately by sampling to determine the initial sulfide concentration. We found that between adding the sulfide in the glove box and the initial sulfide measurement, we lost an average of 14±19% of the sulfide added (Appendix A, Tables A2 and A3), possibly due to abiotic losses such as precipitation (Alvarez et al., 2007) and/or stripping (Suleimenov and Krupp, 1994). Experiments were initiated by adding thirty mL of the washed biomass to each flask to make a final batch volume of 100 mL.

### *3.3.2 Sample collection and analysis*

All samples were collected by first moving the flask from the water bath to the stir plate to ensure samples were taken from a completely mixed system. Ten milliliter samples were collected for nitrogen analysis at 2 min, 30 min, 2 h, 4 h and 8 h into the experiment. Samples were pelleted at 7500 x g for 5 min at 4°C and the supernatant was filtered using a washed 0.45 µm nitrocellulose filter (Fisher Scientific). An aliquot of each filtered sample was acidified to a pH of 3 using 1 N HCl for ammonium analysis via the phenate method 4500-$NH_3$ F (APHA et al., 2005).) Nitrite

was determined using the colorimetric method 4200-$NO_2^-$ B, and nitrate and sulfate were measured using the ion chromatography method 4110-B (APHA et al., 2005).

Samples for sulfide analysis were collected separate from the samples taken for nitrogen analyses at the following time points: immediately after iron addition, at 2 min, 30 min, 2 h, and 4 h into the experiment. All samples were collected, stored, and analysed according to method 4500-$S^{2-}$ G (APHA et al., 2005). Samples were collected into a syringe containing 2 mL of sulfide antioxidant buffer (2x, final sample dilution), immediately transferred to the anaerobic chamber, filtered using a washed 0.45 µm nitrocellulose filter (Fisher Scientific), and preserved in the dark until analysis within 24 hours. The sulfide antioxidant buffer was stored in the anaerobic chamber in an amber bottle and prepared as described in Standard Methods by combining 67 g of disodium EDTA, 35 g of ascorbic acid, and 200 mL of 1 N sodium hydroxide into deoxygenated Milli-Q water to 1 L final volume (APHA et al., 2005). Sulfide was analysed using a silver sulfide electrode (Thermo Scientific, Orion) that was calibrated with a 3% (w/v) sodium sulfide stock solution (Ricca Chemical Company) method 4500-$S^{2-}$ G (APHA et al., 2005).

Two biomass samples (one for DNA analysis, one for cDNA analysis, 1 mL each) were collected for microbial community analysis from each flask between 2.5 hours and 3.75 hours into the experiment to represent a time point when nitrogenous substrates had not been depleted. Samples were collected by moving the flask to a stir plate and pipetting the samples into nuclease free microcentrifuge tubes. Samples were immediately pelleted at 7500 x g for 5 minutes at 4°C, the supernatant was discarded, and one sample was resuspended in RNALater (Qiagen, Valencia, CA). All samples were stored at -80°C until nucleic acids were extracted.

Volatile suspended solids (VSS) were analysed at the end of the experiment (Appendix A, Table A4) and used to normalize rates of oxidation. Rates of nitrification (µ) were determined by taking the slope of the linear range of nitrate concentrations for nitrite amended cultures, or the sum of nitrite and nitrate concentrations for ammonium amended cultures. Data used to take rates of nitrification are shown in Appendix A (Figures A2 and A3). The linear range was between the 34±18 min and 7.0±1.0 h sample points, $R^2$=0.97±0.04.

### *3.3.3 Estimation of inhibition parameters*

We modeled inhibition of AOB and NOB using a noncompetitive inhibition model. Previous studies on nitrification inhibition showed that volatile sulfur compounds inhibit ammonia monooxygenase noncompetitively (Hyman et al., 1990) and this model was used for sulfide inhibition of both AOB and NOB (Kouba et al., 2017); consequently, there is prior evidence that this model form with sulfide inhibition is reasonable. Under the noncompetitive inhibition model, the rate of growth under inhibited conditions ($\mu_{inh}$) is:

$$(1)\ \mu_{inh} = \frac{\mu_{max}[S]}{(1+\frac{[I]}{K_i})(K_S+[S])}$$

Where: $\mu_{max}$ is the uninhibited maximum specific growth rate; [S] is the concentration of electron donor, which in this case is ammonium or nitrite; [I] is the concentration of inhibitor, which for this study was the measured sulfide concentration just prior to biomass addition; $K_i$ is the inhibition constant; and $K_S$ is the half saturation constant. In the absence of an inhibitor, the rate of growth in the controls ($\mu_{cont}$) simplifies to conventional Monod kinetics:

$$(2)\ \mu_{cont} = \frac{\mu_{max}[S]}{(K_S+[S])}$$

Therefore, the rate in the sulfide amended cultures normalized to the controls reduces to:

$$(3)\ \frac{\mu_{inh}}{\mu_{cont}} = \frac{1}{1+\frac{[I]}{K_i}}$$

Sulfide is a reactive inhibitor therefore the nitrifying populations were exposed to lower concentrations of sulfide on average than the concentrations used in our model (Appendix A, Tables A2 and A3). Thus, by using measured sulfide concentration at the beginning of the experiment for I, our $K_I$ estimates represent conservative estimates of nitrification inhibition. Equation 3 was fit to our data using the nonlinear squares function in the R environment (R Core Team, 2016) and the line of best fit was used for the estimate.

### *3.3.4 Estimation of biological and abiotic rates of sulfide oxidation*

To estimate the relative contribution of abiotic and biotic sulfide oxidation in the batch experiments we applied a model developed by Nielson et al. (2006, 2004) for sewer networks. The model accounts for the effect of pH and temperature on chemical and biological sulfide oxidation. Biological oxidation was best described using a power equation. The authors developed calibration constants from two separate sewer systems. We applied this model along with the parameters they estimated for the dissolved oxygen, temperature, and pH used for our batch experiments.

### *3.3.5 Nucleic acid extractions and qPCR*

DNA and RNA were extracted from biomass collected during batch experiments exposed to three different levels of sulfide: below the inhibition constant for NOB inhibition, between the NOB and AOB inhibition constants, and above the AOB inhibition constant. Nucleic acid extractions were performed using three bead-beading steps followed by extraction with a Maxwell 16 LEV automated nucleic acid extractor (Promega, Madison WI) with the DNA blood and simply RNA tissue kits, respectively. Extractions were performed following manufacturer's instructions with a few modifications. The manufacturer's lysis buffer was replaced with Qiagen lysis buffer (RLT) to increase the buffer volume (600 µL total volume). For the RNA extraction, the DNAse 1 solution volume was doubled to 10 µL to remove contaminating DNA. Total DNA and RNA concentrations in all samples were quantified by Nanodrop (ThermoScientific, Waltham, MA) and verified by Qubit (Invitrogen, Waltham, MA). RNA extracts were treated with a second DNAse step using a DNA-*free*™ DNA removal kit (Ambion, Foster City, CA) to further remove contaminating DNA. Two approaches were used to confirm no DNA contamination of RNA extracts: (i) the absence of amplifiable DNA was confirmed using quantitative polymerase chain reaction (qPCR) of the 16S rRNA gene (methods described in Appendix A) and (ii) Qubit was used to confirm that DNA was below detection limits. Lastly, RNA was reverse transcribed to produce complimentary DNA (cDNA) using the SuperScript™ VILO™ cDNA Synthesis Kit according to the manufacturer's instructions (Life Technologies, Grand Island, NY).

### *3.3.6 qPCR, sequencing, and microbial community analysis*

Bacterial ammonia monooxygenase (*amoA*), 16S rRNA, and *Nitrospira* nitrite oxidoreductase (*nxrB*) genes were quantified from cDNA and DNA using qPCR. Standards for the qPCR reaction were obtained using purified products from PCR reactions for each wastewater treatment plant. Samples and standards were analyzed in triplicate and each qPCR plate had a positive control (DNA extracts from a nitrifying enrichment culture for *amoA* and *nxrB* (Stadler and Love, 2016) or genomic DNA from *Pseudomonas aeruginosa* culture for 16S), and duplicate no-template controls. Details on qPCR standard preparation and qPCR conditions are given in Appendix A-4.

Amplicon sequencing of the V4 region of the 16S rRNA gene was performed with DNA and cDNA using the Illumina MiSeq (MiSeq Reagent Kit V2 500 cycles, Illumina Inc., San Diego, CA) platform and the previously developed Dual-indexing sequencing strategy (Kozich et al., 2013). Twenty µL PCR reactions were performed using the following conditions: 1 µL template, 5 µL primers at a concentration of 4 µM, 0.15 µL AccuPrime HiFi Polymerase, 2 µL AccuPrime PCR Buffer II, 11.85 µL molecular grade water. Illumina sequencing results were analyzed using Mothur (version 1.38.1) following the MiSeq SOP (Kozich et al., 2013; Schloss et al., 2009) with two exceptions: data were rarefied only for ordination analysis and archaea were included in the analysis. In addition to aligning sequences to the SILVA database (release 123), sequences were aligned to a custom 16S rRNA sequence database of known nitrifiers created from the NCBI database using BLAST. The database was created March 14$^{th}$, 2016. This additional step was used to identify nitrifier OTUs that are unclassified or unknown based on the SILVA database. All hits had over 230 base pair alignment lengths, e-values below 4E-115 and bit scores above 405. In addition, hits were compared with the entire non-redundant NCBI database using BLAST to ensure that the nitrifying taxonomic assignment was the best available assignment. From this analysis, no ammonia oxidizing archaea (AOA) were identified in either treatment plant, therefore only AOB are considered.

### *3.3.7 Prediction of precipitates formed*

Precipitation reactions were predicted using the sweep function in Visual Minteq version 3.1 (Gustafsson, 2012). A tableau was created for the media used for the batch cultures and possible

chemical precipitates were identified and include: iron sulfide, molybdenum disulfide, wurtzite, covellite, manganese (II) sulfide, cobalt sulfide, nickel sulfide, acanthite, chalcocite, galena, pyrite, spharelite, chalcopyrite. The species tableau is available in Appendix A, Table A1. Equilibrium was determined across 100 concentrations of $HS^-$ between 0 and 32 mg/L as S.

### *3.3.8 Statistical analysis*

Data analysis was conducted in the R environment (R Core Team, 2016). Statistical comparisons between inhibition model coefficients were done using a two-sided t-test. Differences between copy numbers from qPCR data were tested using Spearman's rank coefficient. To evaluate differences in microbial community structure due to the presence of sulfide, relative abundances of samples were standardized to median sequencing depth across all the samples. Sparse data were removed by pruning OTUs with fewer than 5 reads across all the samples. Following this, sulfide amended cDNA relative abundances were normalized to the average cDNA relative abundance in the sulfide-free controls for each batch experiment. Principal coordinate analysis on the Bray-Curtis similarity matrix was plotted using the phyloseq package in R (McMurdie and Holmes, 2013). Overall changes in the microbial community structure under different sulfide concentrations were tested using permutational MANOVA (999 permutations) based on the Bray-Curtis similarity index using the vegan package in R (Oksanen et al., 2007). Following this exploratory data analysis, a subsequent analysis was conducted using the DESeq2 package (Love et al., 2014; McMurdie and Holmes, 2014). For this analysis, instead of normalizing to the sulfide-free controls or median sequencing depth, 16S rRNA cDNA abundances were normalized using the negative binomial model which accounts for differences in library sizes(McMurdie and Holmes, 2014). The Wald parametric test was used to find significant associations between taxa cDNA abundances and sulfide (Love et al., 2014; McMurdie and Holmes, 2014). The OTUs that were determined to be statistically significant and were unclassified OTUs were compared against the NCBI database; however, more resolution on the taxonomic assignment could not be obtained. All *p*-values given were adjusted for multiple comparisons using the Benjamani Hochberg correction.

## 3.4 Results and Discussion

### *3.4.1 NOB from full-scale treatment systems showed different levels of sulfide inhibition*

Sulfide undergoes many abiotic and biological transformations that can occur very rapidly and the loss of sulfide influences how inhibition is modeled. When applying the model developed by Nielson et al. at minimum and maximum sulfide concentrations (2006, 2004), we found that abiotic (1.2 and 16 mg S/L-hr) and biotic (2.1 and 37 mg S/L-hr) rates of sulfide oxidation are within the same order of magnitude and can thus simultaneously drive sulfide oxidation. Inhibition of nitrification was maintained throughout the experiment even after sulfide was lost (i.e. the slopes of lines were constant, Appendix A, Figures A2 and A3 and Tables A2 and A3). Experimentally determining kinetic rates for reactive inhibitors such as sulfide can be tricky, as inhibition constants are impacted by the startup procedure and how sulfide is defined in the inhibition model. Due to the rapid reactivity and subsequent loss of sulfide, it is important to underscore that the sulfide concentrations used to fit our inhibition model were measured at the beginning of each batch experiment, which captures any immediate losses due to precipitation or aerobic oxidation between adding sulfide and the time zero measurement. Therefore, our estimated inhibition constants are conservative estimates of nitrification inhibition. All previous studies of nitrifier inhibition use the concentrations of sulfide they applied rather than measuring sulfide at time zero, as we did, and therefore do not account for rapid sulfide loss (Bejarano-Ortiz et al., 2015; Bejarano Ortiz et al., 2013; Kouba et al., 2017; Zhou et al., 2014); consequently, these studies tend to overestimate inhibition constants. We conclude that our estimates are reasonable and offer a realistic estimate of relative inhibition differences between AOB and NOB cultures.

Nitrification in both plants was inhibited by sulfide and is characterized in Figure 3-1 based on the initial bulk liquid sulfide concentration present when biomass was first exposed. The range (95% confidence intervals) of $K_I$ estimates across both treatment plants for AOB was between 7.8-14 mg/L as S, while the $K_I$ for NOB was between 2.4-6.7 mg/L as S. The lower $K_I$ value for NOB compared to AOB in both treatment plants ($p_{t\text{-}test}<0.05$) indicates that NOB were more sensitive to sulfide than AOB. Our results are consistent with previous studies that showed NOB to be more sensitive to sulfide than AOB (Erguder et al., 2008). Bejarano-Ortiz et al (2015) found lower inhibition constants (0.22 mg/L as S for NOB and 2.54 mg/L as S for AOB) using biomass from

an enrichment culture. Real wastewater microbial communities may be better adapted to sulfide, resulting in higher sulfide inhibition constants. Another study obtained inhibition parameters almost an order of magnitude higher than the parameters we estimated (10 mg/L as S for NOB and 150 mg/L as S for AOB) (Kouba et al., 2017), perhaps reflecting either a more sulfide-resistant nitrifying community or overestimation due to the use of applied rather than measured sulfide concentrations in their inhibition model. Other studies using lab scale nitrifying cultures (Beristain-Cardoso et al., 2010) or activated sludge (Zhou et al., 2014) have only quantified inhibition of complete nitrification and obtained similar inhibition parameters (10-13 mg S/L) to those we have obtained for AOB. While the extent of inhibition is variable, differential inhibition of AOB and NOB in reactors is consistent across processes with different redox environments and microbial communities. Given the variability in the parameter values, calibration and validation are needed before applying inhibition constants from one community to another community in modeling efforts. Overall, these comparisons show that the response of nitrifying communities to sulfide is community-specific. By pairing the analysis of inhibition with an analysis of the microbial community, we can infer how different nitrifying populations respond to sulfide.

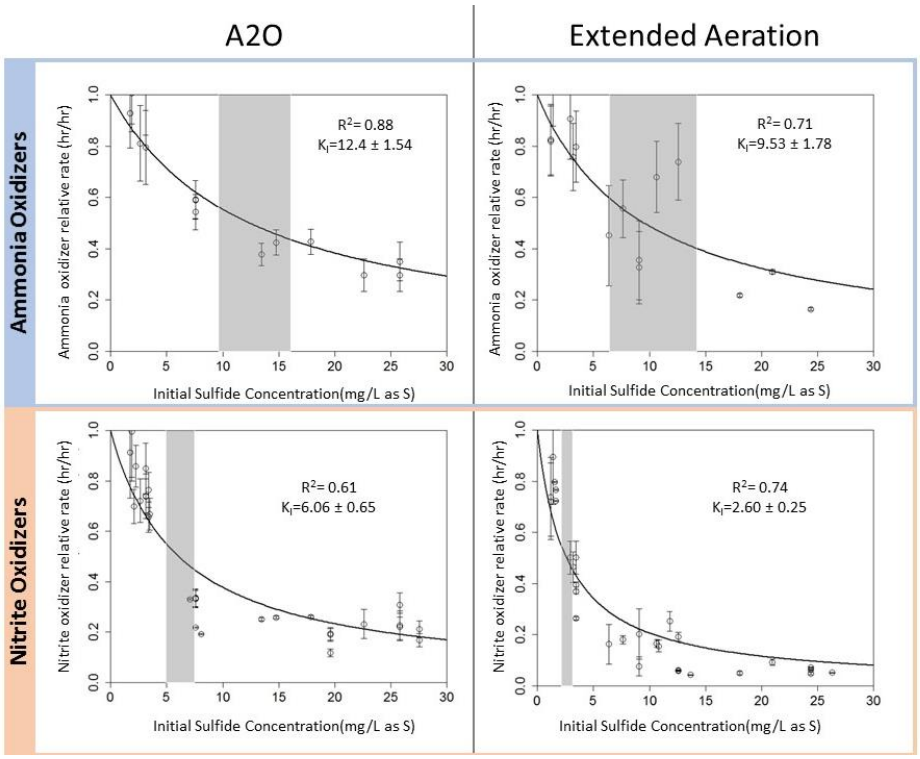


**Figure 3-1.** Rates of nitrification across various sulfide concentrations, normalized to the sulfide-free controls. Each point represents one batch culture. Error bars are the result of normalizing to duplicate sulfide-free control batches. The line represents the best fit for the inhibition model. $K_I$ represents the inhibition constant; the shaded region represents the 95% confidence interval for $K_I$. The rate of ammonium oxidation (as measured the production of nitrite and nitrate) is shown on top. The rates of nitrite oxidation (as measured by nitrate production) are shown on the bottom. The left figures are the results from experiments with biomass from the A2O process and the right figures are the results of experiments with biomass from the extended aeration process.

Understanding the direct and indirect mechanisms of sulfide inhibition can help elucidate whether sulfide inhibition can be harnessed over the long-term. We first consider possible indirect mechanisms of nitrification inhibition such as precipitation of sulfide with trace metals and oxygen deficiencies due to sulfide oxidation. Using equilibrium speciation modeling, we evaluated the possibility that sulfide-induced precipitative loss of trace metals that are enzymatic cofactors for ammonia monooxygenase (copper, zinc, and iron (Gilch et al., 2009; Zahn et al., 1996)) and nitrite oxidoreductase (iron and molybdenum (Meincke et al., 1992)) contributed to the inhibition we observed. In the media used for the batch experiments, the model predicts that ammonia monooxygenase cofactors copper and zinc precipitate at lower sulfide concentrations than the nitrite oxidoreductase cofactor molybdenum (Appendix A, Figure A1). While precipitation did occur and could have contributed to the inhibition patterns observed, our model predictions suggest

that if precipitation was controlling inhibition factor AOB would have been inhibited at lower sulfide concentrations than NOB. Consequently, abiotic precipitation does not appear to be the primary mechanism of differential inhibition between ammonium oxidizers and nitrite oxidizers.

Next, we looked at the oxygen demand that sulfide exerts and asked if it could have limited growth of nitrifying bacteria by causing a deficiency in dissolved oxygen (Appendix A, Table A7). Based on stoichiometric estimates, the oxygen demands of sulfide oxidation are significant. At a maximum, the oxygen diverted to sulfide could have oxidized 2.5 times the total amount of ammonium that was oxidized in the 25 mg S/L for the extended aeration process. On the other hand, nitrite oxidation was more affected by the loss of oxygen; at a maximum, the oxygen diverted to sulfide could have oxidized 8 times the total amount of nitrite that was oxidized in the 15 mg S/L batch for the A2O process. However, this analysis assumes all sulfide was oxidized by oxygen and none precipitated or went to the gas phase. Furthermore, sulfide was oxidized very rapidly (Appendix A, Tables A2 and A3) and therefore, this stochiometric effect should have been short-lived. We did not observe a change in nitrification rate once sulfide was lost, indicating this is probably not the primary inhibition mechanism.

Lastly, we consider direct enzymatic inhibition by quantifying the expression of the ammonia monooxygenase and nitrite oxidoreductase genes using rt-qPCR. We did not observe statistically significant associations between cDNA gene copy numbers and sulfide concentration (Appendix A, Figure A4). The relationship between transcriptional activity and protein abundances is complex and transcriptional activity may not correlate with enzymatic activity (Moran et al., 2013). For example, the inhibitor may change the conformation of the enzyme (Baumann et al., 1997), a mechanism proposed previously for the inhibition of the ammonia monooxygenase enzyme by carbon disulfide and thiourea (Hyman et al., 1990; Wood et al., 1981). An enzyme conformation change could explain why inhibition was maintained after sulfide was no longer detected in the batch reactors; the time to recover from a conformational change may be particularly slow for nitrifiers because of their slow growth rates. While we cannot decipher the exact mechanism of sulfide inhibition, our results support the need for more in-depth (pure culture and proteomic, for example) experiments to further elucidate sulfide-induced inhibition mechanisms between different AOB and NOB taxa.

### *3.4.2 The NOB communities from the two treatment plants had distinct structures.*

The observation that NOB inhibition by sulfide differed among the two full-scale treatment processes ($p_{t\text{-}test}<0.05$), whereas AOB inhibition kinetics were not different ($p_{t\text{-}test}>0.9$), may be due to differences in the composition of the nitrite oxidizing communities between the two plants. Figure 3-2 shows AOB and NOB activity levels in both source biomasses based on cDNA generated from rRNA. It reveals that while transcriptionally active ammonium oxidizers in both plants are dominated by *Nitrosomonas*, the A2O process has more diverse transcriptionally active nitrite oxidizers—and was therefore more functionally redundant with respect to nitrite oxidation—than the extended aeration process. Increased functional redundancy within microbial communities can lead to more resilient communities (Girvan et al., 2005). Our work is consistent with this notion since the culture from the A2O system had greater resistance to sulfide inhibition than the extended aeration process ($K_{I,\,NOB}^{A2O} > K_{I,\,NOB}^{EA}$). While enhanced microbial diversity in wastewater treatment plants has been explored as a strategy to improve process performance (Johnson et al., 2014), our results suggest that increasing diversity of NOB may have undesirable effects on nitritation systems.

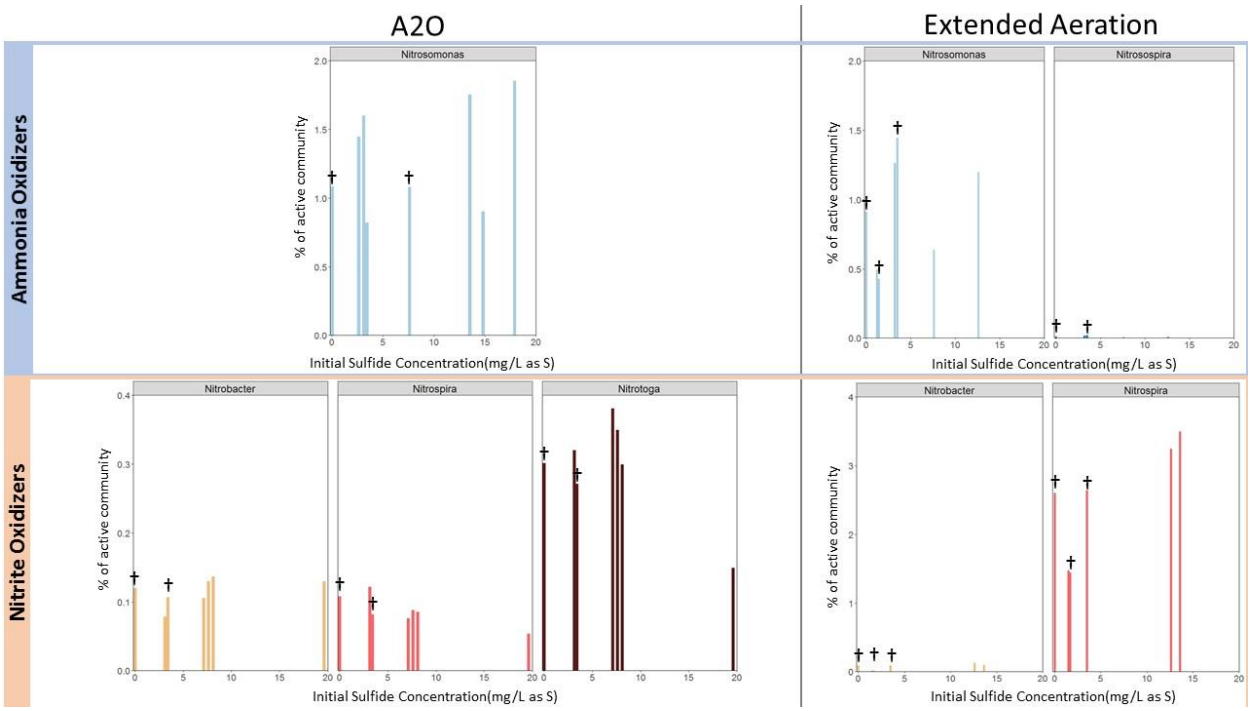


**Figure 3-2.** Relative activity of nitrifying communities based on a sequencing the cDNA from 16S rRNA. The % of active community was calculated relative abundance in the cDNA sequencing data. Results are presented for ammonium oxidizers in ammonium-amended batches (top) and nitrite oxidizers in nitrite-amended batches (bottom) from A2O (left) and extended aeration (right) cultures. A cross symbol indicates that averages of relative abundance in multiple samples at the same sulfide concentration are shown. Some Nitrospira have the ability to completely oxidize ammonia to nitrate (Daims et al., 2015; van Kessel et al., 2015), but we do not have evidence for whether comammox are present in these treatment plants, and therefore are grouped with NOB.

The more sulfide resistant NOB community in the A2O process may be due to differences in the active NOB populations between the two treatment plants. While both plants reported a history of sulfide-related corrosion in their collection systems, the A2O process has temporal changes in redox conditions that create environments favorable for sustaining sulfide for extended time periods (Zhou et al., 2014), possibly exerting a selective pressure on the nitrite oxidizers in the A2O process. The extended aeration treatment plant is dominated by the NOB family *Nitrospira* that appears to be more sensitive to sulfide than the *Nitrotoga* that dominate the A2O plant, and possibly the *Nitrobacter* NOB also present in the A2O biomass. It is worth noting that some *Nitrospira* species uniquely possess the genetic inventory for sulfur oxidation (Lücker et al., 2013), though no studies have found metabolic evidence for this function. Nitrite oxidation by *Nitrospira* may be inherently more sensitive to inhibitors; Blackburne et al. (2007) found *Nitrospira* to be more sensitive to free ammonia and free nitrous acid than *Nitrobacter*. This difference in inhibition

characteristics between *Nitrospira* and *Nitrobacter* could potentially be explained by the location of the substrate binding unit of the nitrite oxidoreductase enzyme (Nxr) within the cell. In *Nitrospira* the Nxr is periplasmic, while in *Nitrobacter* the Nxr is cytoplasmic; therefore, the cell membrane may protect *Nitrobacter* since the charged $HS^-$ molecule must first enter the cell. This explanation does not hold for *Nitrotoga*, which also has a periplasmic Nxr (Nowka et al., 2015) and dominates the A2O nitrite oxidizer microbial community. Our results suggest that not all NOB are equal with respect to sulfide inhibition. The differing metabolic capacities, physiologies, and ecological niches of NOB leads to different sulfide inhibition characteristics and unraveling these differences between NOB is an important area of future research.

### *3.4.3 Sulfide impacted the activity of non-nitrifying microorganisms within the community.*

Considering inhibition of nitrifying populations without considering the effect of the inhibitor on the overall microbial community may miss important interdependencies between nitrifiers and associated populations. Sulfide is both an energetically favorable electron donor and inhibits some microbial processes; consequently, it can have complex effects on the overall microbial community. While sulfide did not significantly change the composition of the microbial community over the course of the batch tests based on sequencing of 16S rRNA genes (permutational MANOVA on Bray-Curtis similarity, $p>0.07$, $R^2<0.05$, Appendix A, Figure A5), the active microbial community based on sequencing of 16S rRNA cDNA shifted due to sulfide (Appendix A, Figure A6). The active microbial communities had statistically significant correlations with sulfide concentration based on the permutational MANOVA on the Bray Curtis dissimilarity matrix ($p=0.001$, $R^2=0.12$, stratified by the wastewater treatment plant). The small effect size ($R^2$) indicates that only a small proportion of the OTUs in the studied communities were affected by the initial sulfide concentration.

Since we found that sulfide affects microbial community activity (16S rRNA) and not composition (16S rRNA gene) over the time scales of these experiments, we focused on the cDNA data to evaluate which OTUs were associated with sulfide. Using the DESeq2 package, we found 55 OTUs with normalized cDNA abundances that statistically significantly correlated with initial sulfide concentration (Wald test, $p<0.05$). The changes in relative activity of these OTUs due to

sulfide are shown in Figure 3-3. Interestingly, despite a loss of nitrifying activity, none of the nitrifying OTUs had statistically significant associations between 16S rRNA relative activity and sulfide and are, therefore, absent from Figure 3-3 (based on both Spearmans rank and Wald test, $p>0.05$). A lack of association between 16S rRNA and activity has previously been observed in pure cultures of AOB under stressed conditions (Bollmann et al., 2005; Chandran and Love, 2008) but we know of no similar studies with NOB. The lack of association between the expression of the ammonia monooxygenase and nitrite oxidoreductase genes observed in this study is an independent measurement that is consistent with the absence of nitrifying OTUs in Figure 3-3. In contrast, many OTUs that were positively associated with sulfide have been implicated in sulfur cycling such as *Desulfonema* and *Desulfovibrio*. Members of the *Desulfovibrio* family have also been shown to oxidize sulfide (Fuseler et al., 1996) and have been implicated in sulfide oxidation using dissimilatory nitrate and nitrite reduction to ammonium (DNRA) (Thorup and Schramm, 2017). Similarly, members of the *Planctomycetacaea* family are involved in sulfur cycling (Elshahed et al., 2007). The *Rhodocyclacaea* OTU with a positive association with initial sulfide concentration was categorized at the genus level to be *Dechloromonas*, which also may contain sulfur oxidation genes (Salinero et al., 2009). Many more statistically significantly associated OTUs ($p_{Wald}<0.05$) were negatively associated (48 OTUs) with initial sulfide concentration than were positively associated (7 OTUs), suggesting sulfide inhibition. The changes in activity we observed indicate that sulfide induced microbial community shifts; however, there is additional research to be done on the relationship, if any, between the community shifts and nitrification inhibition.

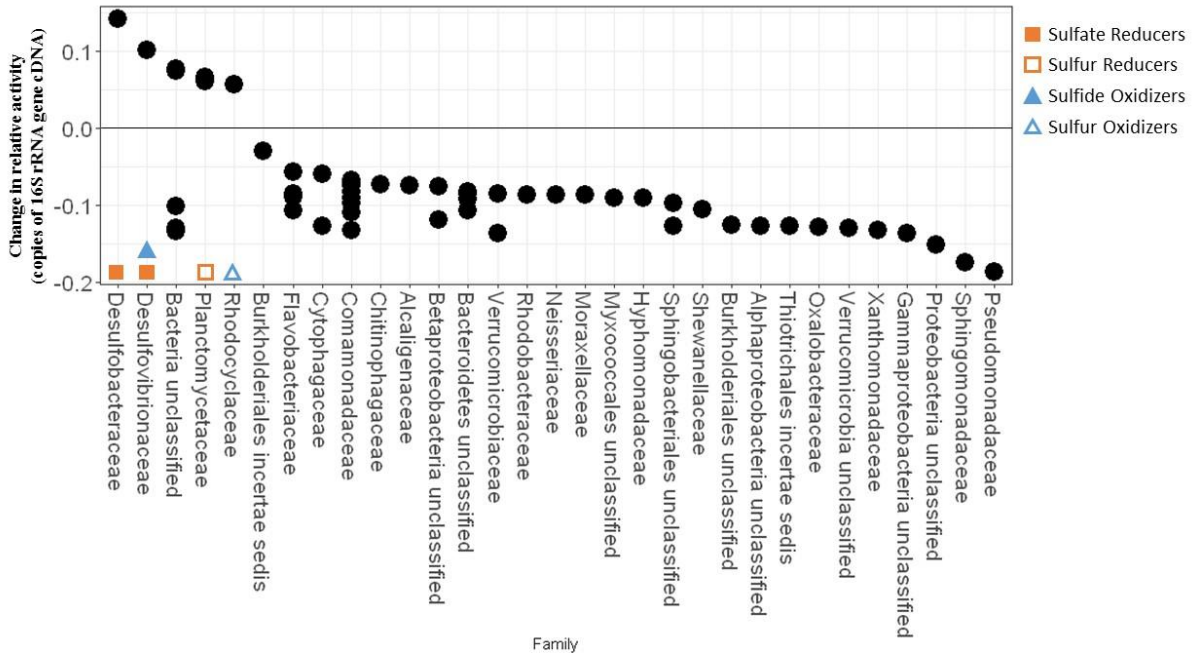


**Figure 3-3.** Sulfide sensitive OTUs (p-Wald<0.05, adjusted for multiple comparisons using Benjamani Hochberg correction). Y-axis indicates the log base 2 fold change in OTU normalized activity (16S rRNA gene in cDNA) for a 1 mg/L as S increase in sulfide concentration. Symbols next to name indicates known functions that exist within the Family or Genera (based on best classification).

## 3.5 Summary and Potential Applications

As the population in coastal cities increases and nitrogen regulations become more stringent, innovations that lead to more energy efficient nitrogen management will be increasingly valuable. Sulfide in wastewater can be harnessed to implement nitritation processes via the differential inhibition of AOB and NOB. Existing treatment processes that use varying redox environments including anoxic and anaerobic zones, or that maintain low DO conditions, will also support environments where nitrifiers could be inhibited by sulfide. Mainstream nitritation due to sulfide could also be supported in emerging technologies such as the SANI process, mainstream anammox, or mainstream anaerobic processes (McCarty et al., 2011) that are known to produce variable and sometimes high concentrations of sulfide (Delgado Vela et al., 2015). Additionally, amid water stress, more densely populated coastal communities may consider seawater toilet flushing and harnessing sulfide during wastewater treatment (Liu et al., 2016). As nitrogen regulations become more stringent and energy conservation in wastewater treatment systems

becomes a priority, sulfide may help reduce energy requirements of nitrogen removal by suppressing NOB and supporting shortcut nitrogen removal technologies. Future research is needed to understand if nitritation can be maintained in a continuously fed system since long-term feeding of sulfide could lead to both physiological adaptation or selection for sulfide-resistant nitrifying populations.

We showed that applying sulfide for the support of NOB suppression requires knowledge of the underlying nitrite oxidizing community. By linking inhibition parameters to the nitrifying community our results show that a more diverse nitrite oxidizing community is more resistant to sulfide inhibition and that *Nitrospira*-rich communities are more sensitive to sulfide inhibition. Further, we found that sulfide impacts the activity of the microbial community, suggesting that sulfide has impacts on the wastewater treatment processes that have yet to be identified.

### 3.6 Conclusions

- Nitrite oxidizing bacteria are more sensitive to sulfide than ammonia oxidizing microorganisms in the two processes considered.
- Distinct communities of nitrite-oxidizing bacteria showed different responses to sulfide, consistent with *Nitrospira* being more sensitive to sulfide than *Nitrobacter* and *Nitrotoga*.
- Sulfide affects microbial community activity, and many OTUs had lower activities with increased sulfide concentration.

### 3.7 References

Alvarez, M.T., Crespo, C., Mattiasson, B., 2007. Precipitation of Zn(II), Cu(II) and Pb(II) at bench-scale using biogenic hydrogen sulfide from the utilization of volatile fatty acids. Chemosphere 66, 1677–1683. doi:10.1016/j.chemosphere.2006.07.065

Anthonisen, A., Loehr, R., Prakasam, T., Srinath, E., 1976. Inhibition of Nitrification by Ammonia and Nitrous Acid. J. Water Pollut. Control Fed. 48, 835–852. doi:10.1017/CBO9781107415324.004

APHA, AWWA, WEF, 2005. Standard methods for the examination of water and wastewater, 21st ed. Washington D.C.

Baumann, B., Van Der Meer, J.R., Snozzi, M., Zehnder, A.J.B., 1997. Inhibition of denitrification activity but not of mRNA induction in Paracoccus dentrificans by nitrite at a suboptimal pH. Antonie van Leeuwenhoek, Int. J. Gen. Mol. Microbiol. 72, 183–189.

doi:10.1023/A:1000342125891

Bejarano-Ortiz, D.I., Huerta-Ochoa, S., Thalasso, F., Cuervo-López, F. de M., Texier, A.C., 2015. Kinetic Constants for Biological Ammonium and Nitrite Oxidation Processes Under Sulfide Inhibition. Appl. Biochem. Biotechnol. 177, 1665–1675. doi:10.1007/s12010-015-1844-3

Bejarano Ortiz, D.I., Thalasso, F., Cuervo López, F.D.M., Texier, A.C., 2013. Inhibitory effect of sulfide on the nitrifying respiratory process. J. Chem. Technol. Biotechnol. 88, 1344–1349. doi:10.1002/jctb.3982

Beristain-Cardoso, R., Gómez, J., Méndez-Pampín, R., 2010. The behavior of nitrifying sludge in presence of sulfur compounds using a floating biofilm reactor. Bioresour. Technol. 101, 8593–8598. doi:10.1016/j.biortech.2010.06.084

Blackburne, R., Vadivelu, V.M., Yuan, Z., Keller, J., 2007. Kinetic characterisation of an enriched Nitrospira culture with comparison to Nitrobacter. Water Res. 41, 3033–42. doi:10.1016/j.watres.2007.01.043

Blackburne, R., Yuan, Z., Keller, J., 2008. Partial nitrification to nitrite using low dissolved oxygen concentration as the main selection factor. Biodegradation 19, 303–312. doi:10.1007/s10532-007-9136-4

Bollmann, A., Schmidt, I., Saunders, A.M., Nicolaisen, M.H., 2005. Influence of starvation on potential ammonia-oxidizing actvity and amoA mRNA levels in Nitrospira briensis. Appl. Environ. Microbiol. 71, 1276–1282. doi:10.1128/AEM.71.3.1276-1282.2005

Burton, F.L., Stensel, H.D., Tchobanoglous, G., 2014. Wastewater engineering: treatment and resource recovery. McGraw-Hill.

Canfield, D.E., Stewart, F.J., Thamdrup, B., Brabandere, L. De, Delong, E.F., Revsbech, N.P., Ulloa, O., De Brabandere, L., Dalsgaard, T., Delong, E.F., Revsbech, N.P., Ulloa, O., Brabandere, L. De, Delong, E.F., Revsbech, N.P., Ulloa, O., 2010. A cryptic sulfur cycle in oxygen-minimum-zone waters off the Chilean coast. Science 330, 1375–1378. doi:10.1126/science.1196889

Chandran, K., Love, N.G., 2008. Physiological state, growth mode, and oxidative stress play a role in Cd(II)-Mediated inhibition of Nitrosomonas europaea 19718. Appl. Environ. Microbiol. 74, 2447–2453. doi:10.1128/AEM.01940-07

Daims, H., Lebedeva, E. V., Pjevac, P., Han, P., Herbold, C., Albertsen, M., Jehmlich, N., Palatinszky, M., Vierheilig, J., Bulaev, A., Kirkegaard, R.H., Bergen, M. von, Rattei, T., Bendinger, B., Nielsen, P.H., Wagner, M., 2015. Complete nitrification by Nitrospira bacteria. Nature. doi:10.1038/nature16461

Delgado Vela, J., Stadler, L.B., Martin, K.J., Raskin, L., Bott, C., Love, N.G., 2015. Prospects for Biological Nitrogen Removal from Anaerobic Effluents during Mainstream Wastewater Treatment. Environ. Sci. Technol. Lett. 2, 233–244. doi:10.1021/acs.estlett.5b00191

Elshahed, M.S., Youssef, N.H., Luo, Q., Najar, F.Z., Roe, B.A., Sisk, T.M., Bühring, S.I., Hinrichs, K.U., Krumholz, L.R., 2007. Phylogenetic and metabolic diversity of

Planctomycetes from anaerobic, sulfide- and sulfur-rich Zodletone Spring, Oklahoma. Appl. Environ. Microbiol. 73, 4707–4716. doi:10.1128/AEM.00591-07

Erguder, T.H., Boon, N., Vlaeminck, S.E., Verstraete, W., 2008. Partial nitrification achieved by pulse sulfide doses in a sequential batch reactor. Environ. Sci. Technol. 42, 8715–8720. doi:10.1021/es801391u

Fuseler, K., Krekeler, D., Sydow, U., Cypionka, H., 1996. A common pathway of sulfide oxidation by sulfate-reducing bacteria.

Gilbert, E.M., Agrawal, S., Brunner, F.C., Schwartz, T., Horn, H., Lackner, S., 2014. Response of different Nitrospira sp. to anoxic periods depends on operational DO. Environ. Sci. Technol. doi:10.1021/es404992g

Gilch, S., Meyer, O., Schmidt, I., 2009. A soluble form of ammonia monooxygenase in Nitrosomonas europaea. Biol. Chem. 390, 863–873. doi:10.1515/BC.2009.085

Girvan, M.S., Campbell, C.D., Killham, K., Prosser, J.I., Glover, L.A., 2005. Bacterial diversity promotes community stability and functional resilience after perturbation. Environ. Microbiol. 7, 301–313. doi:10.1111/j.1462-2920.2004.00695.x

Gustafsson, J.P., 2012. Visual Minteq, a free equilibrium speciation model. KTH, Dep. L. Water Resour. Eng.

Hyman, M.R., Kim, C.Y., Arp, D.J., 1990. Inhibition of ammonia monooxygenase in Nitrosomonas europaea by carbon disulfide. J. Bacteriol. 172, 4775–5782.

Isa, Z., Grusenmeyer, S., Verstraete, W., 1986. Sulfate Reduction Relative to Metane Production in High-Rate Anaerobic Digestion: Technical Aspects. Appl. Environ. Microbiol. 51, 572–579.

Johnson, D.R., Lee, T.K., Park, J., Fenner, K., Helbling, D.E., 2014. The functional and taxonomic richness of wastewater treatment plant microbial communities are associated with each other and with ambient nitrogen and carbon availability. Environ. Microbiol. 17, 1–34. doi:10.1111/1462-2920.12429

Kouba, V., Proksova, E., Wiesinger, H., Vejmelkova, D., Bartacek, J., 2017. Good servant, bad master: sulfide and dissolved methane influence on partial nitritation of sewage. Water Sci. Technol. wst2017490. doi:10.2166/wst.2017.490

Kozich, J.J., Westcott, S.L., Baxter, N.T., Highlander, S.K., Schloss, P.D., 2013. Development of a Dual-Index Sequencing Strategy and Curation Pipeline for Analyzing Amplicon Sequence Data on the MiSeq Illumina Sequencing Platform. Appl. Environ. Microbiol. 79, 5112–5120. doi:10.1128/AEM.01043-13

Liu, X., Dai, J., Wu, D., Jiang, F., Chen, G., Chui, H.K., van Loosdrecht, M.C.M., 2016. Sustainable Application of a Novel Water Cycle Using Seawater for Toilet Flushing. Engineering 2, 460–469. doi:10.1016/J.ENG.2016.04.013

Love, M.I., Huber, W., Anders, S., 2014. Moderated estimation of fold change and dispersion for

RNA-seq data with DESeq2. Genome Biol. 15, 550. doi:10.1186/s13059-014-0550-8

Lu, H., Ekama, G.A., Wu, D., Feng, J., van Loosdrecht, M.C.M., Chen, G.H., 2012. SANI ?? process realizes sustainable saline sewage treatment: Steady state model-based evaluation of the pilot-scale trial of the process. Water Res. 46, 475–490. doi:10.1016/j.watres.2011.11.031

Lücker, S., Nowka, B., Rattei, T., Spieck, E., Daims, H., 2013. The genome of Nitrospina gracilis illuminates the metabolism and evolution of the major marine nitrite oxidizer. Front. Microbiol. 4, 1–19. doi:10.3389/fmicb.2013.00027

McCarty, P.L., Bae, J., Kim, J., 2011. Domestic wastewater treatment as a net energy producer--can this be achieved? Environ. Sci. Technol. 45, 7100–6. doi:10.1021/es2014264

McMurdie, P.J., Holmes, S., 2014. Waste Not, Want Not: Why Rarefying Microbiome Data Is Inadmissible. PLoS Comput. Biol. 10. doi:10.1371/journal.pcbi.1003531

McMurdie, P.J., Holmes, S., 2013. phyloseq: An R package for reproducible interactive analysis and graphics of microbiome census data. PLoS One 8, e61217.

Meincke, M., Bock, E., Kastrau, D., Kroneck, P.M.H., 1992. Nitrite oxidoreductase from Nitrobacter hamburgensis: Redox centers and their catalytic role. Arch. Microbiol. 158, 127–131. doi:10.1007/BF00245215

Moran, M.A., Satinsky, B., Gifford, S.M., Luo, H., Rivers, A., Chan, L.K., Meng, J., Durham, B.P., Shen, C., Varaljay, V.A., Smith, C.B., Yager, P.L., Hopkinson, B.M., 2013. Sizing up metatranscriptomics. ISME J. 7, 237–243. doi:10.1038/ismej.2012.94

Nielsen, A.H., Vollertsen, J., Hvitved-jacobsen, T., 2006. Kinetics and Stoichiometry of Aerobic Sulfide Oxidation in Wastewater from Sewers — Effects of pH and Temperature. Water Environ. Res. 78, 275–283.

Nielsen, A.H., Vollertsen, J., Hvitved-Jacobsen, T., 2004. Chemical sulfide oxidation of wastewater - Effects of pH and temperature. Water Sci. Technol. 50, 185–192.

Nowka, B., Daims, H., Spieck, E., 2015. Comparative oxidation kinetics of nitrite-oxidizing bacteria: nitrite availability as key factor for niche differentiation. Appl. Environ. Microbiol. 81, 745–753. doi:10.1128/AEM.02734-14

Oksanen, J., Kindt, R., Legendre, P., O'Hara, B., Stevens, M.H.H., Oksanen, M.J., Suggests, M., 2007. The vegan package. Community Ecol. Packag. 631–637.

R Core Team, 2016. R: A Language and Environment for Statistical Computing.

Regmi, P., Miller, M.W., Holgate, B., Bunce, R., Park, H., Chandran, K., Wett, B., Murthy, S., Bott, C.B., 2014. Control of aeration, aerobic SRT and COD input for mainstream nitritation/denitritation. Water Res. 57, 162–71. doi:10.1016/j.watres.2014.03.035

Rosso, D., Larson, L.E., Stenstrom, M.K., 2008. Aeration of large-scale municipal wastewater treatment plants: state of the art. Water Sci. Technol. 57, 973–978.

Sabba, F., Devries, A., Vera, M., Druschel, G., Bott, C., Nerenberg, R., 2016. Potential use of

sulfite as a supplemental electron donor for wastewater denitrification. Rev. Environ. Sci. Bio/Technology 15, 563–572. doi:10.1007/s11157-016-9413-y

Salinero, K.K., Keller, K., Feil, W.S., Feil, H., Trong, S., Di Bartolo, G., Lapidus, A., 2009. Metabolic analysis of the soil microbe Dechloromonas aromatica str. RCB: indications of a surprisingly complex life-style and cryptic anaerobic pathways for aromatic degradation. BMC Genomics 10, 351. doi:10.1186/1471-2164-10-351

Schloss, P.D., Westcott, S.L., Ryabin, T., Hall, J.R., Hartmann, M., Hollister, E.B., Lesniewski, R. a., Oakley, B.B., Parks, D.H., Robinson, C.J., Sahl, J.W., Stres, B., Thallinger, G.G., Van Horn, D.J., Weber, C.F., 2009. Introducing mothur: Open-source, platform-independent, community-supported software for describing and comparing microbial communities. Appl. Environ. Microbiol. 75, 7537–7541. doi:10.1128/AEM.01541-09

Shannon, J.M., Hauser, L.W., Liu, X., Parkin, G.F., Mattes, T.E., Just, C.L., 2015. Partial nitritation ANAMMOX in submerged attached growth bioreactors with smart aeration at 20 °C. Environ. Sci. Process. Impacts 17, 81–9. doi:10.1039/c4em00481g

Stadler, L.B., Love, N.G., 2016. Impact of microbial physiology and microbial community structure on pharmaceutical fate driven by dissolved oxygen concentration in nitrifying bioreactors. Water Res. 104, 189–199.

Suleimenov, O.M., Krupp, R.E., 1994. Solubility of hydrogen sulfide in pure water and in NaCl solutions, from 20 to 320°C and at saturation pressures. Geochim. Cosmochim. Acta 58, 2433–2444. doi:10.1016/0016-7037(94)90022-1

Thorup, C., Schramm, A., 2017. Disguised as a Sulfate Reducer: Growth of the Deltaproteobacterium Desulfurivibrio alkaliphilus by Sulfide Oxidation with Nitrate. MBio 8, 1–9.

Vadivelu, V.M., Yuan, Z., Fux, C., Keller, J., 2006. The Inhibitory Effects of Free Nitrous Acid on the Energy Generation and Growth Processes of an Enriched Nitrobacter Culture. Environ. Sci. Technol. 40.

van Kessel, M. a. H.J., Speth, D.R., Albertsen, M., Nielsen, P.H., Op den Camp, H.J.M., Kartal, B., Jetten, M.S.M., Lücker, S., 2015. Complete nitrification by a single microorganism. Nature 1–17. doi:10.1038/nature16459

Villaverde, S., García-Encina, P. a., Fdz-Polanco, F., 1997. Influence of pH over nitrifying biofilm activity in submerged biofilters. Water Res. 31, 1180–1186. doi:10.1016/S0043-1354(96)00376-4

Wang, J., Lu, H., Chen, G.H., Lau, G.N., Tsang, W.L., van Loosdrecht, M.C.M., 2009. A novel sulfate reduction, autotrophic denitrification, nitrification integrated (SANI) process for saline wastewater treatment. Water Res. 43, 2363–2372. doi:10.1016/j.watres.2009.02.037

Wood, L.B., Hurley, B.J.E., Matthews, P.J., 1981. Some observations on the biochemistry and inhibition of nitrification. Water Res. 15, 543–551. doi:10.1016/0043-1354(81)90017-8

Wu, D., Ekama, G.A., Chui, H.K., Wang, B., Cui, Y.X., Hao, T.W., van Loosdrecht, M.C.M.,

Chen, G.H., 2016. Large-scale demonstration of the sulfate reduction autotrophic denitrification nitrification integrated (SANI®) process in saline sewage treatment. Water Res. 100, 496–507. doi:10.1016/j.watres.2016.05.052

Yang, W., Zhao, Q., Lu, H., Ding, Z., Meng, L., Chen, G.-H., 2016. Sulfide-driven autotrophic denitrification significantly reduces N2O emissions. Water Res. 90, 176–184. doi:10.1016/j.watres.2015.12.032

Zahn, J.A., Arciero, D.M., Hooper, A.B., DiSpirito, A.A., 1996. Evidence for an iron center in the ammonia monooxygenase from Nitrosomonas europaea. FEBS Lett. 397, 35–38. doi:10.1016/S0014-5793(96)01116-7

Zhang, L., De Schryver, P., De Gusseme, B., De Muynck, W., Boon, N., Verstraete, W., 2008. Chemical and biological technologies for hydrogen sulfide emission control in sewer systems: A review. Water Res. 42, 1–12. doi:10.1016/j.watres.2007.07.013

Zhou, Z., Xing, C., An, Y., Hu, D., Qiao, W., Wang, L., 2014. Inhibitory effects of sulfide on nitrifying biomass in the anaerobic-anoxic-aerobic wastewater treatment process. J. Chem. Technol. Biotechnol. 89, 214–219. doi:10.1002/jctb.4104

# CHAPTER 4.

## SULFIDE CHANGES MICROBIAL INTERACTIONS IN A NITROGEN CYCLING BIOFILM REACTOR

Jeseth Delgado Vela[1], Laura Bristow[2], Hannah Marchant[3], Nancy Love[1], Greg Dick[4]

[1]Department of Civil and Environmental Engineering, University of Michigan
[2]Department of Biology, University of Southern Denmark
[3]Department of Biogeochemistry, Max Planck Institute for Marine Microbiology
[4]Department of Earth and Environmental Sciences, University of Michigan

### 4.1 Summary

Microbial cross-feeding leads to complex and interconnected elemental cycling but we need an improved understanding of how cross-feeding influences overall community function and how changes in substrates perturb these relationships. Here, we used a membrane aerated biofilm reactor that was fed methane, sulfide, and ammonium to study potential cross-feeding relationships. Results from isotopic rate measurements and metagenomic sequencing showed that sulfide (i) could inhibit nitrite oxidizing bacteria (NOB) but did not affect ammonium oxidation rates and (ii) induced dissimilatory nitrite reduction to ammonium (DNRA) in the bioreactor. When nitrite oxidation was inhibited, more nitrite is available for DNRA, anammox, and nitrite-dependent anaerobic methane oxidation. Recovery and analysis of a near complete genome sequence related to the nitrite-dependent anaerobic methane oxidizer *Candidatus* Methylomirabilis confirmed that a nitrite source was needed for this organism to grow. It appears that sulfide disrupted microbial cross-feeding between AOB and NOB but induced cross-feeding between AOB and nitrite reducing organisms. The results indicate that DNRA may occur and produce ammonium in engineered systems that use sulfide as an electron donor, which is generally not desirable and would need to be controlled.

## 4.2 Introduction

Although essential to cellular life, nitrogen can contaminate natural water bodies and contribute to global warming. Microbial processes control the nitrogen cycle; hence, regulating microbial activity can help mitigate environmental pollution. Understanding coupled biogeochemical cycling of nitrogen, sulfur, and carbon is complex due to the metabolic flexibility of the bacteria that cycle these substrates, but new molecular and cultivation techniques have spurred rapid discovery in this area (Kuypers et al., 2018). For instance, marine nitrite oxidizing bacteria have been shown to oxidize sulfide (Füssel et al., 2017), anammox bacteria can oxidize organic matter (Kartal et al., 2007), and sulfate reducing bacteria can also denitrify (Thorup and Schramm, 2017). This metabolic flexibility means that taxonomic markers such as the 16S rRNA gene are insufficient to determine the key players in the sulfur, nitrogen, and carbon cycles. Higher resolution methods are needed because understanding microbial interactions within these elemental cycles which is important in both environmental (Arshad et al., 2017) and engineered systems (Delgado Vela et al., 2015b).

Few studies have evaluated the interactions between microbial cycling of methane, nitrogen, and sulfur in mixed redox environments. A study in an anoxic bioreactor that considered methane, sulfide, and nitrate in one system revealed the co-existence and beneficial cross-feeding relationship between anammox, sulfide oxidizers, and denitrifying anaerobic methane oxidizers (Arshad et al., 2017). The presence of anammox in a system fed sulfide is somewhat surprising because sulfide is typically thought to inhibit anammox bacteria (Jin et al., 2013). However, this is consistent with previous studies and the evidence suggests that anammox can grow in the presence of sulfide because sulfide-based denitrifiers consume the inhibitory sulfide and reduce the nitrate produced by anammox to either nitrite (Rios-Del Toro and Cervantes, 2016; Russ et al., 2014) or ammonia (Jones et al., 2017). Once oxic environments are introduced, the growth of aerobic bacteria such as nitrifiers, methanotrophs, and sulfur oxidizers introduces additional possible cross-feeding relationships. Coupled oxic and anoxic environments are abundant in natural (e.g. Bristow et al., 2016; Lüke et al., 2016; Reim et al., 2012) and engineered (e.g. Morgenroth et al., 1997; Pochana and Keller, 1999) environments and we need to understand how

the microbial interactions in these systems shape elemental cycling and how interactions change under different substrate conditions.

Since it is possible to precisely create and control oxic and anoxic environments, bioreactor systems are advantageous for understanding microbial interactions between nitrifying and denitrifying organisms. Controlled experiments that create distinct environments in lab-scale bioreactors can be used to develop and test hypotheses on the microbial interactions that may occur between different metabolic groups. For example, a membrane aerated biofilm reactor (MABR) uses oxygen-permeable membranes to produce a counter-current biofilm where the flux of dissolved oxygen (from the membrane) moves in the opposite direction to the flow of electron donor (from the bulk liquid) (Martin and Nerenberg, 2012; Terada et al., 2007). Consequently, an MABR provides a unique redox environment to study nitrogen and sulfur cycling because redox can dictate microbial population selection and consequently control nitrogen and sulfur speciation. An added benefit of using the MABR to study microbial interactions is that due to its energy efficiency it is a technology increasingly being considered for full-scale wastewater treatment (Heffernan et al., 2017; Houweling et al., 2017; Peeters et al., 2017). Therefore, understanding how microbes interact in this system can inform bioreactor design to improve nitrogen removal in an emerging technology.

In this study we operated a lab-scale MABR and applied metagenomic and isotope labeling techniques to evaluate interactions between microbial populations. We evaluated how hydrogen sulfide changes rates of oxidation over short-term batch experiments and how sulfide shifts the microbial community functional potential over long-term stepwise increases in sulfide concentrations. During treatment of synthetic anaerobic effluents containing dissolved methane, sulfide, and ammonia, simultaneous oxic and anoxic cycling of nitrogen, sulfur, and carbon occurred. We found that differential sulfide inhibition of ammonia oxidizing bacteria (AOB) and nitrite oxidizing bacteria (NOB) can provide a nitrite source for other metabolisms including anammox, denitrifying anaerobic methane oxidizers, and denitrifying sulfur oxidizers. We also found that an important sink for nitrite in the presence of sulfide was the dissimilatory nitrite reduction to ammonia. These findings can help us understand interactions between sulfur and

nitrogen cycling in engineered environments to ultimately improve the efficiency of nitrogen removal.

## 4.3 Results and Discussion

### *4.3.1 Sulfide increased nitrite accumulation and nitrite reduction to ammonia.*

We conducted rate experiments to reveal the functional potential in the reactor. Experiments with heavy nitrogen ($^{15}N$) were used to obtain rates of ammonia oxidation, nitrite oxidation, nitrate reduction and dissimilatory nitrite/nitrate reduction to ammonia (DNRA). Results show that with the exception of nitrite oxidation, all processes were faster in the presence of sulfide (Figure 4-1).

Experiments in the reduction of nitrate and nitrite showed that DNRA was an important process. DNRA occurred when sulfide and nitrite were in the influent (161 ± 30 µmol/L-hr with sulfide; 0.2±0.7 µmol/L-hr without sulfide, $p_{t\text{-}test}$=0.02, Figure 4-1D). During experiments with $^{15}NO_3^-$ in the influent there was little measurable ammonium produced (Appendix B Figure B4) regardless of the presence of sulfide. This could be because ammonium produced was very rapidly consumed by AOB or because DNRA only occurred with nitrite as the electron acceptor. In both cases DNRA was only measurable when sulfide was present in the influent. The rate of nitrate reduction to nitrite was faster in the presence of sulfide (175 ± 35 µmol/L-hr with sulfide 127±9 µmol/L-hr without sulfide, Figure 4-1C and Appendix B Figure B4). However, the rate of DNRA when sulfide and nitrite were present was comparable to the rate of nitrate reduction. This indicates that DNRA has the potential to be an important and significant process in this system.

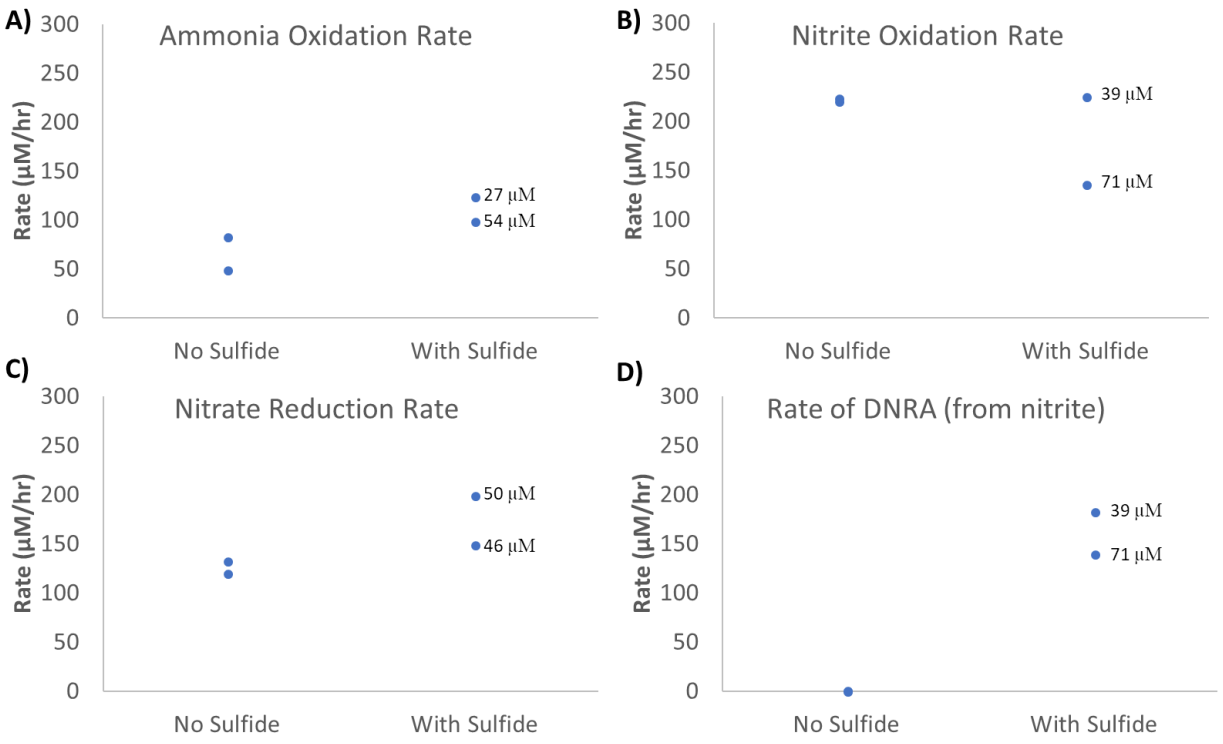


**Figure 4-1.** Rates derived from $^{15}N$ experiments. Concentrations next to rates with sulfide indicate the concentration of sulfide in time zero sample. Average $R^2$ from the linear estimate was 0.96 ± 0.05.

Experiment C revealed that nitrite oxidation was generally very fast, but when sulfide was present in the influent nitrite oxidation rates were slower (181 ± 63 µmol/L-hr with sulfide and 223 ± 3 µmol/L-hr Figure 4-1B). Consistent with previous studies (Bejarano-Ortiz et al., 2015; Delgado Vela et al., 2018; Erguder et al., 2008), NOB were inhibited by sulfide. As shown in Figure 4-1B at the lower initial concentration of sulfide, differences in the nitrite oxidation rate were not discernable. These results are consistent with the inhibition index determined in Chapter 3 for a *Nitrospira*-dominated NOB population (81 ± 8 µM) (Delgado Vela et al., 2018). It is also worth noting that the concentrations listed were the concentrations in the time zero sample. However rapid sulfide oxidation was occurring during the filling of the reactor; therefore, these concentrations are likely underestimates of the true-initial concentrations in the reactor. Despite the uncertainty in the initial sulfide exposure, it is clear that inhibition of NOB with sulfide in this multi-redox bioreactor was possible.

In contrast to nitrite oxidation, rates of ammonia oxidation were higher in the presence of sulfide (111 ± 18 μmol/L-hr) compared to without sulfide (66 ± 24 μmol/L-hr). This indicates that unlike batch systems (Bejarano-Ortiz et al., 2015; Delgado Vela et al., 2018), ammonia oxidation was not affected by sulfide in a continuously fed MABR. However, these initial concentrations are significantly lower than those previously determined inhibition constants for AOB (298-388 μM) (Delgado Vela et al., 2018) therefore at higher initial concentrations of sulfide inhibition of AOB may still be an important process to consider. An important consideration for comparing previously determined inhibition constants to these experiments is that, unlike the batch experiments from Chapter 3, anaerobic metabolisms are present in the bioreactor and can consume nitrite. Interestingly, in the presence of sulfide the rates of DNRA are faster than the rates of ammonia oxidation. Sulfide has been shown to increase DNRA in both natural (Brunet and Garcia-Gil, 1996; Jones et al., 2017) and engineered systems (Dolejs et al., 2014; Yin et al., 2015). Hydrogen sulfide acts as a reducing agent, and electron-rich environments are more prone to DNRA (Van Den Berg et al., 2015). In studies published to date, it is unclear whether the organisms responsible for DNRA are using sulfide as an electron donor. In this study, the rate of DNRA was faster in the bioreactor with the lower initial sulfide concentration, however there were no organic compounds in the influent that are typically thought to be involved in DNRA present in the reactor (e.g. acetate). The only other electron donor that was present in the reactor was methane, which is not a known electron donor for DNRA. This suggests that sulfide may have been the electron donor for DNRA during these experiments.

From a treatment standpoint, it is more desirable to reduce nitrite to nitrogen gas instead of ammonia. Previous literature says that at higher sulfide/N ratios, nitrate gets reduced to ammonia, while at lower sulfide/N ratios denitrification occurs (Dolejs et al., 2014; Yin et al., 2015). Future work should assess the operating conditions that would limit DNRA and induce denitrification, which is preferential for meeting wastewater treatment goals. Our results underscore the importance of considering DNRA when describing sulfur-nitrogen interactions and their effect on overall community function and reactor performance.

### *4.3.2 Metabolic functions were partitioned between planktonic and biofilm communities.*

To further explore mechanisms by which sulfide affects nitrogen cycling, we evaluated the long-term effect of stepwise increases in sulfide on the microbial community present in different reactor compartments using metagenomic sequencing. The change in relative abundance of genes of key metabolic processes over time and space in the reactor (Figure 4-2) showed a division of labor between physical compartments of the reactor; sulfur oxidation and denitrification (except for denitrifying anaerobic methane oxidizers and anammox denitrifiers) were concentrated in the planktonic portion of the reactor while nitrification was concentrated in the biofilm. The planktonic growth was not present until sulfide was added to the influent. Since there were no electron acceptors other than nitrate available in the bulk liquid, the sulfide oxidizers present in the planktonic phase were likely associated with nitrate-linked denitrification processes. Consistent with this inference, the majority of the planktonic denitrifying genes had top hits to NCBI's nonredundant database with taxonomy that matched that of the top hits of the sulfur oxidation genes (Appendix B, Figure B5). This analysis suggests that a majority of planktonic denitrification and sulfur oxidation potential were from the genus *Thiobacillus*. Collectively, these results show that MABRs can provide an environment for sulfide-based denitrifiers.

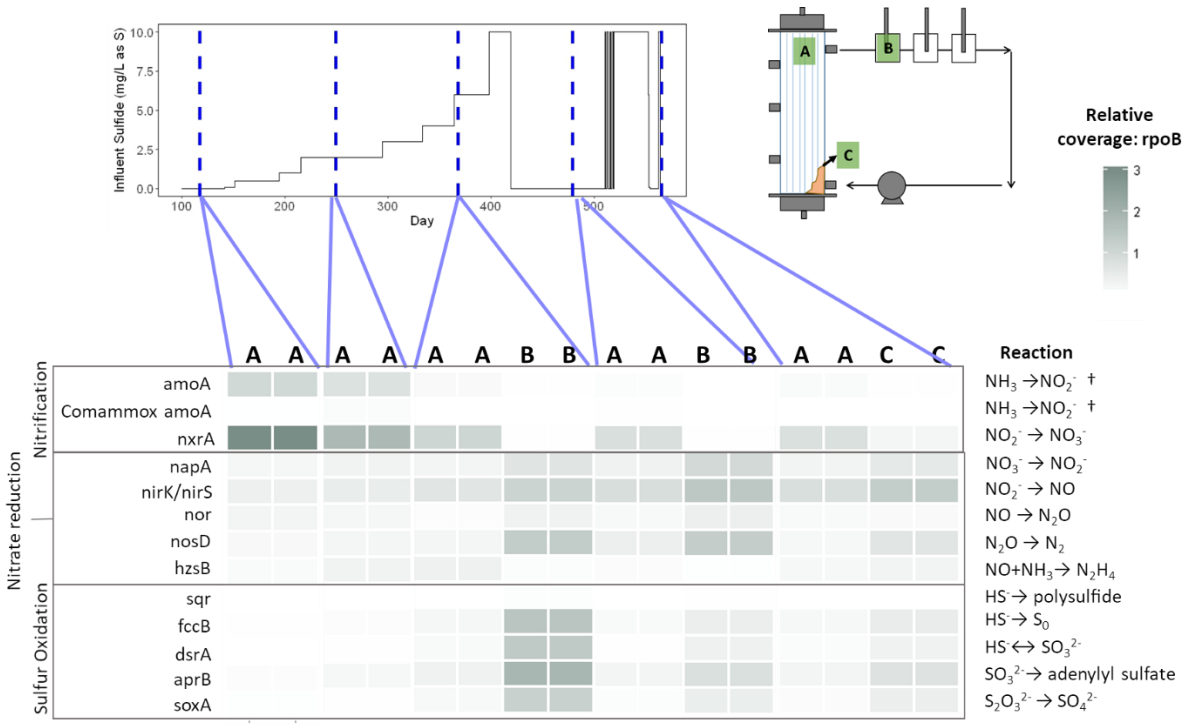


**Figure 4-2.** Relative abundance of genes for key metabolic functions in the reactor. The day and influent sulfide are indicated in the figure on top. The physical location of the samples are indicated with the letters on top of the heatmap, (A) biofilm samples, (B) samples are planktonic, suspended, and (C) samples are sloughed and settled biomass. Coverage scale is based on the coverage of each gene normalized to total coverage of all bacterial *rpoB* genes. Nitrifying gene marker are ammonia monooxygenase gene (*amoA*), comammox *amoA*, and nitrite oxidoreductase gene (*nxrB*). Denitrifyng gene markers are nitrate reductase (*napA*), nitrite reductase (*nirK/nirS*), nitric oxide reductase (*nor*), nitrous oxide reductase (*nosD*), and hydrazine synthase for the anammox process (*hzsB*). Sulfur oxidation genes are the sulfide-quionone reductase (*sqr*), the sulfide dehydrogenase (flavocytochrome c) (*fccB*) and dissimilatory sulfite reductase (*dsrA*), the adenylylsulfate reductase (*aprB*) and the Sox enzyme complex (*soxA*). *nirB*, *narG*, and *narH* are not shown because they were at low abundances. † ammonia monooxygenase converts ammonia to hydroxylamine, but full AOB reaction is shown here.

The concentrated sulfur oxidation and denitrification in the planktonic phase has implications for using sulfide-based denitrification in an MABR. A previous study of nitrogen removal in an MABR achieved almost 100% nitrogen removal and described a “hybrid” system where the biofilm was nitrifying while denitrification occurred in the suspended portion of the reactor (Downing and Nerenberg, 2008). These results highlight that biofilm reactor studies need to account for planktonic growth and potential division of labor between planktonic cells and biofilm communities. Nitrogen removal in these bioreactor systems can be improved by harnessing the denitrification potential present in the planktonic growth.

### *4.3.3 Sulfide addition decreased the relative abundance of nitrifier genes and increased those for DNRA, anammox, and denitrifying anaerobic methane oxidation.*

As sulfide increased, the abundance of both *nxr* and *amo* genes significantly decreased ($p_{ANOVA}$<0.05), suggesting sulfide inhibition of organisms carrying these genes (Figure 4-2 and Appendix B Figure B6). The abundances of nitrifying bacteria as indicated by these gene markers did not recover over the 90 days in which sulfide was removed from the influent. The only nitrite oxidizing bacteria detected in the reactor were in the family *Nitrospira*. Some *Nitrospira* can oxidize ammonia to nitrate (termed comammox) (Daims et al., 2015; van Kessel et al., 2015) and the relative abundance of the *Nitrospira nxr* compared to *amo* genes suggest that the bioreactor is a candidate for comammox metabolism. However, we detected comammox ammonia monooxygenase genes in the biofilm only at low abundances. On day 117, when nitrifying genes were most abundant, coverage of the comammox ammonia monooxygenase in the biofilm only accounted for about 0.5% of the total coverage of ammonia monooxygenase genes. This finding was confirmed using qPCR; gene copies of comammox *amoA* were two orders of magnitude lower than copies of canonical AOB and *Nitrospira* (Appendix B, Figure B6). Canonical *Nitrospira* that do not oxidize ammonia have a high affinity for nitrite (Nowka et al., 2015) relative to other NOB, and can grow in low DO environments (Keene et al., 2017; Regmi et al., 2014). High affinity for oxygen could be advantageous in an MABR where microbes are competing for oxygen in the biofilm, resulting in enrichment for such microorganisms in an MABR biofilm. The oxygen affinity of comammox bacteria is unknown and although comammox bacteria have one of the highest ammonia affinities of all terrestrial ammonia oxidizing bacteria, they do not have a similar affinity for nitrite. In this reactor, ammonia was not limiting but nitrite was, so the high ammonia affinity did not give comammox a competitive advantage over other AOB and canonical *Nitrospira* outcompeted comammox bacteria for nitrite. Both relative and absolute abundances of AOB and NOB decreased with increasing sulfide, providing molecular evidence of sulfide inhibition of nitrification.

The abundance of nitrite reductase genes responsible for DNRA (*nrfA*) increased with increasing sulfide (Figure 4-3 and Appendix B, Figure B7), which corresponds with the measured increase in the potential DNRA rate observed in the heavy nitrogen experiments. This provides two

independent indications that sulfide-induced DNRA was a substantial process occurring in the MABR. Interestingly, *nrfA* genes are more abundant in the biofilm than the suspended growth. In the reactor as a whole on day 368, over 40% of the *nrfA* genes had top hits to NCBI's nonredundant database with taxonomy assigned to anammox bacteria (Appendix B, Figure B6). DNRA by anammox is known to occur (Kartal et al., 2007), but so far has been limited to the use of volatile fatty acids as electron donors, which were not present in the reactor. Interestingly, unlike conventional DNRA, low COD/N ratios have been shown to induce DNRA by anammox (Castro-Barros et al., 2017). It is unlikely that volatile fatty acids that are typically used by anammox were formed in sufficient quantities from decay to support anammox growth via DNRA. Thus, we infer that the increased abundances of anammox-associated DNRA genes was likely a byproduct of anammox growth. Although over a quarter of the DNRA potential did not have clear top taxonomic hits compared to NCBI's nonredundant database, 23% of the overall DNRA present in the bioreactor had top hits to a denitrifying anaerobic methane oxidizer, *Candidatus* Methylomirabilis. Similar to the DNRA associated with anammox, this could be a byproduct of the growth of denitrifying anaerobic methane oxidizers. However, the high potential rates at which DNRA occurred suggest that some of these most abundant organisms contributed to this process.

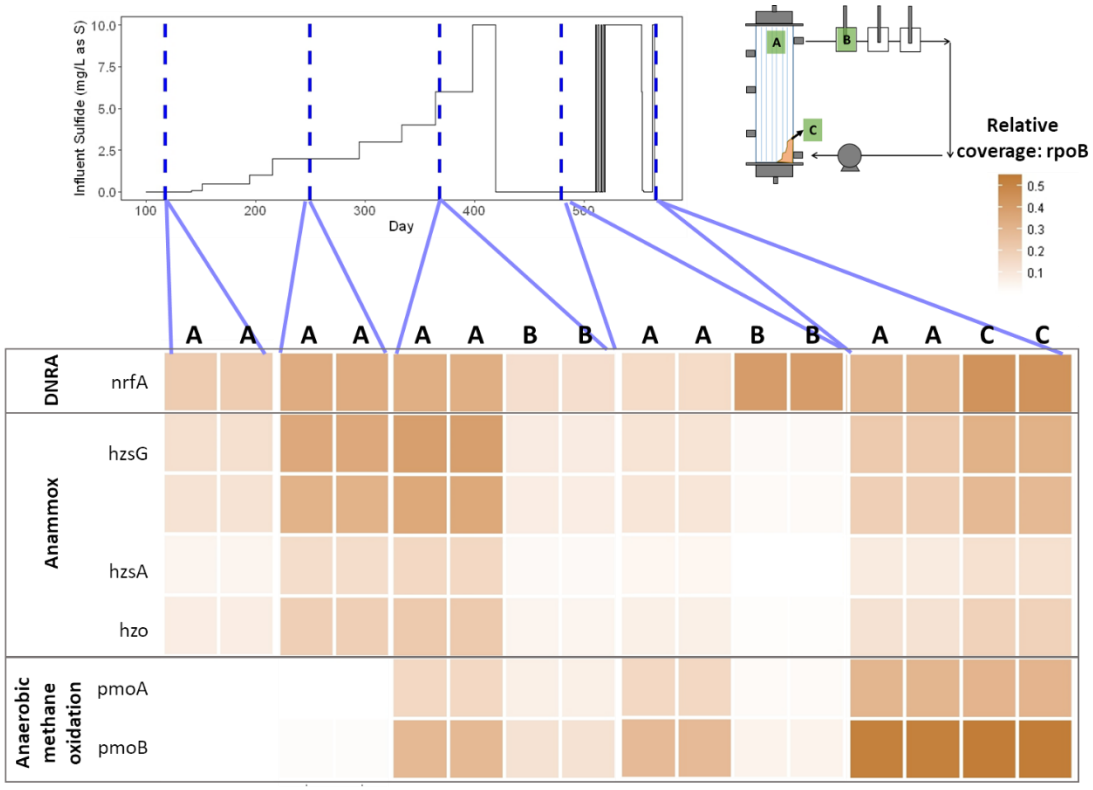


**Figure 4-3.** Relative abundances of key genes for DNRA (formate-dependent nitrite reductase, *nrfA*) anammox (hydrazine synthase, *hzsG*, *hzsB, hzsA,* and hydrazine oxidase, *hzo*) and denitrifying anaerobic methane oxidizer (particulate methane monooxygenase *pmoA* and *pmoB*). The location of the samples are indicated with the letters on top of the heatmap, (A) biofilm samples, (B) samples are planktonic, suspended, and (C) samples are sloughed and settled biomass. Coverage scale is based on the coverage of each gene normalized to total coverage of all bacterial *rpoB* genes.

The abundance of both anammox and denitrifying anaerobic methane oxidizers increased with increased sulfide (Figure 4-3) and methane oxidizer abundances in the biofilm were statistically correlated with influent sulfide ($p_{ANOVA}$=0.03). On day 479, coverage of nitrite reductase genes associated with anaerobic methane oxidizers account for 14% of biofilm nitrite reduction potential and 7% percent of the total reactor nitrite reduction potential. The potential inhibition of nitrite oxidation by sulfide that was observed in the rate experiments could have aided in providing substrate for anammox and denitrifying anaerobic methane oxidizers. The increased abundances of anammox and denitrifying anaerobic methane oxidizers could also be because sulfide served as a reducing agent. The oxidation reduction potential (Appendix B, Figure B8) shows a change in redox state with increased sulfide and this may have helped these oxygen sensitive organisms to grow. These results indicate that there is the potential to support anammox and denitrifying

anaerobic methane oxidizers in a multi-redox MABR and sulfide helps this process by inhibiting NOB and acting as a reducing agent.

### *4.3.4 The MABR enriched for a novel denitrifying anaerobic methane oxidizer.*

Given that denitrifying anaerobic methane oxidation increased with increasing sulfide, we sought to evaluate the metabolic potential within this organism. From metagenomic assembly and binning we recovered a near-complete bin (95% complete, 3% contamination). Based on Phylosift analysis 100% of the contigs in the bin could be classified within the NC10 phyla, and 67% were classified within the genus *Candidatus* Methylomirabilis, Furthermore, the bin contains markers similar to *Ca.* Methylomirabilis oxyfera: an RNA polymerase (91% identical), a 23S rRNA gene (96% identical), and a 16S rRNA gene (97% identical). Figure 4-4A shows that based on the average nucleotide identity (ANI) the organism in the reactor is a distinct species from the NC10 organisms that have previously been described, its closest relative shares an average nucleotide identity of 85%. Collectively, this means that the genome recovered is in the genus of *Ca* Methylomirabilis (within 82% ANI of all other *Ca* Methylomirabilis) but is a distinct species. Based on these results, we compared the gene content of this genomic bin to related genomes described in the literature to evaluate potential differences in functional potential.

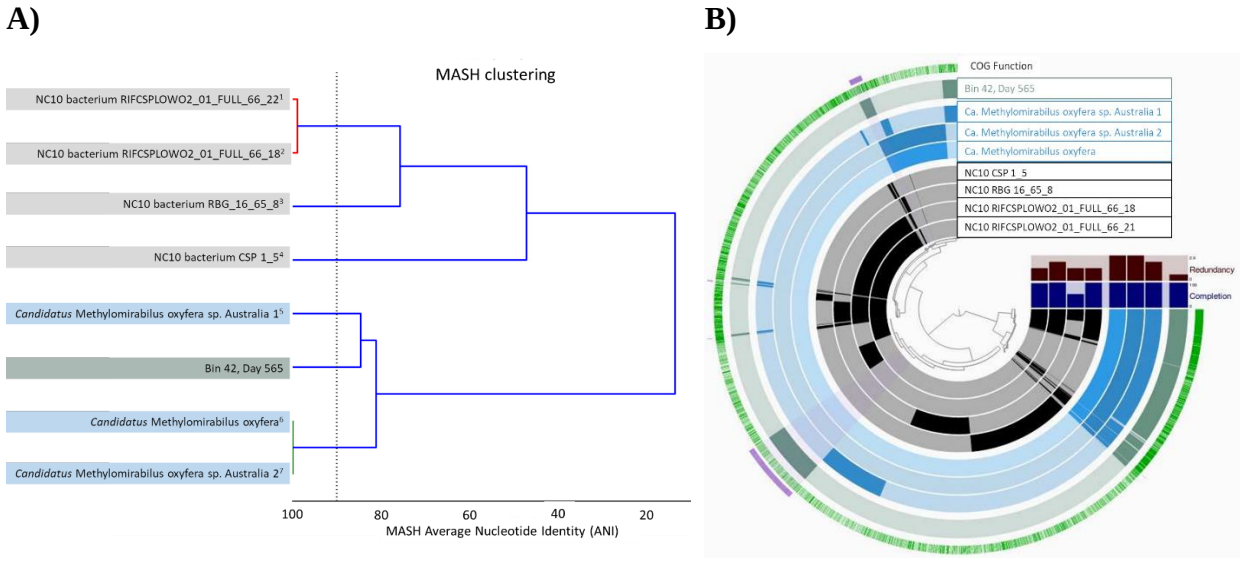


**Figure 4-4.** (A) Average nucleotide identities of new bins 42 compared with public ally available genomes from the NC10 phyla. Accession numbers on IMG GOLD Analysis Project IDs: [1]Ga0155960 (Wrighton et al., 2012), [2]Ga0156237 (Wrighton et al., 2012), [3]Ga0154810 (Wrighton et al., 2012), [5]Ga0011360, [6]Ga0169943 (Ettwig et al.,

2010), [7]Ga0011361 and NCBI BioSample [4]SAMN03462098 (Hug et al., 2016). The bin is indicated in olive, *Ca.* Methylomirabilis genomes are blue, and other genomes in the NC10 phyla are grey. Dotted line represents an ANI of 90%. (B) Pangenome analysis of bin (olive), oxyfera genomes (blue), and NC10 genomes (black). Purple bars and highlighting indicate distinct protein clusters from other NC10 genomes.

Using a pangenome analysis, we identified 307 gene clusters in this organism that were not present in other genomes in the NC10 phylum (Figure 4-4B, Appendix B, Table B6). While many of these gene clusters encode functions that are present in other *Ca.* Methylomirabilis genomes, we identified 88 unique functions. Most of these unique functions were associated with COG category V, defense mechanisms, but this comparison also revealed a denitrification pathway that is distinct from other *Ca.* Methylomirabilis organisms. Nitrate reduction genes (*narG* and *narJ)* were absent, a finding confirmed by searching for the *narG* and *narJ* specific to *Ca.* Methylomirabilis in the unbinned scaffolds and individual sequence reads. Previous studies have shown that *Ca.* Methylomirabilis oxyfera does not contain the nitrous oxide reductase protein (Ettwig et al., 2010), but the *Ca.* Methylomirabilis organism in the MABR did have a gene encoding for the nitrous oxide reductase protein (*nosD*) that was absent from all other NC10 genomes, again indicating that the denitrification pathway in the *Ca.* Methylomirabilis present in our bioreactor was distinct. The *Ca.* Methylomirabilis genome from our bioreactor did have a *narK* gene, which is used for nitrate assimilation. Although *narK* is present in other distantly related bacteria from the NC10 phyla it is not present in any other *Ca.* Methylomirabilis bacteria. Overall, these results suggest that the organism in the bioreactor does not have the capacity to use nitrate as an electron acceptor and is consistent with use of nitrite as an electron acceptor. This further supports that residual nitrite was needed to support *Ca.* Methylomirabilis, likely the result of NOB inhibition.

One function that was uniform across all *Ca.* Methylomirabilis genomes was the potential to conduct DNRA. All *Ca.* Methylomirabilis genomes have a *nrfA* gene for reduction of nitrite to ammonia. Although *Ca.* Methylomirabilis organisms and the archaeal anaerobic methane oxidizers (Haroon et al., 2013) all have the genetic capacity to conduct DNRA, DNRA coupled to anaerobic methane oxidation has not been described, but it is worth considering in this system for two reasons. First, we observed the growth of *Ca.* Methylomirabilis without any increases in overall denitrification, and second, a significant portion of the overall DNRA genetic potential in the reactor was associated with *Ca.* Methylomirabilis. Understanding the conditions under which

DNRA is expressed in anaerobic methane oxidizers is an important gap in the literature that warrants further exploration.

We have shown the potential functions and microbial interactions that result from increases in sulfur in a MABR (Figure 4-5). NOB were more inhibited by sulfide than AOB. Through both the metagenomic and experimental rate data we showed that this inhibition resulted in production of nitrite and led to increased dissimilatory reduction of nitrite to ammonia. Furthermore, this nitrite accumulation supported growth of an organism related to *Ca.* Methylomirabilis. We suggest that methane may be serving as an electron donor for DNRA, but this inference as well as the conditions that promote DNRA by anaerobic methane oxidizers need to be evaluated further. In summary, sulfide changed microbial cross-feeding relationships. Due to these tight interactions within the community, it was only through the application of metagenomic data and isotopic rate data that we could uncover these relationships. In order to apply these results to engineered treatment systems pursuing nitrogen removal, it will be important to understand how to encourage denitrification over DNRA.

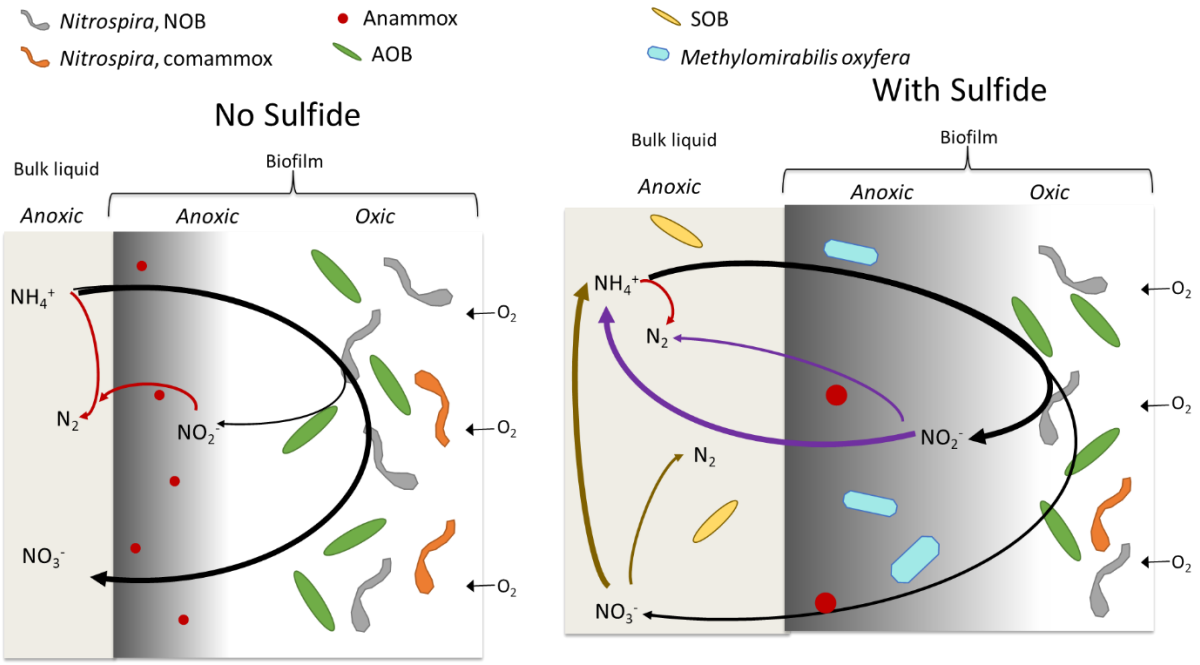


**Figure 4-5.** Potential nitrogen metabolisms with and without sulfide. Sulfide shifts redox in the biofilm. Arrow color indicates metabolism responsible: Black is nitrifying bacteria, purple DNRA or denitrification linked to either anammox or anaerobic methane oxidation, red is anammox, dark yellow is DNRA and denitrification by sulfide

oxidizing bacteria (SOB). Arrow color (other than black) also indicates electron donor: purple is either methane or ammonia, red is ammonia, and dark yellow is sulfide.

## 4.4 Experimental Procedures

### *4.4.1 Reactor design and inoculation*

The MABR system (1.93 L working volume, Appendix B, Figure B1) was modeled after Gilmore et al. (2013), inspired by systems operated by a research team at the NASA Kennedy Space Center (Tansel et al., 2005). The module consisted of an acrylic cylinder column approximately 0.3 m long x 0.08 m inner diameter with flanges on either end. Fibers (n=157) of Silastic™ silicone laboratory tubing (Dow Corning, Midland, MI) were potted in milled end caps. The tubing has an outer diameter of 3.18 mm and an inner diameter of 1.98 mm and was roughened with sand paper to improve biofilm adhesion. The specific surface area of the membrane was 248 $m^2/m^3$ of reactor volume. The reactor was operated with membranes in an open-ended, flow-through configuration. Synthetic wastewater was recirculated parallel to the membranes at flow rates greater than fifty times the influent flow rate. A tracer study using sodium chloride was conducted prior to inoculation and showed the reactor is best modeled as a continuously stirred tank reactor; thus, bulk concentrations are approximately uniform in the reactor (Appendix B, Figure B2). Dissolved oxygen (DO), oxidation-reduction potential (ORP), pH, ammonia, and nitrate sensors (YSI/Xylem, Yellow Springs, Ohio, USA) were used to continuously monitor performance. Data were logged using a data acquisition device (NI 6008) and Labview program (National Instruments, Austin, Texas, USA). The program was also used to control pH (by controlling a pump feeding a 30 g/L sodium bicarbonate solution) and air addition (by controlling a mass flow controller connected to a pressurized air cylinder (GFCS17A, Aalborg, Aalborg, Denmark)).

Prior to the experiments described here, the reactor was operated for over 500 days while being fed synthetic anaerobic membrane bioreactor effluent, which contained ammonium (50 mg N/L), methane at saturation, volatile fatty acids (30 mg chemical oxygen demand (COD)/L, equal parts propionate and acetate), and sulfide (5 mg/L as S). The reactor was inoculated with a blend of sludge from a sidestream anammox based DEMON (DEamMONification) process and a mainstream activated sludge process performing ammonia oxidation with NOB suppression (Regmi et al., 2015), both provided by the Hampton Roads Sanitation District (Virginia Beach, Virginia). During this phase, the reactor achieved moderate nitrogen removal (40-60%) (Delgado

Vela et al., 2015a). On day zero for the experiments described here, suspended growth was aggressively removed, which caused a significant fraction of the biofilm to detach, and volatile fatty acids were eliminated from the reactor feed. On days 9 and 15, the reactor was re-inoculated with activated sludge from an Anaerobic-Anoxic-Aerobic activated sludge process (Ann Arbor, MI) by adding 5 mL of concentrated and washed mixed liquor, then turning down the recirculation pump for 24 hours to allow for adhesion of the inoculum to the membrane.

### *4.4.2 Reactor influent and operation*

The reactor was operated to simulate treatment of an effluent from a mainstream anaerobic process. Synthetic influent (twenty liters) was prepared by first combining 20 mL of the acidic trace metals and basic trace metals solution. The acidic trace metals solution consisted of (per liter): $CoCl_2 \cdot 6H_2O$, 280 mg; $ZnSO_4 \cdot 7H_2O$, 340 mg; $H_3BO_3$, 37 mg; $MnCl_2 \cdot 4H_2O$, 110 mg; $AlCl_3 \cdot 6H_2O$, 28 mg; $NiCl_2 \cdot 6H_2O$, 140 mg; $CuCl_2 \cdot 2H_2O$, 100 mg. The basic trace metals solution consisted of (per liter): $(NH_4)_2MoO_4 \cdot 4H_2O$, 160 mg; $Na_2SeO_4$, 22 mg; $Na_2WO_4 \cdot 2H_2O$, 39.5 mg. Twenty mL of a NaEDTA stock was added to the trace metals mixture, followed by 100 mL of a 56 g/L ammonium bicarbonate stock solution to achieve a final ammonium concentration of 50 mg N/L. After mixing, 20 mL of a divalent cation solution was added and contained (per liter): $CaCl_2 \cdot 2H_2O$, 5g; $MgCl_2 \cdot 6H_2O$, 33 g; KCl, 16 g; $KH_2PO_4$, 11 g. The synthetic influent was diluted with deionized water for a final volume 20 L to which 65 mL of 1 N HCl was added. The solution was then sparged with methane for 25 minutes to both saturate with methane and purge dissolved oxygen. Sparging stripped the influent of carbonate; therefore, 95 mL of a 30 g/L sodium bicarbonate stock was added after sparging. Additionally, 20 mL of a 6.6 g/L $FeSO_4 \cdot 7H_2O$ stock, which was stored in an anaerobic glove chamber to prevent Fe (II) oxidation, was added. The influent was sparged with methane for 5 more minutes after sodium bicarbonate and iron addition. The synthetic influent was prepared approximately every two days using glassware that was autoclaved prior to influent preparation.

For the first 120 days of operation (Phase A), a nitrifying biofilm was established with steady increases in influent ammonium loading (Appendix B, Figure B3 and Table B1). After this initial period, phase B was begun with stepwise increases in the sulfide concentration over the course of 299 days (Table B1). To minimize precipitation, sodium sulfide was added via a separate

peristaltic pump to achieve the desired influent concentration. The sulfide feed was made using a sodium sulfide nonahydrate stock (5 g/L as sulfur) stored in an anaerobic chamber. The feed jar with sodium sulfide was connected to a gas bag with nitrogen gas to prevent aerobic oxidation.

### *4.4.3 Bulk reactor rate experiments*

To obtain rates for nitrification, nitrate reduction, and DNRA, we conducted experiments with $^{15}N$ labeled nitrogen (> 98% purity, Sigma Aldrich). The reactor was emptied, refilled with influent containing $^{15}N$ labeled nitrogen, and operated in batch mode with recirculation but no new influent for two hours. Initial rates of reaction were obtained during the batch experiments and, consequently, represent potential rates of oxidation and growth, not extant rates. The benefit of conducting the experiments in this manner is that multiple substrate profiles could be assessed in replicate experiments.

Three batch experiments were conducted in duplicate with and without sulfide in the influent (12 batch experiments total). To obtain rates of ammonia oxidation the influent contained labeled ammonia and unlabeled nitrite (Experiment A). Ammonium oxidation rates were based on $^{15}NO_2^-$ production. Experiment B was used to obtain rates of nitrate reduction with labeled nitrate, unlabeled nitrite, and unlabeled ammonia, and measuring $^{15}NO_2^-$ produced. Experiment C included feeding labeled nitrite and unlabeled nitrate to obtain rates of nitrite oxidation based on $^{15}NO_3^-$ production. DNRA rates were measured in Experiments B and C by measuring the rate of $^{15}NH_4^+$ production. Standard protocols were used to measure $^{14}N$-nitrite, -nitrate and -ammonium. Measurements of these nutrients were used to correct the isotope labeling ratio throughout the experiments.

To initiate an experiment, the reactor was filled with new influent, which took between 15 and 20 minutes. It is likely that biologically-mediated oxidation started before mixing (via recirculation pump) could begin. However this potential activity is ignored in the rate calculations and time zero used in plots and in rate calculations was taken to the time at which mixing was turned on. In this way, the rates calculated are a conservative estimate of rates. The reactor was sampled immediately after the recirculation pump was turned on and 10, 30, 60, 90, and 120 minutes thereafter. The time between the experiments was at a minimum equivalent to four hydraulic residence times

(HRT=5.1 hours) to minimize the residual label in the bioreactor. To correct for any residual label from the previous experiment, the reactor was also sampled approximately 30 minutes before the experiment and a few hours after the experiment was over. Any labeled substrate or product measured in the samples taken before the experiment began, were used as initial concentrations in rate calculations. Since the reactor was emptied prior to adding new influent, this is a conservative approach and accounts for any residual label. All the experiments with sulfide were conducted first, between days 547 and 552. Sulfide was removed from the influent long enough for effluent nitrogen to mimic previous sulfide-free operation (2 days), then experiments without sulfide were conducted on days 557-562.

Collected samples were filtered (0.2 µm PES, Titan3$^{TM}$, Thermo Fisher Scientific) and measured for pH. To avoid introducing air into the recirculation line, the liquid taken for each sample was replenished with either sodium bicarbonate or distilled water (depending on if any pH adjustment was needed). The volume replenished was tracked and used to correct the dilution in the final rate calculations. Samples were frozen and shipped to the University of Southern Denmark, Odense, Denmark for analysis. Methods for isotope analysis have been previously described (Bristow et al., 2016). Briefly, for analysis of $^{15}NO_3^-$, residual $^{15}NO_2^-$ was first removed from the sample using sulfamic acid (Füssel et al., 2012), followed by cadmium reduction to convert $^{15}NO_3^-$ to $^{15}NO_2^-$ and sulfamic acid to reduce the $^{15}NO_2^-$ to $N_2$ (McIlvin and Altabet, 2005). This preparation process produced $^{14}N^{15}N$ and $^{15}N^{15}N$ forms of $N_2$, and were measured using a gas chromatography-isotope ratio mass spectrometer (GC-IRMS) (Dalsgaard et al., 2012). $^{15}NH_4^+$ was analyzed using GC-IRMS by converting the labeled ammonium to $^{14}N^{15}N$ and $^{15}N^{15}N$ using hypobromite (Warembourg, 1993).

For experiments with sulfide in the influent, samples for sulfide analysis were collected separately immediately after nitrogen samples. Samples were collected, stored, and analyzed according to method 4500-$S^{2-}$ G in Standard Methods(APHA et al., 2005). Sulfide samples were diluted (2x) in sulfide antioxidant buffer. They were immediately transferred to the anaerobic chamber, filtered (0.45 µm, nitrocellulose filter, Fisher Scientific), and preserved in the dark. All samples were analyzed within 24 hours. Sulfide was analyzed using a silver sulfide electrode (Thermo Scientific,

Orion) that was calibrated by making standards with a 3% (w/v) sodium sulfide stock solution (Ricca Chemical Company), according to method 4500-$S^{2-}$ G (APHA et al., 2005).

### *4.4.4 Biomass sampling, DNA extraction, qPCR, and metagenomic sequencing*

Biofilm samples were collected by opening the top flange of the reactor and carefully scraping the lumen of the membrane. When there was sufficient planktonic growth, biomass samples from the monitoring probe flow cells were also collected. Duplicate biomass samples collected during reactor operation on days 117, 249, 368, 479 were submitted for sequencing. In addition, samples were taken when the reactor was decommissioned (day 565). Duplicate samples taken from the outer membranes at a midpoint vertical height and from biomass that had settled at the bottom of the reactor chamber were submitted for sequencing. DNA extractions were performed by combining bead beating with the Maxwell automatic DNA extractor as described in Chapter 3, section 3.3.5.

Gene copies of bacterial ammonia monooxygenase (*amoA*), 16S rRNA, *Nitrospira* nitrite oxidoreductase genes (*nxrB*), anammox 16S genes, and comammox clade A *amoA* genes were quantified in triplicate using qPCR. Purified products from PCR reactions on reactor samples were used as standards for the qPCR reaction. For all qPCR targets except the 16S rRNA gene, standards were confirmed using Sanger Sequencing. Positive controls (DNA extracts from a nitrifying enrichment culture for AOB and *Nitrospira* (Stadler and Love, 2016), DEMON sludge for anammox, drinking water biofilter for comammox (Pinto et al., 2015), or genomic DNA from *Pseudomonas aeruginosa* pure culture for 16S) and duplicate no-template controls were analyzed on each qPCR plate. Details on qPCR conditions and primers are given in Appendix B.

Samples were submitted for sequencing on the Illumina HiSeq 4000 platform with 150 base pair paired-end reads with a target insert size of 350 base pairs at the University of Michigan DNA Sequencing Core. DNA was fragmented using standard Covaris sonication (Covaris, Woburn, MA). Fragmented DNA was then prepared as a standard Illumina library using Wafergen reagents on the Apollo 324™ instrument, where the fragments are end repaired, A tailed, and adapter ligated. Then, the samples are PCR amplified and pooled. Final libraries were checked for quality and quantity by TapeStation (Agilent, Santa Clara, CA) and qPCR using Roche's library quantification

kit for Illumina Sequencing platforms (catalog # KK4835). They were clustered on the cBot (Illumina) and were pooled and sequenced on a 300 cycle paired end run on a HiSeq 4000 using software version 3.4.0.38.

### *4.4.5 Whole genome assembly and annotation*

Raw sequencing reads were dereplicated (100% identity over 100% of the length for both forward and reverse reads), trimmed using Sickle (Joshi and Fass, 2011), and adaptors were removed using Scythe version 0.994-4. Trimming removed 5 ± 1 % of the data. Whole genome de novo assembly was performed on pooled duplicate samples using MEGAHIT v 1.1.2 (Li et al., 2015) with mink=27, maxk=87, and a step size of 10. Assembled data resulted in 390,000 ± 78,000 contigs (of which 150,000 ± 29,000 contigs were > 1,000 bp). The N50 of the assembled contigs was 3,600 ± 490 bp. Reads were mapped to assembled contigs using the Burrows-Wheeler Aligner (BWA version 0.7.15) and default parameters (Li and Durbin, 2009). The mapped read counts were extracted using SAMtools version 1.3.1 (Li et al., 2009). Each duplicate sample was mapped to the pooled assembly separately. Gene calling on assembled data was performed using Prodigal v2.6.2. The predicted amino acid sequences were then compared to a custom database of relevant functions (Appendix B, Table B4) using BLASTp. The database was generated using relevant functions from whole genomes of taxa represented in previously analyzed 16S rRNA gene amplicon sequencing data. The outputs were filtered based on an alignment length of at least 100 amino acids, bitscores above 250 and percent identities greater than 50%. Gene annotation was confirmed by manually checking the annotations against the entire NCBI non-redundant database. Assembled data were submitted to the DOE JGI-IMG/MER annotation pipeline (GOLD Study ID Gs0134229). To determine relative abundances of genes, coverages were normalized to the coverage of the *rpoB* gene and the length of the genes.

### *4.4.6 Metagenomic binning and pangenome analysis*

The annotation and blast analysis revealed that genome coverages of important organisms were high (greater than 200x coverage). To improve the assembly and binning on important organisms, trimmed reads were subsampled and reassembled as previously described (Hug et al., 2016). Subsampling percentages were based on the coverage of markers of important metabolisms with the goal of obtaining a coverage between 15x and 25x. Reads were downsampled between 10 and

50% to achieve this goal. Assemblies and mapping on downsampled reads were performed using the same methods as the complete samples. CONCOCT v0.4.1 was used to bin assembled reads using default parameters. Bin completeness and contamination were evaluated using CheckM v1.0.11 and PhyloSift was used to taxonomically classify bins. Metagenome assembled genomes were compared to existing draft and complete genomes from the literature based on average nucleotide identities using MASH clustering (Ondov et al., 2016) and dRep v2.0.5 (Olm et al., 2017). Differences between genomes were assessed using the pangenome workflow (Delmont and Eren, 2018) of Anvi'o version 4 (Eren et al., 2015). NCBI's BLASTp was used to calculate protein similarities. Weak matches were eliminated using the minbit heuristic (Benedict et al., 2014), and the MCL algorithm was used to cluster proteins (van Dongen and Abreu-Goodger, 2012).

### *4.4.7 Statistical analysis*

Associations between gene coverages and sulfide concentration were tested using a repeated measures ANOVA and corrected for multiple comparisons using the Benjamani-Hochberg correction factor. Differences in rate measurements were tested using a two-sided t-test. The R environment was used to analyze all data (R Core Team, 2016).

## 4.5 References


APHA, AWWA, WEF, 2005. Standard methods for the examination of water and wastewater, 21st ed. Washington D.C.

Arshad, A., Martins, P.D., Frank, J., Jetten, M.S.M., Op den Camp, H.J.M., Welte, C.U., 2017. Mimicking microbial interactions under nitrate-reducing conditions in an anoxic bioreactor: enrichment of novel Nitrospirae bacteria distantly related to Thermodesulfovibrio. Environ. Microbiol. 00, 1–41. doi:10.1111/1462-2920.

Bejarano-Ortiz, D.I., Huerta-Ochoa, S., Thalasso, F., Cuervo-López, F. de M., Texier, A.C., 2015. Kinetic Constants for Biological Ammonium and Nitrite Oxidation Processes Under Sulfide Inhibition. Appl. Biochem. Biotechnol. 177, 1665–1675. doi:10.1007/s12010-015-1844-3

Benedict, M.N., Henriksen, J.R., Metcalf, W.W., Whitaker, R.J., Price, N.D., 2014. ITEP: An integrated toolkit for exploration of microbial pan-genomes. BMC Genomics 15. doi:10.1186/1471-2164-15-8

Bristow, L.A., Dalsgaard, T., Tiano, L., Mills, D.B., Bertagnolli, A.D., Wright, J.J., Hallam, S.J., Ulloa, O., Canfield, D.E., Revsbech, N.P., Thamdrup, B., 2016. Ammonium and nitrite oxidation at nanomolar oxygen concentrations in oxygen minimum zone waters. Proc. Natl. Acad. Sci. 113, 10601–10606. doi:10.1073/pnas.1600359113

Brunet, R.C., Garcia-Gil, L.J., 1996. Sulfide-induced dissimilatory nitrate reduction to ammonia in anaerobic freshwater sediments. FEMS Microbiol. Ecol. 21, 131–138. doi:10.1016/0168-6496(96)00051-7

Castro-Barros, C.M., Jia, M., van Loosdrecht, M.C.M., Volcke, E.I.P., Winkler, M.K.H., 2017. Evaluating the potential for dissimilatory nitrate reduction by anammox bacteria for municipal wastewater treatment. Bioresour. Technol. 233, 363–372. doi:10.1016/j.biortech.2017.02.063

Daims, H., Lebedeva, E. V., Pjevac, P., Han, P., Herbold, C., Albertsen, M., Jehmlich, N., Palatinszky, M., Vierheilig, J., Bulaev, A., Kirkegaard, R.H., Bergen, M. von, Rattei, T., Bendinger, B., Nielsen, P.H., Wagner, M., 2015. Complete nitrification by Nitrospira bacteria. Nature. doi:10.1038/nature16461

Dalsgaard, T., Thamdrup, B., Farías, L., Revsbech, N.P., 2012. Anammox and denitrification in the oxygen minimum zone of the eastern South Pacific. Limnol. Oceanogr. 57, 1331–1346. doi:10.4319/lo.2012.57.5.1331

Delgado Vela, J., Dick, G.J., Love, N.G., 2018. Sulfide inhibition of nitrite oxidation in activated sludge depends on microbial community composition. Water Res. 138, 241–249.

Delgado Vela, J., Martin, K.J., Beaton, N., McFarland, A., Stadler, L.B., Bott, C.B., Skerlos, S.J., Raskin, L., Love, N.G., 2015a. Nutrient Removal from Mainstream Anaerobic Processes using a Membrane Biofilm Reactor and a Granular Sludge Sequencing Batch Reactor, in: Proceedings of the Water Environment Federation.

Delgado Vela, J., Stadler, L.B., Martin, K.J., Raskin, L., Bott, C., Love, N.G., 2015b. Prospects for Biological Nitrogen Removal from Anaerobic Effluents during Mainstream Wastewater Treatment. Environ. Sci. Technol. Lett. 2, 233–244. doi:10.1021/acs.estlett.5b00191

Delmont, T.O., Eren, A.M., 2018. Linking pangenomes and metagenomes: the *Prochlorococcus* metapangenome. PeerJ 6, e4320. doi:10.7717/peerj.4320

Dolejs, P., Paclík, L., Maca, J., Pokorna, D., Zabranska, J., Bartacek, J., Paclik, L., Maca, J., Pokorna, D., Zabranska, J., Bartacek, J., Paclík, L., Maca, J., Pokorna, D., Zabranska, J., Bartacek, J., 2014. Effect of S/N ratio on sulfide removal by autotrophic denitrification. Appl. Microbiol. Biotechnol. 99, 2383–2392. doi:10.1007/s00253-014-6140-6

Downing, L.S., Nerenberg, R., 2008. Total nitrogen removal in a hybrid, membrane-aerated activated sludge process. Water Res. 42, 3697–3708. doi:10.1016/j.watres.2008.06.006

Eren, A.M., Esen, Ö.C., Quince, C., Vineis, J.H., Morrison, H.G., Sogin, M.L., Delmont, T.O., 2015. Anvi'o: an advanced analysis and visualization platform for 'omics data. PeerJ 3, e1319. doi:10.7717/peerj.1319

Erguder, T.H., Boon, N., Vlaeminck, S.E., Verstraete, W., 2008. Partial nitrification achieved by pulse sulfide doses in a sequential batch reactor. Environ. Sci. Technol. 42, 8715–8720. doi:10.1021/es801391u

Ettwig, K.F., Butler, M.K., Le Paslier, D., Pelletier, E., Mangenot, S., Kuypers, M.M.M.,

Schreiber, F., Dutilh, B.E., Zedelius, J., de Beer, D., Gloerich, J., Wessels, H.J.C.T., van Alen, T., Luesken, F., Wu, M.L., van de Pas-Schoonen, K.T., Op den Camp, H.J.M., Janssen-Megens, E.M., Francoijs, K.-J., Stunnenberg, H., Weissenbach, J., Jetten, M.S.M., Strous, M., 2010. Nitrite-driven anaerobic methane oxidation by oxygenic bacteria. Nature 464, 543–8. doi:10.1038/nature08883

Füssel, J., Lam, P., Lavik, G., Jensen, M.M., Holtappels, M., Günter, M., Kuypers, M.M.M., 2012. Nitrite oxidation in the Namibian oxygen minimum zone. ISME J. 6, 1200–1209. doi:10.1038/ismej.2011.178

Füssel, J., Lücker, S., Yilmaz, P., Nowka, B., van Kessel, M.A.H.J., Bourceau, P., Hach, P.F., Littmann, S., Berg, J., Spieck, E., Daims, H., Kuypers, M.M.M., Lam, P., 2017. Adaptability as the key to success for the ubiquitous marine nitrite oxidizer *Nitrococcus*. Sci. Adv. 3, e1700807. doi:10.1126/sciadv.1700807

Gilmore, K.R., Terada, A., Smets, B.F., Love, N.G., Garland, J.L., 2013. Autotrophic Nitrogen Removal in a Membrane-Aerated Biofilm Reactor Under Continuous Aeration: A Demonstration. Environ. Eng. Sci. 30, 38–45. doi:10.1089/ees.2012.0222

Guo, Q., Hu, H.-Y., Shi, Z.-J., Yang, C.-C., Li, P., Huang, M., Ni, W.-M., Shi, M.-L., Jin, R.-C., 2016. Towards simultaneously removing nitrogen and sulfur by a novel process: Anammox and autotrophic desulfurization–denitrification (AADD). Chem. Eng. J. 297, 207–216. doi:10.1016/j.cej.2016.03.138

Haroon, M.F., Hu, S., Shi, Y., Imelfort, M., Keller, J., Hugenholtz, P., Yuan, Z., Tyson, G.W., 2013. Anaerobic oxidation of methane coupled to nitrate reduction in a novel archaeal lineage. Nature 2–7. doi:10.1038/nature12375

Heffernan, A.B., Shrivastava, A., Toniolo, D., Semmens, M., Syron, E., 2017. Operation of a Large Scale Membrane Aerated Biofilm Reactor for the treatment of Municipal Wastewater. Proc. Water Environ. Fed. 285–297.

Houweling, D., Peeters, J., Cote, P., Long, Z., Adams, N., 2017. Proving Membrane Aerated Biofilm Reactor (MABR) Performance and Reliability: Results from Four Pilots and a Full-Scale Plant. Proc. Water Environ. Fed. 272–284.

Hug, L.A., Thomas, B.C., Sharon, I., Brown, C.T., Sharma, R., Hettich, R.L., Wilkins, M.J., Williams, K.H., Singh, A., Banfield, J.F., 2016. Critical biogeochemical functions in the subsurface are associated with bacteria from new phyla and little studied lineages. Environ. Microbiol. 18, 159–173. doi:10.1111/1462-2920.12930

Jin, R.C., Yang, G.F., Zhang, Q.Q., Ma, C., Yu, J.J., Xing, B.S., 2013. The effect of sulfide inhibition on the ANAMMOX process. Water Res. 47, 1459–1469. doi:10.1016/j.watres.2012.12.018

Jones, Z.L., Jasper, J.T., Sedlak, D.L., Sharp, J.O., 2017. Sulfide Induced Dissimilatory Nitrate Reduction to Ammonium Supports Anaerobic Ammonium Oxidation (Anammox) in an Open-Water Unit Process Wetland. Appl. Environ. Microbiol. 83, 1–14.

Joshi, N.A., Fass, J.N., 2011. Sickle: A sliding-window, adaptive, quality-based trimming tool for FastQ files (Version 1.33)[Software].

Kartal, B., Kuypers, M.M.M., Lavik, G., Schalk, J., Op den Camp, H.J.M., Jetten, M.S.M., Strous, M., 2007. Anammox bacteria disguised as denitrifiers: nitrate reduction to dinitrogen gas via nitrite and ammonium. Environ. Microbiol. 9, 635–42. doi:10.1111/j.1462-2920.2006.01183.x

Keene, N.A., Reusser, S.R., Scarborough, M.J., Grooms, A.L., Seib, M., Santo Domingo, J., Noguera, D.R., 2017. Pilot plant demonstration of stable and efficient high rate biological nutrient removal with low dissolved oxygen conditions. Water Res. 121, 72–85. doi:10.1016/j.watres.2017.05.029

Kuypers, M.M.M., Marchant, H.K., Kartal, B., 2018. The microbial nitrogen-cycling network. Nat. Rev. Microbiol. doi:10.1038/nrmicro.2018.9

Li, D., Liu, C.M., Luo, R., Sadakane, K., Lam, T.W., 2015. MEGAHIT: An ultra-fast single-node solution for large and complex metagenomics assembly via succinct de Bruijn graph. Bioinformatics 31, 1674–1676. doi:10.1093/bioinformatics/btv033

Li, H., Durbin, R., 2009. Fast and accurate short read alignment with Burrows-Wheeler transform. Bioinformatics 25, 1754–60. doi:10.1093/bioinformatics/btp324

Li, H., Handsaker, B., Wysoker, A., Fennell, T., Ruan, J., Homer, N., Marth, G., Abecasis, G., Durbin, R., Subgroup, 1000 Genome Project Data Processing, 2009. The Sequence Alignment/Map format and SAMtools. Bioinformatics 25, 2078–2079. doi:10.1093/bioinformatics/btp352

Lüke, C., Speth, D.R., Kox, M.A.R., Villanueva, L., Jetten, M.S.M., 2016. Metagenomic analysis of nitrogen and methane cycling in the Arabian Sea oxygen minimum zone. PeerJ 4, e1924. doi:10.7717/peerj.1924

Martin, K.J., Nerenberg, R., 2012. The membrane biofilm reactor (MBfR) for water and wastewater treatment: principles, applications, and recent developments. Bioresour. Technol. 122, 83–94. doi:10.1016/j.biortech.2012.02.110

McIlvin, M.R., Altabet, M.A., 2005. Chemical conversion of nitrate and nitrite to nitrous oxide for nitrogen and oxygen isotopic analysis in freshwater and seawater. Anal. Chem. 77, 5589–5595. doi:10.1021/ac050528s

Morgenroth, E., Sherden, T., Van Loosdrecht, M.C.M., Heijnen, J.J., Wilderer, P. a., 1997. Aerobic granular sludge in a sequencing batch reactor. Water Res. 31, 3191–3194. doi:10.1016/S0043-1354(97)00216-9

Nowka, B., Daims, H., Spieck, E., 2015. Comparison of oxidation kinetics of nitrite-oxidizing bacteria: Nitrite availability as a key factor in niche differentiation. Appl. Environ. Microbiol. 81, 745–753. doi:10.1128/AEM.02734-14

Olm, M.R., Brown, C.T., Brooks, B., Banfield, J.F., 2017. DRep: A tool for fast and accurate genomic comparisons that enables improved genome recovery from metagenomes through

de-replication. ISME J. 11, 2864–2868. doi:10.1038/ismej.2017.126

Ondov, B.D., Treangen, T.J., Melsted, P., Mallonee, A.B., Bergman, N.H., Koren, S., Phillippy, A.M., 2016. Mash: Fast genome and metagenome distance estimation using MinHash. Genome Biol. 17, 1–14. doi:10.1186/s13059-016-0997-x

Peeters, J., Long, Z., Houweling, D., Côté, P., Daigger, G.T., Snowling, S., 2017. Nutrient Removal Intensification with MABR–Developing a Process Model Supported by Piloting. Proc. Water Environ. Fed. 2017, 657–669.

Pinto, A.J., Marcus, D.N., Ijaz, Z., Bautista-de los Santos, Q.M., Dick, G.J., Raskin, L., 2015. Metagenomic Evidence for the Presence of Comammox Nitrospira-Like Bacteria in a Drinking Water System. mSphere 1, e00054-15. doi:10.1128/mSphere.00054-15

Pochana, K., Keller, J., 1999. Study of Factors Affecting Simultaneous Nitrification and Denitrification (SND). Water Sci. Technol. 39, 61–68.

R Core Team, 2016. R: A Language and Environment for Statistical Computing.

Regmi, P., Bunce, R., Miller, M.W., Park, H., Chandran, K., Wett, B., Murthy, S., Bott, C.B., 2015. Ammonia-based intermittent aeration control optimized for efficient nitrogen removal. Biotechnol. Bioeng. 112, n/a-n/a. doi:10.1002/bit.25611

Regmi, P., Miller, M.W., Holgate, B., Bunce, R., Park, H., Chandran, K., Wett, B., Murthy, S., Bott, C.B., 2014. Control of aeration, aerobic SRT and COD input for mainstream nitritation/denitritation. Water Res. 57, 162–71. doi:10.1016/j.watres.2014.03.035

Reim, A., Lüke, C., Krause, S., Pratscher, J., Frenzel, P., 2012. One millimetre makes the difference: high-resolution analysis of methane-oxidizing bacteria and their specific activity at the oxic-anoxic interface in a flooded paddy soil. ISME J. 6, 2128–39. doi:10.1038/ismej.2012.57

Rios-Del Toro, E.E., Cervantes, F.J., 2016. Coupling between anammox and autotrophic denitrification for simultaneous removal of ammonium and sulfide by enriched marine sediments. Biodegradation 27, 107–118. doi:10.1007/s10532-016-9759-4

Russ, L., Speth, D.R., Jetten, M.S.M.M., Op den Camp, H.J.M.M., Kartal, B., 2014. Interactions between anaerobic ammonium and sulfur-oxidizing bacteria in a laboratory scale model system. Environ. Microbiol. 16, 3487–3498. doi:10.1111/1462-2920.12487

Stadler, L.B., Love, N.G., 2016. Impact of microbial physiology and microbial community structure on pharmaceutical fate driven by dissolved oxygen concentration in nitrifying bioreactors. Water Res. 104, 189–199.

Tansel, B., Sager, J., Rector, T., Garland, J., Strayer, R.F., Levine, L., Roberts, M., Hummerick, M., Bauer, J., 2005. Integrated evaluation of a sequential membrane filtration system for recovery of bioreactor effluent during long space missions. J. Memb. Sci. 255, 117–124. doi:10.1016/j.memsci.2005.01.028

Terada, A., Lackner, S., Tsuneda, S., Smets, B.F., 2007. Redox-stratification controlled biofilm

(ReSCoBi) for completely autotrophic nitrogen removal: the effect of co- versus counter-diffusion on reactor performance. Biotechnol. Bioeng. 97, 40–51. doi:10.1002/bit.21213

Thorup, C., Schramm, A., 2017. Disguised as a Sulfate Reducer: Growth of the Deltaproteobacterium Desulfurivibrio alkaliphilus by Sulfide Oxidation with Nitrate. MBio 8, 1–9.

Van Den Berg, E.M., Van Dongen, U., Abbas, B., Van Loosdrecht, M.C.M., 2015. Enrichment of DNRA bacteria in a continuous culture. ISME J. 9, 2153–2161. doi:10.1038/ismej.2015.26

van Dongen, S., Abreu-Goodger, C., 2012. Using MCL to Extract Clusters from Networks, in: van Helden, J., Toussaint, A., Thieffry, D. (Eds.), Bacterial Molecular Networks: Methods and Protocols. Springer New York, New York, NY, pp. 281–295. doi:10.1007/978-1-61779-361-5_15

van Kessel, M.A.H.J., Speth, D.R., Albertsen, M., Nielsen, P.H., Huub, J.M., 2015. Complete nitrification by a single microorganism. Nature 528, 555–559. doi:10.1038/nature16459

Warembourg, F.R., 1993. Nitrogen fixation in soil and plant systems. Nitrogen Isot. Tech. 127–156.

Wrighton, K.C., Thomas, B.C., Sharon, I., Miller, C.S., Castelle, C.J., Verberkmoes, N.C., Wilkins, M.J., Hettich, R.L., Lipton, M.S., Williams, K.H., Long, P.E., Banfield, J.F., 2012. Fermentation, Hydrogen, and Sulfur Metabolism in Multiple Uncultivated Bacterial Phyla. Science. 337, 1661–1665.

Yin, Z., Xie, L., Zhou, Q., 2015. Effects of sulfide on the integration of denitrification with anaerobic digestion. J. Biosci. Bioeng. 120, 426–431. doi:10.1016/j.jbiosc.2015.02.004

# CHAPTER 5.

## THE IMPACT OF SULFIDE ON THE PERFORMANCE OF A MEMBRANE AERATED BIOFILM REACTOR

Jeseth Delgado Vela[1], Kelly J. Gordon[2], Zerihun A. Bekele[1], Judith Klatt[3], Greg Dick[4], Nancy Love[1]

[1]Department of Civil and Environmental Engineering, University of Michigan
[2]Black and Veatch
[3]Max Planck Institute for Marine Microbiology
[4]Department of Earth and Environmental Sciences, University of Michigan

### 5.1 Abstract

As the population in coastal communities continues to increase and nitrogen regulations become more stringent in these coastal regions, innovation can help build more resource efficient wastewater treatment. An emerging innovation in the wastewater treatment field is the application of membrane aerated biofilm reactors (MABRs) as low-energy and small-footprint technologies. MABRs use membranes to supply diffused oxygen to a bioreactor and to support a biofilm that removes nitrogen. The purpose of this study was to evaluate the impact of sulfide on nitrogen cycling in a MABR. Influent sulfide was increased stepwise into a nitrifying MABR over 420 days, resulting in higher effluent ammonium concentrations. In addition, nitrous oxide emissions were higher when sulfide was in the influent. We show that apparent inhibition of nitrification was likely magnified by the presence of dissimilatory nitrate/nitrite reduction to ammonia (DNRA). Lastly, modeling was used to evaluate the potential importance of DNRA using nitrite or nitrate as an electron acceptor. Results show that future experimental work is needed to determine the sulfide to nitrogen ratios that select for denitrification or DNRA, because this affects model outcomes. In general, the results described here are an initial step for implementing coupled sulfur and nitrogen cycling in a membrane aerated biofilm reactor for wastewater treatment.

## 5.2 Introduction

There is growing interest in linking the carbon, nitrogen, and sulfur cycles for biological wastewater treatment. This could be advantageous in parts of the country that are facing stringent effluent nitrogen requirements and must add external carbon to meet regulations. Using hydrogen sulfide as an electron donor for denitrification can reduce the need for external carbon. Using sulfide for denitrification is appropriate for wastewaters that have relatively high concentrations of sulfur such as systems under the influence of seawater intrusion into sewers or systems that use seawater for toilet flushing as a water conservation strategy. Sulfide-rich wastewater would also result from anaerobic treatment processes because sulfate reducing bacteria convert the sulfate to hydrogen sulfide. For these reasons, there is ongoing research on harnessing sulfide as an electron donor for denitrification (Guo et al., 2016; Kalyuzhnyi et al., 2006; Sahinkaya et al., 2014; Sánchez-Ramírez et al., 2014; Souza and Foresti, 2013; Wang et al., 2009; Yang et al., 2016a). Many published studies have focused on two stage nitrogen removal but there have been relatively few studies evaluating the impact of hydrogen sulfide on nitrogen removal in single-stage nitrogen removal reactors that support oxic and anoxic environments (Moraes et al., 2012; Xue et al., 2017).

One challenge with using hydrogen sulfide as an electron donor for denitrification is that sulfide is known to inhibit both anammox and heterotrophic denitrifiers (Russ et al., 2014; Sorensen et al., 1980). Inhibition constants for anammox bacteria are as low as 0.32 mg/L as S (Russ et al., 2014). However inhibition is not always observed and active anammox bacteria can be found in the presence of sulfide (Jones et al., 2017; Russ et al., 2014). In these studies, sulfide oxidizing bacteria reduce the concentrations of sulfide to below inhibitory levels and reduce nitrate to ammonium (Jones et al., 2017) or nitrite (Russ et al., 2014), providing necessary substrates for anammox growth. In heterotrophic denitrification, sulfide can inhibit the nitrous oxide reductase enzyme (Schonharting et al., 1998; Sorensen et al., 1980), which would increase nitrous oxide ($N_2O$) emissions (Liu et al., 2016; Zhang et al., 2015). Similar to annamox inhibition, increased $N_2O$ due to sulfide is not always observed (Yang et al., 2016b). Understanding what is driving sulfide-induced $N_2O$ emissions is critical because $N_2O$ is almost 300 times more potent a greenhouse gas than $CO_2$ over a 100 year timescale (Solomon et al., 2007). Furthermore, in the U.S., emissions of $N_2O$ during wastewater treatment have been increasing over the past 10 years

(U.S. Environmental Protection Agency, 2017), and $N_2O$ can represent more than half of the total greenhouse gas emissions from wastewater treatment processes (Foley et al., 2010). The use of sulfide as an electron donor for denitrification necessitates an improved understanding of how to minimize sulfide inhibition to avoid higher $N_2O$ emissions and diminishes anammox activity.

Sulfide also inhibits nitrification processes (Erguder et al., 2008; Zhou et al., 2014). However, one aspect that complicates our understanding of sulfide inhibition of nitrification in mixed redox environments is that sulfide can induce dissimilatory nitrate reduction to ammonium (DNRA) (Brunet and Garcia-Gil, 1996). At higher sulfide/N ratios, nitrate gets reduced to ammonium, while at lower sulfide/N ratios denitrification occurs (Dolejs et al., 2014; Yin et al., 2015). Importantly, it is difficult to differentiate between increases in effluent ammonium due to its by DNRA and its accumulation due to nitrification inhibition. Multiple redox environments in close proximity can further obfuscate differentiating between these processes. In Chapter 4 we demonstrated rapid sulfide-induced DNRA in a mixed-redox biofilm system—rates of DNRA could be higher than rates of ammonia oxidation. Therefore, in mixed redox environments, it is important to consider that DNRA may appear to be sulfide inhibition of nitrification.

In this study, we tested the impact of stepwise sulfur increases on nitrogen cycling in a membrane aerated biofilm reactor (MABR) over 420 days. In an MABR reactor configuration, air is supplied to a biofilm by oxygen permeable membranes. This system provides multiple redox environments that support the growth of both aerobic and anaerobic metabolisms (Downing and Nerenberg, 2008; Gilmore et al., 2013). The electron donor and acceptor flow into the biofilm in opposite directions, so unlike conventional biofilms used in wastewater bioprocesses, MABRs uniquely maintain a counter-diffusional biofilm. In this counter-diffusional biofilm, sulfide is amended into an anoxic bulk liquid, preventing rapid sulfide oxidation with oxygen. Furthermore, membrane aeration eliminates gas stripping, preserving hydrogen sulfide in the liquid phase. Together, these features of an MABR enable the use of sulfide as an electron donor for denitrification. Here, we show that nitrification was inhibited by sulfide in the MABR but we suggest that the extent of nitrification inhibition appeared higher due to the activity of DNRA. We used one-dimensional biofilm modeling to evaluate the potential impact of DNRA in the MABR. From this, we found that nitrate based DNRA is more likely to be important, but more work is needed to understand

the metabolic switch between denitrification and DNRA and to evaluate electron donors for DNRA beyond sulfide. In addition, we observed increased nitrous oxide emissions in the presence of sulfide, indicating inhibition during the last step of denitrification. We show that metal precipitation occurred and may also be an indirect mechanism of inhibition. Overall, we present advantages and impediments that need to be addressed for the implementation of coupled sulfur and nitrogen cycling in a membrane aerated biofilm reactor for wastewater treatment.

## 5.3 Materials and Methods

### *5.3.1 Sample analysis*

The MABR was inoculated and operated as described in Chapter 4. Approximately three times per week, samples were collected in the recirculation line of the reactor. All samples were filtered using a washed 0.45 µm nitrocellulose filter (Fisher Scientific), and analyzed for multiple soluble inorganic species based on Standard Methods (APHA et al., 2005). The phenate method (method 4500-$NH_3$ F) was used to determine ammonium concentrations. Nitrite was determined colorimetrically (method 4200-$NO_2^-$ B), and ion chromatography was used to determine nitrate and sulfate concentrations (method 4110-B). Iron, molybdenum, and copper were monitored because these metals readily precipitate with sulfide and are in the active site of nitrifying enzymes (Gilch et al., 2009; Meincke et al., 1992; Zahn et al., 1996). For analysis of these metals, samples were acidified (1% nitric acid) and analyzed via ICP/MS according to methods 3010, 3125B, 3111B, and 3111D (APHA et al., 2005). Approximately every two weeks, samples were collected, stored, and analyzed for sulfide according to method 4500-$S^{2-}$ G. Sulfide samples were diluted (2x) in sulfide antioxidant buffer, were immediately transferred to the anaerobic chamber, filtered (0.45 µm) and preserved in the dark. All samples were analyzed within 2 hours. Sulfide was analyzed using a silver sulfide electrode (Thermo Scientific, Orion) that was calibrated by making standards with a 3% (w/v) sodium sulfide stock solution (Ricca Chemical Company), according to method 4500-$S^{2-}$ G (APHA et al., 2005). In addition to analyzing inorganic species influent and effluent dissolved methane were sampled and analyzed approximately weekly using established methods (Rudd et al., 1974). Briefly, 30 mL of sample was collected into a vial with 30 mL of $N_2$ gas. The syringe was shaken by hand for 1 min to strip dissolved methane into the gas phase. The gas phase was analyzed immediately using gas chromatography with a flame ionization detector.

From days 509-519 was cycled on and off twice at 24-hour intervals to test the impact of a short-term pulsing condition. Samples for nitrogen, sulfide, metals, and sulfate were collected 30 minutes, 5 hours, 10 hours, and 23.5 hours after each change in sulfide concentration and analyzed according to the methods identified previously.

### *5.3.2 Microsensor measurements*

Microsensors were used to evaluate the profiles of sulfide, nitrous oxide, and oxygen in the reactor. Microsensor data were collected on days 505 and 545 at sulfide concentrations of 0 and 10 mg/L as S. For hydrogen sulfide and oxygen profiles, custom-made microsensors were built and calibrated as previously described (Jeroschewski et al., 1996; Revsbecht and Ward, 1983) with tip diameters of 50 and 15 µm, respectively. Microsensor signals of the $O_2$ and $H_2S$ sensors were processed by a custom-made picoampermeter and recorded with the Profix software (PyroScience, Aachen, Germany). For pH and nitrous oxide measurements, commercially available microsensors with 25 µm diameter tips were used (Unisense, Aarhus, Denmark). The $N_2O$ and pH microsensors were calibrated according to manufacturer's instructions. Signals were processed with a Unisense multimeter and the Unisense SensorTrace Logger software. Calculation of total sulfide from the local $H_2S$ concentrations and pH was carried out according to Millero (1986), using the $pK_a$ value of 7.04 (Jeroschewski et al., 1996; Wieland and Kühl, 2000).

Oxygen profiles were measured in intervals as low as 25 µm. The datum was taken to be the point of membrane deflection and profiles (at least 5) were made after the datum was established (Gilmore et al., 2009). The measured oxygen concentration at the point of membrane deflection (datum) was used to calculate the mass transfer of oxygen into the biofilm (oxygen flux). Oxygen flux was calculated by assuming the oxygen in the lumen was at saturation. This is justified because our flow-through MABR design allowed for constant air flow through the lumen (35 mL/minute); the gas residence time through the lumen was 3.7 seconds. This is significantly lower than a similarly designed system where a gas residence time of 3 minutes was sufficient to ensure oxic regions across the length of the reactor (Gilmore et al., 2009). While operating with this rapid gas flow did not maximize oxygen transfer efficiencies, the intent was to maintain a uniform oxygen gradient across the length of the biofilm and maximize the extent of oxygen mass transfer. The tradeoffs between oxygen mass transfer (i.e. flux) and oxygen transfer efficiencies (i.e. flux

relative to air supplied) have previously been described (Martin and Nerenberg, 2012; Perez-Calleja et al., 2017).

The flux through the lumen was calculated using the following equation:

$$J_{O2} = \frac{(S_l - S_m) * D}{t}$$

Where $S_l$ is the oxygen concentration in the lumen (assumed to be at saturation at room temperature, 8.3 mg/L), and $S_m$ is the measured oxygen concentration at the datum. D is the diffusion coefficient of oxygen for the membrane material which has previously been determined to be 2.22 X $10^{-5}$ $cm^2/s$ (Gilmore et al., 2009), and t is the thickness of the membrane, 0.06 cm.

### *5.3.3 Statistical analysis*

Associations between effluent parameters and sulfide were assessed using a repeated measures ANOVA. Differences in oxygen fluxes and nitrous oxide emissions were tested using the Wilcoxon rank sum test. All *p* values were corrected for multiple comparisons using the Benjamani-Hochberg correction factor.

### *5.3.4 One-dimensional biofilm model*

A one-dimensional biofilm model was developed using the well-established AQUASIM software (Reichert, 1994). The details of the kinetic equations and the parameters used are provided in Appendix C, Tables C1, C2, C3, and C4. The model simulation included relevant metabolisms: AOB, NOB, aerobic methanotrophs, denitrifying anaerobic methane oxidizers (nitrite and nitrate utilizing), anammox, aerobic heterotrophs, sulfide oxidizing bacteria, sulfate reducers, and sulfide-based denitrifiers (nitrite and nitrate utilizing). To calibrate the model, the parameters targeted for calibration were identified first using the normalized absolute-relative sensitivity function within AQUASIM. This function identifies how much each kinetic parameter impacts the simulated steady-state effluent total nitrogen concentrations (sensitivity and uncertainty). The sensitivity of the kinetic parameters were ranked to determine which parameters would be used for model calibration (Appendix C, Table C7). The three parameters that had the largest impact on the effluent ammonium, nitrite, and nitrate concentrations (top sensitivity ranking) were selected for parameter estimations. To test the potential importance of DNRA a switching function was added

between denitrification and DNRA with sulfide as an electron donor. The details of this function are outlined in Appendix C, Tables C5 and C6.

To conduct parameter estimation, effluent ammonia, nitrite, nitrate, and methane concentrations were randomly generated based on the distribution of effluent from the lab-scale bioreactor when the influent sulfide was 2 mg/L. This influent sulfide concentration was selected the 2 mg/L feeding regime had the highest number of effluent data points and allowed for model calibration. The simplex technique within AQUASIM's parameter estimation tool was used to estimate parameters based a randomly generated effluent. From this, we obtained a distribution of expected values for each parameter based on estimations from 200 distinct randomly generated effluent concentrations. Using this procedure, we calibrated the model while accounting for the variation and random effects in the lab-scale bioreactor (Appendix C, Figure C2). The parameter estimates were constrained by the upper and lower limits of values found in the literature (Delgado Vela et al., 2015). Following parameter estimation, the model calibration was validated by testing simulations across the range of influent sulfide concentrations utilized during the physical MABR experiments and evaluating whether model outputs were within the range of experimental results. The validation results are given in Appendix C, Figure C3.

## 5.4 Results and Discussion

### *5.4.1 Higher levels of effluent ammonium were observed as a result of sulfide addition.*

Over the stepwise increases in sulfide that lasted 420 days, we observed a decrease in the extent of ammonium oxidation, as measured by both increased ammonium and decreased nitrate in the effluent (Figure 5-1A). For example, 70±20% of the influent ammonium was oxidized prior to sulfide addition, but at the end of stepwise sulfide increases only 40±10% of influent ammonium was oxidized (ANOVA $p<0.001$). Sulfide was significantly associated with the concentrations of both effluent ammonium and nitrate (ANOVA $p<0.001$) specifically; increases in sulfide led to increased effluent ammonium and decreased effluent nitrate concentrations. Initially, a loss of ammonium oxidation could be observed with an increase in sulfide to just 0.1 mg S/L. Ammonium oxidation subsequently recovered, and it took higher concentrations of sulfide (between 2 and 3 mg/L as S) to reach the same effluent ammonium concentrations that were observed when influent sulfide was 0.1 mg S/L. This implies that there was an initial inhibition shock, but the nitrifiers

subsequently adapted to sulfide. Furthermore, we found that when ammonium concentrations were elevated due to the presence of sulfide, the higher ammonium levels were maintained even after the sulfide concentration was reduced; therefore the extent of nitrification did not return to pre-sulfide levels over reactor operation (Figure 5-1, shaded region). The sustained increases in effluent ammonium after sulfide addition is similar to a previous study (Erguder et al., 2008). In both this study and previous studies, sulfide inhibition of ammonia oxidation was sustained even after sulfide was removed from the influent, but we do not know the mechanism for this phenomenon.

One potential explanation for the loss of nitrification is that sulfide is rapidly oxidized aerobically through both biotic and abiotic processes and exerts an oxygen demand that competes with nitrification. Assuming that sulfide was fully oxidized to sulfate (Appendix C, Figure C4, average recoveries are 99 ± 27 %), and that ammonium was oxidized completely to nitrate (no nitrite accumulation, Figure 5-1) stoichiometric calculations predict that the additional oxygen demand due to sulfide would only account for a 9% loss of nitrification (calculations summarized in Appendix C). This is less than the loss of nitrification we observed (30% of the influent nitrogen). Furthermore, the molecular evidence from Chapter 4 suggest that the sulfide was oxidized biologically in anoxic regions of the bioreactor by denitrifying organisms, so sulfide would not exert an oxygen demand. In fact, measured oxygen fluxes significantly decreased with the addition of sulfide from an average oxygen flux of 2.1±0.4 g $O_2/m^2$-day in the absence of sulfide to 1.4±0.2g $O_2/m^2$-day when sulfide was present (Appendix C Figure C5, Wilcoxon $p<0.05$). For these reasons, oxygen limitation due to the addition of sulfide is not a likely mechanism of nitrification inhibition.

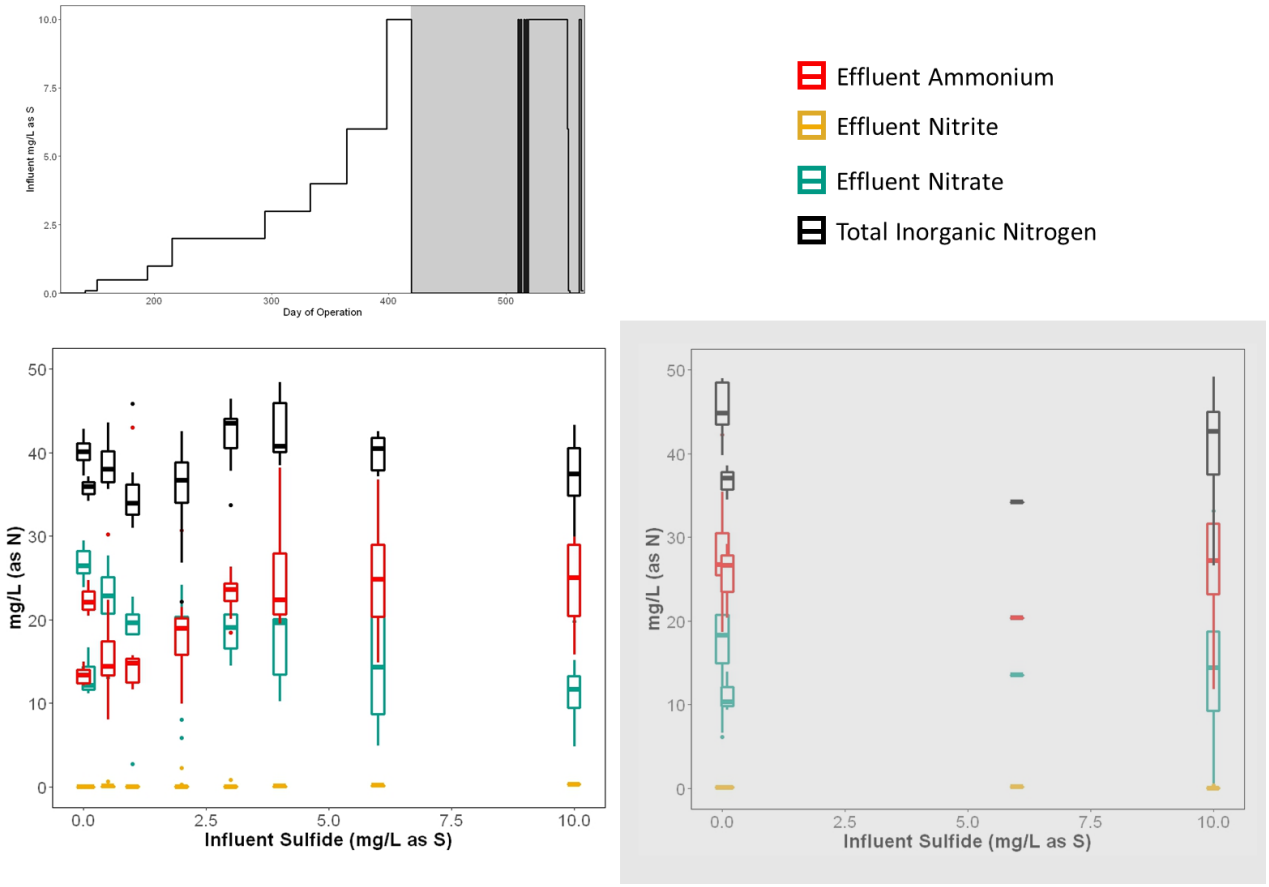


**Figure 5-1.** Effluent nitrogen quality. Top left is sulfide feeding regime during stepwise increases and subsequent experiments (shaded). Bottom left is sulfide during stepwise increases in sulfide. Bottom right is after stepwise experiments were complete (shaded timeframe in top left).

In contrast to Chapter 3 and other studies of nitrification in the presence of sulfide (Bejarano-Ortiz et al., 2015; Erguder et al., 2008), nitrite accumulation was not observed. Most previous studies of sulfide inhibition of nitrification were conducted under batch conditions. We therefore chose to test whether nitrite accumulation would occur in the MABR under short term pulses. We found that even under 24-hour sulfide pulses, there was no nitrite accumulation in the reactor (Figure 5-2). However, ammonium increased and nitrate decreased during the 24-hour period. It is worth noting that the pulse experiment occurred after the long-term experiment (days 509-512). Therefore, the response from nitrifying populations was likely affected by the history of sulfide exposure. The findings may have been different if the pulse experiment was done before the long-term step increases in sulfide. In any case, the results from these short-term pulse experiments

confirm that even under short-term exposures, sulfide increased effluent ammonia concentrations and reduced effluent nitrate, but did not result in nitrite accumulation.

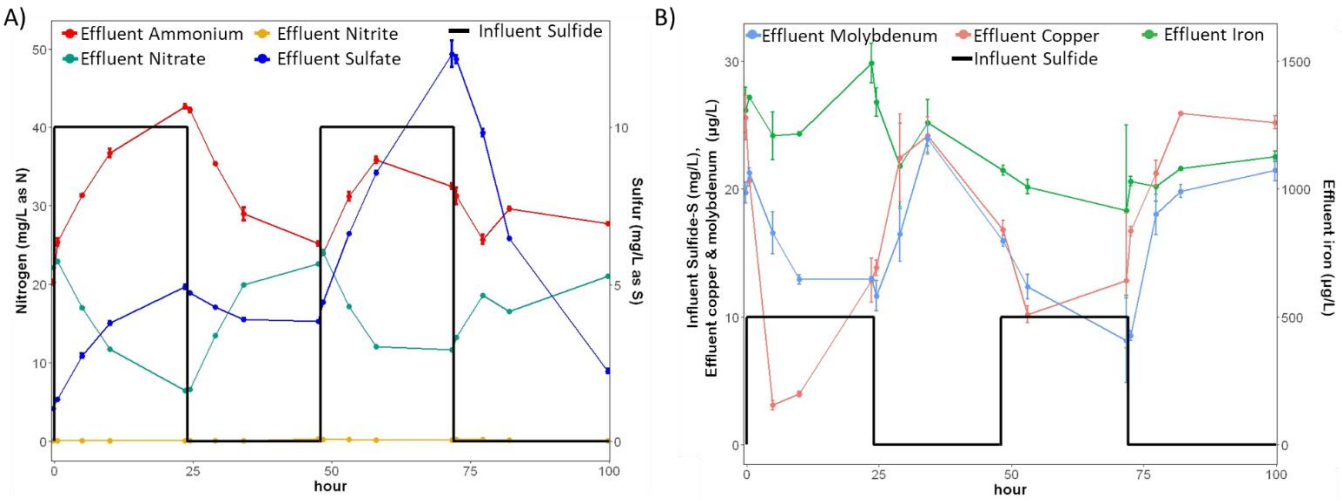


**Figure 5-2.** Effluent concentrations under short-term pulses of sulfide (Phase D-1). Ammonium, nitrite, nitrate, and sulfate are on the left plot; Trace metals (molybdenum, copper, and iron) are on the right plot. The solid black line represents the influent concentration of sulfide during the experiment.

DNRA would make bulk liquid profiles appear as a loss of nitrification, and a previous study of this MABR system (Chapter 4) indicated that DNRA with nitrite as the electron acceptor was very favorable in the presence of sulfide. To further evaluate if DNRA was possible, we conducted a stoichiometric analysis comparing oxygen fluxes and measured effluent data. Since sulfide was consumed in the anoxic regions and there was no change in methane oxidation, the decreases in oxygen fluxes are assumed to be associated with reduced oxygen consumption due to sulfide-inhibition of nitrifying organisms because nitrifying organisms. Measured changes in oxygen fluxes result in a 33% reduction in oxygen consumption. However, for the extent of inhibition observed, oxygen fluxes should be reduced by 43% percent, assuming complete nitrification to nitrate (calculations detailed in Appendix C). Therefore, the stoichiometrically-determined decrease in oxygen consumption for nitrification in the presence of sulfide inhibition was larger than the measured decrease in oxygen flux. Stoichiometry predicts that DNRA with sulfide as the electron donor and nitrite as the electron acceptor would result in an increase of ammonium concentrations to 5.8 mg N/L, which is less than the observed increases of 12 mg N/L. Figure 5-3A shows the combination of these calculations. The results show that there was likely some

combination of DNRA and nitrification inhibition due to sulfide that contributed to the observed effluent ammonium concentration. Furthermore, we previously showed that DNRA rates were almost 50% faster than ammonia oxidation rates when sulfide was present, thus DNRA is an important process to consider in this system. An important distinction between these two studies is that in Chapter 4 the DNRA rates were determined when the reactor was operated in batch mode, so the initial sulfide exposure was higher (10 mg/L at the beginning of the experiment) than what was observed throughout this study. In addition, operating in batch mode will create a different physiological state by the bacteria and, possibly, different metabolic outcomes. However, in combination with the rates and genetic markers discussed in Chapter 4, this analysis indicates that DNRA was likely contributing to the observed accumulation of ammonium.

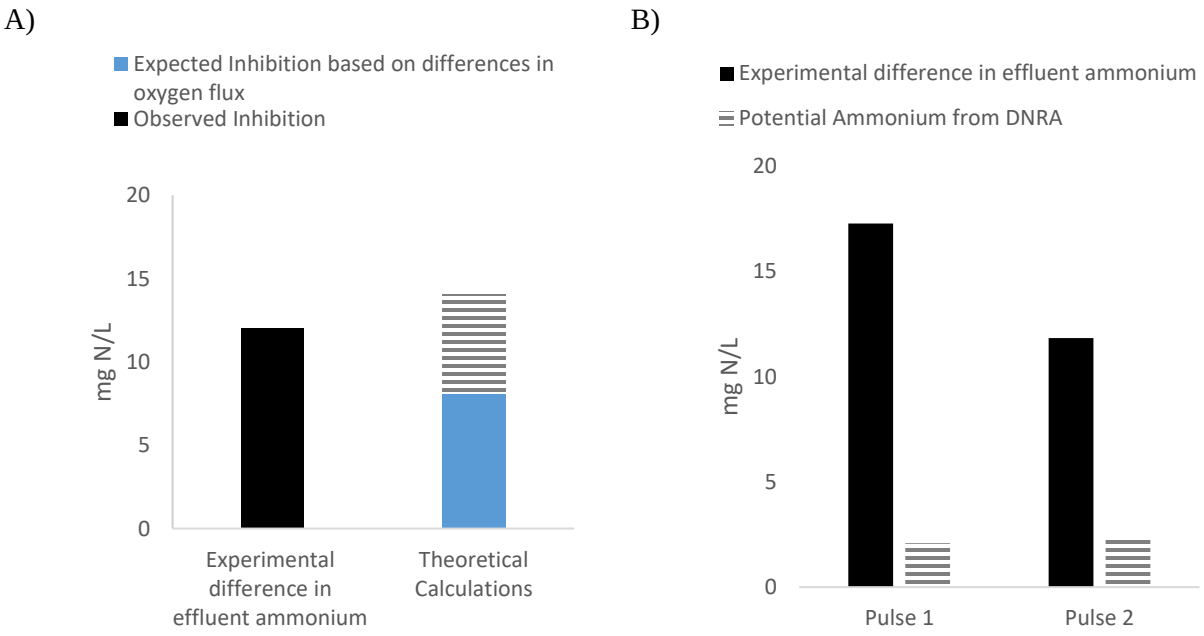


**Figure 5-3.** A) Comparison of observed differences in effluent ammonium (0 vs 10 mg S/L in influent) compared with theoretical contributions of inhibition (based on change of oxygen flux) and DNRA (assuming all sulfide is used to reduce nitrite to ammonia) B)Comparison of observed differences in effluent ammonium for sulfide-pulse experiments (first data point versus last data point for each pulse) and potential DNRA calculated from the sulfate produced over that time period assuming nitrite is electron acceptor. All calculations summarized in Appendix C.

An additional line of evidence supporting the presence of DNRA in this system is the close association between effluent sulfate and effluent ammonium during the pulse experiment (Figure 5-2), especially evident the initial pulse. As shown in Figure 5-3B, based on the increase in sulfate,

effluent ammonium exceeds the potential ammonium produced from DNRA. During these experiments, the rates of ammonium production (1 ±0.4 mg N/L-hr, average between first and second pulse) exceed the rates of sulfate production (0.3 ± 0.2 mg S/L-hr). For a DNRA process using nitrite as an electron acceptor, the molar ratio of sulfate to ammonium is 3:4. Therefore, this rate of sulfate production would produce ammonium at a rate of 0.2 ± 0.1 mg N/L-hr. These results indicate that sulfide-based DNRA is not the only reason for ammonium accumulation during the pulse experiments. However, these predicted rates are plausible as they are well below the predicted rates based on experiments from Chapter 4 (2 ± 0.4 mg N/L-hr). In these calculations (Figure 5-3) from both the long-term operation and the pulse experiments, DNRA had the potential to account for up to 50% of the effluent ammonium observed in the reactor. The DNRA potentials we have presented assume sulfide is being used as the electron donor. As indicated in Chapter 4, methane-based reduction of nitrite to ammonium would contribute to additional effluent ammonia and warrants further study. Overall, the results show that the effect of DNRA can be significant and needs to be accounted for in processes that aim to use sulfide for denitrification.

An additional point that supports the potential for DNRA masking observed inhibition is the spatial distribution of bacteria in the MABR. The nitrifying populations were in the aerobic region, which is the innermost portion of the biofilm. Our bulk liquid sulfide measurements and microsensor profiles showed that the bulk liquid concentration of sulfide in the reactor was low. The bulk liquid sulfide measurements were below the detection limit of the silver/sulfide electrode(<0.6 mg S/L) over the course of reactor operation, and the microsensor measurements in the bulk liquid were 0.5 ±0.4 mg S/L. Using the most conservative inhibition parameters that were previously determined (7.4 mg S/L for AOB (Delgado Vela et al., 2018)), we predict that AOB inhibition would be 6 percent at most (calculations detailed in Appendix C), whereas our observed increases in ammonium concentration were 30 percent. Inhibition constants were generated in batch cultures, so long-term inhibition may be different. Furthermore, there was a loss of nitrifying populations as sulfide increased (Chapter 4), so some degree of inhibition did contribute to the loss of ammonium oxidation. Nevertheless, the observed inhibition is higher than what one would predict given the inhibition constants that are available in the literature.

To effectively utilize sulfide as an electron donor during wastewater treatment we need to understand the conditions where sulfide-induced DNRA exceeds denitrification. Previous studies of wastewater treatment systems have shown that DNRA occurs when sulfide to $NO_3^-$-N ratios are above 1.6-3 g S/g N (Dolejs et al., 2014; Yin et al., 2015). In this study, sulfide was rapidly consumed, so sulfide to nitrate ratios were low. However, we did not find sulfide to $NO_2^-$-N ratios in the literature that encourage DNRA. Although both effluent sulfide and nitrite were very low, the concentration of sulfide exceeded nitrite substantially (4.1±2.02 g S/g N). Overall, these findings show that there is an opportunity to use the existing literature to test a dynamic process of how to induce denitrification over DNRA in engineered systems.

### *5.4.1 Modeling reveals the potential importance of DNRA.*

Biofilm modeling was used to expand our understanding of MABR operation and test operational conditions to promote denitrification over DNRA. After calibration, NOB were predicted to two times faster $\mu_{max}$ values (Appendix C, Table C3) than AOB. Although these values were constrained by what is present in the literature (previously reviewed (Delgado Vela et al., 2015)), the calibrated NOB was in the upper range of what the literature suggests is possible. This is consistent with Chapter 4 where the rates of NOB were an order of magnitude faster than rates of AOB. Substrate affinity affects rates of oxidation, so the $\mu_{max}$ value is not directly comparable to the rates presented in Chapter 4. Nevertheless, the rates still function as an independent validation of the model calibration procedure. Despite this independent check of the calibration procedure, the outcomes of the model are not representative of the effluent chemistry observed in the lab-scale bioreactor (Appendix C, Figure C3). The model consistently predicts higher effluent ammonia and lower effluent nitrate than what was observed experimentally. This indicates that there are some processes occurring that are not captured in our current model.

We chose to test whether incorporating sulfide-based DNRA would generate results that are more consistent with our experimental results. We developed a version of the model that incorporated DNRA from nitrite or nitrate using sulfide as the electron donor. To achieve this goal we incorporated a switching function based on two studies that determined the ratio of sulfide to nitrate needed to go from denitrification to DNRA processes (Dolejs et al., 2014; Yin et al., 2015). In this modeling framework, sulfide-based denitrifies will produce ammonium or nitrate,

depending on the ratio of sulfide to nitrate. We applied this ratio to both nitrite and nitrate based denitrifiers. Results show that the approach used to incorporate DNRA had a minimal impact on modeling results (Figure 5-4). DNRA increased ammonium concentrations by at most 1% over baseline concentrations and this only occurred when nitrate was the electron acceptor and when the denitrification to DNRA switching function was minimized (Figure 5-4, Nitrate Low Switch). These results indicated that sulfide-based DNRA is possible in the MABR, but is not sufficient to account for observed increases in ammonium. However, future work should focus on a more thorough evaluation of the switching function since the value selected can have a significant impact on simulated results. Furthermore, modeling frameworks for alternative electron donors for DNRA need to be developed to fully understand the potential impact of DNRA.

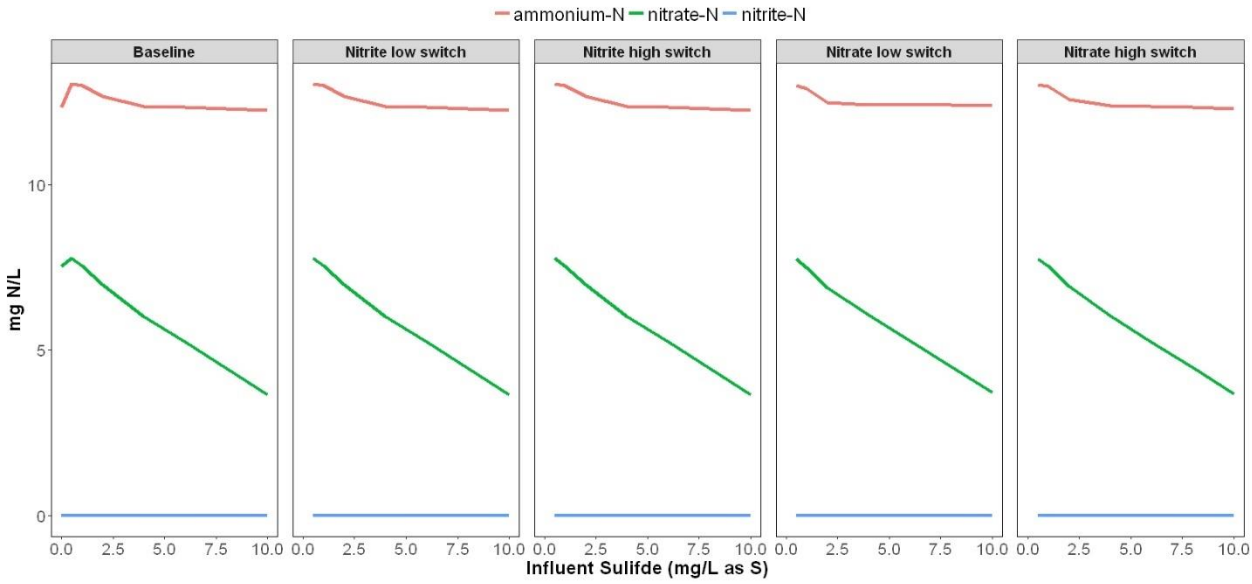


**Figure 5-4.** Results from modeling. Left panel is baseline results. Right panes indicate electron acceptor used for DNRA (nitrite or nitrate) and value of critical S to N ratio where DNRA occurs. "Low switch" indicates S to N ratio was 1.5; "high switch" indicates S to N ratio was 3.

### *5.4.2 The MABR mitigated methane emissions, but sulfide inhibited nitrous oxide reduction.*

To assess the environmental sustainability of using an MABR for anaerobic effluents we tested the effect of sulfide on greenhouse gas emissions. Over the course of the experiment on average 81±15 % of the influent methane was oxidized, and this did not change with increasing sulfide concentration. Therefore, the MABR is suitable for mitigating the global warming potential associated with methane emissions from mainstream anaerobic effluents. Previous studies have

shown that MABRs have low nitrous oxide ($N_2O$) emissions (Gilmore et al., 2013; Peng et al., 2016) because the counter diffusional nature of the MABR biofilm provides $N_2O$ sinks (Kinh et al., 2017). However, sulfide inhibition of nitrous oxide reduction causes increased $N_2O$ emissions (Liu et al., 2016; Zhang et al., 2015) and $N_2O$ represents an important contributor to greenhouse gas emissions from wastewater treatment plants. Therefore, it is important to understand how increased $N_2O$ emissions due to sulfide compare with the overall low $N_2O$ emissions we expect from an MABR system.

Nitrous oxide emissions were higher when sulfide was in the influent compared to measurements done without sulfide (Wilcoxon $p$< 2.2E-16). According to nitrous oxide microsensor profiles, we found that the bulk liquid nitrous oxide concentrations were 0.13 ± 0.02 mg N/L with sulfide (day 544) and 0.001 ± 0.007 mg N/L without sulfide (day 467). Without sulfide these emissions (0.002% of influent ammonium, Appendix C) are well below what has been previously reported for other simultaneous nitrification and denitrification systems (Kampschreur et al., 2009) and are consistent with previous MABR studies (Gilmore et al., 2013; Kinh et al., 2017). When sulfide was in the influent the emissions factor (0.25%) was higher than what was previously reported for MABR systems. However, these emissions factors are still lower than what has been reported for many other simultaneous nitrification and denitrification systems (Kampschreur et al., 2009). Our finding that increased sulfide led to increased emissions of $N_2O$ is consistent with previous studies in a variety of environments (Brunet and Garcia-Gil, 1996; Senga et al., 2006), including activated sludge (Manconi et al., 2006; Tugstas and Pavlostathis, 2007). The most likely explanation is that sulfide inhibits the nitrous oxide reductase (Sorensen et al., 1980). Understanding the mechanisms of inhibition of the nitrous oxide reductase can help identify strategies to mitigate this inhibition effect and reduce the greenhouse gas emissions of the process.

### *5.4.3 Sulfide precipitation with trace metals is a potential mechanism of inhibition for both nitrifying and denitrifying bacteria.*

One potential mechanism of sulfide inhibition is the loss of enzyme cofactors and trace nutrients due to precipitation with sulfide. We evaluated this inhibition mechanism by monitoring dissolved iron, copper, and molybdenum in the influent and effluent of the reactor. To mimic anaerobic effluents, we added a reduced form of iron (II) that has a favorable precipitation reaction with

sulfide. Over the course of the reactor operation, both influent and effluent iron decreased with increased sulfide concentrations (Appendix C, Figure C6, ANOVA $p<0.01$). Black precipitates were observed in the tubing at the mixing point between the sulfide feed and the influent line, consistent with formation of iron sulfides. Iron is found in the catalytic core of both the ammonia monooxygenase (Zahn et al., 1996) and the nitrite oxidoreductase enzymes (Meincke et al., 1992), and is known to stimulate the activity of enzymes involved in both nitrification and denitrification (Chen et al., 2018). However, when we compared both influent and effluent iron with concentrations of nitrogen species we found no statistically significant associations (ANOVA $p>0.2$). Consequently, although iron precipitation occurred, there is no evidence that it was a primary mechanism of inhibition.

Effluent molybdenum and influent copper were also significantly associated with the influent sulfide (Appendix B Figure C7, ANOVA $p<0.01$). The rapid precipitation of copper and molybdenum was also evident in our pulse exposure experiments (Figure 5-2B). Copper is found in the catalytic core of the ammonia monooxygenase enzyme (Gilch et al., 2009) and molybdenum is found in the catalytic core of the nitrite oxidoreductase enzyme (Meincke et al., 1992). When we compared effluent copper and molybdenum to the effluent nitrogen data we found that both species had significant associations with ammonium removal (ANOVA $p<0.05$). While this test of statistical significance could be an artifact of sulfide precipitation, copper has been known to have a strong effect on ammonia loss in nitrifying activated sludge (Braam and Klapwijk, 1981). Interestingly, one study showed that copper limitations due to sulfide precipitation caused inhibition of the nitrous oxide reductase enzyme (Manconi et al., 2006). The media concentrations used in that study (0.2 µM) are similar to the influent concentrations we measured during reactor operation (0.38 µM ± 0.07 µM). When Manconi and co-authors supplemented their cultures with 60 µM of copper, effluent $N_2O$ decreased. This mechanism could explain why increased $N_2O$ due to sulfide is not consistently shown in the literature (Yang et al., 2016b). Accordingly, studies showing no effect of sulfide on $N_2O$ emissions could have higher soluble copper levels so the nitrous oxide reductase is unaffected by sulfide. In contrast to copper, fewer studies have evaluated the importance of molybdenum (Finstein and Delwiche, 1965). Although precipitation of copper and molybdenum was not as clear of an effect compared to iron precipitation (Appendix C, Figures

C6 and C7), the limitation of copper and molybdenum is an important possible mechanism of sulfide inhibition that warrants future study.

In conclusion we found evidence of inhibition of nitrification and denitrification. Importantly, the apparent extent of nitrification inhibition observed in the reactor was likely magnified due to the presence of DNRA. Simulation results suggest that DNRA with sulfide can increase effluent ammonium concentrations. Denitrification inhibition manifested with increased nitrous oxide emissions. An important candidate mechanism of inhibition that warrants further study is sulfide precipitation with copper. Indeed, if copper limitation is a primary mechanism of inhibition, it could serve as a means for mitigating the higher nitrous oxide emissions observed with sulfide-based denitrification systems.

## 5.5 References


APHA, AWWA, WEF, 2005. Standard methods for the examination of water and wastewater, 21st ed. Washington D.C.

Bejarano-Ortiz, D.I., Huerta-Ochoa, S., Thalasso, F., Cuervo-López, F. de M., Texier, A.C., 2015. Kinetic Constants for Biological Ammonium and Nitrite Oxidation Processes Under Sulfide Inhibition. Appl. Biochem. Biotechnol. 177, 1665–1675. doi:10.1007/s12010-015-1844-3

Braam, F., Klapwijk, A., 1981. Effect of copper on nitrification in activated sludge. Water Res. 15, 1093–1098. doi:10.1016/0043-1354(81)90077-4

Brunet, R.C., Garcia-Gil, L.J., 1996. Sulfide-induced dissimilatory nitrate reduction to ammonia in anaerobic freshwater sediments. FEMS Microbiol. Ecol. 21, 131–138. doi:10.1016/0168-6496(96)00051-7

Castro-Barros, C.M., Jia, M., van Loosdrecht, M.C.M., Volcke, E.I.P., Winkler, M.K.H., 2017. Evaluating the potential for dissimilatory nitrate reduction by anammox bacteria for municipal wastewater treatment. Bioresour. Technol. 233, 363–372. doi:10.1016/j.biortech.2017.02.063

Chen, H., Zhao, X., Cheng, Y., Jiang, M., Li, X., Xue, G., 2018. Iron Robustly Stimulates Simultaneous Nitrification and Denitrification Under Aerobic Conditions. Environ. Sci. Technol. acs.est.7b04751. doi:10.1021/acs.est.7b04751

Chen, X., Ni, B., 2016. Model-based evaluation on simultaneous nitrate and arsenite removal in a membrane biofilm reactor. Chem. Eng. Sci. doi:10.1016/j.ces.2016.06.049

Delgado Vela, J., Dick, G.J., Love, N.G., 2018. Sulfide inhibition of nitrite oxidation in activated sludge depends on microbial community composition. Water Res. 138, 241–249.

Delgado Vela, J., Stadler, L.B., Martin, K.J., Raskin, L., Bott, C., Love, N.G., 2015. Prospects for

Biological Nitrogen Removal from Anaerobic Effluents during Mainstream Wastewater Treatment. Environ. Sci. Technol. Lett. 2, 233–244. doi:10.1021/acs.estlett.5b00191

Dolejs, P., Paclík, L., Maca, J., Pokorna, D., Zabranska, J., Bartacek, J., Paclik, L., Maca, J., Pokorna, D., Zabranska, J., Bartacek, J., Paclík, L., Maca, J., Pokorna, D., Zabranska, J., Bartacek, J., 2014. Effect of S/N ratio on sulfide removal by autotrophic denitrification. Appl. Microbiol. Biotechnol. 99, 2383–2392. doi:10.1007/s00253-014-6140-6

Downing, L.S., Nerenberg, R., 2008. Total nitrogen removal in a hybrid, membrane-aerated activated sludge process. Water Res. 42, 3697–3708. doi:10.1016/j.watres.2008.06.006

Erguder, T.H., Boon, N., Vlaeminck, S.E., Verstraete, W., 2008. Partial nitrification achieved by pulse sulfide doses in a sequential batch reactor. Environ. Sci. Technol. 42, 8715–8720. doi:10.1021/es801391u

Fajardo, C., Mora, M., Fernández, I., Mosquera-Corral, A., Campos, J.L., Méndez, R., 2014. Cross effect of temperature, pH and free ammonia on autotrophic denitrification process with sulphide as electron donor. Chemosphere 97, 10–5. doi:10.1016/j.chemosphere.2013.10.028

Finstein, M.S., Delwiche, C.C., 1965. Molybdenum as a Micronutrient for Nitrobacter. J. Bacteriol. 89, 123–128.

Foley, J., de Haas, D., Hartley, K., Lant, P., 2010. Comprehensive life cycle inventories of alternative wastewater treatment systems. Water Res. 44, 1654–1666. doi:10.1016/j.watres.2009.11.031

Gilch, S., Meyer, O., Schmidt, I., 2009. A soluble form of ammonia monooxygenase in Nitrosomonas europaea. Biol. Chem. 390, 863–873. doi:10.1515/BC.2009.085

Gilmore, K.R., Little, J.C., Smets, B.F., Love, N.G., 2009. Oxygen Transfer Model for a Flow-Through Hollow-Fiber Membrane Biofilm Reactor. J. Environ. Eng. 135, 806–814. doi:10.1061/(ASCE)EE.1943-7870.0000035

Gilmore, K.R., Terada, A., Smets, B.F., Love, N.G., Garland, J.L., 2013. Autotrophic Nitrogen Removal in a Membrane-Aerated Biofilm Reactor Under Continuous Aeration: A Demonstration. Environ. Eng. Sci. 30, 38–45. doi:10.1089/ees.2012.0222

Guo, Q., Hu, H.-Y., Shi, Z.-J., Yang, C.-C., Li, P., Huang, M., Ni, W.-M., Shi, M.-L., Jin, R.-C., 2016. Towards simultaneously removing nitrogen and sulfur by a novel process: Anammox and autotrophic desulfurization–denitrification (AADD). Chem. Eng. J. 297, 207–216. doi:10.1016/j.cej.2016.03.138

Hubaux, N., Wells, G., Morgenroth, E., 2014. Impact of coexistence of flocs and biofilm on performance of combined nitritation-anammox granular sludge reactors. Water Res. 68, 127–139. doi:10.1016/j.watres.2014.09.036

Jeroschewski, P., Steuckart, C., Kühl, M., 1996. An Amperometric Microsensor for the Determination of $H_2S$ in Aquatic Environments. Anal. Chem. 68, 4351–4357. doi:10.1021/ac960091b

Jones, Z.L., Jasper, J.T., Sedlak, D.L., Sharp, J.O., 2017. Sulfide Induced Dissimilatory Nitrate Reduction to Ammonium Supports Anaerobic Ammonium Oxidation (Anammox) in an Open-Water Unit Process Wetland. Appl. Environ. Microbiol. 83, 1–14.

Kalyuzhnyi, S., Gladchenko, M., Mulder, A., Versprille, B., 2006. DEAMOX-New biological nitrogen removal process based on anaerobic ammonia oxidation coupled to sulphide-driven conversion of nitrate into nitrite. Water Res. 40, 3637–3645. doi:10.1016/j.watres.2006.06.010

Kampschreur, M.J., Temmink, H., Kleerebezem, R., Jetten, M.S.M., van Loosdrecht, M.C.M., 2009. Nitrous oxide emission during wastewater treatment. Water Res. 43, 4093–103. doi:10.1016/j.watres.2009.03.001

Kinh, C.T., Suenaga, T., Hori, T., Riya, S., Hosomi, M., Smets, B.F., Terada, A., 2017. Counter-diffusion biofilms have lower N 2 O emissions than co-diffusion biofilms during simultaneous nitrification and denitrification: Insights from depth-profile analysis. Water Res. doi:10.1016/j.watres.2017.07.058

Liu, Y., Peng, L., Ngo, H.H., Guo, W., Wang, D., Pan, Y., Sun, J., Ni, B.-J., 2016. Evaluation of Nitrous Oxide Emission from Sulfide- and Sulfur-Based Autotrophic Denitrification Processes. Environ. Sci. Technol. acs.est.6b02202. doi:10.1021/acs.est.6b02202

Manconi, I., van der Maas, P., Lens, P., 2006. Effect of copper dosing on sulfide inhibited reduction of nitric and nitrous oxide. Nitric Oxide - Biol. Chem. 15, 400–407. doi:10.1016/j.niox.2006.04.262

Martin, K.J., Nerenberg, R., 2012. The membrane biofilm reactor (MBfR) for water and wastewater treatment: principles, applications, and recent developments. Bioresour. Technol. 122, 83–94. doi:10.1016/j.biortech.2012.02.110

Meincke, M., Bock, E., Kastrau, D., Kroneck, P.M.H., 1992. Nitrite oxidoreductase from Nitrobacter hamburgensis: Redox centers and their catalytic role. Arch. Microbiol. 158, 127–131. doi:10.1007/BF00245215

Millero, F.J., 1986. The thermodynamics and kinetics of the hydrogen sulfide system in natural waters. Mar. Chem. 18, 121–147. doi:10.1016/0304-4203(86)90003-4

Moraes, B.S., Orrú, J.G.T., Foresti, E., 2012. Nitrogen and sulfide removal from effluent of UASB reactor in a sequencing fed-batch biofilm reactor under intermittent aeration. J. Biotechnol. 164, 378–385. doi:10.1016/j.jbiotec.2012.06.032

Mozumder, M.S.I., Picioreanu, C., Van Loosdrecht, M.C.M., Volcke, E.I.P., 2014. Effect of heterotrophic growth on autotrophic nitrogen removal in a granular sludge reactor. Environ. Technol. (United Kingdom) 35, 1027–1037. doi:10.1080/09593330.2013.859711

Peng, L., Sun, J., Liu, Y., Dai, X., Ni, B.-J., 2016. Nitrous Oxide Production in Co- Versus Counter-Diffusion Nitrifying Biofilms. Sci. Rep. 6, 28880. doi:10.1038/srep28880

Perez-Calleja, P., Aybar, M., Picioreanu, C., Esteban-Garcia, A.L., Martin, K.J., Nerenberg, R., 2017. Periodic venting of MABR lumen allows high removal rates and high gas-transfer

efficiencies. Water Res. 121, 349–360. doi:10.1016/j.watres.2017.05.042

Reichert, P., 1994. AQUASIM - A Tool for Simulation and Data Analysis of Aquatic Systems. Water Sci. Technol. 30, 21–30.

Revsbecht, N.P., Ward, D.M., 1983. Oxygen Microelectrode That Is Inssensitive to Medium Chemical Composition: Use in an Acid Microibal Mat Dominated by Cyanidium caldarium. Appl. Environ. Microbiol. 45, 755–759.

Rios-Del Toro, E.E., Cervantes, F.J., 2016. Coupling between anammox and autotrophic denitrification for simultaneous removal of ammonium and sulfide by enriched marine sediments. Biodegradation 27, 107–118. doi:10.1007/s10532-016-9759-4

Rudd, J.W.M., Hamilton, R.D., Campbell, N.E.R., 1974. Measurement of microbial oxidation of methane in lake water. Limnol. Oceanogr. 19, 519–524.

Russ, L., Speth, D.R., Jetten, M.S.M.M., Op den Camp, H.J.M.M., Kartal, B., 2014. Interactions between anaerobic ammonium and sulfur-oxidizing bacteria in a laboratory scale model system. Environ. Microbiol. 16, 3487–3498. doi:10.1111/1462-2920.12487

Sahinkaya, E., Kilic, A., Duygulu, B., 2014. Pilot and full scale applications of sulfur-based autotrophic denitrification process for nitrate removal from activated sludge process effluent. Water Res. 60C, 210–217. doi:10.1016/j.watres.2014.04.052

Sánchez-Ramírez, J.E., Seco, a, Ferrer, J., Bouzas, a, García-Usach, F., 2014. Treatment of a submerged anaerobic membrane bioreactor (SAnMBR) effluent by an activated sludge system: The role of sulphide and thiosulphate in the process. J. Environ. Manage. 147, 213–218. doi:10.1016/j.jenvman.2014.04.043

Schonharting, B., Rehner, R., Metzger, J.W., Krauth, K., Rizzi, M., 1998. Release of Nitrous Oxide (N2O) from denitrifying activated sludge caused by H2S-Containing Wastewater: Quantification and Application of a new mathematical model. Water Sci. Technol. 38, 237–246.

Senga, Y., Mochida, K., Fukumori, R., Okamoto, N., Seike, Y., 2006. N2O accumulation in estuarine and coastal sediments: The influence of H2S on dissimilatory nitrate reduction. Estuar. Coast. Shelf Sci. 67, 231–238. doi:10.1016/j.ecss.2005.11.021

Solomon, S., Qin, D., Manning, M., Chen, Z., Marquis, M., Averyt, K.B., Tignor, M., Miller, H.L., 2007. Contribution of working group I to the fourth assessment report of the intergovernmental panel on climate change, 2007.

Sorensen, J., Tiedje, J.M., Firestone, R.B., 1980. Inhibition by Sulfide of Nitric and Nitrous-Oxide Reduction by Denitrifying Pseudomonas-Fluorescens. Appl. Environ. Microbiol. 39, 105–108.

Souza, T.S.O., Foresti, E., 2013. Sulfide-oxidizing autotrophic denitrification: an evaluation for nitrogen removal from anaerobically pretreated domestic sewage. Appl. Biochem. Biotechnol. 170, 1094–103. doi:10.1007/s12010-013-0261-8

Tugstas, A.E., Pavlostathis, S.G., 2007. Effect of Sulfide on Nitrate Reduction in Mixed Methanogenic Cultures. Biotechnol. Bioeng. 97, 1448–1459. doi:10.1002/bit

U.S. Environmental Protection Agency, ', 2017. Inventory of U.S. Greenhouse Gas Emissions and Sinks, 1990-2015.

Wang, J., Lu, H., Chen, G.H., Lau, G.N., Tsang, W.L., van Loosdrecht, M.C.M., 2009. A novel sulfate reduction, autotrophic denitrification, nitrification integrated (SANI) process for saline wastewater treatment. Water Res. 43, 2363–2372. doi:10.1016/j.watres.2009.02.037

Wieland, A., Kühl, M., 2000. Short-term temperature effects on oxygen and sulfide cycling in a hypersaline cyanobacterial mat (Solar Lake, Egypt). Mar. Ecol. Prog. Ser. 196, 87–102. doi:10.3354/meps196087

Xue, W., Hao, T., Mackey, H.R., Li, X., Chan, R.C., Chen, G., 2017. The role of sulfate in aerobic granular sludge process for emerging sulfate-laden wastewater treatment. Water Res. 124, 513–520. doi:10.1016/j.watres.2017.08.009

Yang, W., Lu, H., Khanal, S.K., Zhao, Q., Meng, L., Chen, G.H., 2016a. Granulation of sulfur-oxidizing bacteria for autotrophic denitrification. Water Res. 104, 507–519. doi:10.1016/j.watres.2016.08.049

Yang, W., Zhao, Q., Lu, H., Ding, Z., Meng, L., Chen, G.-H., 2016b. Sulfide-driven autotrophic denitrification significantly reduces N2O emissions. Water Res. 90, 176–184. doi:10.1016/j.watres.2015.12.032

Yin, Z., Xie, L., Zhou, Q., 2015. Effects of sulfide on the integration of denitrification with anaerobic digestion. J. Biosci. Bioeng. 120, 426–431. doi:10.1016/j.jbiosc.2015.02.004

Zahn, J.A., Arciero, D.M., Hooper, A.B., DiSpirito, A.A., 1996. Evidence for an iron center in the ammonia monooxygenase from Nitrosomonas europaea. FEBS Lett. 397, 35–38. doi:10.1016/S0014-5793(96)01116-7

Zhang, L., Zhang, C., Hu, C., Liu, H., Bai, Y., Qu, J., 2015. Sulfur-based mixotrophic denitrification corresponding to different electron donors and microbial profiling in anoxic fluidized-bed membrane bioreactors. Water Res. 85, 422–431. doi:10.1016/j.watres.2015.08.055

Zhou, Z., Xing, C., An, Y., Hu, D., Qiao, W., Wang, L., 2014. Inhibitory effects of sulfide on nitrifying biomass in the anaerobic-anoxic-aerobic wastewater treatment process. J. Chem. Technol. Biotechnol. 89, 214–219. doi:10.1002/jctb.4104

# CHAPTER 6.

## CONCLUSIONS, SIGNIFICANCE, AND FUTURE RESEARCH DIRECTIONS

### 6.1 Overview

Developing an equitable, resource efficient, and cost efficient urban water cycle for the 21st century requires an interdisciplinary approach that integrates novel tools in research and technology. For centuries, the activated sludge process has been a black box; however, we can advance our understanding of the microbial communities within wastewater treatment systems with the help of new research tools and develop new treatment technologies that improve environmental health. The goal of this dissertation research was to understand how sulfur can affect nitrogen cycling in ways that are relevant to wastewater treatment and to identify beneficial uses of sulfur that may improve the resource efficiency of wastewater treatment. As highlighted in Chapter 2, our current understanding of how nitrogen and sulfur interact in wastewater treatment demonstrates both potential benefits and pitfalls associated with using sulfur to improve treatment. Ultimately, understanding how to maximize the benefits while minimizing the pitfalls will improve the resource efficiency of treatment in the rapidly growing and increasingly urbanized coastal regions of the world.

This dissertation tested the impact of hydrogen sulfide in three distinct systems: two full-scale treatment plants with different redox environments that had distinct microbial communities and one lab-scale membrane-aerated biofilm reactor (MABR). The MABR employs a counter-diffusional biofilm with a redox gradient and consequently supports mixed microbial metabolisms. Overall, the results show that hydrogen sulfide could have beneficial impacts on nitrogen removal in engineered systems, but the effect of hydrogen sulfide is complex because microbial communities are interconnected and adaptable and the microbial community response depends on reactor configuration. This dissertation research gives new insights into the beneficial and detrimental effects of using hydrogen sulfide for nitrogen removal and highlights future areas of

research needed to minimize the potential pitfalls associated with applying sulfide for nitrogen removal in wastewater treatment systems.

## 6.2 Using Hydrogen Sulfide to Inhibit Nitrite Oxidizing Bacteria

Sulfide could help induce nitritation processes in activated sludge, thus reducing the resource requirements wastewater treatment (Chapter 3). By linking microbial community characteristics to process rates, this research showed that different communities of nitrite oxidizing bacteria (NOB) have distinct propensities for sulfide inhibition. The results highlight that links between treatment process data and microbial community characteristics are needed to generalize results and improve process models.

When the application of sulfide for nitritation was tested in an MABR, the results show that active NOB could be inhibited by sulfide (Chapter 4). Consistent with Chapter 3, the NOB were more sensitive to sulfide than the ammonia oxidizing bacteria (AOB). Unlike the fully aerobic batches discussed in Chapter 3, the MABR supports multiple redox environments, so rapid consumption of nitrite may mask NOB inhibition due to sulfide. The results from Chapter 5 showed that nitrite did not accumulate over the course of stepwise increases in sulfide. In isolation, the data from Chapter 5 show that sulfide inhibited complete nitrification; it is only with the knowledge of potential rates from Chapter 4 that we know nitrite accumulation due to sulfide occurred in the MABR. The distinction between the batch experiments and the MABR is important because it highlights that responses to hydrogen sulfide can be both community and reactor specific. Furthermore, in complex biofilms where microbial cross-feeding can occur, multiple methods are needed to understand the system.

## 6.3 Community-Wide Effects from Hydrogen Sulfide

An important theme of this dissertation is that hydrogen sulfide had community-wide effects. In Chapter 3, these community-wide effects were demonstrable even in the short-term batch experiments with 16S rRNA cDNA sequencing showing a decreased activity of many taxa at higher sulfide concentrations. Community-wide effects were also demonstrable over the long-term experiments in the MABR whereby addition of sulfide resulted in a division of labor between physical compartments of the reactor; sulfur oxidation and denitrification (except for denitrifying

anaerobic methane oxidizers and anammox denitrifiers) were concentrated in the planktonic portion of the reactor while nitrification was concentrated in the biofilm. Understanding the distinct niches that can form in engineered systems is important and can inform the design of treatment systems. Microbial communities do not necessarily mold themselves to environmental engineers; we may be better served to design our systems with the microbial community in mind. In this case, in an effort to maximize biomass concentrations the lab-scale MABR was designed to maximize biofilm surface area. A design which could have allowed for more nitrogen removal may have been to have more space for bulk liquid growth in order to support a "hybrid" system (Downing and Nerenberg, 2008) with heterotrophic and sulfide-based denitrifiers growing in the bulk liquid. Regardless of this potential opportunity to improve nitrogen removal, we showed that sulfide addition to the MABR promoted the formation of new ecological niches.

Sulfide also induced dissimilatory nitrite reduction to ammonia (DNRA). While this phenomenon was previously shown in wetland (Jones et al., 2017) and freshwater sediments (Brunet and Garcia-Gil, 1996), few studies have shown sulfide-induced DNRA in an engineered community (Dolejs et al., 2014; Yin et al., 2015). As with the results from NOB inhibition, in isolation, the data from Chapter 5 show that sulfide inhibited complete nitrification; it is only by using molecular and isotopic labeling methods in Chapter 4 that we discovered the rapid conversion of nitrite to ammonia that was occurring. Sulfide-induced DNRA in wastewater treatment systems can be beneficial, especially in anammox systems where the reduction of nitrate to ammonia can provide additional substrate for anammox (Castro-Barros et al., 2017; Wang et al., 2018). However, Chapter 5 shows that these benefits have limits because nitrite reduction to ammonia can reduce the overall nitrogen removal from the system.

## 6.4 Implications for the Use of Sulfide for Nitrogen Removal

Denitrifying communities such as anammox and denitrifying anaerobic methane oxidizers developed from increased sulfide concentrations and both of these metabolic microbial groups can reduce the resource requirements for nitrogen removal. Anammox directly consumes ammonium therefore only half of it needs to be oxidized, which reduces the energy needed for aeration. Denitrifying anaerobic methane oxidizers require the oxidation of ammonia, but these organisms consume dissolved methane which is a potent greenhouse gas. This is particularly advantageous

for the treatment of anaerobic effluents which contain dissolved methane that constitutes an important life cycle cost (Smith et al., 2014). Since mainstream anaerobic effluents are also sulfide-rich and require nitrogen treatment (Delgado Vela et al., 2015), they are ideally suited for the application of denitrifying anaerobic methane oxidizers. The potential benefit of hydrogen sulfide for creating a more reduced environment and a nitrite source for denitrifying anaerobic methane oxidizers and anammox is an outcome from this dissertation research that has substantial engineering significance.

An additional result of significance is that hydrogen sulfide addition led to increases in nitrous oxide emissions. This is likely due to partial inhibition of denitrification. A benefit of the MABR system is that it exhibits overall lower nitrous oxide emissions compared with conventional biological nitrogen removal systems (Kinh et al., 2017). Even with sulfide inhibition of nitrous oxide reduction, nitrous oxide emissions were lower in the lab-scale MABR than in conventional systems. Nevertheless, these emissions need to be remedied because the global warming potential of nitrous oxide is approximately 300 times higher than that of carbon dioxide. Therefore, nitrous oxide emissions due to sulfide addition need to be understood and mitigated if the benefits of sulfide-based nitrogen removal to be realized.

## 6.5 Future Research Needs

There are numerous benefits of applying sulfur cycling to nitrogen removal in wastewater. Sulfide can inhibit nitrite oxidizing bacteria, thereby providing a nitrite source for denitrifying anaerobic methane oxidizers and anammox. Sulfide is also a reducing agent that establishes environments favorable for these oxygen sensitive microorganisms. A critical challenge in applying sulfide to nitrogen removal is that denitrification needs to be encouraged in lieu of DNRA. This is an important area of future research if sulfide is to be used for nitrogen removal from wastewater.

The mechanisms of nitrification and denitrification inhibition are still unknown. An important hypothesis to test is if inhibition is indirect via precipitation of trace metals that are used as micronutrients. In Chapters 3 and 5, precipitation was examined as a potential mechanism of inhibition. In particular, copper limitations can affect ammonia oxidation, nitrite oxidation, and nitrous oxide reduction to nitric oxide. If micronutrient limitations are found to be the mechanism

of inhibition, controlling sulfide inhibition may be as simple as supplementing these nutrients. Understanding the mechanism of inhibition is especially important to eliminate the harmful effect of $N_2O$ emission.

Lastly, much of the data presented in Chapter 4 where the importance of DNRA is established was based on functional potential. A better understanding of the transcriptome and proteome would improve the links between functional potential and microbial community activity. This could help us understand which organisms are responsible for the DNRA process and help elucidate strategies for controlling DNRA and supporting denitrification.

This dissertation shows that engineered systems can serve as a platform for understanding microbial community interactions. Different microbial communities can respond to stressors in different ways, so characterizing the microbial community can guide biotechnology development. Understanding microbial community interactions such as cross-feeding relationships and how they differ in current and emerging treatment systems is important. This dissertation shows that by enhancing our understanding of microbial community interactions, we can guide technology development and improve the resource efficiency of treatment.

## 6.6 References


Brunet, R.C., Garcia-Gil, L.J., 1996. Sulfide-induced dissimilatory nitrate reduction to ammonia in anaerobic freshwater sediments. FEMS Microbiol. Ecol. 21, 131–138. doi:10.1016/0168-6496(96)00051-7

Castro-Barros, C.M., Jia, M., van Loosdrecht, M.C.M., Volcke, E.I.P., Winkler, M.K.H., 2017. Evaluating the potential for dissimilatory nitrate reduction by anammox bacteria for municipal wastewater treatment. Bioresour. Technol. 233, 363–372. doi:10.1016/j.biortech.2017.02.063

Delgado Vela, J., Stadler, L.B., Martin, K.J., Raskin, L., Bott, C., Love, N.G., 2015. Prospects for Biological Nitrogen Removal from Anaerobic Effluents during Mainstream Wastewater Treatment. Environ. Sci. Technol. Lett. 2, 233–244. doi:10.1021/acs.estlett.5b00191

Dolejs, P., Paclík, L., Maca, J., Pokorna, D., Zabranska, J., Bartacek, J., Paclik, L., Maca, J., Pokorna, D., Zabranska, J., Bartacek, J., Paclík, L., Maca, J., Pokorna, D., Zabranska, J., Bartacek, J., 2014. Effect of S/N ratio on sulfide removal by autotrophic denitrification. Appl. Microbiol. Biotechnol. 99, 2383–2392. doi:10.1007/s00253-014-6140-6

Downing, L.S., Nerenberg, R., 2008. Total nitrogen removal in a hybrid, membrane-aerated activated sludge process. Water Res. 42, 3697–3708. doi:10.1016/j.watres.2008.06.006

Jones, Z.L., Jasper, J.T., Sedlak, D.L., Sharp, J.O., 2017. Sulfide Induced Dissimilatory Nitrate Reduction to Ammonium Supports Anaerobic Ammonium Oxidation (Anammox) in an Open-Water Unit Process Wetland. Appl. Environ. Microbiol. 83, 1–14.

Kinh, C.T., Suenaga, T., Hori, T., Riya, S., Hosomi, M., Smets, B.F., Terada, A., 2017. Counter-diffusion biofilms have lower N 2 O emissions than co-diffusion biofilms during simultaneous nitrification and denitrification: Insights from depth-profile analysis. Water Res. doi:10.1016/j.watres.2017.07.058

Smith, A.L., Stadler, L.B., Cao, L., Love, N.G., Raskin, L., Skerlos, S.J., 2014. Navigating Wastewater Energy Recovery Strategies: A Life Cycle Comparison of Anaerobic Membrane Bioreactor and Conventional Treatment Systems with Anaerobic Digestion. Environ. Sci. Technol. doi:10.1021/es5006169

Wang, S., Wang, W., Liu, L., Zhuang, L., Zhao, S., Su, Y., Li, Y., Wang, M., Wang, C., Xu, L., Zhu, G., 2018. Microbial nitrogen cycle hotspots in the plant-bed/ditch system of a constructed wetland with N2O mitigation. Environ. Sci. Technol. acs.est.7b04925. doi:10.1021/acs.est.7b04925

Yin, Z., Xie, L., Zhou, Q., 2015. Effects of sulfide on the integration of denitrification with anaerobic digestion. J. Biosci. Bioeng. 120, 426–431. doi:10.1016/j.jbiosc.2015.02.004

# APPENDICES

# Appendix A.

# Supplementary Information for Chapter 3.

## A-1. Visual MINTEQ Methods

The species tableau used for the precipitation characterization is given in Table A1. The sulfide concentration was varied using the sweep function from 0-35 mg/L as S.

**Table A1.** Species tableau for influent characteristics

| Species | Conc (mM) | Ca | Cl | Mg | K | H | PO4 | NH4 | CO3 | Na | Fe (III) | SO4 | Co (II) | Zn | B | Mn | Mo | Al | Ni | Se | W | Cu | EDTA |
|---|---|---|---|---|---|---|---|---|---|---|---|---|---|---|---|---|---|---|---|---|---|---|---|
| CaCl2*2H2O | 0.03 | 0.0 | 0.1 | | | | | | | | | | | | | | | | | | | | |
| MgCl2*6H2O | 0.2 | | 0.3 | 0.2 | | | | | | | | | | | | | | | | | | | |
| KH2PO4 | 7.1 | | | | 7.1 | 14.1 | 7.1 | | | | | | | | | | | | | | | | |
| Na2HPO4 | 29.0 | | | | | 29.0 | 29.0 | | | 57.9 | | | | | | | | | | | | | |
| NH4HCO3 | 3.6 | | | | | 3.6 | | 3.6 | 3.6 | | | | | | | | | | | | | | |
| NaHCO3 | 6.0 | | | | | 6.0 | | | 6.0 | 6.0 | | | | | | | | | | | | | |
| Fe ($FeCl_3 \cdot 6H_2O$) | 0.0240 | | 0.0720 | | | | | | | | 0.0240 | | | | | | | | | | | | |
| Co (CoCl2*6H2O) | 0.0012 | | 0.0024 | | | | | | | | | | 0.0012 | | | | | | | | | | |
| Zn (ZnSO4*7H2O) | 0.0012 | | | | | | | | | | | 0.0012 | | 0.0012 | | | | | | | | | |
| B (H3BO3) | 0.0006 | | | | | | | | | | | | | | 0.0006 | | | | | | | | |
| Mn (MnSO4*H2O) | 0.0006 | | | | | | | | | | | 0.0006 | | | | 0.0006 | | | | | | | |
| Mo ((NH4)6Mo7O24*4H2O) | 0.0001 | | | | | | | 0.0005 | | | | | | | | | 0.0006 | | | | | | |
| Al (AlCl3*6H2O) | 0.0001 | | 0.0004 | | | | | | | | | | | | | | | 0.0001 | | | | | |
| Ni (NiCl2*6H2O) | 0.0006 | | 0.0012 | | | | | | | | | | | | | | | | 0.0006 | | | | |
| Se (Na2SeO4) | 0.0001 | | | | | | | | | 0.0002 | | | | | | | | | | 0.0001 | | | |
| W (Na2WO4*2H2O) | 0.0001 | | | | | | | | | 0.0002 | | | | | | | | | | | 0.0001 | | |
| Cu (CuCl2*2H2O) | 0.0006 | | 0.0012 | | | | | | | | | | | | | | | | | | | 0.0006 | |
| EDTA (NaEDTA) | 0.0300 | | | | | | | | | 0.0300 | | | | | | | | | | | | | 0.0300 |
| HCl | 1.0 | | 1.0 | | | 1.0 | | | | | | | | | | | | | | | | | |
| | Totals | 0.0 | 1.5 | 0.2 | 7.1 | 53.6 | 36.0 | 3.6 | 9.6 | 63.9 | 0.0 | 0.0 | 0.0 | 0.0 | 0.0 | 0.0 | 0.0 | 0.0 | 0.0 | 0.0 | 0.0 | 0.0 | 0.0 |

## A-2. Visual Minteq Results

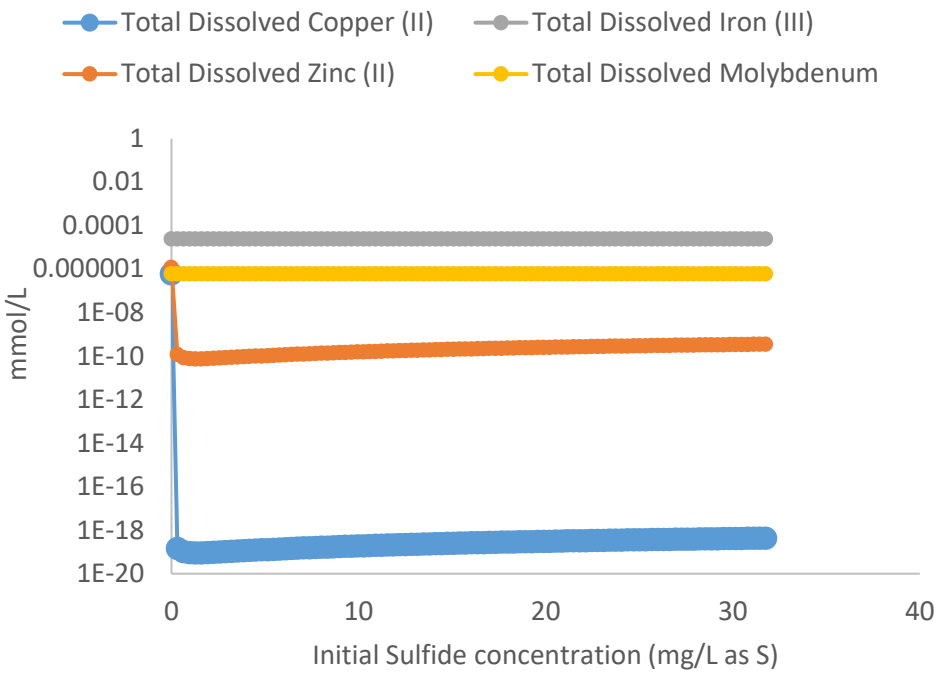


**Figure A1.** Total dissolved copper, iron, zinc, and molybdenum at varying sulfide concentrations.

## A-3. Raw Batch Experiment Data

### *A-3.1. Sulfide Data*

Concentrations of sulfide for the A2O process are given in Table A2. Concentrations of sulfide for the extended aeration process are given in Table A3.

**Table A2.** Sulfide measurements in batch experiments for A2O plant. All concentrations are in mg/L as S. The limit of detection for the silver sulfide electrode is 0.64 mg/L as S.

| Target sample time (hr) | Ammonia fed | | | Nitrite Fed | | |
|---|---|---|---|---|---|---|
| **Target Influent Sulfide- 2 mg/L as S.** | | | | | | |
| Initial | 1.9 | 1.9 | 1.7 | 2.1 | 3.5 | 2.3 |
| [% recovered] | [95] | [95] | [87] | [103] | [175] | [113] |
| 0:02:00 | 0.9 | 0.8 | 0.9 | 0.7 | 0.8 | 1 |
| 0:30:00 | <0.6 | <0.6 | <0.6 | <0.6 | <0.6 | <0.6 |
| 2:00:00 | <0.6 | <0.6 | <0.6 | <0.6 | <0.6 | <0.6 |
| 4:00:00 | 1 | <0.6 | <0.6 | <0.6 | <0.6 | <0.6 |
| **Target Initial Sulfide- 4 mg/L as S** | | | | | | |
| Initial | 2.6 | 3.1 | 3.1 | 3.4 | 3.4 | 3.1 |
| [% recovered] | [66] | [78] | [78] | [84] | [84] | [78] |
| 0:02:00 | 1.5 | 1.7 | 1.7 | 1.7 | 1.6 | 1.9 |
| 0:30:00 | <0.6 | <0.6 | <0.6 | <0.6 | <0.6 | <0.6 |
| 2:00:00 | <0.6 | <0.6 | <0.6 | <0.6 | <0.6 | <0.6 |
| 4:00:00 | <0.6 | <0.6 | <0.6 | <0.6 | <0.6 | <0.6 |
| **Target Initial Sulfide- 7.7 mg/L as S** | | | | | | |
| Initial | 7.6 | 7.6 | 7.6 | 7.1 | 7.6 | 8.1 |
| [% recovered] | [98] | [98] | [98] | [92] | [98] | [105] |
| 0:02:00 | 6.2 | 5.8 | 5.4 | 3.4 | 4.1 | 8.3 |
| 0:30:00 | 1.5 | 0.7 | 1.3 | 1.4 | 1.1 | 2.2 |
| 2:00:00 | 0.9 | 0.8 | 1.0 | 1.0 | 1.2 | 2.4 |
| 4:00:00 | 0.9 | 0.7 | 0.8 | 1.0 | 0.9 | 1.7 |
| **Target Initial Sulfide- 15 mg/L as S** | | | | | | |
| Initial | 13.4 | 14.8 | 17.9 | 19.6 | 19.6 | 19.6 |
| [% recovered] | [90] | [99] | [119] | [130] | [130] | [130] |
| 0:02:00 | 7.5 | 7.5 | 7.5 | 8.2 | 9.9 | 9.9 |
| 0:30:00 | 1.4 | 1.7 | 2.9 | 3.5 | 3.5 | 3.5 |
| 2:00:00 | <0.6 | <0.6 | <0.6 | 0.9 | <0.6 | <0.6 |
| 4:00:00 | <0.6 | <0.6 | <0.6 | 0.7 | 0.7 | 0.7 |
| **Target Initial Sulfide- 35 mg/L as S** | | | | | | |
| Initial | 22.6 | 25.8 | 25.8 | 27.6 | 25.8 | 27.6 |
| [% recovered] | [65] | [74] | [74] | [79] | [74] | [79] |
| 0:02:00 | 15.7 | 17.9 | 13.7 | 12.9 | 12.9 | 12.0 |
| 0:30:00 | 13.7 | 4.2 | 9.3 | 4.2 | 4.2 | 4.8 |
| 2:00:00 | 17.9 | <0.6 | 0.9 | 1.9 | 1.5 | 1.7 |
| 4:00:00 | 0.8 | 0.7 | <0.6 | 0.8 | <0.6 | 0.92 |

**Table A3.** Sulfide measurements in batch experiments for extended aeration plant. All concentrations are in mg/L as S. The limit of detection for the silver sulfide electrode is 0.64 mg/L as S.

| Target sample time (hr) | Ammonia fed | | | Nitrite Fed | | |
|---|---|---|---|---|---|---|
| **Target Influent Sulfide- 2 mg/L as S.** | | | | | | |
| Initial | 1.2 | 1.2 | 1.4 | 1.5 | 1.7 | 1.7 |
| [% recovered] | [59] | [59] | [70] | [76] | [83] | [83] |
| 0:02:00 | <0.6 | 0.9 | <0.6 | <0.6 | <0.6 | <0.6 |
| 0:30:00 | <0.6 | <0.6 | <0.6 | <0.6 | <0.6 | <0.6 |
| 2:00:00 | <0.6 | <0.6 | <0.6 | <0.6 | <0.6 | <0.6 |
| 4:00:00 | <0.6 | <0.6 | <0.6 | <0.6 | <0.6 | <0.6 |
| **Target Initial Sulfide- 5 mg/L as S** | | | | | | |
| Initial | 3.5 | 3.2 | 2.9 | 3.5 | 3.5 | 3.5 |
| [% recovered] | [69] | [64] | [59] | [69] | [69] | [69] |
| 0:02:00 | 0.8 | 0.7 | 0.8 | 0.8 | <0.6 | <0.6 |
| 0:30:00 | <0.6 | <0.6 | <0.6 | <0.6 | <0.6 | <0.6 |
| 2:00:00 | 0.7 | 0.8 | <0.6 | <0.6 | <0.6 | <0.6 |
| 4:00:00 | <0.6 | <0.6 | <0.6 | <0.6 | <0.6 | <0.6 |
| **Target Initial Sulfide- 10mg/L as S** | | | | | | |
| Initial | 6.4 | 9.1 | 9.1 | 11.8 | 10.8 | 10.8 |
| [% recovered] | [64] | [91] | [91] | [118] | [108] | [108] |
| 0:02:00 | 3.5 | 2.9 | 2.5 | 2.2 | 2.3 | 2.9 |
| 0:30:00 | 1.6 | 1.2 | 1.3 | 1.6 | 1.7 | 1.5 |
| 2:00:00 | <0.6 | <0.6 | <0.6 | 1.3 | 0.9 | 1.0 |
| 4:00:00 | <0.6 | <0.6 | <0.6 | <0.6 | <0.6 | <0.6 |
| **Target Initial Sulfide- 15 mg/L as S** | | | | | | |
| Initial | 7.6 | 10.6 | 12.6 | 12.6 | 12.6 | 13.6 |
| [% recovered] | [51] | [71] | [84] | [84] | [84] | [91] |
| 0:02:00 | 2.9 | 4.0 | 4.5 | 5.2 | 2.5 | 2.5 |
| 0:30:00 | 1.5 | 1.8 | 1.3 | 1.5 | 1.5 | 1.6 |
| 2:00:00 | <0.6 | <0.6 | <0.6 | <0.6 | <0.6 | <0.6 |
| 4:00:00 | <0.6 | <0.6 | <0.6 | <0.6 | <0.6 | <0.6 |
| **Target Initial Sulfide- 35 mg/L as S** | | | | | | |
| Initial | 18.0 | 21.0 | 24.3 | 24.3 | 24.3 | 26.3 |
| [% recovered] | [52] | [60] | [70] | [70] | [70] | [75] |
| 0:02:00 | 7.7 | 8.3 | 11.3 | 8.3 | 6.7 | 6.7 |
| 0:30:00 | 4.9 | 3.6 | 3.6 | 3.6 | 3.6 | 3.9 |
| 2:00:00 | 1.4 | 1.6 | 1.5 | 2.9 | 3.1 | 3.1 |
| 4:00:00 | 1.3 | <0.6 | 0.8 | 1.3 | 1.5 | 1.6 |

### *A-3.2. Volatile suspended solids concentrations*

Final volatile suspended solids concentrations are given in Table A4. Generally, solids in the extended aeration plant experiments were higher than solids in A2O process, which was expected since the mixed liquor suspended solids from this process were higher. All rates were normalized to solids to eliminate this effect.

**Table A4.** Volatile suspended solids concentrations from the end of the experiment, standard deviations are the result of duplicate analysis. A indicates Ammonia and sulfide amended flask; B indicates ammonia amended controls; N indicates nitrite and sulfide amended flask; C indicates nitrite amended controls. Numeric indicate replicate numbers.

| | **A2O Process** | **Extended Aeration Process** |
|---|---|---|
| | **Average ±Standard Deviation (mg/L)** | |
| **Target Sulfide** | **2 mg/L as S** | |
| A1 | 1510±190 | 2475±25 |
| A2 | 1390±90 | 2475±25 |
| A3 | 1417±17 | 2325±75 |
| B1 | 1383±17 | 2125±25 |
| B2 | 1417±50 | 2175±75 |
| N1 | 950±17 | 2150±200 |
| N2 | 1700±100 | 2125±25 |
| N3 | 1400±67 | 2275±75 |
| C1 | 1367±33 | 2075±125 |
| C2 | 1317±17 | 2350±250 |
| **Target Sulfide** | **4 mg/L as S** | **5 mg/L as S** |
| A1 | 1470±30 | 2310±190 |
| A2 | 1560±40 | 2500±50 |
| A3 | 1280±40 | 2575±25 |
| B1 | 1400±120 | 2500±150 |
| B2 | 1240±40 | 2225±75 |
| N1 | 1400±120 | 2100±250 |
| N2 | 1420±60 | 2225±125 |
| N3 | 1460±100 | 2925±175 |
| C1 | 1540±60 | 2850±0 |
| C2 | 1420±60 | 2400±100 |
| **Target Sulfide** | **7.7 mg/L as S** | **10 mg/L as S** |
| A1 | 1500±50 | 2275±25 |
| A2 | 1375±125 | 2450±200 |
| A3 | 1325±75 | 2200±150 |
| B1 | 1450±0 | 2425±75 |
| B2 | 1375±75 | 2525±125 |

| | | |
|---|---|---|
| N1 | 1275±75 | 2225±25 |
| N2 | 1250±50 | 2000±200 |
| N3 | 1275±25 | 2325±75 |
| C1 | 1325±25 | 2050±0 |
| C2 | 1375±125 | 2150±50 |
| **Target Sulfide** | **15 mg/L as S** | |
| A1 | 1350±83 | 2175±125 |
| A2 | 1367±67 | 2143±108 |
| A3 | 1317±50 | 1900±250 |
| B1 | 1350±83 | 2075±125 |
| B2 | 1283±50 | 3025±525 |
| N1 | 1233±33 | 2150±350 |
| N2 | 1217±17 | 2400±150 |
| N3 | 1333±33 | 2350±0 |
| C1 | 1383±150 | 2175±75 |
| C2 | 1400±67 | 2100±0 |
| **Target Sulfide** | **35 mg/L as S** | |
| A1 | 1120±40 | 2250±50 |
| A2 | 1220±220 | 2175±25 |
| A3 | 1160±80 | 2375±75 |
| B1 | 1220±60 | 2075±25 |
| B2 | 1160±0 | 2200±100 |
| N1 | 1260±60 | 2150±0 |
| N2 | 1380±100 | 2375±25 |
| N3 | 840±40 | 2175±75 |
| C1 | 530±10 | 2225±25 |
| C3 | 1320±0 | 2350±50 |

### *A-3.3. Nitrogen Data*

Raw nitrogen data is given in Figure A2 and Figure A3. All rates were taken using the initial slopes and normalized to biomass concentration. It is noteworthy that despite loss of sulfide (below detection typically within 2 hours, Table A3), we don't have clear or consistent change in rates between two and eight hour, for example.

## Ammonia Amended


### A2O Process

**Target: 2 mg S/L**

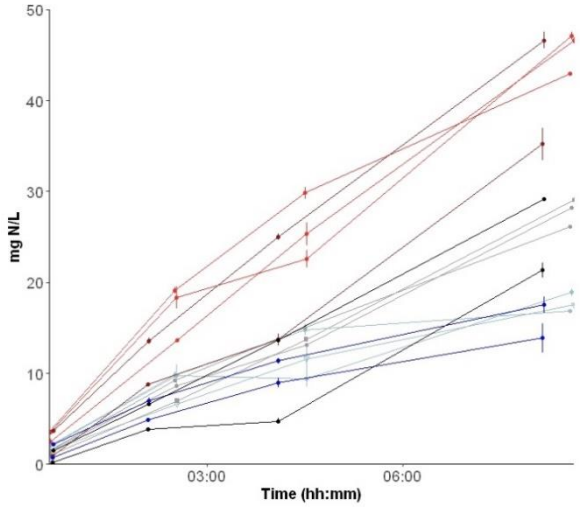


**Target: 4 mg S/L**

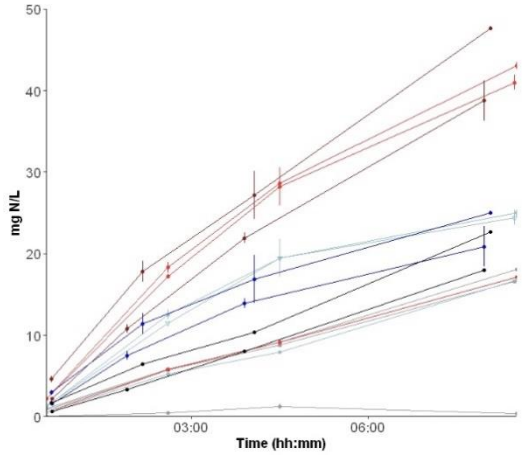


**Target: 7.7 mg S/L**

### Extended Aeration Process

**Target: 2 mg S/L**

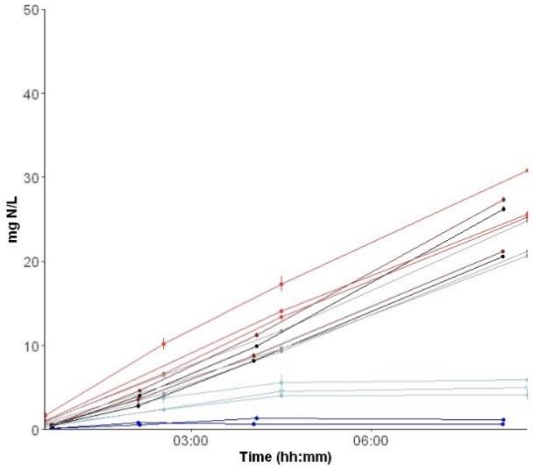


**Target 5 mg S/L**

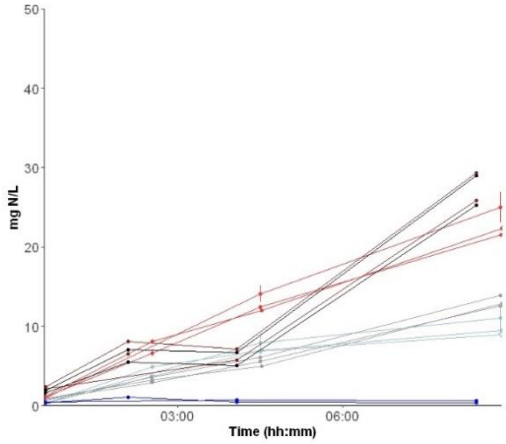


**Target: 10 mg S/L**

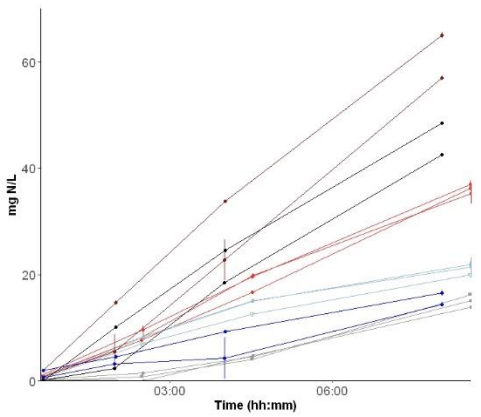


**Target: 15 mg S/L**

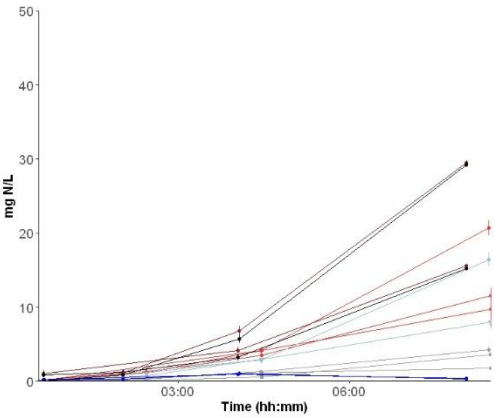


**Target: 15 mg S/L**

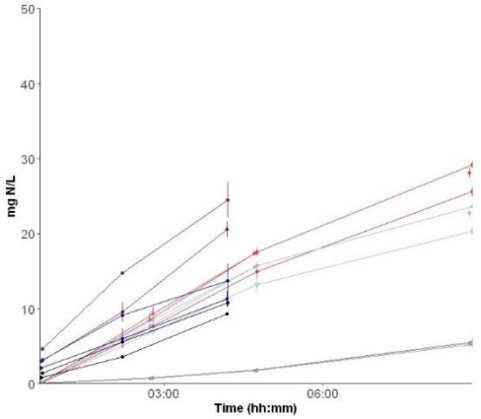


**Target 35 mg S/L**

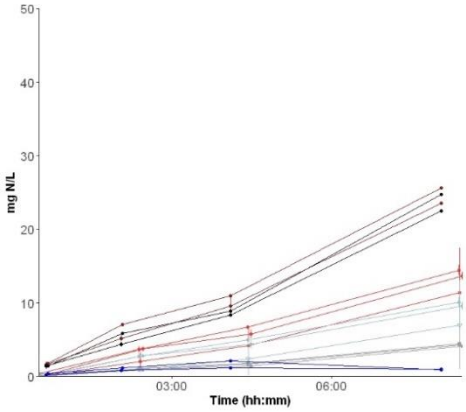


**Target 35 mg S/L**

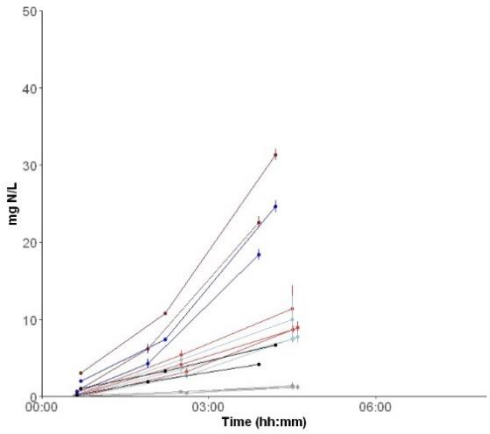


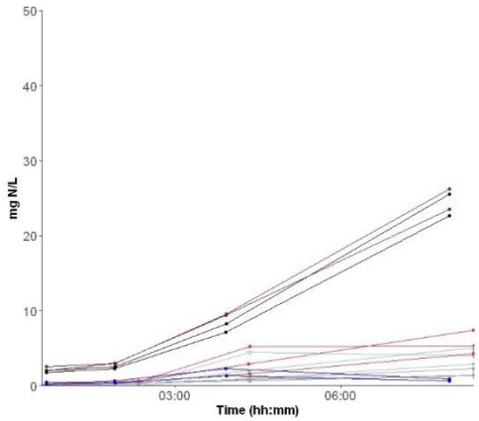


**Figure A2.** Raw data used for rates, ammonia fed batches from A2O process (right) and extended aeration process (left).

## Nitrite Amended

Nitrate, Control  Nitrate, Sulfide

### Anaerobic-Anoxic-Aerobic

**Target: 2 mg S/L**

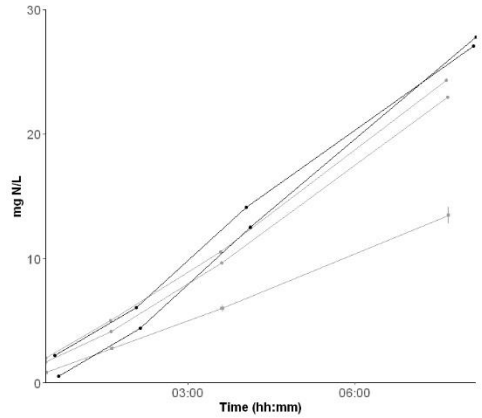


**Target: 4 mg S/L**

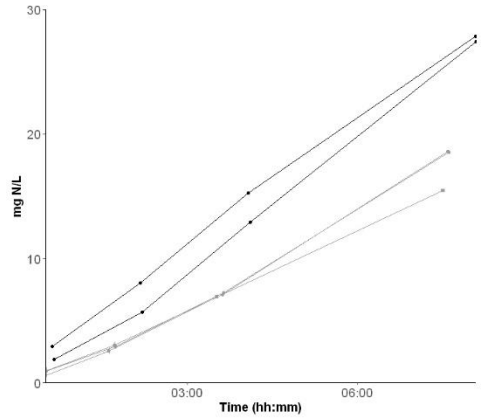


**Target: 7.7 mg S/L**

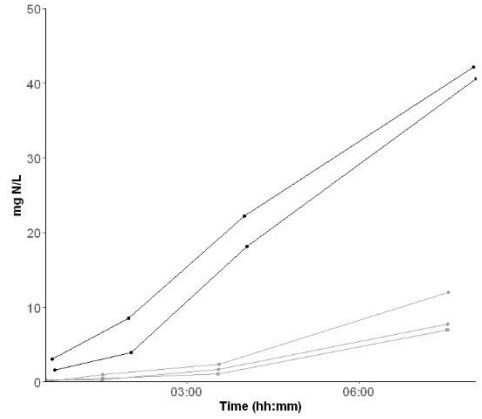


### Extended Aeration

**Target: 2 mg S/L**

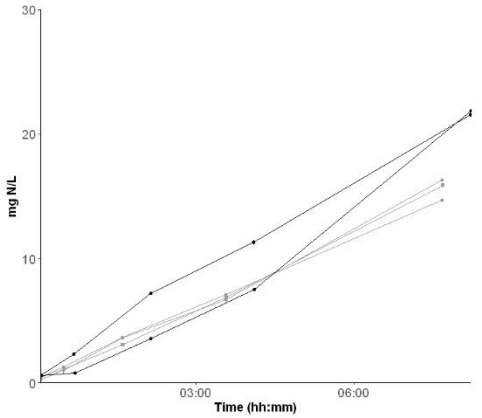


**Target 5 mg S/L**

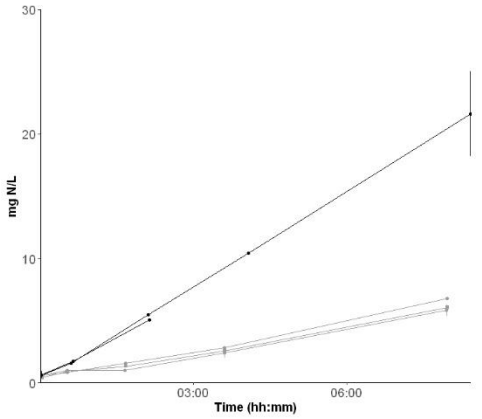


**Target: 10 mg S/L**

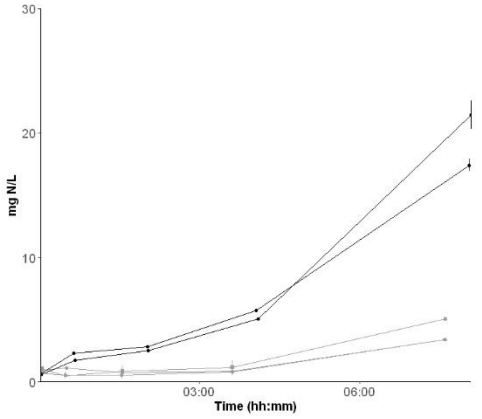

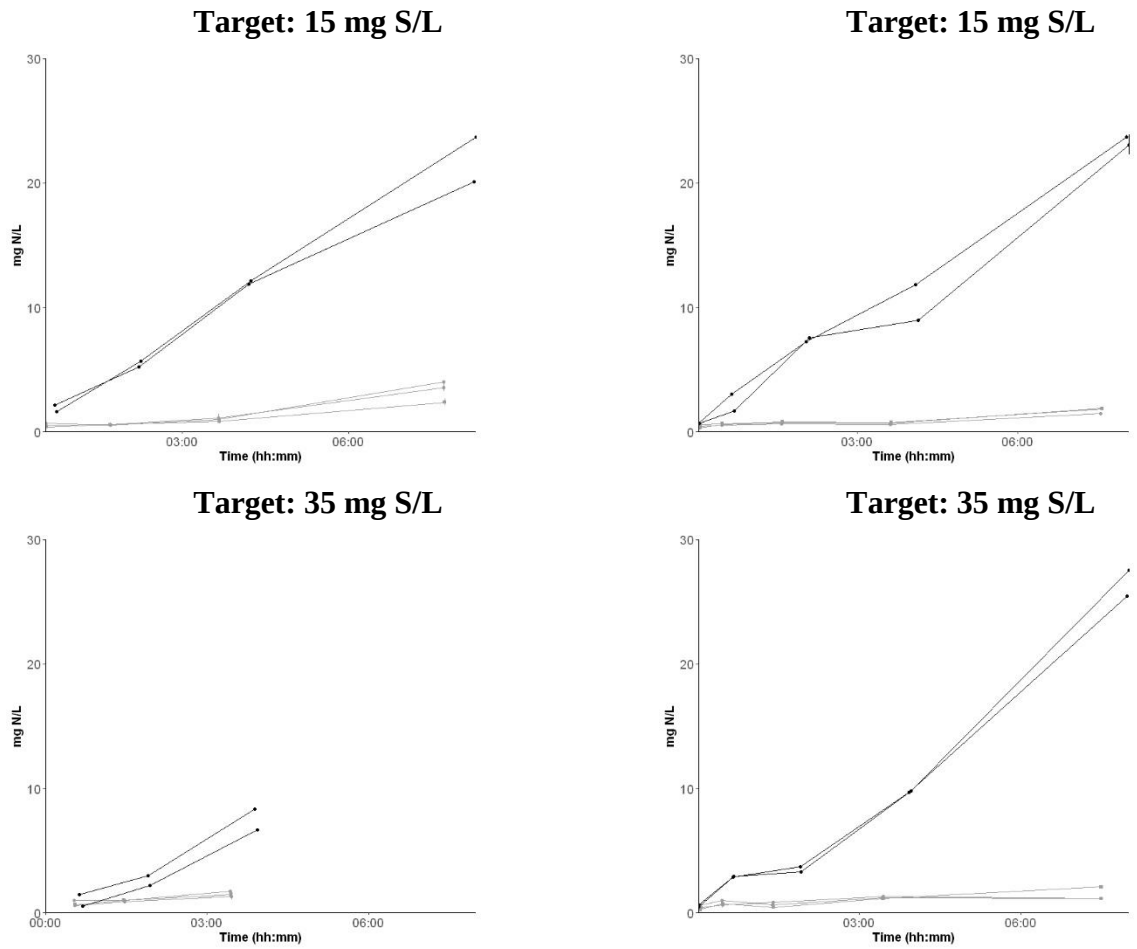


**Figure A3.** Raw data used for rates, nitrite fed batches from A2O process (right) and extended aeration process (left).

## A-4. Quantitative PCR

### *A-4.1. Methods*

qPCR primers used for bacterial ammonia monooxygenase, *Nitrospira nxrB*, and the V4 region of the 16S rRNA gene are given in Table A5. qPCR standards were prepared using DNA extracts from ammonia oxidizing controls from each wastewater treatment plant. PCR was used to amplify the amoA, nxrB, and 16S gene in the extracts. For PCR, each 10 µL reaction volume consisted of: 5 µL Phusion Flash High Fidelity PCR Master Mix (Thermo Fisher Scientific), 0.1 µL of a 50 µM forward and reverse primer (final concentration of 0.5 µM), 0.125 µL of 50 mg/mL ultrapure bovine serum albumin (Ambion, final concentration 0.625 mg/mL), 1 µL of template, and 3.675µL ultrapure water. Thermocycling conditions are given in Table A6. The PCR products were visualized using a 1.5% agarose gel electrophoresis. The resultant band was excised from the gel using a sterile scalpel and the PCR products were purified using the QIAquick Gel Extraction Kit (Qiagen, Valencia, CA). The DNA concentration of the purified amplicon was determined using Qubit Flourometric Quantitation and the two wastewater treatment plants were pooled. The pooled purified amplicon was verified using Sanger sequencing (for the *nxrB* and *amoA* gene). Serial dilutions of the purified PCR products were used as qPCR standards. Standards consisted of serial dilutions ranging from $10^7$-$10^1$ for ammonia monooxygenase genes, $10^7$-$10^2$ for nitrite oxidoreductase genes, and $10^8$-$10^3$ for 16S genes.

**Table A5.** Primers utilized for qPCR

| Target | Forward (5'→3') | Reverse (5'→3') | Citation |
|---|---|---|---|
| amoA | GGG GTT TCT ACT GGT GGT | CCC CTC KGS AAA GCC TTC TTC | (Rotthauwe et al., 1997) |
| nxrB | TAC ATG TGG TGG AAC A | CGG TTC TGG TCR ATC A | (Pester et al., 2014) |
| 16S | GCG CCA GCM GCC GCG GTA A | GGA CTA CHV GGG TWT CTA AT | |

**Table A6.** PCR conditions used to make standards

| Step | Initial Denaturation | Denaturation | Annealing | Extension | Final Extension |
|---|---|---|---|---|---|
| Temperature | 98°C | 98°C | 52°C (nxrB) | 72°C | 72°C |
| | | | 55°C (amoA) | | |
| | | | 55°C (16S) | | |
| Duration | 10 sec | 1 sec | 5 sec | 5 sec | 1 min |
| Number of cycles | 1 | 35 (nxrB) | | | 1 |
| | | 35 (amoA) | | | |
| | | 30 (16S) | | | |

The Mastercycler Realplex Ep (Eppendorf, Hamburg, Germany) was used for all qPCR reactions. 10 µL reaction volumes were used consisting of 5 µL Fast Plus EvaGreen Master Mix (Biotium, Hayward, CA), 0.3 mg/mL bovine serum albumin (BSA, Life Technologies, Grand Island, NY), 0.5 µM primer and 1 µL template. For ammonia monooxygenase cycles consisted of an initial denaturation of 2 minutes at 95°C, followed by 40 cycles of 20 seconds at 95°C, 15 seconds at 59°C, and 30 seconds at 72°C. For nitrite oxidoreductase cycles consisted of an initial denaturation of 2 minutes at 95°C, followed by 40 cycles of 5 seconds at 95°C, 5 seconds at 56.2°C, and 25 seconds at 72°C. For the 16S gene, cycles consisted of an initial denaturation of 2 minutes at 95°C, followed by 35 cycles of 20 seconds at 95°C, 15 seconds at 55°C, and 30 seconds at 72°C. Efficiencies averaged 0.90±0.06 for ammonia monooxygenase, 0.64±0.05 for nitrite oxidoreductase, and 0.88±0.07 for 16S reactions; $R^2$ averaged 0.996±0.002 for all reactions.

### *A-4.2. Results*

Results for the A2O and extended aeration nitrite oxidoreductase, ammonia monooxygenase and 16S transcripts are given in Figure A4. For both genes the amoA and the nxrB, many samples did not have any ammonia monooxygenase or nitrite oxidoreductase transcripts detected in the samples. Only samples with results detected are shown in Figure A4. Other studies of nitrifier inhibition have shown patterns between oxidation rates and *amoA* transcript abundances (Chandran and Love, 2008; Ouyang et al., 2016). However, our data did not clearly follow trends of rate of oxidation. It is important to note that the primers used may not be encapsulating the full

diversity of the ammonia and nitrite oxidizers in the sample. In fact, the primers used for the nitrite oxidoreductase gene only encapsulate Nitrospira nitrite oxidizers. Nitrotoga and Nitrobacter are not incorporated in the qPCR analysis. In addition, in a batch culture over such short time scales, transcript activity may be rapidly responding to environmental conditions, while protein activity may not be responding at the same rate. Although sulfide is a favorable electron donor that could enhance overall activity, we observed no associations between total 16S rRNA transcript copy numbers and sulfide concentration ($p_{spearmans}$>0.06).

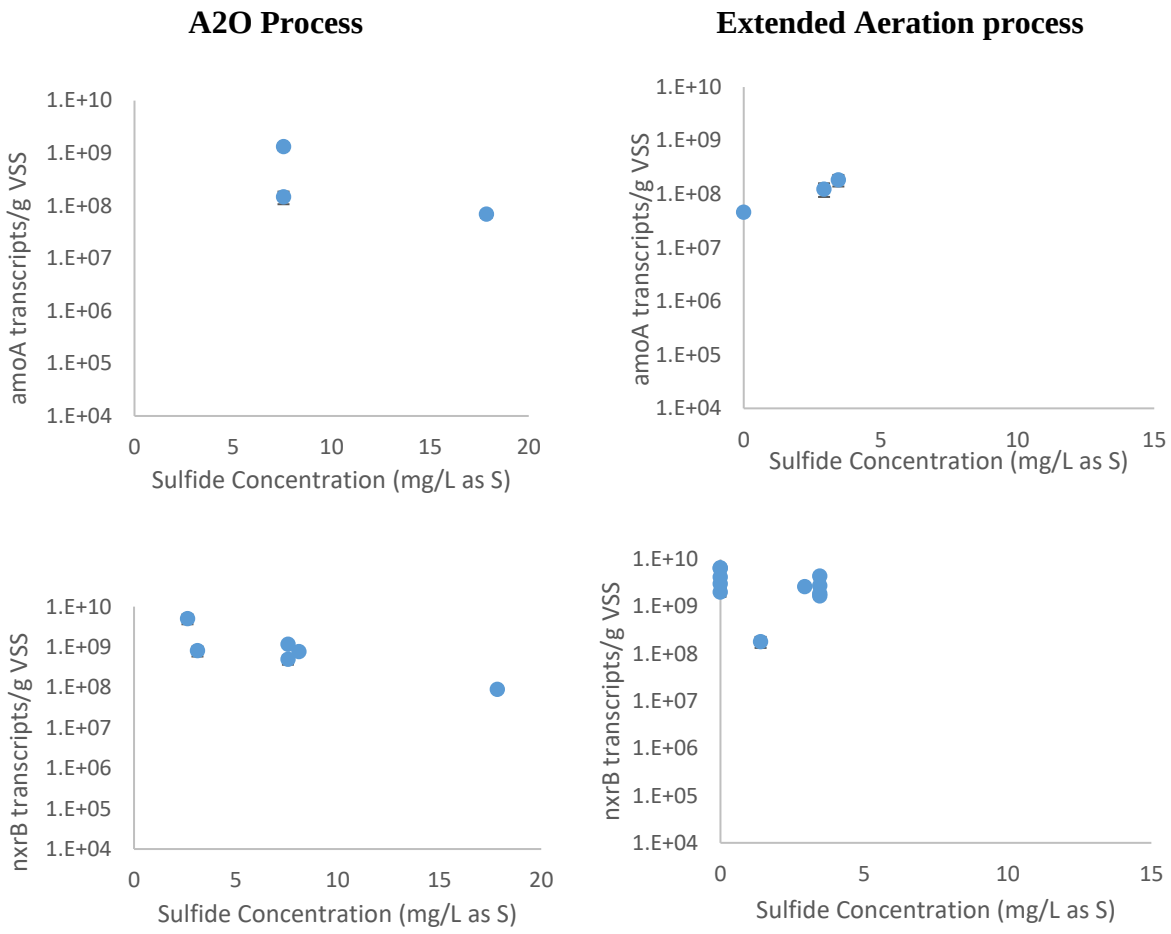

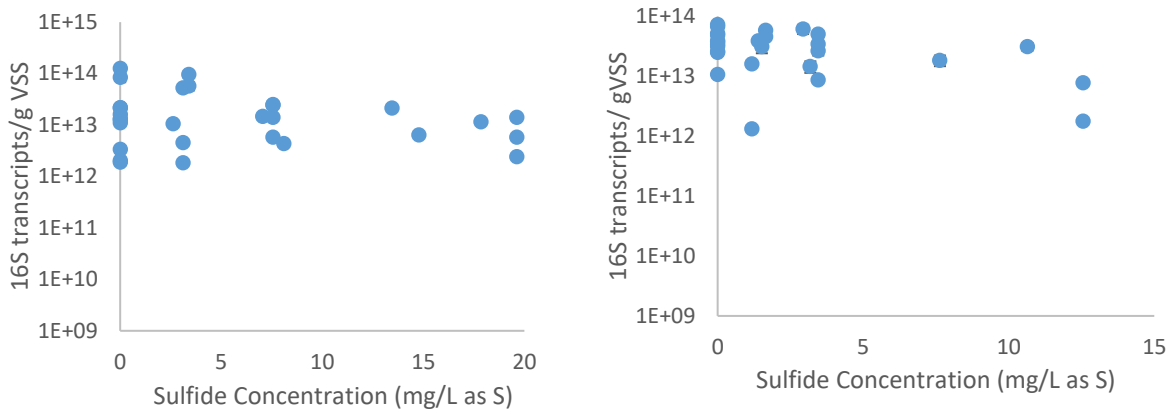


**Figure A4.** Ammonia monooxygenase (top), Nitrospira nitrite oxidoreductase (middle), and 16S (bottom) transcript abundances normalized to VSS at varying sulfide concentrations for the A2O process (left) and the extended aeration process (right)

### A-5. Impact of potential oxygen loses due to sulfide oxidation nitrification

We calculated the potential impact of oxygen loses due to sulfide oxidation on nitrification (Table A7). These calculations were done based on stochiometric demands, given the oxygen requirements of sulfide oxidation to sulfate (2 moles of oxygen/mole of sulfide), ammonium oxidation to nitrite (1.5 moles of oxygen/mole of sulfide), and nitrite oxidation to nitrate (0.5 moles of oxygen/mole of sulfide). The purpose of the calculation was to determine the impact of oxygen diversion to sulfide oxidation on nitrification. For example, for batch experiments at 35 mg sulfide-S/L, 0.1 mg $NH_4$-N/L could not be oxidized due to loses of oxygen diverted for sulfide oxidation (ammonia-N diverted):

$$35\ \frac{mg\ S}{L} \cdot \frac{1\ mmol\ S}{32\ mg\ S} \cdot \frac{2\ mmole\ O_2}{mmol\ S} \cdot \frac{1\ mmole\ NH_4^+}{1.5\ mmol\ O_2} \frac{14\ mg\ N}{mmol\ N} = 20\ mg\ N/L$$

**Table A7.** Potential nitrification loss due to aerobic sulfide oxidation and the actual nitrogen oxidized during batches. *Sulfide concentrations in A2O batches were slightly lower.

| Sulfide (mg/L as S) | Ammonia-N Diverted (mg/L) | A2O ammonia-N oxidized (mg/L) [diverted/oxidized] % | Extended Aeration ammonia-N oxidized (mg/L) [diverted/oxidized] % | Nitrite-N Diverted (mg/L) | A2O nitrite-N oxidized (mg/L) [diverted/oxidized] % | Extended Aeration nitrite-N oxidized (mg/L) [diverted/oxidized] % |
|---|---|---|---|---|---|---|
| 2 | 1.2 | 46±2.3 [2.6] | 27±3.1 [4.4] | 3.5 | 20±5.9 [18] | 16±0.8 [22] |
| 5 | 2.9 | *43±1.9 [6.7] | 23±1.9 [13] | 8.8 | *17±1.8 [52] | 6.2±0.5 [140] |
| 10 | 5.8 | *36±0.9 [16] | 14±5.8 [41] | 18 | *8.9±2.7 [200] | 3.9±0.9 [450] |
| 15 | 8.8 | 28±1.9 [31] | 13±1.5 [68] | 26 | 3.3±0.9 [800] | 1.7±0.2 [150] |
| 25 | 15 | 9.6±1.3 [150] | 5.7±1.6 [260] | 44 | 1.5±0.2 [290] | 1.5±0.5 [290] |

### A-6. 16S rRNA sequencing data

The microbial community structure based on DNA is shown in Figure A5. There were no associations between sulfide concentration and microbial community structure using DNA data.

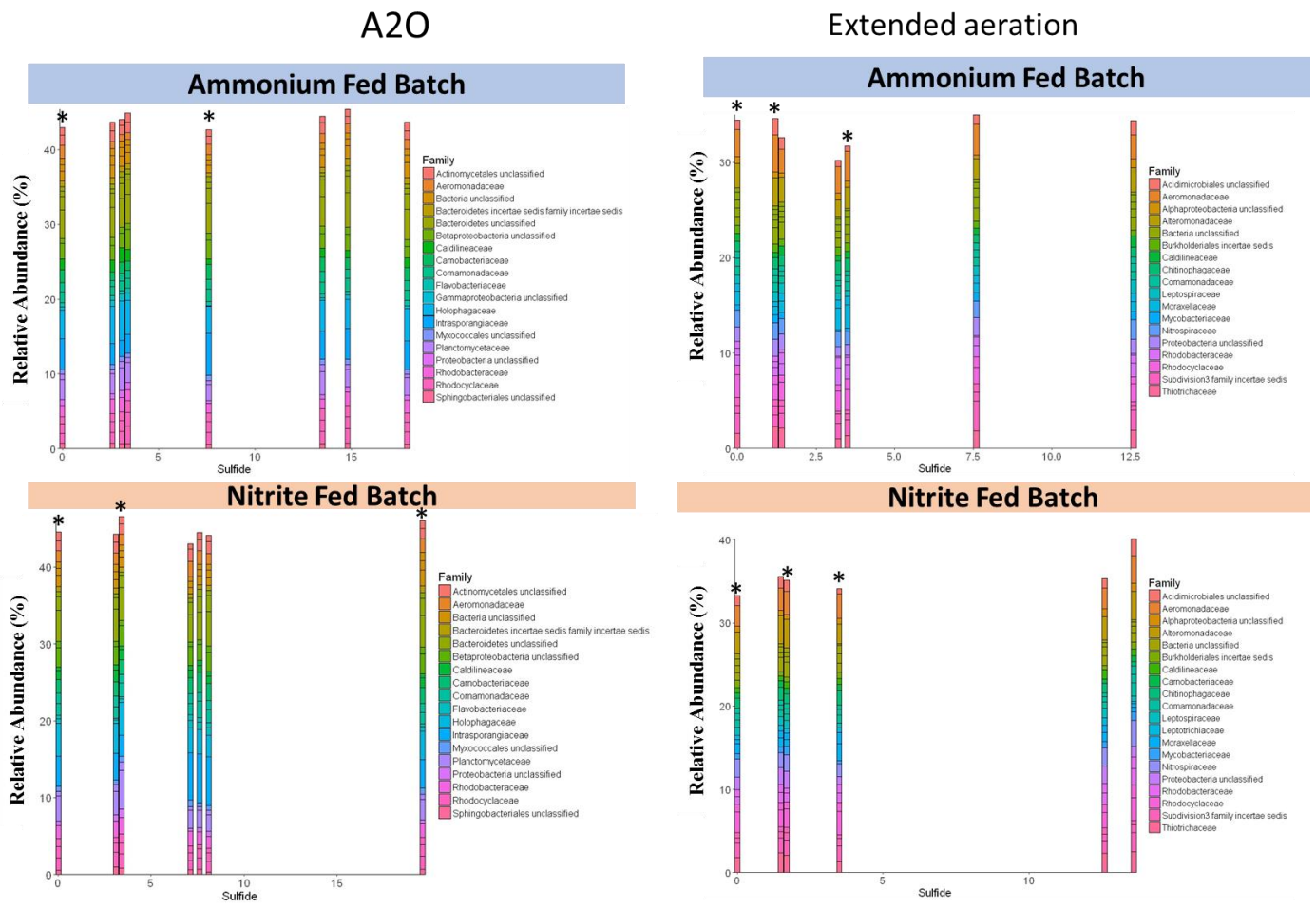


**Figure A5.** Relative abundance of top 30 most abundant OTUs based on DNA data. An asterisk above the bar indicates multiple samples at the same sulfide concentration were averaged for the plot.

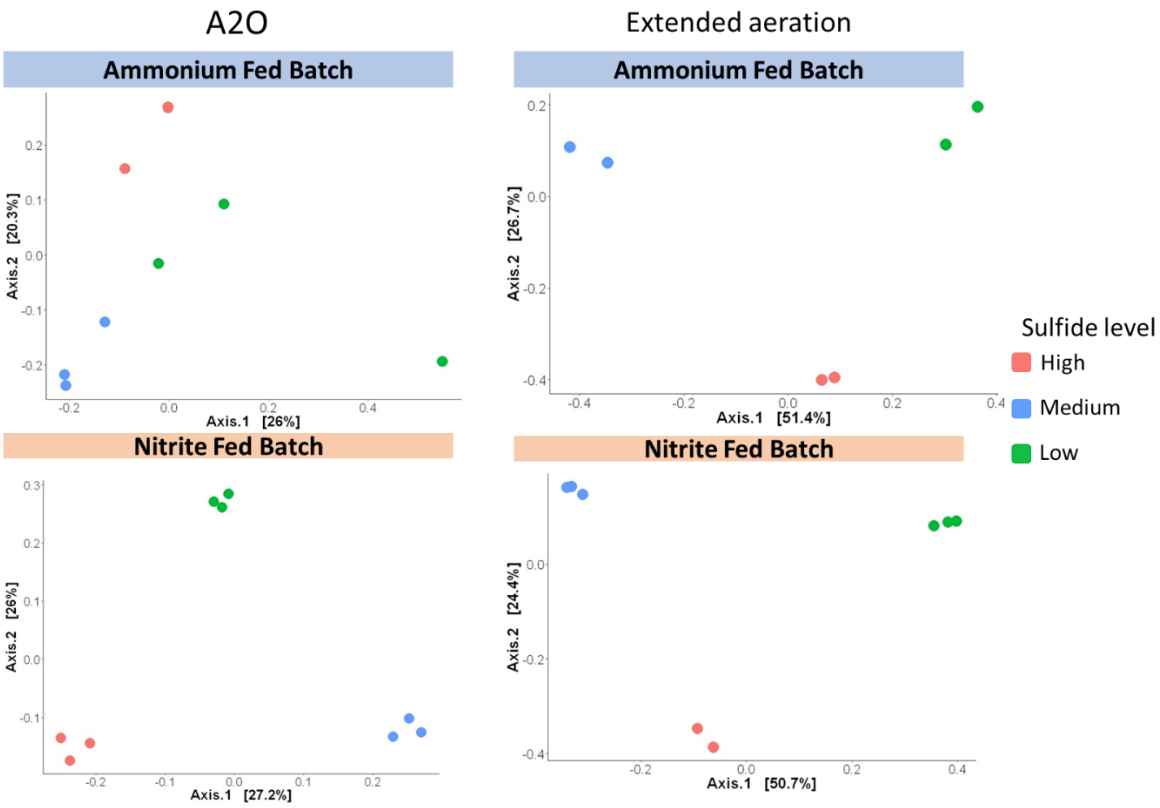


**Figure A6.** Principle Coordinate Analysis on Bray Curtis dissimilarity of cDNA relative abundances of OTUs. High represents sulfide levels above the AOB inhibition index, medium represents sulfide levels between the AOB and NOB inhibition indices, and low represents sulfide levels below the NOB inhibition index.

# Appendix B.

## Supplementary Information for Chapter 4.

### Reactor Operation and Startup

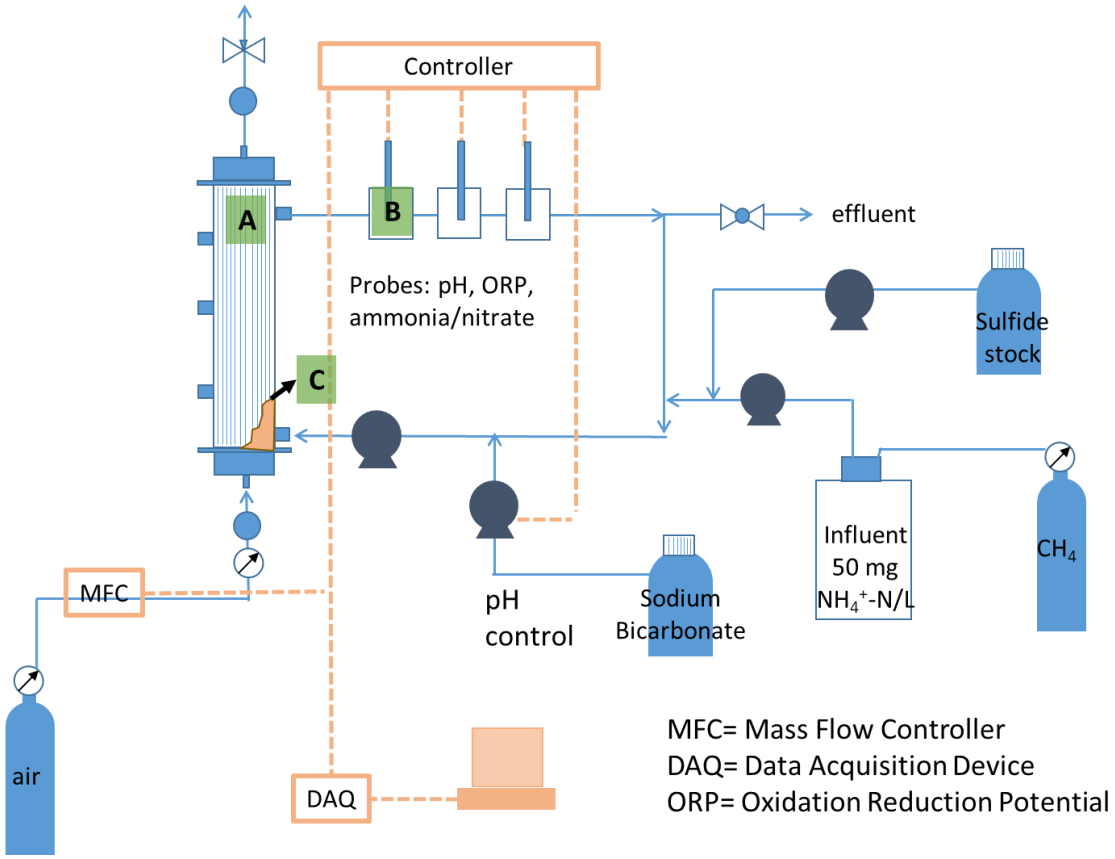


**Figure B1.** MABR reactor schematic. Letters indicate biomass sampling location.

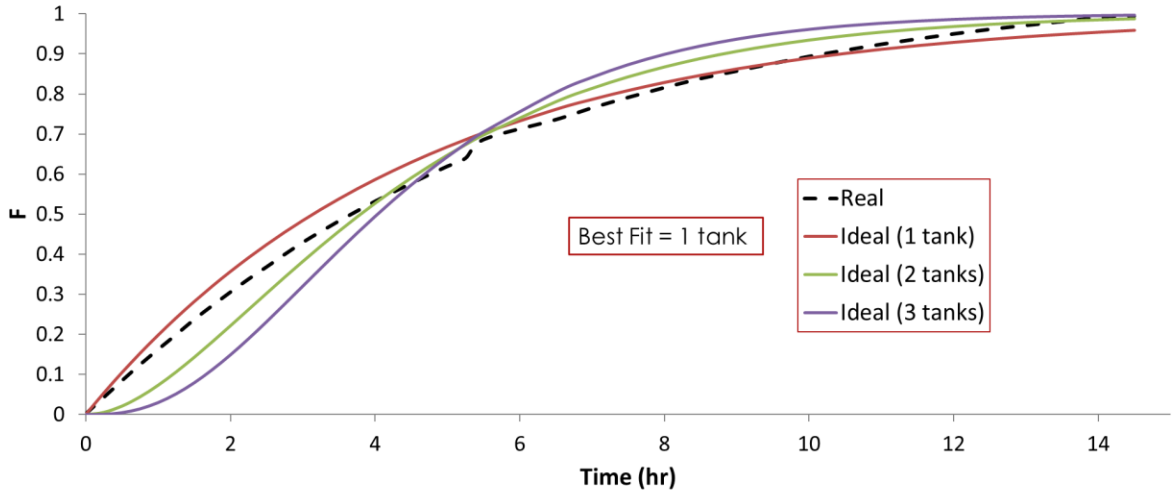


**Figure B2.** F curve from tracer test.

**Table B1.** Reactor Loading Characteristics

| Experiment | Phase | Days | Ammonium load (g N/m$^2$-day) | Sulfide concentration (mg S/L) [load (mg S/m$^2$-day)] |
|---|---|---|---|---|
| A. Reactor startup | A-1 | 0-1 | 0.33 | 0 [0] |
| | A-2 | 1-11 | 0.45 | |
| | A-3 | 11-15 | 0.53 | |
| | A-4 | 15-20 | 0.60 | |
| | A-5 | 20-62 | 0.68 | |
| | A-6 | 62-70 | 0.75 | |
| | A-7 | 70-81 | 0.78 | |
| | A-8 | 81-83 | 0.83 | |
| | A-9 | 83-85 | 0.86 | |
| | A-10 | 85-92 | 0.89 | |
| | A-11 | 92-110 | 0.92 | |

| | | | | |
|---|---|---|---|---|
| | A-12 | 110-120 | 0.95 | |
| B. Long term increase in sulfide | B-1 | 120-141 | 0.95 | 0 [0] |
| | B-2 | 141-151 | | 0.1 [0.04] |
| | B-3 | 151-194 | | 0.5 [0.20] |
| | B-4 | 194-215 | | 1 [0.39] |
| | B-5 | 215-294 | | 2 [0.78] |
| | B-6 | 294-333 | | 3 [1.17] |
| | B-7 | 333-364 | | 4 [1.56] |
| | B-8 | 364-398 | | 6 [2.35] |
| | B-9 | 398-419 | | 10 [3.91] |
| C. Stabilize Operation Between Experiments | C-1 | 419-509 | 0.95 | 0 [0] |
| D. Pulse experiments (not described here) | D-1 | 509-512 | 0.95 | Daily pulses: 0 & 10 [0 & 3.91] |
| C. Stabilize Operation Between Experiments | C-2 | 512-514 | 0.95 | 0 [0] |
| D. Pulse experiments (not described here) | D-2 | 514-519 | 0.95 | Daily pulses: 0 & 10 [0 & 3.91] |
| C. Stabilize Operation Between Experiments | C-3 | 519-546 | 0.95 | 10 [3.91] |
| E. $^{15}N$ experiments with sulfide | E-1 | 547-551 | 0.95 | 10 [3.91] |
| C. Stabilize Operation Between Experiments | C-4 | 552 | 0.95 | 6 [2.35] |
| | C-5 | 553 | | 0.1 [0.04] |

| | | | | |
|---|---|---|---|---|
| | C-6 | 554-556 | | 0 [0] |
| E. $^{15}$N experiments with sulfide | E-2 | 557-562 | 0.95 | 0 [0] |

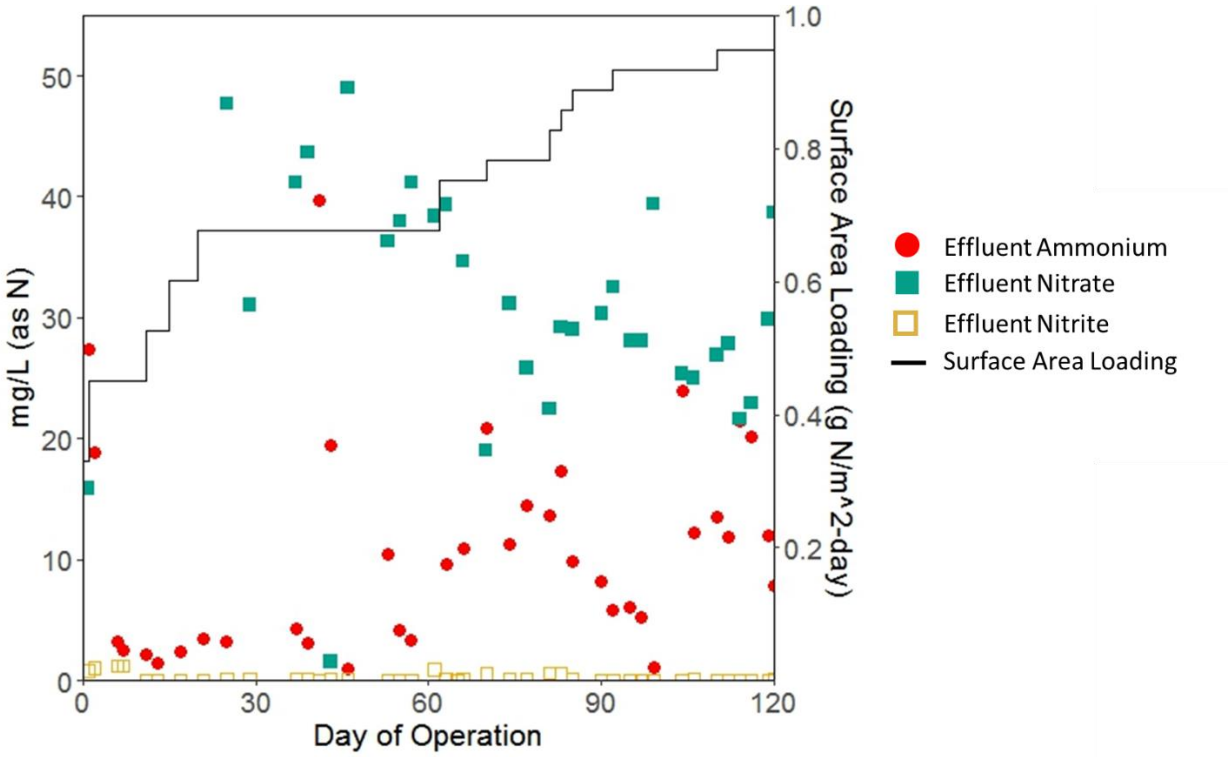


**Figure B3.** Effluent quality during phase A, reactor startup

## qPCR methods

qPCR primers used for bacterial ammonia monooxygenase, anammox 16S gene, *Nitrospira nxrB*, and the V4 region of the 16S rRNA gene, and comammox *amoA* gene are given in Table B2. Clade B of comammox could not be detected in our samples. qPCR standards were prepared using DNA extracts from the reactor. PCR was used to amplify the *amoA*, *nxrB*, comammox *amoA*, anammox 16S, and 16S gene in the extracts. For PCR, each 10 µL reaction volume consisted of: 5 µL Phusion Flash High Fidelity PCR Master Mix (Thermo Fisher Scientific), 0.1 µL of a 50 µM forward and reverse primer (final concentration of 0.5 µM), 0.125 µL of 50 mg/mL ultrapure bovine serum

albumin (Ambion, final concentration 0.625 mg/mL), 1 µL of template, and 3.675µL ultrapure water. Thermocycling conditions are given in Table B3. The PCR products were visualized using a 1.5% agarose gel electrophoresis. The resultant band was excised from the gel using a sterile scalpel and the PCR products were purified using the QIAquick Gel Extraction Kit (Qiagen, Valencia, CA). The DNA concentration of the purified amplicon was determined using Qubit Flourometric Quantitation. The purified amplicon was verified using Sanger sequencing. Serial dilutions of the purified PCR products were used as qPCR standards. Standards consisted of serial dilutions ranging from $10^6$-$10^1$ for ammonia monooxygenase genes, $10^7$-$10^2$ for nitrite oxidoreductase genes, anammox 16S genes, and comammox *amoA* genes, and $10^8$-$10^3$ for 16S genes.

**Table B2.** Primers utilized for qPCR

| Target | Forward (5'→3') | Reverse (5'→3') | Citation |
|---|---|---|---|
| amoA | GGG GTT TCT ACT GGT GGT | CCC CTC KGS AAA GCC TTC TTC | (Rotthauwe et al., 1997) |
| nxrB | TAC ATG TGG TGG AAC A | CGG TTC TGG TCR ATC A | (Pester et al., 2014) |
| 16S | GCG CCA GCM GCC GCG GTA A | GGA CTA CHV GGG TWT CTA AT | (Caporaso et al., 2011) |
| Anammox 16S | ATGGGCACTMRGTAGAGGGGTTT | AACGTCTCACGACACGAGCTG | (Tsushima et al., 2007) |
| Comammox *amoA*-clade A | Equimolar mixture of:<br>TACAACTGGGTGAACTA<br>TATAACTGGGTGAACTA<br>TACAATTGGGTGAACTA<br>TACAACTGGGTCAACTA<br>TACAACTGGGTCAATTA<br>TATAACTGGGTCAATTA | Equimolar mixture of:<br>AGATCATGGTGCTATG<br>AAATCATGGTGCTATG<br>AGATCATGGTGCTGTG<br>AAATCATGGTGCTGTG<br>AGATCATCGTGCTGTG<br>AAATCATCGTGCTGTG | (Pjevac et al., 2016) |

**Table B3.** PCR conditions used to make standards

| Step | Initial Denaturation | Denaturation | Annealing | Extension | Final Extension |
|---|---|---|---|---|---|
| Temperature | 98°C | 98°C | 65°C anammox | 72°C | 72°C |
| | | | 47°C (coma) | | |
| | | | 52°C (nxrB) | | |
| | | | 55°C (amoA) | | |
| | | | 55°C (16S) | | |
| Duration | 10 sec | 1 sec | 5 sec | 5 sec | 1 min |
| Number of cycles | 1 | 35 anammox | | | 1 |
| | | 30 (coma) | | | |
| | | 35 (nxrB) | | | |
| | | 35 (amoA) | | | |
| | | 30 (16S) | | | |

The Mastercycler Realplex Ep (Eppendorf, Hamburg, Germany) was used for all qPCR reactions. 10 µL reaction volumes were used consisting of 5 µL Fast Plus EvaGreen Master Mix (Biotium, Hayward, CA), 0.3 mg/mL bovine serum albumin (BSA, Life Technologies, Grand Island, NY), 0.5 µM primer and 1 µL template. For ammonia monooxygenase cycles consisted of an initial denaturation of 2 minutes at 95°C, followed by 40 cycles of 20 seconds at 95°C, 15 seconds at 59°C, and 30 seconds at 72°C. For nitrite oxidoreductase cycles consisted of an initial denaturation of 2 minutes at 95°C, followed by 40 cycles of 5 seconds at 95°C, 5 seconds at 56.2°C, and 25 seconds at 72°C. For the 16S gene, cycles consisted of an initial denaturation of 2 minutes at 95°C, followed by 30 cycles of 20 seconds at 95°C, 15 seconds at 55°C, and 30 seconds at 72°C. For comammox *amoA* cycles consisted of initial denaturation of 2 minutes at 95°C, followed by

45 cycles of 5 seconds at 95°C, 10 seconds at 52°C, and 25 seconds at 72°C. For anammox reactions cycles consisted of initial denaturation of 2 minutes at 95°C, followed by 40 cycles of 5 seconds at 95°C, 5 seconds at 61°C, and 25 seconds at 72°C. All qPCR programs had a melt curve analysis at the end of the program to evaluate nonspecific binding. Efficiencies averaged 0.88±0.04 for ammonia monooxygenase, 0.56±0.02 for nitrite oxidoreductase, 0.84±0.06 for comammox reactions, 0.91±0.02 for anammox reactions, and 0.85±0.11 for 16S reactions; $R^2$ averaged 0.997±0.002 for all reactions.

**Table B4.** Accession numbers for custom database

| NCBI Accession Number | Gene | Organism |
|---|---|---|
| BAJ14738.1 | soxB | Sulfuritalea hydrogenivorans |
| BAJ14737.1 | aprA | |
| WP_041098216.1 | dsrB | |
| WP_041098218.1 | dsrB | |
| WP_041100037.1 | aprA | |
| WP_041100039.1 | aprB | |
| WP_084207406.1 | soxB | |
| WP_084207482.1 | soxA | |
| WP_041096647.1 | napA | |
| WP_041101723.1 | nirK/nirS | |
| WP_041099757.1 | nirK/nirS | |
| WP_041100219.1 | nirK/nirS | |
| WP_041099729.1 | nosD | |
| WP_084207398.1 | nosD | |
| WP_009205081.1 | dsrB | Sulfuritalea denitrificans |
| WP_009207523.1 | dsrB | |
| WP_041673408.1 | aprA | |
| WP_009205410.1 | soxB | |
| WP_009205411.1 | soxA | |
| WP_009206827.1 | napA | |
| WP_009206840.1 | nirK/nirS | |

| | | |
|---|---|---|
| WP_009205117.1 | nirK/nirS | |
| WP_009205268.1 | nirB | |
| WP_009206853.1 | nosD | |
| WP_009206232.1 | nosD | |
| WP_011311919.1 | sqr | Thiobacillus denitrificans |
| WP_011312546.1 | fccA | |
| WP_011312547.1 | fccB | |
| WP_011311821.1 | dsrA | |
| WP_011311881.1 | dsrA | |
| WP_011312996.1 | dsrB | |
| WP_011312997.1 | dsrA | |
| WP_011311384.1 | aprA | |
| WP_011311385.1 | aprB | |
| WP_011312794.1 | aprA | |
| WP_011312795.1 | aprB | |
| WP_041432283.1 | soxB | |
| WP_011311076.1 | soxA | |
| WP_041432283.1 | soxB | |
| WP_011312822.1 | napA | |
| WP_011312991.1 | narI/narV | |
| WP_011310590.1 | nirK/nirS | |
| WP_041432744.1 | nirB | |
| WP_011311073.1 | nor | |
| WP_009206748.1 | nor | |
| WP_011311335.1 | nor | |
| WP_011311903.1 | nosD | |
| AKX33668.1 | pmoA | Methylococcaceae bacterium Sn10-6 |
| CAD84854.1 | amoB | Nitrosomonas europaea ATCC 19718 |
| CAD84855.1 | amoA | |
| AL954747.1 | amoC | |

| | | |
|---|---|---|
| CAD84856.1 | amoC | |
| CAD85973.1 | amoB | |
| CAD85974.1 | amoA | |
| CAD85975.1 | amoC | |
| CAD84873.1 | hao | |
| CAD85955.1 | hao | |
| CAD86251.1 | hao | |
| ALA56693.1 | nxrB | Nitrospira moscoviensis |
| ALA56694.1 | nxrA | |
| CUS35558.1 | amoC | Candidatus Nitrospira nitrificans |
| CUS34405.1 | amoC | |
| CUS38776.1 | nxrA | |
| CUS36764.1 | nxrA | |
| CUS34648.1 | nxrA | |
| CUS34649.1 | nxrA | |
| CUS34650.1 | nxrB | |
| CUS36762.1 | nxrB | |
| WP_062484767.1 | amoA | Candidatus Nitrospira inopinata |
| WP_062484768.1 | amoB | |
| WP_062484140.1 | amoC | |
| WP_062483313.1 | amoC | |
| OYT21943.1 | amoA | Nitrospira sp. UW-LDO-01 |
| OYT21942.1 | amoB | |
| OYT19804.1 | nxrG | |
| GAN35163.1 | nrfA | Candidatus Brocadia sinica JPN1 |
| GAN33811.1 | hzo | |
| GAN32119.1 | hzsA | |
| GAN32120.1 | hzsB | |
| KKO18415.1 | nirK | Candidatus Brocadia sinica fulgida |
| CBE69519.1 | pmoA | Candidatus Methylomirabilis oxyfera |

| | | |
|---|---|---|
| CBE69517.1 | pmoB | |
| CBE69387.1 | pmoC | |
| CBE69521.1 | pmoC | |
| 2713528256 (IMG, Gene ID) | narH | |
| 2713528258 (IMG, GeneID) | narG | |
| 2713528254 (IMG, Gene ID) | narG | |
| 2713528255(IMG, Gene ID) | narJ | |
| 2713529904 (IMG, Gene ID) | napA | |
| 2517502826 (IMG, Gene ID) | nirB | |
| 2517302091 (IMG, Gene ID) | nirB | |
| 2713528341 (IMG, Gene ID) | nirB | |
| WP_050343474.1 | nrfA | Selenomonas sp. oral taxon 478 |
| PJF26186.1 | nrfA | Chloroflexi bacterium |
| WP_011342651.1 | nrfA | Pelobacter carbinolicus |
| WP_062418934.1 | nrfA | Levilinea saccharolytica |
| gi\|266618717 | rpoB | Conserved |
| gi\|239938700 | rpoB | |
| gi\|6831647 | rpoB | |
| gi\|6094125 | rpoB | |
| gi\|2507343 | rpoB | |
| WP_000037868.1 | rpoB | |
| WP_005873809.1 | rpoB | |
| WP_010931849.1 | rpoB | |
| WP_011015993.1 | rpoB | |
| WP_011056489.1 | rpoB | |
| WP_011029792.1 | rpoB | |
| WP_010918390.1 | rpoB | |

## $^{15}$N rate experiments

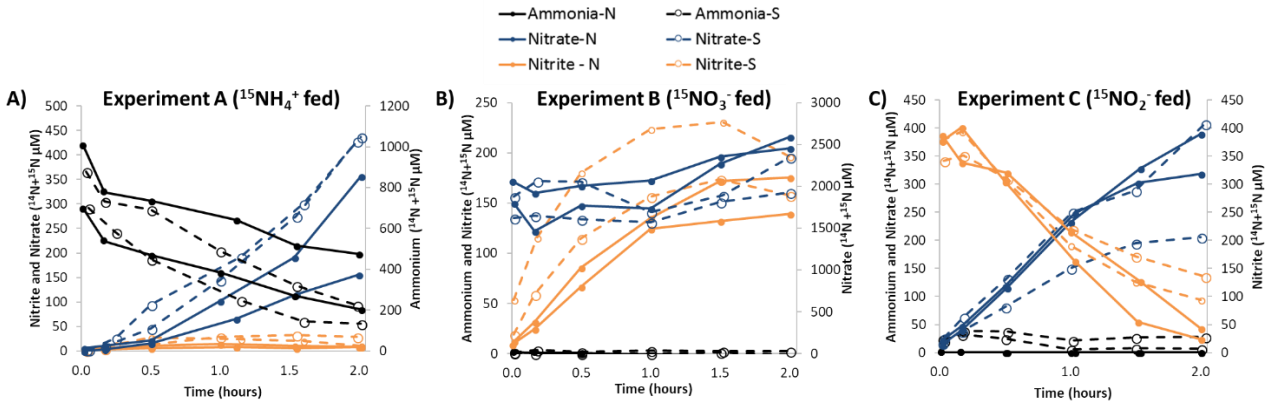


**Figure B4.** Results from $^{15}$N experiments. Left rates of ammonia loss, right, rates of nitrite production. Non-filled points and dashed lines indicate sulfide amended experiments.

**Table B5.** Sulfur Concentrations during batch experiments. Numbers in parenthesis are the rates of sulfide loss.

| Experiment A | | | | | | |
|---|---|---|---|---|---|---|
| **A1 (-97 µmol S/L-hr)** | | | | | | |
| **Time (min)** | **Time (hr)** | **Sulfide (mg S/L)** | **Sulfate (mg S/L)** | **Sulfate (stdev)** | **Sulfate produced** | **Sulfate produced (stdev)** |
| 14 | 0.2 | 1.7 | 4.6 | 0.1 | 4.0 | 0.1 |
| 22 | 0.4 | 0.9 | 1.5 | 0.0 | 0.9 | 0.0 |
| 41 | 0.7 | 0.2 | 4.7 | 0.0 | 4.1 | 0.0 |
| 81 | 1.3 | 0.1 | 3.9 | 0.1 | 3.2 | 0.1 |
| 107 | 1.8 | 0.1 | 6.5 | 0.0 | 5.8 | 0.0 |
| 132 | 2.2 | 0.1 | 5.1 | 0.0 | 4.5 | 0.0 |
| **A2 (-140 µmol/L-hr)** | | | | | | |
| 13 | 0.2 | 0.9 | 5.0 | 0.0 | 3.7 | 0.1 |
| 21 | 0.3 | 0.3 | 5.5 | 0.0 | 4.2 | 0.1 |
| 42 | 0.7 | 0.4 | 8.2 | 0.0 | 6.9 | 0.0 |
| 71 | 1.2 | 0.1 | 9.5 | 0.0 | 8.2 | 0.0 |
| 106 | 1.8 | 0.1 | 11.5 | 0.1 | 10.3 | 0.1 |
| 130 | 2.2 | 0.1 | 6.0 | 0.0 | 4.8 | 0.0 |
| **Experiment B** | | | | | | |
| **B1 (-72 µmol/L-hr)** | | | | | | |
| 12 | 0.2 | 1.6 | 3.4 | 0.1 | 1.0 | 0.1 |
| 22 | 0.4 | 0.5 | 3.1 | 0.0 | 0.7 | 0.1 |
| 42 | 0.7 | 0.3 | 4.1 | 0.0 | 1.7 | 0.0 |
| 71 | 1.2 | 0.2 | 5.4 | 0.0 | 3.0 | 0.1 |

| | | | | | | |
|---|---|---|---|---|---|---|
| 102 | 1.7 | 0.2 | 4.9 | 0.0 | 2.5 | 0.0 |
| 135 | 2.3 | 0.1 | 8.1 | 0.0 | 5.7 | 0.1 |
| **B2 (-78 µmol/L-hr)** | | | | | | |
| 12 | 0.2 | 1.5 | 3.8 | 0.0 | 2.4 | 0.0 |
| 22 | 0.4 | 0.5 | 6.3 | 0.0 | 5.0 | 0.0 |
| 42 | 0.7 | 0.1 | 7.2 | 0.1 | 5.8 | 0.1 |
| 71 | 1.2 | 0.1 | 6.2 | 0.0 | 4.8 | 0.0 |
| 101 | 1.7 | 0.1 | 8.6 | 0.0 | 7.2 | 0.0 |
| 131 | 2.2 | 0.0 | 6.9 | 0.0 | 5.5 | 0.0 |
| **Experiment C** | | | | | | |
| **C1 (-120 µmol/L-hr)** | | | | | | |
| 12 | 0.2 | 2.3 | 5.2 | 0.0 | 4.0 | 0.0 |
| 20 | 0.3 | 1.0 | 3.9 | 0.0 | 2.7 | 0.0 |
| 40 | 0.7 | 0.2 | 6.5 | 0.1 | 5.3 | 0.1 |
| 70 | 1.2 | 0.1 | 11.7 | 0.0 | 10.5 | 0.0 |
| 100 | 1.7 | 0.2 | 12.2 | 0.1 | 11.0 | 0.1 |
| 131 | 2.2 | 0.2 | 15.2 | 0.1 | 14.0 | 0.2 |
| **C2 (-45 µmol/L-hr)** | | | | | | |
| 12 | 0.2 | 1.2 | 6.8 | 0.0 | 5.5 | 0.0 |
| 22 | 0.4 | 0.3 | 5.6 | 0.0 | 4.2 | 0.0 |
| 49 | 0.8 | 0.2 | 7.2 | 0.1 | 5.8 | 0.1 |
| 73 | 1.2 | 0.1 | 12.6 | 0.2 | 11.2 | 0.2 |
| 101 | 1.7 | 0.1 | 11.7 | 0.0 | 10.4 | 0.0 |
| 133 | 2.2 | 0.1 | 16.9 | 0.0 | 15.5 | 0.0 |

## Supplementary Coverage figures

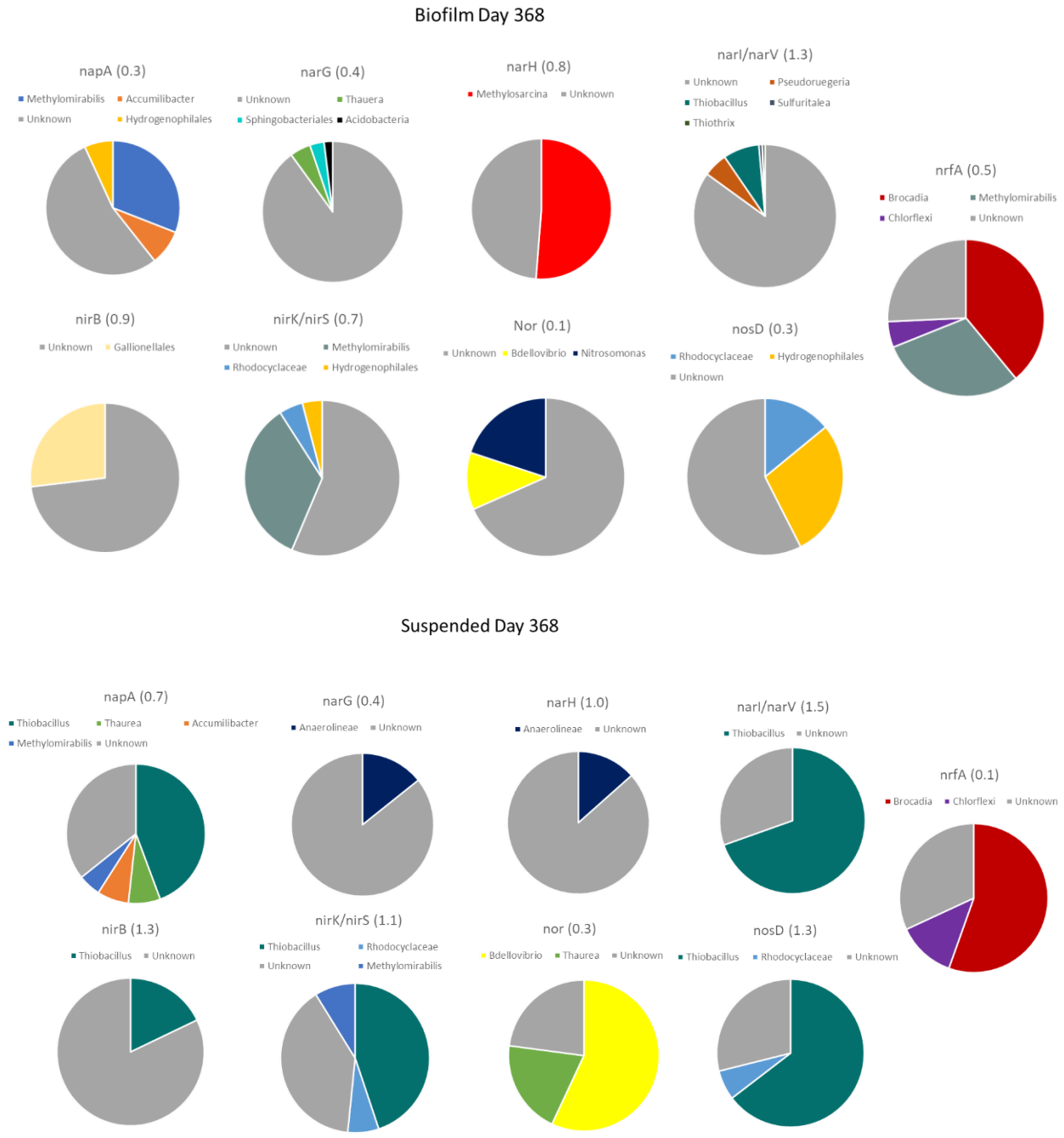


**Figure B5.** Best hit of denitrification genes in Biofilm (top) and (suspended) samples. Numbers in parenthesis represent total coverage of that gene. Unknown samples were either hits to unknown organisms or had multiple hits to distinct organisms with cutoffs.

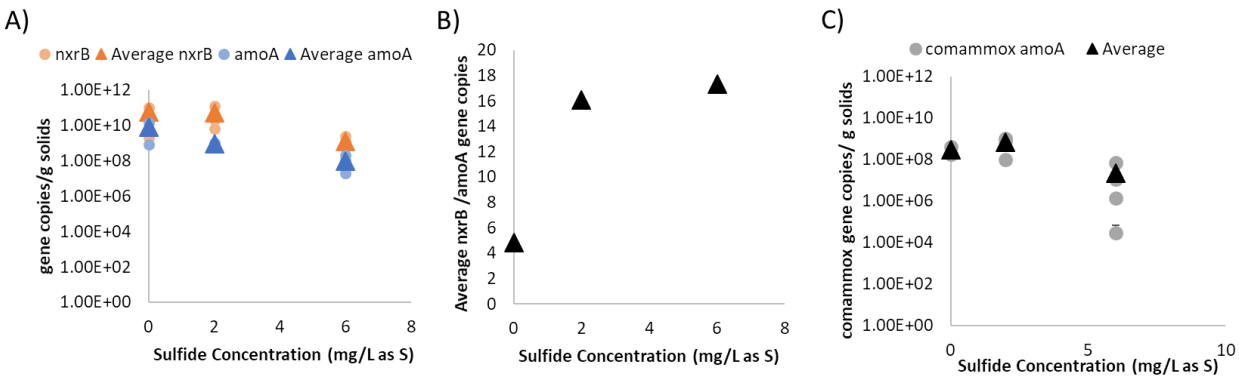


**Figure B6.** Nitrifying organisms measured by qPCR. A) Absolute abundances of *Nitrospira* and AOB expressed as abundnaces of gene copies of *nxrB* and *amoA*, respectively. B) *Nitrospira nxrB* abundances relative to *amoA*. C) Absolute abundances of comammox expressed as abundances of gene copies of comammox *amoA*.

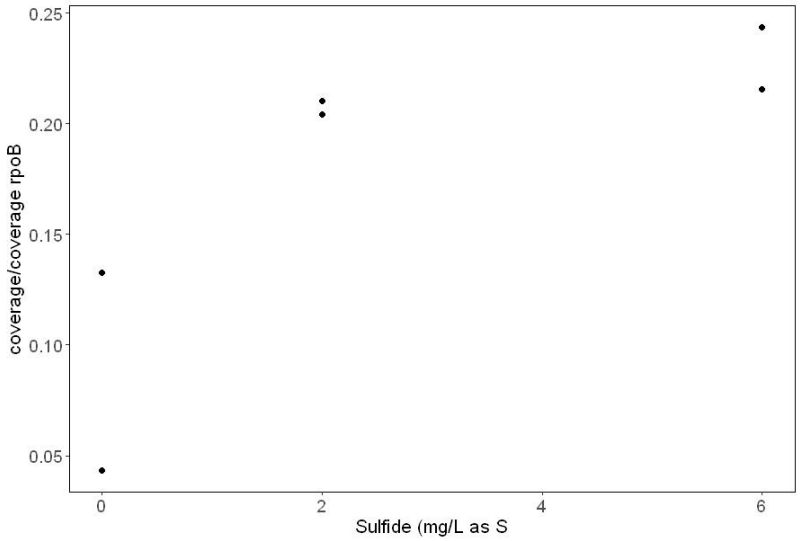


**Figure B7.** Coverage of *nrfA* in biofilm during sulfide increases

## Supplementary Reactor Data figure

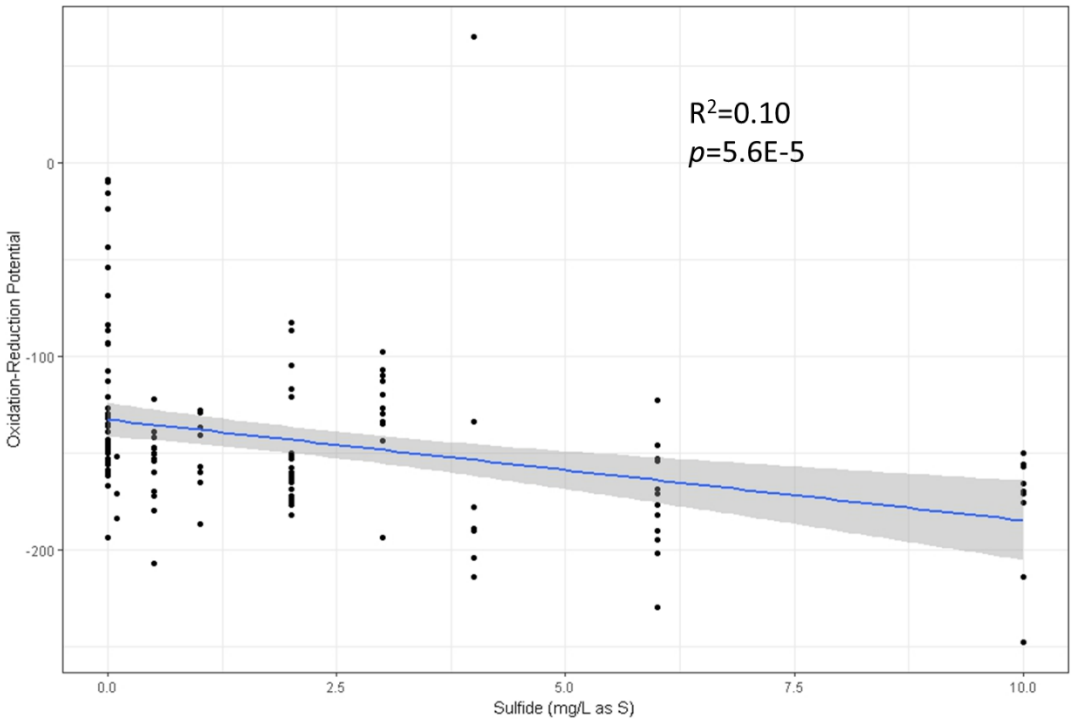


**Figure B8.** Relationship between sulfide and redox (as measured by ORP)

## Unique COG Categories

**Table B6.** Unique protein clusters in DAMO bin. Shaded lines refer to unique functions in the bin.

| COG Identifier | Number of clusters | COG Category | Description |
|---|---|---|---|
| COG0282 | 1 | C | Acetate kinase |
| COG0546 | 1 | C | Phosphoglycolate phosphatase, HAD superfamily |
| COG1012 | 1 | C | Acyl-CoA reductase or other NAD-dependent aldehyde dehydrogenase |
| COG4659 | 1 | C | Na+-translocating ferredoxin:NAD+ oxidoreductase RNF, RnfG subunit |
| COG0849 | 1 | D | Cell division ATPase FtsA |
| COG4641 | 1 | D | Spore maturation protein CgeB |
| COG0334 | 1 | E | Glutamate dehydrogenase/leucine dehydrogenase |
| COG0421 | 1 | E | Spermidine synthase |
| COG2095 | 1 | E | Small neutral amino acid transporter SnatA, MarC family |

| | | | |
|---|---|---|---|
| COG2309 | 1 | E | Leucyl aminopeptidase (aminopeptidase T) |
| COG0175 | 1 | E\|H | 3'-phosphoadenosine 5'-phosphosulfate sulfotransferase (PAPS reductase)/FAD synthetase or related enzyme |
| COG0241\|COG0859 | 1 | E\|M | Histidinol phosphatase or a related phosphatase\|ADP-heptose:LPS heptosyltransferase |
| COG1864 | 1 | F | DNA/RNA endonuclease G, NUC1 |
| COG1109 | 1 | G | Phosphomannomutase |
| COG1216 | 7 | G | Glycosyltransferase, GT2 family |
| COG1449 | 1 | G | Alpha-amylase/alpha-mannosidase, GH57 family |
| COG1523 | 1 | G | Pullulanase/glycogen debranching enzyme |
| COG2814 | 1 | G | Predicted arabinose efflux permease, MFS family |
| COG0726 | 2 | G\|M | Peptidoglycan/xylan/chitin deacetylase, PgdA/CDA1 family |
| COG1011 | 1 | H | FMN phosphatase YigB, HAD superfamily |
| COG1477 | 1 | H | Thiamine biosynthesis lipoprotein ApbE |
| COG2226 | 4 | H | Ubiquinone/menaquinone biosynthesis C-methylase UbiE |
| COG2227 | 1 | H | 2-polyprenyl-3-methyl-5-hydroxy-6-metoxy-1,4-benzoquinol methylase |
| COG0558 | 1 | I | Phosphatidylglycerophosphate synthase |
| COG0764 | 1 | I | 3-hydroxymyristoyl/3-hydroxydecanoyl-(acyl carrier protein) dehydratase |
| COG1213 | 1 | I | Choline kinase |
| COG1960 | 1 | I | Acyl-CoA dehydrogenase related to the alkylation response protein AidB |
| COG0304 | 3 | I\|Q | 3-oxoacyl-(acyl-carrier-protein) synthase |
| COG0013 | 1 | J | Alanyl-tRNA synthetase |
| COG0223 | 1 | J | Methionyl-tRNA formyltransferase |
| COG0349 | 1 | J | Ribonuclease D |
| COG0590 | 1 | J | tRNA(Arg) A34 adenosine deaminase TadA |
| COG1234 | 1 | J | Ribonuclease BN, tRNA processing enzyme |
| COG3481 | 1 | J | 3'-5' exoribonuclease YhaM, can participate in 23S rRNA maturation, HD superfamily |
| COG1208 | 1 | J\|M | NDP-sugar pyrophosphorylase, includes eIF-2Bgamma, eIF-2Bepsilon, and LPS biosynthesis proteins |
| COG1309 | 1 | K | DNA-binding transcriptional regulator, AcrR family |
| COG1595 | 1 | K | DNA-directed RNA polymerase specialized sigma subunit, sigma24 family |
| COG1846 | 1 | K | DNA-binding transcriptional regulator, MarR family |
| COG2214 | 1 | K | Curved DNA-binding protein CbpA, contains a DnaJ-like domain |

| | | | |
|---|---|---|---|
| COG2865 | 1 | K | Predicted transcriptional regulator, contains HTH domain |
| COG3177 | 1 | K | Fic family protein |
| COG4190 | 1 | K | Predicted transcriptional regulator |
| COG1349 | 1 | K\|G | DNA-binding transcriptional regulator of sugar metabolism, DeoR/GlpR family |
| COG0553\|COG1502 | 2 | K\|I\|L | Superfamily II DNA or RNA helicase, SNF2 family\|Phosphatidylserine/phosphatidylglycerophosphate/cardiolipin synthase or related enzyme |
| COG0553 | 2 | K\|L | Superfamily II DNA or RNA helicase, SNF2 family |
| COG1061 | 1 | K\|L | Superfamily II DNA or RNA helicase |
| COG2197 | 2 | K\|T | DNA-binding response regulator, NarL/FixJ family, contains REC and HTH domains |
| COG2203\|COG2203\|COG3604 | 1 | K\|T | GAF domain\|GAF domain\|Transcriptional regulator containing GAF, AAA-type ATPase, and DNA-binding Fis domains |
| COG3604 | 1 | K\|T | Transcriptional regulator containing GAF, AAA-type ATPase, and DNA-binding Fis domains |
| COG2002 | 2 | K\|V | Bifunctional DNA-binding transcriptional regulator of stationary/sporulation/toxin gene expression and antitoxin component of the YhaV-PrlF toxin-antitoxin module |
| COG0270 | 1 | L | Site-specific DNA-cytosine methylase |
| COG0433 | 1 | L | Archaeal DNA helicase HerA or a related bacterial ATPase, contains HAS-barrel and ATPase domains |
| COG0507\|COG1112\|COG2852 | 1 | L | ATP-dependent exoDNAse (exonuclease V), alpha subunit, helicase superfamily I\|Superfamily I DNA and/or RNA helicase\|Very-short-patch-repair endonuclease |
| COG0513\|COG1205\|COG2852 | 1 | L | Superfamily II DNA and RNA helicase\|ATP-dependent helicase YprA, contains C-terminal metal-binding DUF1998 domain\|Very-short-patch-repair endonuclease |
| COG0863 | 1 | L | DNA modification methylase |
| COG0863\|COG2189 | 1 | L | DNA modification methylase\|Adenine specific DNA methylase Mod |
| COG1074 | 1 | L | ATP-dependent exoDNAse (exonuclease V) beta subunit (contains helicase and exonuclease domains) |
| COG1484 | 3 | L | DNA replication protein DnaC |
| COG1743 | 2 | L | Adenine-specific DNA methylase, contains a Zn-ribbon domain |
| COG2003 | 1 | L | DNA repair protein RadC, contains a helix-hairpin-helix DNA-binding motif |
| COG2189 | 3 | L | Adenine specific DNA methylase Mod |
| COG2887 | 2 | L | RecB family exonuclease |
| COG3727 | 1 | L | G:T-mismatch repair DNA endonuclease, very short patch repair protein |
| COG4974 | 2 | L | Site-specific recombinase XerD |

| | | | |
|---|---|---|---|
| COG0399 | 1 | M | dTDP-4-amino-4,6-dideoxygalactose transaminase |
| COG0438 | 5 | M | Glycosyltransferase involved in cell wall bisynthesis |
| COG0451 | 3 | M | Nucleoside-diphosphate-sugar epimerase |
| COG0463 | 1 | M | Glycosyltransferase involved in cell wall bisynthesis |
| COG0744 | 1 | M | Membrane carboxypeptidase (penicillin-binding protein) |
| COG0769 | 2 | M | UDP-N-acetylmuramyl tripeptide synthase |
| COG1136 | 1 | M | ABC-type lipoprotein export system, ATPase component |
| COG1368 | 1 | M | Phosphoglycerol transferase MdoB or a related enzyme of AlkP superfamily |
| COG1538 | 2 | M | Outer membrane protein TolC |
| COG1835 | 1 | M | Peptidoglycan/LPS O-acetylase OafA/YrhL, contains acyltransferase and SGNH-hydrolase domains |
| COG1898 | 1 | M | dTDP-4-dehydrorhamnose 3,5-epimerase or related enzyme |
| COG2244 | 1 | M | Membrane protein involved in the export of O-antigen and teichoic acid |
| COG3064 | 1 | M | Membrane protein involved in colicin uptake |
| COG3203 | 1 | M | Outer membrane protein (porin) |
| COG3307 | 2 | M | O-antigen ligase |
| COG3409 | 1 | M | Peptidoglycan-binding (PGRP) domain of peptidoglycan hydrolases |
| COG3637\|COG3659 | 1 | M | Opacity protein and related surface antigens\|Carbohydrate-selective porin OprB |
| COG3267\|COG3409 | 1 | M\|U | Type II secretory pathway, component ExeA (predicted ATPase)\|Peptidoglycan-binding (PGRP) domain of peptidoglycan hydrolases |
| COG1192 | 1 | N | Cellulose biosynthesis protein BcsQ |
| COG1215 | 1 | N | Glycosyltransferase, catalytic subunit of cellulose synthase and poly-beta-1,6-N-acetylglucosamine synthase |
| COG3144 | 1 | N | Flagellar hook-length control protein FliK |
| COG4786 | 1 | N | Flagellar basal body rod protein FlgG |
| COG5653 | 1 | N | Acetyltransferase involved in cellulose biosynthesis, CelD/BcsL family |
| COG0071 | 1 | O | Molecular chaperone IbpA, HSP20 family |
| COG0526 | 1 | O | Thiol-disulfide isomerase or thioredoxin |
| COG1404 | 1 | O | Serine protease, subtilisin family |
| COG1572 | 1 | O | Serine protease, subtilase family |
| COG1651 | 1 | O | Protein-disulfide isomerase |
| COG4930 | 1 | O | Predicted ATP-dependent Lon-type protease |
| COG4934 | 1 | O | Serine protease, subtilase family |

| | | | |
|---|---|---|---|
| COG1086 | 2 | O\|M | NDP-sugar epimerase, includes UDP-GlcNAc-inverting 4,6-dehydratase FlaA1 and capsular polysaccharide biosynthesis protein EpsC |
| COG0004 | 1 | P | Ammonia channel protein AmtB |
| COG0288 | 1 | P | Carbonic anhydrase |
| COG0475 | 1 | P | Kef-type K+ transport system, membrane component KefB |
| COG0475\|COG0490\|COG1226 | 1 | P | Kef-type K+ transport system, membrane component KefB\|K+/H+ antiporter YhaU, regulatory subunit KhtT\|Voltage-gated potassium channel Kch |
| COG0672 | 1 | P | High-affinity Fe2+/Pb2+ permease |
| COG0715 | 1 | P | ABC-type nitrate/sulfonate/bicarbonate transport system, periplasmic component |
| COG0803 | 1 | P | ABC-type Zn uptake system ZnuABC, Zn-binding component ZnuA |
| COG1108 | 1 | P | ABC-type Mn2+/Zn2+ transport system, permease component |
| COG1116 | 1 | P | ABC-type nitrate/sulfonate/bicarbonate transport system, ATPase component |
| COG1121 | 1 | P | ABC-type Mn2+/Zn2+ transport system, ATPase component |
| COG2223 | 1 | P | Nitrate/nitrite transporter NarK |
| COG3221 | 1 | P | ABC-type phosphate/phosphonate transport system, periplasmic component |
| COG3420 | 1 | P | Nitrous oxidase accessory protein NosD, contains tandem CASH domains |
| COG3696 | 1 | P | Cu/Ag efflux pump CusA |
| COG4773 | 1 | P | Outer membrane receptor for ferric coprogen and ferric-rhodotorulic acid |
| COG4986 | 1 | P | ABC-type anion transport system, duplicated permease component |
| COG2041\|COG4117 | 1 | P\|C | Periplasmic DMSO/TMAO reductase YedYZ, molybdopterin-dependent catalytic subunit\|Thiosulfate reductase cytochrome b subunit |
| COG0425\|COG1416 | 1 | P\|O | TusA-related sulfurtransferase\|Intracellular sulfur oxidation protein, DsrE/DsrF family |
| COG1116\|COG4754 | 1 | P\|S | ABC-type nitrate/sulfonate/bicarbonate transport system, ATPase component\|Uncharacterized protein |
| COG0038\|COG0517 | 1 | P\|T | H+/Cl- antiporter ClcA\|CBS domain |
| COG1233 | 1 | Q | Phytoene dehydrogenase-related protein |
| COG1647 | 1 | Q | Esterase/lipase |
| COG2162 | 1 | Q | Arylamine N-acetyltransferase |
| COG0385 | 1 | R | Predicted Na+-dependent transporter |
| COG0535 | 2 | R | Radical SAM superfamily enzyme, MoaA/NifB/PqqE/SkfB family |
| COG0667 | 1 | R | Predicted oxidoreductase (related to aryl-alcohol dehydrogenase) |

| | | | |
|---|---|---|---|
| COG0693 | 1 | R | Putative intracellular protease/amidase |
| COG1032 | 1 | R | Radical SAM superfamily enzyme YgiQ, UPF0313 family |
| COG1373 | 4 | R | Predicted ATPase, AAA+ superfamily |
| COG1483 | 1 | R | Predicted ATPase, AAA+ superfamily |
| COG1487 | 2 | R | Predicted nucleic acid-binding protein, contains PIN domain |
| COG1569 | 1 | R | Predicted nucleic acid-binding protein, contains PIN domain |
| COG1569 | 1 | R | Predicted nucleic acid-binding protein, contains PIN domain |
| COG1708 | 2 | R | Predicted nucleotidyltransferase |
| COG1724 | 1 | R | Predicted RNA binding protein YcfA, dsRBD-like fold, HicA-like mRNA interferase family |
| COG1741 | 2 | R | Redox-sensitive bicupin YhaK, pirin superfamily |
| COG1848 | 1 | R | Predicted nucleic acid-binding protein, contains PIN domain |
| COG1988 | 1 | R | Membrane-bound metal-dependent hydrolase YbcI, DUF457 family |
| COG2081 | 1 | R | Predicted flavoprotein YhiN |
| COG2374 | 2 | R | Predicted extracellular nuclease |
| COG2391 | 1 | R | Uncharacterized membrane protein YedE/YeeE, contains two sulfur transport domains |
| COG2402 | 1 | R | Predicted nucleic acid-binding protein, contains PIN domain |
| COG2405 | 1 | R | Predicted nucleic acid-binding protein, contains PIN domain |
| COG2522 | 1 | R | Predicted transcriptional regulator |
| COG3146 | 1 | R | Predicted N-acyltransferase |
| COG3153 | 1 | R | Predicted N-acetyltransferase YhbS |
| COG3173 | 1 | R | Predicted kinase, aminoglycoside phosphotransferase (APT) family |
| COG3179 | 1 | R | Predicted chitinase |
| COG3391 | 1 | R | DNA-binding beta-propeller fold protein YncE |
| COG3919 | 1 | R | Predicted ATP-dependent carboligase, ATP-grasp superfamily |
| COG4113 | 1 | R | Predicted nucleic acid-binding protein, contains PIN domain |
| COG4113 | 1 | R | Predicted nucleic acid-binding protein, contains PIN domain |
| COG4634 | 2 | R | Predicted nuclease, contains PIN domain, potential toxin-antitoxin system component |
| COG4782 | 1 | R | Esterase/lipase superfamily enzyme |
| COG4804 | 1 | R | Predicted nuclease of restriction endonuclease-like (RecB) superfamily, DUF1016 family |
| COG5573 | 1 | R | Predicted nucleic acid-binding protein, contains PIN domain |
| COG5610 | 1 | R | Predicted hydrolase, HAD superfamily |
| COG1063 | 1 | R\|E | Threonine dehydrogenase or related Zn-dependent dehydrogenase |

| | | | |
|---|---|---|---|
| COG1028 | 2 | R\|I\|Q | NAD(P)-dependent dehydrogenase, short-chain alcohol dehydrogenase family |
| COG1361 | 1 | S | Uncharacterized conserved protein |
| COG1479\|COG3472 | 1 | S | Uncharacterized conserved protein, contains ParB-like and HNH nuclease domains\|Uncharacterized protein |
| COG1512 | 1 | S | Uncharacterized membrane protein YgcG, contains a TPM-fold domain |
| COG1704 | 1 | S | Uncharacterized conserved protein |
| COG1808 | 1 | S | Uncharacterized membrane protein |
| COG2340 | 1 | S | Uncharacterized conserved protein YkwD, contains CAP (CSP/antigen 5/PR1) domain |
| COG2442 | 3 | S | Uncharacterized conserved protein, DUF433 family |
| COG2445 | 3 | S | Uncharacterized conserved protein YutE, UPF0331/DUF86 family |
| COG2929 | 3 | S | Uncharacterized conserved protein, DUF497 family |
| COG3174 | 1 | S | Uncharacterized membrane protein, DUF4010 family |
| COG3514 | 1 | S | Uncharacterized conserved protein, DUF4415 family |
| COG3584 | 1 | S | 3D (Asp-Asp-Asp) domain |
| COG3762 | 1 | S | Uncharacterized membrane protein |
| COG4089 | 1 | S | Uncharacterized membrane protein |
| COG4372 | 1 | S | Uncharacterized conserved protein, contains DUF3084 domain |
| COG4487 | 1 | S | Uncharacterized protein |
| COG4737 | 1 | S | Uncharacterized protein |
| COG5428 | 2 | S | Uncharacterized protein YuzE |
| COG5483 | 1 | S | Uncharacterized conserved protein, DUF488 family |
| COG0515 | 1 | T | Serine/threonine protein kinase |
| COG2203\|COG2770\|COG5002 | 1 | T | GAF domain\|HAMP domain\|Signal transduction histidine kinase |
| COG2204 | 2 | T | DNA-binding transcriptional response regulator, NtrC family, contains REC, AAA-type ATPase, and a Fis-type DNA-binding domains |
| COG2205 | 1 | T | K+-sensing histidine kinase KdpD |
| COG2336 | 1 | T | Antitoxin component of the MazEF toxin-antitoxin module |
| COG5635 | 1 | T | Predicted NTPase, NACHT family domain |
| COG0464 | 1 | T\|D\|M | AAA+-type ATPase, SpoVK/Ycf46/Vps4 family |
| COG0286 | 2 | V | Type I restriction-modification system, DNA methylase subunit |
| COG0577 | 1 | V | ABC-type antimicrobial peptide transport system, permease component |
| COG0732\|COG0732 | 3 | V | Restriction endonuclease S subunit\|Restriction endonuclease S subunit |
| COG0841 | 2 | V | Multidrug efflux pump subunit AcrB |

| | | | |
|---|---|---|---|
| COG0842 | 1 | V | ABC-type multidrug transport system, permease component |
| COG1002 | 1 | V | Type II restriction/modification system, DNA methylase subunit YeeA |
| COG1131 | 1 | V | ABC-type multidrug transport system, ATPase component |
| COG1203 | 1 | V | CRISPR/Cas system-associated endonuclease/helicase Cas3 |
| COG1337 | 1 | V | CRISPR/Cas system CSM-associated protein Csm3, group 7 of RAMP superfamily |
| COG1343 | 1 | V | CRISPR/Cas system-associated endoribonuclease Cas2 |
| COG1353 | 1 | V | CRISPR/Cas system-associated protein Cas10, large subunit of type III CRISPR-Cas systems, contains HD superfamily nuclease domain |
| COG1403 | 1 | V | 5-methylcytosine-specific restriction endonuclease McrA |
| COG1421 | 1 | V | CRISPR/Cas system CSM-associated protein Csm2, small subunit |
| COG1468 | 1 | V | CRISPR/Cas system-associated exonuclease Cas4, RecB family |
| COG1518 | 1 | V | CRISPR/Cas system-associated endonuclease Cas1 |
| COG1567 | 1 | V | CRISPR/Cas system CSM-associated protein Csm4, group 5 of RAMP superfamily |
| COG1598 | 4 | V | Predicted nuclease of the RNAse H fold, HicB family |
| COG1680 | 1 | V | CubicO group peptidase, beta-lactamase class C family |
| COG1715 | 2 | V | Restriction endonuclease Mrr |
| COG2076 | 2 | V | Multidrug transporter EmrE and related cation transporters |
| COG2161 | 1 | V | Antitoxin component YafN of the YafNO toxin-antitoxin module, PHD/YefM family |
| COG2253 | 2 | V | Predicted nucleotidyltransferase component of viral defense system |
| COG2337 | 1 | V | mRNA-degrading endonuclease, toxin component of the MazEF toxin-antitoxin module |
| COG3093 | 1 | V | Plasmid maintenance system antidote protein VapI, contains XRE-type HTH domain |
| COG3440 | 1 | V | Predicted restriction endonuclease |
| COG3649 | 1 | V | CRISPR/Cas system type I-B associated protein Csh2, Cas7 group, RAMP superfamily |
| COG3657 | 1 | V | Putative component of the toxin-antitoxin plasmid stabilization module |
| COG3744 | 3 | V | PIN domain nuclease, a component of toxin-antitoxin system (PIN domain) |
| COG4006 | 1 | V | CRISPR/Cas system-associated protein Csm6, COG1517 family |
| COG4118 | 1 | V | Antitoxin component of toxin-antitoxin stability system, DNA-binding transcriptional repressor |
| COG4257 | 2 | V | Streptogramin lyase |
| COG5340 | 2 | V | Transcriptional regulator, predicted component of viral defense system |

| | | | |
|---|---|---|---|
| COG0551\|COG1787 | 1 | V\|L | ssDNA-binding Zn-finger and Zn-ribbon domains of topoisomerase 1\|Endonuclease, HJR/Mrr/RecB family |
| COG0845 | 4 | V\|M | Multidrug efflux pump subunit AcrA (membrane-fusion protein) |
| COG1332\|COG3064 | 1 | V\|M | CRISPR/Cas system CSM-associated protein Csm5, group 7 of RAMP superfamily\|Membrane protein involved in colicin uptake |
| COG2442\|COG3587 | 1 | V\|S | Uncharacterized conserved protein, DUF433 family\|Restriction endonuclease |
| COG2801 | 1 | X | Transposase InsO and inactivated derivatives |
| COG2963 | 1 | X | Transposase and inactivated derivatives |
| COG3039 | 2 | X | Transposase and inactivated derivatives, IS5 family |
| COG3328 | 3 | X | Transposase (or an inactivated derivative) |
| COG3335 | 1 | X | Transposase |
| COG3385 | 2 | X | IS4 transposase |
| COG3415 | 1 | X | Transposase |
| COG3636 | 1 | X | DNA-binding prophage protein |
| COG3668 | 2 | X | Plasmid stabilization system protein ParE |
| COG4584 | 4 | X | Transposase |
| COG4644 | 1 | X | Transposase and inactivated derivatives, TnpA family |
| COG4679 | 3 | X | Phage-related protein |

# Appendix C.

## Supplementary information for Chapter 5.

### Supplemental information on modeling

The rate of change in biomass in the model is equivalent to the rate of growth minus the rate of decay. For example, the anammox biomass concentration is given by the differential equation:

$$\frac{dX_{ANA}}{dt} = \hat{\mu}_{ANA}\left(\frac{S_{NO2}}{K_{NO2,ANA} + S_{NO2}}\right)\left(\frac{S_{NH4}}{K_{NH4,NO2} + S_{NH4}}\right)X_{ANA} - b_{ANA}X_{ANA}$$

For electron donors the substrate utilization rate is related to the rate of growth by the yield of the organism. The yield is the ratio of mass of biomass produced to mass of electron donor consumed. For electron acceptors, the relation is more complex and requires some stoichiometric calculations of electrons going to biomass production versus electrons going to the electron acceptor. Other considerations in this model are the consumption of ammonium-nitrogen used for biomass growth and the production of ammonium-nitrogen from biomass decay. Decay products get converted either to inert or soluble particulates. Soluble particulates are then converted to soluble substrates via hydrolysis. These calculations are outlined in most environmental biotechnology textbooks(Grady et al., 2011; Rittmann and Mccarty, 2001). The Peterson matrix below is used to give the differential equations used in the model. For each soluble species (i), the differential equation describing the concentration is equal to the sum of the rate equation (j) times the matrix coefficient. For example, the rate of methane consumption is equal to:

$$\frac{dCH_4}{dt} = -\frac{1}{Y_{MOB}}\hat{\mu}_{MOB}\left(\frac{S_O}{K_{O,MOB}+S_O}\right)\left(\frac{S_{CH4}}{K_{CH4,MOB}+S_{CH4}}\right)X_{MOB} - \frac{1}{Y_{n-damo}}\hat{\mu}_{NO2-damo}\left(\frac{K_{O,NO2-damo}}{K_{O,NO2-damo}+S_O}\right)\left(\frac{S_{NO2}}{K_{NO2,n-damo}+S_{NO2}}\right)\left(\frac{S_{CH4}}{K_{CH4,NO2-damo}+S_{CH4}}\right)X_{NO2-damo} - \frac{1}{Y_{n-damo}}\hat{\mu}_{NO3-damo}\left(\frac{K_{O,NO3-damo}}{K_{O,NO3-damo}+S_O}\right)\left(\frac{S_{NO3}}{K_{NO3,n-damo}+S_{NO3}}\right)\left(\frac{S_{CH4}}{K_{CH4,NO3-damo}+S_{CH4}}\right)X_{NO3-damo}$$

**Table C1.** Process rates in model

| # | Process(j): | Process Rate |
|---|---|---|
| 1 | **Growth of Aerobic ammonia oxidizers** | $\hat{\mu}_{AOB}\left(\frac{S_O}{K_{O,AOB}+S_O}\right)\left(\frac{S_{NH4}}{K_{NH4,AOB}+S_{NH4}}\right)\left(\frac{K_{S,AOB}}{K_{S,AOB}+S_S}\right)X_{AOB}$ |
| 2 | **Growth of Aerobic nitrite Oxidizers** | $\hat{\mu}_{NOB}\left(\frac{S_O}{K_{O,NOB}+S_O}\right)\left(\frac{S_{NO2}}{K_{NO2,NOB}+S_{NO2}}\right)\left(\frac{K_{S,NOB}}{K_{S,NOB}+S_S}\right)X_{NOB}$ |
| 3 | **Growth of Anaerobic ammonia oxidizers** | $\hat{\mu}_{ANA}\left(\frac{K_{O,ANA}}{K_{O,ANA}+S_O}\right)\left(\frac{S_{NO2}}{K_{NO2,ANA}+S_{NO2}}\right)\left(\frac{S_{NH4}}{K_{NH4,NO2}+S_{NH4}}\right)\left(\frac{K_{S,ANA}}{K_{S,ANA}+S_S}\right)X_{ANA}$ |
| 4 | **Growth of Aerobic methane oxidizers** | $\hat{\mu}_{MOB}\left(\frac{S_O}{K_{O,MOB}+S_O}\right)\left(\frac{S_{CH4}}{K_{CH4,MOB}+S_{CH4}}\right)X_{MOB}$ |
| 5 | **Growth of DAMO (Nitrite dependent)** | $\hat{\mu}_{NO2-damo}\left(\frac{K_{O,NO2-damo}}{K_{O,NO2-damo}+S_O}\right)\left(\frac{S_{NO2}}{K_{NO2,n-damo}+S_{NO2}}\right)\left(\frac{S_{CH4}}{K_{CH4,NO2-damo}+S_{CH4}}\right)X_{NO2-damo}$ |
| 6 | **Growth of DAMO (Nitrate dependent)** | $\hat{\mu}_{NO3-damo}\left(\frac{K_{O,NO3-damo}}{K_{O,NO3-damo}+S_O}\right)\left(\frac{S_{NO3}}{K_{NO3,n-damo}+S_{NO3}}\right)\left(\frac{S_{CH4}}{K_{CH4,NO3-damo}+S_{CH4}}\right)X_{NO3-damo}$ |
| 7 | **Growth of heterotrophs** | $\hat{\mu}_h\left(\frac{S_{COD}}{K_{COD,h}+S_{COD}}\right)\left(\frac{S_O}{K_{O,h}+S_O}\right)X_h$ |
| 8 | **Growth of sulfide based denitrifiers (nitrite)** | $\hat{\mu}_{sulf,NO2-}\left(\frac{S_{NO2-}}{K_{NO2-,sulf}+S_{NO2-}}\right)\left(\frac{S_{HS-}}{K_{HS-,sulf}+S_{HS-}}\right)\left(\frac{K_{O,ANA}}{K_{O,ANA}+S_O}\right)X_{NO2,sulf}$ |
| 9 | **Growth of sulfide based denitrifiers (nitrate)** | $\hat{\mu}_{sulf,NO3-}\left(\frac{S_{NO3-}}{K_{NO3-,sulf}+S_{NO3-}}\right)\left(\frac{S_{HS-}}{K_{HS-,sulf}+S_{HS-}}\right)\left(\frac{K_{O,ANA}}{K_{O,ANA}+S_O}\right)X_{NO3,sulf}$ |
| 10 | **Growth of Sulfide Oxidizing bacteria** | $\hat{\mu}_{SOB}\left(\frac{S_{HS-}}{K_{HS-,SOB}+S_{HS-}}\right)\left(\frac{S_O}{K_{O,SOB}+S_O}\right)X_{SOB}$ |
| 11 | **Growth of sulfate reducing bacteria** | $\hat{\mu}_{SRB}\left(\frac{S_{COD}}{K_{COD,SRB}+S_{COD}}\right)\left(\frac{S_{SO4}}{K_{SO4,SRB}+S_{SO4}}\right)X_{SRB}$ |
| 12 | **Decay of Aerobic ammonia oxidizers** | $b_{AOB}X_{AOB}$ |
| 13 | **Decay of Aerobic nitrite Oxidizers** | $b_{NOB}X_{NOB}$ |
| 14 | **Decay of Anaerobic ammonia oxidizers** | $b_{ANA}X_{ANA}$ |
| 15 | **Decay of Aerobic methane oxidizers** | $b_{MOB}X_{MOB}$ |
| 16 | **Decay of DAMO (Nitrite)** | $b_{NO2-damo}X_{NO2-damo}$ |
| 17 | **Decay of DAMO (Nitrate)** | $b_{NO3-damo}X_{NO3-damo}$ |
| 18 | **Decay of heterotrophs** | $b_{HET}X_{HET}$ |
| 19 | **Decay of denitrifying heterotrophs (nitrite)** | $b_{denit,NO2}X_{denite,NO2}$ |
| 20 | **Decay of denitrifying heterotrophs (nitrate)** | $b_{denit,NO3}X_{denite,NO3}$ |
| 21 | **Decay of sulfide based denitrifiers (nitrite)** | $b_{sulf,NO2}X_{sulf,NO2}$ |
| 22 | **Decay of sulfide based denitrifiers (nitrate)** | $b_{sulf,NO3}X_{sulf,NO2}$ |
| 23 | **Decay of SOB** | $b_{SOB}X_{SOB}$ |
| 24 | **Decay of SRB** | $b_{SRB}X_{SRB}$ |
| 25 | **Hydrolysis** | $k_H\left(\frac{X_S}{K_X}\right)$ |
| 26 | **Hydrolysis of nitrogen compounds** | $k_H\left(\frac{X_N}{K_X}\right)$ |

**Table C2.** Peterson Matrix for Model. Each row has a distinct yield (Y) for that metabolism

| (i): | $X_{AOB}$ | $X_{NOB}$ | $X_{ANA}$ | $X_{MOB}$ | $X_{NO2\text{-}damo}$ | $X_{NO3\text{-}damo}$ | $X_{het}$ | $X_{NO2,sulf}$ | $X_{NO3,sulf}$ | $X_s$ | $X_N$ | $X_I$ | $X_{SOB}$ | $X_{SRB}$ | $S_O$ | $S_{COD}$ | $S_{CH4}$ | $S_{NH4}$ | $S_{NO2}$ | $S_{NO3}$ | $S_{SO4}$ | $S_{HS\text{-}}$ |
|---|---|---|---|---|---|---|---|---|---|---|---|---|---|---|---|---|---|---|---|---|---|---|
| (j) | mg/L as COD | | | | | | | | | | | | | | | | | mg/L as N | | | mg/L as S | |
| **1** | 1 | | | | | | | | | | | | | | $-\frac{3.43-Y}{Y}$ | | | $-\frac{1}{Y}-i_{N,X}$ | $\frac{1}{Y}$ | | | |
| **2** | | 1 | | | | | | | | | | | | | $-\frac{1.14-Y}{Y}$ | | | $-i_{N,X}$ | $-\frac{1}{Y}$ | $\frac{1}{Y}$ | | |
| **3** | | | 1 | | | | | | | | | | | | | | | $-\frac{1}{Y}-i_{N,X}$ | $-\frac{1-0.87Y}{Y}$ | 0.87 | | |
| **4** | | | | 1 | | | | | | | | | | | $-\frac{1-Y}{Y}$ | | $-\frac{1}{Y}$ | $-i_{N,X}$ | | | | |
| **5** | | | | | 1 | | | | | | | | | | | | $-\frac{1}{Y}$ | $-i_{N,X}$ | $-\frac{0.58-0.58*Y}{Y}$ | | | |
| **6** | | | | | | 1 | | | | | | | | | | | $-\frac{1}{Y}$ | $-i_{N,X}$ | $-\frac{0.35-0.35Y}{Y}$ | | | |
| **7** | | | | | | | 1 | | | | | | | | $-\frac{1-Y}{Y}$ | $-\frac{1}{Y}$ | | $-i_{N,X}$ | | | | |
| **8** | | | | | | | | 1 | | | | | | | | | | $-i_{N,X}$ | $-\frac{1.17-.585Y}{Y}$ | | $\frac{1}{Y}$ | $-\frac{1}{Y}$ |
| **9** | | | | | | | | | 1 | | | | | | | | | $-i_{N,X}$ | | $-\frac{0.7-}{Y}$ | $\frac{1}{Y}$ | $-\frac{1}{Y}$ |
| **10** | | | | | | | | | | | | | 1 | | $-\frac{2-Y}{Y}$ | | | $-i_{N,X}$ | | | $\frac{1}{Y}$ | $-\frac{1}{Y}$ |
| **11** | | | | | | | | | | | | | | 1 | | $-\frac{1}{Y}$ | | $-i_{N,X}$ | | | $-\frac{1-0.5Y}{Y}$ | $\frac{1-0.5Y}{Y}$ |
| **12** | -1 | | | | | | | | | (1-$f_I$) | $i_{N,X}-i_{NX}*fi$ | $f_I$ | | | | | | | | | | |
| **13** | | -1 | | | | | | | | (1-$f_I$) | $i_{N,X}-i_{NX}*fi$ | $f_I$ | | | | | | | | | | |

| | | | | | | | | | | | | | | | | | | | | | |
|---|---|---|---|---|---|---|---|---|---|---|---|---|---|---|---|---|---|---|---|---|---|
| **14** | | | -1 | | | | | | | (1-$f_I$) | $i_{N,X} - i_{NX} * fi$ | $f_I$ | | | | | | | | | |
| **15** | | | | -1 | | | | | | (1-$f_I$) | $i_{N,X} - i_{NX} * fi$ | $f_I$ | | | | | | | | | |
| **16** | | | | | -1 | | | | | (1-$f_I$) | $i_{N,X} - i_{NX} * fi$ | $f_I$ | | | | | | | | | |
| **17** | | | | | | -1 | | | | (1-$f_I$) | $i_{N,X} - i_{NX} * fi$ | $f_I$ | | | | | | | | | |
| **18** | | | | | | | -1 | | | (1-$f_I$) | $i_{N,X} - i_{NX} * fi$ | $f_I$ | | | | | | | | | |
| **19** | | | | | | | | | | (1-$f_I$) | $i_{N,X} - i_{NX} * fi$ | $f_I$ | | | | | | | | | |
| **20** | | | | | | | | | | (1-$f_I$) | $i_{N,X} - i_{NX} * fi$ | $f_I$ | | | | | | | | | |
| **21** | | | | | | | | -1 | | (1-$f_I$) | $i_{N,X} - i_{NX} * fi$ | $f_I$ | | | | | | | | | |
| **22** | | | | | | | | | -1 | (1-$f_I$) | $i_{N,X} - i_{NX} * fi$ | $f_I$ | | | | | | | | | |
| **23** | | | | | | | | | | (1-$f_I$) | $i_{N,X} - i_{NX} * fi$ | $f_I$ | -1 | | | | | | | | |
| **24** | | | | | | | | | | (1-$f_I$) | $i_{N,X} - i_{NX} * fi$ | $f_I$ | | -1 | | | | | | | |
| **25** | | | | | | | | | | -1 | $i_{N,X} - i_{NX} * fi$ | | | | | 1 | | | | | |
| **26** | | | | | | | | | | | -1 | | | | | | | 1 | | | |

**Table C3.** Kinetic Parameters. All methane values are presented as COD; sulfate and sulfide are as S; ammonia, nitrite, and nitrate are as N. References are: [1] (Delgado Vela et al., 2015), [2] (Munz et al., 2009). [3] (Chen et al., 2014), [4] (Ni et al., 2014), [5] (Mora et al., 2015), [6] (Xu et al., 2013) [7] (Trapani et al., 2010), [8] (Grady et al., 2011), [9] (Chang and Alvarez-Cohen, 1997), [10] (Cema et al., 2012), [11] (Doğan et al., 2012), [12] (Plattes et al., 2007), [13] (Moussa et al., 2005) [14] (van Bodegom et al., 2001) [15] (He et al., 2014), [16] (Dale et al., 2006). [17](Oshiki et al., 2013), [18] (Kappler and Gujer, 1992). [19] (Chang and Criddle, 1997), [20] (Zeng and Zhang, 2005) [21] (Weismann, 1994) [22] (Delgado Vela et al., 2018), [23] (Jetten et al., 1999), [24] (Russ et al., 2014) *reliable parameters not found, assumed same as anammox

| Metabolism | e⁻ donor | e⁻ acceptor | $\mu_{max}$ | | Y | | | $K_{donor}$ | | $K_{acceptor}$ | | b | | $K_{inhib}$ | | |
|---|---|---|---|---|---|---|---|---|---|---|---|---|---|---|---|---|
| | | | $day^{-1}$ | Ref. | | Units | Ref. | mg/L | Ref. | mg/L | Ref. | $day^{-1}$ | Ref. | mg/L | Inhibitor | Ref. |
| Aerobic Ammonia Oxidation | Ammonia | Oxygen | 2.2 | Calibrated | 0.07 | $\frac{gCOD}{g\ N}$ | [8] | 0.26 | [12] | 0.39 | Calibrated | 0.072 | [8] | 12.15 | sulfide | [22] |
| Aerobic Nitrite Oxidation | nitrite | oxygen | 5.39 | Calibrated | 0.08 | $\frac{gCOD}{g\ N}$ | [8] | 2.00 | [13] | 0.25 | Calibrated | 0.072 | [8] | 2.6 | sulfide | [22] |
| Aerobic Methane Oxidation | methane | oxygen | 3.66 | Median from [1] | 0.12 | $\frac{gCOD}{g\ COD}$ | [9] | 1.79 | [14] | 0.21 | [14] | 0.549 | [19] | | | |
| Aerobic Sulfide Oxidation | sulfide | oxygen | 7.40 | [2] | 0.12 | $\frac{gCOD}{g\ S}$ | [2] | 0.32 | [5] | 0.15 | [5] | 0.130 | [2] | 0.06 | oxygen | * |
| Anaerobic Methane Oxidation | methane | nitrite | 0.04 | [3] | 0.06 | $\frac{gCOD}{g\ COD}$ | [3] | 5.50 | [15] | 0.01 | [3] | 0.002 | [15] | 0.06 | oxygen | * |
| Anaerobic Methane Oxidation | methane | nitrate | 0.04 | [3] | 0.07 | $\frac{gCOD}{g\ COD}$ | [3] | 5.50 | [15] | 0.11 | [3] | 0.002 | [15] | | | |
| Anammox | ammonia | nitrite | 0.22 | [4] | 0.16 | $\frac{gCOD}{g\ N}$ | [10] | 0.08 | [10] | 0.47 | [17] | 0.006 | [17] | 0.06<br>0.32 | oxygen<br>sulfide | [23]<br>[23] |
| Sulfide based denitrification | sulfide | nitrite | 4.49 | [5] | 0.80 | $\frac{gCOD}{g\ S}$ | [11] | 0.32 | [5] | 7.15 | [5] | 0.090 | [20] | 0.06 | oxygen | * |
| Sulfide based denitrification | sulfide | nitrate | 4.49 | [5] | 0.80 | $\frac{gCOD}{g\ S}$ | [11] | 0.32 | [5] | 1.30 | [5] | 0.090 | [20] | 0.06 | oxygen | * |
| Sulfate reducing bacteria | org matter | sulfate | 1.46 | [6] | 1.24 | $\frac{gCOD}{g\ S}$ | [6] | 82 | [16] | 96 | [16] | 0.002 | * | 0.06 | oxygen | * |
| Heterotrophic Denitrifiers | org matter | nitrite | 2.06 | [7] | 0.39 | $\frac{gCOD}{gCOD}$ | [8] | 8.82 | [7] | 0.10 | [8] | 0.100 | [21] | 0.25 | oxygen | [18] |
| Heterotrophic Denitrifiers | org matter | nitrate | 2.06 | [7] | 0.39 | $\frac{gCOD}{gCOD}$ | [8] | 8.82 | [7] | 0.10 | [8] | 0.100 | [21] | 0.25 | oxygen | [18] |
| Heterotrophs | org matter | oxygen | 2.06 | [7] | 0.88 | $\frac{gCOD}{gCOD}$ | [7] | 8.82 | [7] | 0.25 | [18] | 0.549 | [18] | | | |

**Table C4.** Additional physical and chemical constants in the model.

| Constants | Value | Units | Reference |
|---|---|---|---|
| Diffusivity of methane | $1.62 \cdot 10^{-4}$ | $m^2$/day | (Witherspoon and Saraf, 1965) |
| Diffusivity of ammonium | $1.60 \cdot 10^{-4}$ | $m^2$/day | (Tijhuis, 1994) |
| Diffusivity of oxygen | $1.73 \cdot 10^{-4}$ | $m^2$/day | (Tijhuis, 1994) |
| Diffusivity of nitrate & nitrite | $1.46 \cdot 10^{-4}$ | $m^2$/day | (Tijhuis, 1994) |
| Diffusivity of volatile fatty acids | $6.41 \cdot 10^{-5}$ | $m^2$/day | (Yu and Pinder, 1994) |
| Diffusivity of particulate matter | 8.64 | $m^2$/day | |
| Diffusivity of hydrogen sulfide | $1.66 \cdot 10^{-4}$ | $m^2$/day | (Lindh et al., 1994) |
| Diffusivity of sulfate | $4.32 \cdot 10^{-5}$ | $m^2$/day | (Krom and Berner, 1980) |
| Diffusivity of membrane | $1.92 \cdot 10^{-4}$ | $m^2$/day | (Gilmore et al., 2009) |
| Volume of lumen | $1.30 \cdot 10^{-4}$ | $m^3$ | Calculated from reactor |
| Maximum biofilm thickness | 600 | µm | Measured during reactor breakdown |
| Volume of reactor | $2.12 \cdot 10^{-3}$ | $m^3$ | - |
| Length of reactor | 0.31 | m | - |
| Thickness of membrane | $6.4 \cdot 10^{-4}$ | m | - |
| Radius of membrane | $1.59 \cdot 10^{-3}$ | m | - |
| Flow of influent | $9.07 \cdot 10^{-3}$ | $m^3$/day | - |
| Decay constant ($f_i$) | 0.08 | - | (Grady et al., 2011) |
| N content of biomass ($i_{N,X}$) | 0.087 | g N/g COD | Calculated (Grady et al., 2011) |
| N content of inerts ($i_{N,X}$) | 0.02 | g N/g COD | (Grady et al., 2011) |
| Hydrolysis rate constant ($k_H$) | 2.21 | $day^{-1}$ | (Grady et al., 2011) |
| Half saturation, hydrolysis ($K_X$) | 0.03 | g COD/ $m^3$ | (Grady et al., 2011) |
| Biofilm porosity | 0.8 | $m^3$ liquid/$m^3$ biofilm | assumed |
| Liquid diffusion layer | 0.0001 | m | assumed |
| Density of bacteria in biofilm | 150000 | g COD/ $m^3$ | assumed |

**Table C5.** Changes to model Peterson Matrix with DNRA.

| Nitrite as acceptor | |
|---|---|
| **Process** | **Rate** |
| **Growth of sulfide based denitrifiers (nitrite)** | $\hat{\mu}_{sulf,NO2-} * DNRA_{switch,inv}\left(\frac{S_{NO2-}}{K_{NO2-,sulf}+S_{NO2-}}\right)\left(\frac{S_{HS-}}{K_{HS-,sulf}+S_{HS-}}\right)\left(\frac{K_{O,ANA}}{K_{O,ANA}+S_O}\right)X_{NO2,sulf}$ |
| **Growth of sulfide based DNRA (nitrite)** | $\hat{\mu}_{sulf,NO2-} * DNRA_{switch}\left(\frac{S_{NO2-}}{K_{NO2-,sulf}+S_{NO2-}}\right)\left(\frac{S_{HS-}}{K_{HS-,sulf}+S_{HS-}}\right)\left(\frac{K_{O,ANA}}{K_{O,ANA}+S_O}\right)X_{NO2,sulf}$ |
| **Nitrate as acceptor** | |
| **Process** | **Rate** |
| **Growth of sulfide based denitrifiers (nitrate)** | $\hat{\mu}_{sulf,NO3-} * DNRA_{switch,inv}\left(\frac{S_{NO3-}}{K_{NO3-,sulf}+S_{NO3-}}\right)\left(\frac{S_{HS-}}{K_{HS-,sulf}+S_{HS-}}\right)\left(\frac{K_{O,ANA}}{K_{O,ANA}+S_O}\right)X_{NO3,sulf}$ |
| **Growth of sulfide based DNRA (nitrate)** | $\hat{\mu}_{sulf,NO3-} * DNRA_{switch}\left(\frac{S_{NO3-}}{K_{NO3-,sulf}+S_{NO3-}}\right)\left(\frac{S_{HS-}}{K_{HS-,sulf}+S_{HS-}}\right)\left(\frac{K_{O,ANA}}{K_{O,ANA}+S_O}\right)X_{NO3,sulf}$ |

**Table C6.** DNRA stoichiometry

| Process | $X_{NO2,sulf}$ | $X_{NO3,sulf}$ | $S_{NH4}$ | $S_{NO2}$ | $S_{NO3}$ | $S_{SO4}$ | $S_{HS-}$ |
|---|---|---|---|---|---|---|---|
| **Growth of sulfide based denitrifiers (nitrite)** | 1 | | $-i_{N,X}+\frac{0.59-0.295Y}{Y}$ | $-\frac{0.59-0.295Y}{Y}$ | | $\frac{1}{Y}$ | $-\frac{1}{Y}$ |
| **Growth of sulfide based DNRA (nitrate)** | | 1 | $-i_{N,X}+\frac{0.48-0.24Y}{Y}$ | | $-\frac{0.48-0.2}{Y}$ | $\frac{1}{Y}$ | $-\frac{1}{Y}$ |

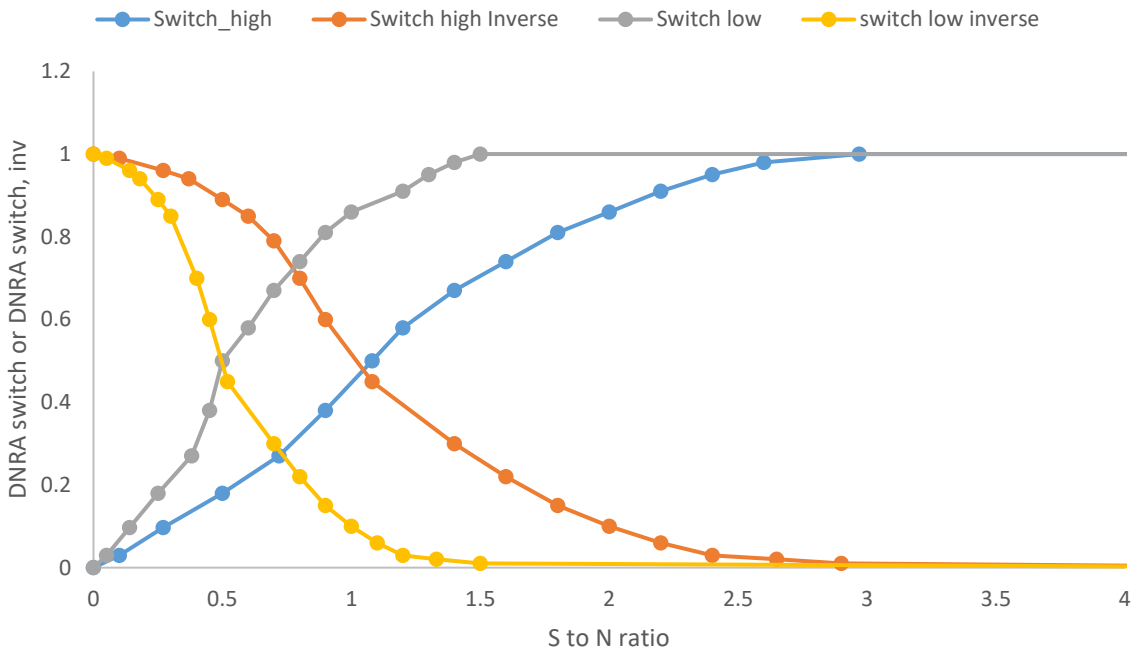


**Figure C1.** DNRA switch and DNRA switch, inverse values as a function of S to N ratio

**Table C7**. Ranked list of sensitivity and uncertainty of parameter vales on effluent nitrogen. Only parameters ranked in top 10 for at least one nitrogenous compound are shown.

| **Sensitivity rankings** | | | | |
|---|---|---|---|---|
| | **Ammonium** | **Nitrite** | **Nitrate** | **Average** |
| $\mu_{AOB}$ | 2 | 3 | 2 | 2.3 |
| $\mu_{NOB}$ | 7 | 1 | 1 | 3.0 |
| $K_{O,AOB}$ | 4 | 4 | 3 | 3.7 |
| $Y_{ANA}$ | 1 | 8 | 4 | 4.3 |
| $\mu_{ANA}$ | 3 | 2 | 10 | 5.0 |
| $b_{AOB}$ | 5 | 9 | 6 | 6.7 |
| $K_{O,NOB}$ | 15 | 5 | 5 | 8.3 |
| $Y_{MOB}$ | 6 | 12 | 9 | 9.0 |
| $Y_{NOB}$ | 17 | 6 | 7 | 10.0 |
| $b_{NOB}$ | 20 | 7 | 8 | 11.7 |
| $b_{MOB}$ | 8 | 13 | 15 | 12.0 |
| $K_{NO2,NOB}$ | 24 | 10 | 12 | 15.3 |
| $K_{NO2,ANA}$ | 10 | 19 | 19 | 16.0 |
| $\mu_{MOB}$ | 9 | 22 | 22 | 17.7 |
| **Uncertainty rankings** | | | | |
| $\mu_{NOB}$ | 3 | 2 | 2 | 2.3 |
| $K_{O,NOB}$ | 5 | 1 | 1 | 2.3 |

| | | | | |
|---|---|---|---|---|
| $K_{O,AOB}$ | 2 | 4 | 3 | 3 |
| $b_{AOB}$ | 1 | 5 | 5 | 3.7 |
| $\mu_{AOB}$ | 4 | 6 | 6 | 5.3 |
| $b_{NOB}$ | 12 | 3 | 4 | 6.3 |
| $K_{O,SOB}$ | 6 | 9 | 9 | 8 |
| $K_{HS,SOB}$ | 7 | 8 | 10 | 8.3 |
| $\mu_{ANA}$ | 8 | 7 | 17 | 10.7 |
| $Y_{ANA}$ | 9 | 15 | 8 | 10.7 |
| $K_{COD,denit}$ | 14 | 14 | 7 | 11.7 |
| $K_{NO2,ANA}$ | 10 | 12 | 15 | 12.3 |
| $K_{NO2,NOB}$ | 28 | 10 | 12 | 16.7 |

**A)**

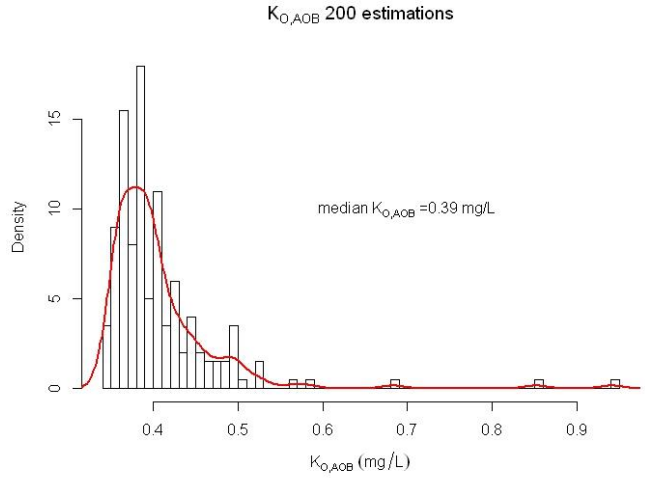


**B)**

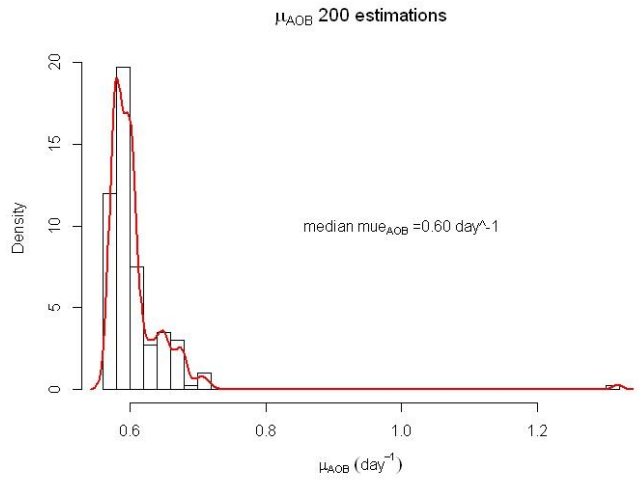

**C)**

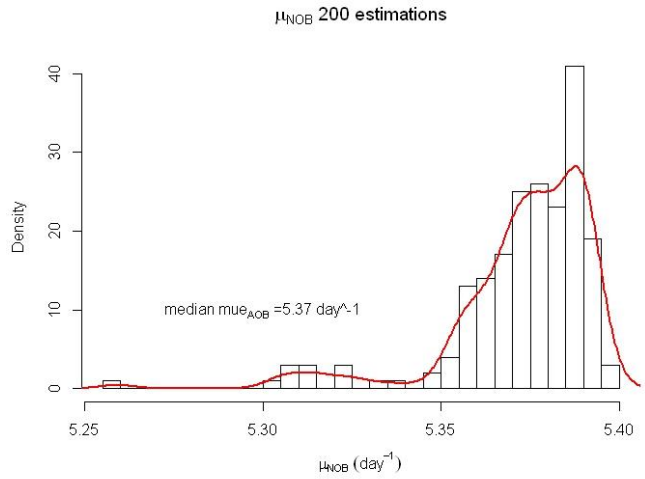


**Figure C2.** Results of parameter estimation

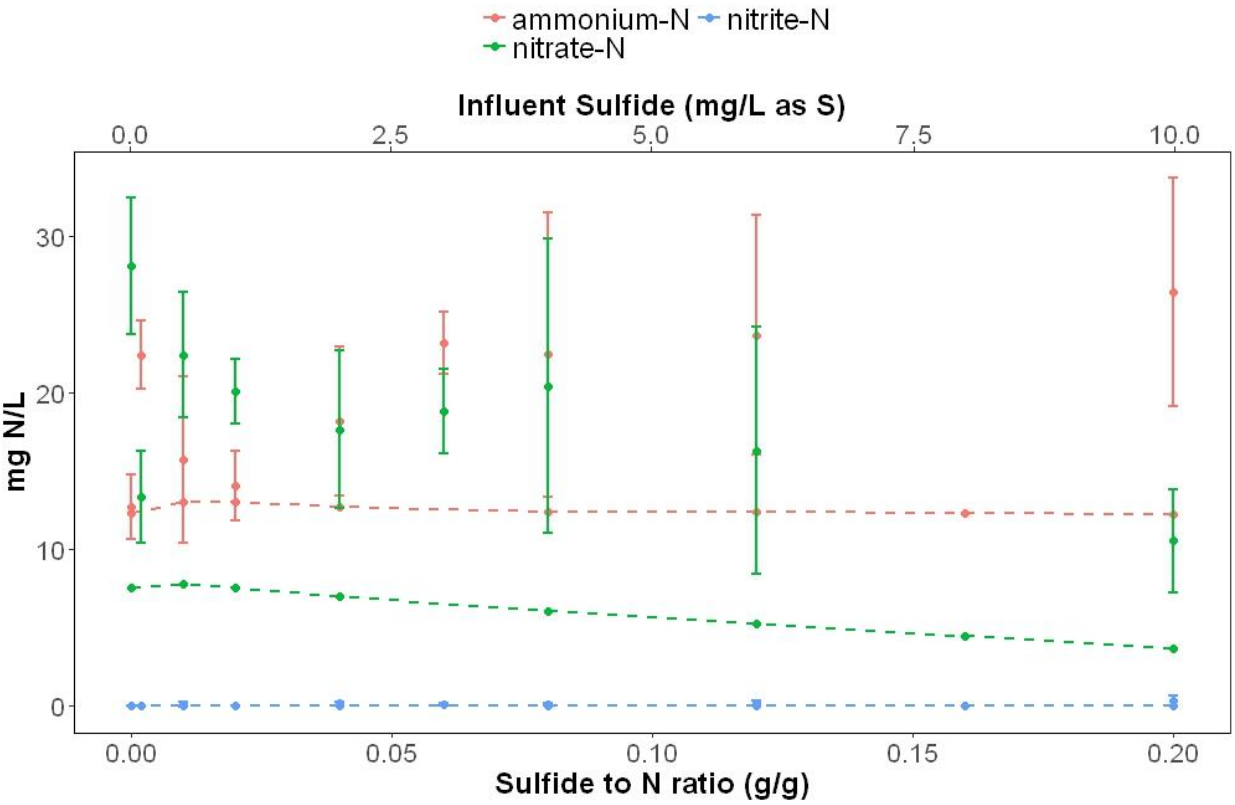


**Figure C3.** Model resulting from calibration procedure. Dashed lines represent model outputs. Dots with error bars represent reactor average effluent and standard deviation.

**Supplemental information calculations**

***Aeration demand from sulfide oxidation calculations***

The balanced equation for sulfide oxidation is:

$$HS^- + 2O_2 \leftrightarrow SO_4^{2-} + H^+$$

Therefore, two moles of oxygen are consumed for each mole of hydrogen sulfide, given the molecular weights of S and $O_2$ (both 32 g/mol), this is equivalent to 2 grams of oxygen consumed per gram of sulfide. So, 20 mg $O_2$/L are needed to oxidize 10 mg sulfide/L. The balanced equation for complete nitrification is:

$$NH_4^+ + 2\ O_2 \leftrightarrow NO_3^- + H_2O + 2\ H^+$$

Therefore, two moles of oxygen are consumed for each mole of ammonium, given the molecular weights of N and $O_2$ (14 and 32 g/mol, respectively), this is equivalent to 4.57 grams of oxygen consumed per gram of nitrogen. Therefore, the 20 mg $O_2$/L can oxidize 4.4 mg $NH_4^+$-N/L. This is equivalent to 8.75% of the influent (50 mg $NH_4^+$-N/L).

***Calculations used on Figure 5-3***

At the beginning of the experiment when nitrification efficiency was 70%, 0.67 g $NH_4^+$-N/$m^2$-day were oxidized (influent loading is 0.95 g $NH_4^+$-N/$m^2$-day). Given the ratio of oxygen demand to nitrification indicated previously (4.57 g $O_2$/g N), this is equivalent to 3.06 g $O_2$/$m^2$-day. The inhibition observed (30%) is based on the nitrification efficiency before (70%) and at end of stepwise increases (40%). 30% of the influent ammonium load is 0.29 g $NH_4^+$-N/$m^2$-day. Given the ratio of oxygen demand to nitrification indicated previously (4.57 g $O_2$/g N), this is equivalent to 1.31 g $O_2$/$m^2$-day. So, the relative change in oxygen flux (100*1.31 g $O_2$/$m^2$-day/3.06 g $O_2$/$m^2$-day) is equal to 43%.

The analogous calculation is to calculate the change in concentration given the differences in flux (which is shown in Figure 5-3A). The difference between the before and after fluxes is 0.7 g $O_2$/$m^2$-day. Given the ratio of oxygen demand to nitrification indicated previously (4.57 g $O_2$/g N), this

is equivalent to 0.15 $NH_4^+$-N /$m^2$-day, which given the flow rate, volume, and membrane surface area of the reactor translates to 8.1 mg $NH_4^+$-N/L.

The balanced equation for sulfide- based DNRA with nitrite as the electron acceptor is:

$$3HS^- + 4NO_2^- + 5H^+ + 4H_2O \leftrightarrow 3SO_4^{2-} + 4NH_4^+$$

Therefore, 4 moles of ammonium are produced for each mole of hydrogen sulfide consumed, given the molecular weights of N and S (14 and 32 g/mol, respectively), this is equivalent to 0.58 grams of ammonium produced per gram of sulfide consumed. So, 10 mg $HS^-$-S/L have to potential to produce 5.8 mg N/L.

For the pulse experiments, a similar calculation is done, but only taking the difference in sulfate concentrations over points where concentrations of ammonium were increasing. For the first pulse this is the difference in concentratin at the beginning and end of each pulse. For the second pulse, this is the difference between the first and third points in the pulse. For the first pulse this was 3.6 mg $SO_4^{2-}$ -S/L, and for the second pulse this was 4.1 mg $SO_4^{2-}$ -S/L. So, with the stochiometric ratio, this is equivalent to 2.1 and 2.4 mg $NH_4^+$/L, respectively.

***Potential inhibition calculations***

As described in Chapter 3, the comparison of rates in a noncompetitive inhibiton model results in the following equation:

$$\frac{\mu_{inh}}{\mu_{cont}} = \frac{1}{1 + \frac{[I]}{K_i}}$$

So given the inhibiton constant ($K_I$) from Chapter 3 of 7.4 mg/L as S, and the concentration measured of sulfide 0.5 mg/L as S this simplifies to:

$$\frac{1}{1 + \frac{0.5}{7.4}} = 0.94$$

***Nitrous oxide emissions factor calculations***

No sulfide:

$$100 * \frac{0.001\ mg\ \frac{N_2O - N}{L}}{50\ mg\ \frac{NH_4^+ - N}{L}\ in\ influent} = 0.002\%$$

With sulfide:

$$100 * \frac{0.13 mg\ \frac{N_2O - N}{L}}{50\ mg\ \frac{NH_4^+ - N}{L}\ in\ influent} = 0.25\%$$

**Supplemental information on reactor effluent**

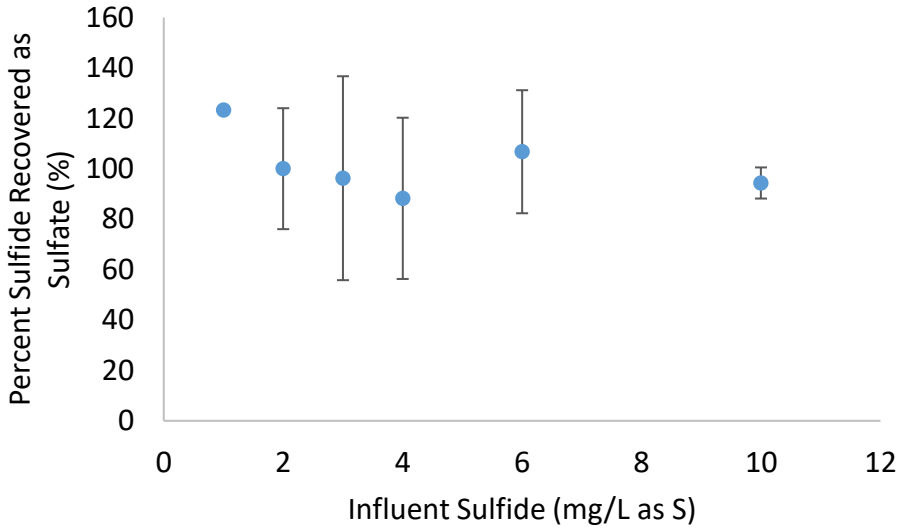


**Figure C4.** Percentage of Sulfide Recovered as Sulfate. Points below 1 mg/L are not shown because differences are below LOD on IC method

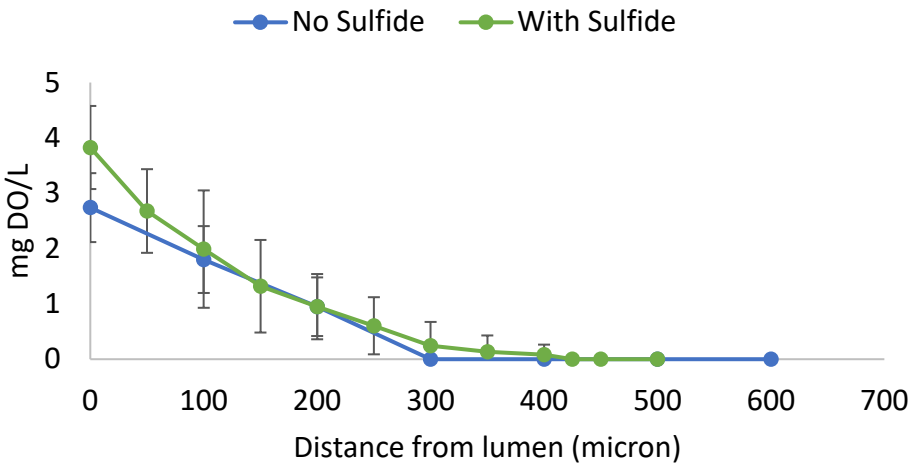


**Figure C5.** Dissolved oxygen microsensor profiles

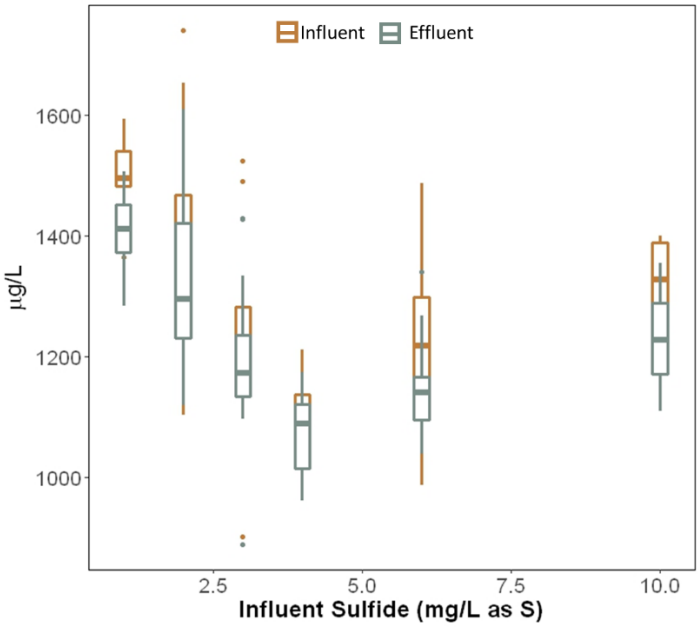


**Figure C6.** Influent and effluent iron concentrations during stepwise increases in sulfide

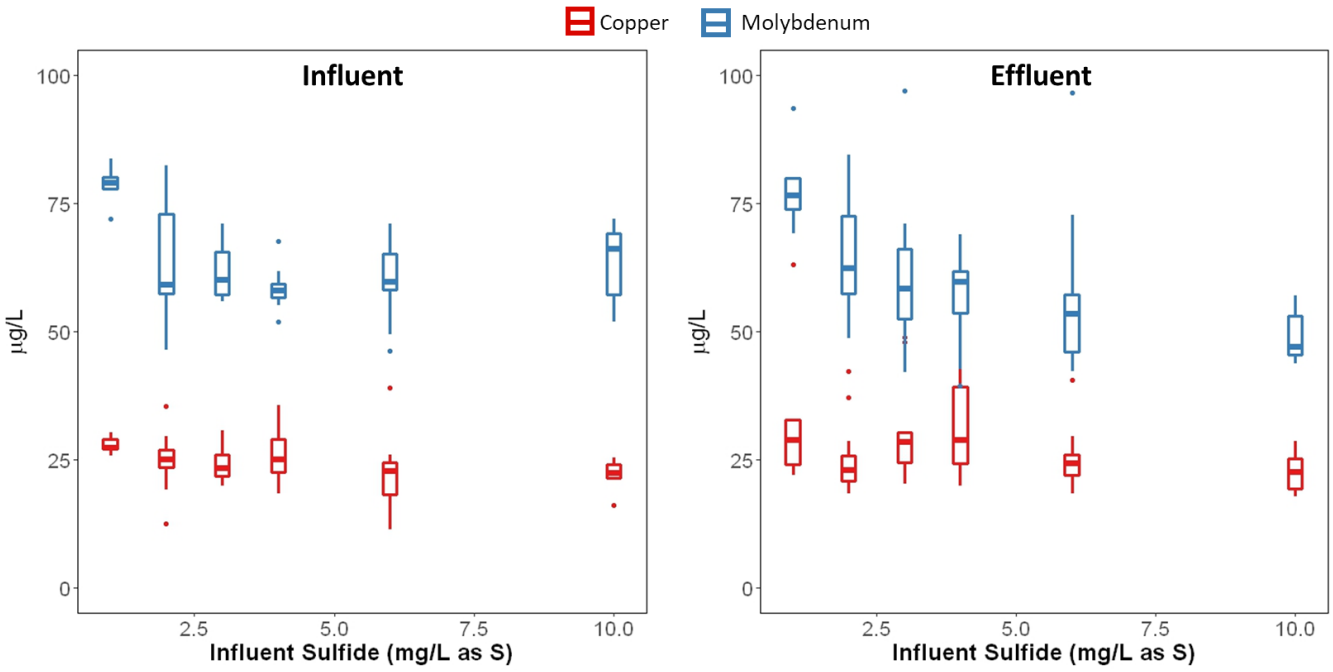


**Figure C7**. Influent and effluent copper and molybdenum concentrations during stepwise increases in sulfide

## References

Cema, G., Sochacki, A., Kubiatowicz, J., Gutwinski, P., Surmacz-Gorska, J., 2012. Start-up, modelling, and simulation of the anammox process in a membrane bioreactor. Chem. Process Eng. 33, 639–650. doi:10.2478/v10176-012-0054-6

Chang, H.-L., Alvarez-Cohen, L., 1997. Two-Stage Methanotrophic Bioreactor for the Treatment of Chlorinated Organic Wastewater. Water Res. 31, 2026–2036.

Chang, W.K., Criddle, C.S., 1997. Experimental evaluation of a model for cometabolism: Prediction of simultaneous degradation of trichloroethylene and methane by a methanotrophic mixed culture. Biotechnol. Bioeng. 56, 492–501. doi:10.1002/(SICI)1097-0290(19971205)56:5<492::AID-BIT3>3.0.CO;2-D

Chen, J., Zhou, Z.-C., Gu, J.-D., 2014. Occurrence and diversity of nitrite-dependent anaerobic methane oxidation bacteria in the sediments of the South China Sea revealed by amplification of both 16S rRNA and pmoA genes. Appl. Microbiol. Biotechnol. doi:10.1007/s00253-014-5733-4

Dale, A.W., Regnier, P., Van Cappellen, P., 2006. Bioenergetic controls on anaerobic oxidation of methane (AOM) in coastal marine sediments: A theoretical analysis. Am. J. Sci. 306, 246–294. doi:10.2475/04.2006.02

Delgado Vela, J., Dick, G.J., Love, N.G., 2018. Sulfide inhibition of nitrite oxidation in activated sludge depends on microbial community composition. Water Res. 138, 241–249.

Delgado Vela, J., Stadler, L.B., Martin, K.J., Raskin, L., Bott, C., Love, N.G., 2015. Prospects for

Biological Nitrogen Removal from Anaerobic Effluents during Mainstream Wastewater Treatment. Environ. Sci. Technol. Lett. 2, 233–244. doi:10.1021/acs.estlett.5b00191

Doğan, E.C., Türker, M., Dağaçsan, L., Arslan, A., 2012. Simultaneous sulfide and nitrite removal from industrial wastewaters under denitrifying conditions. Biotechnol. Bioprocess Eng. 17, 661–668. doi:10.1007/s12257-011-0677-3

Gilmore, K.R., Little, J.C., Smets, B.F., Love, N.G., 2009. Oxygen Transfer Model for a Flow-Through Hollow-Fiber Membrane Biofilm Reactor. J. Environ. Eng. 135, 806–814. doi:10.1061/(ASCE)EE.1943-7870.0000035

Grady, C.P.L., Daigger, G.T., Love, N.G., Filipe, C.D.M., 2011. Biological Wastewater Treatment, 3rd ed. CRC Press, Boca Raton.

He, Z., Cai, C., Shen, L., Lou, L., Zheng, P., Xu, X., Hu, B., 2014. Effect of inoculum sources on the enrichment of nitrite-dependent anaerobic methane-oxidizing bacteria. Appl. Microbiol. Biotechnol. doi:10.1007/s00253-014-6033-8

Jetten, M.S.M., Strous, M., van de Pas-schoonen, K.T., Schalk, J., van Dongen, U.G.J.M., van de Graaf, A.A., Logemann, S., Muyzer, G., van Loosdrecht, M.C.M., Kuenen, J.G., 1999. The anaerobic oxidation of ammonium. FEMS Microbiol. Rev. 22, 421–437.

Kappler, J., Gujer, W., 1992. Estimation of Kinetic Parameters of Heterotrophic Biomass under Aerobic Conditions and Characterization of Wastewater for Activated Sludge Modeling. Water Sci. Technol. 25, 125–139.

Krom, M.D., Berner, R. a., 1980. The diffusion coefficients of sulfate, ammonium, and phosphate ions in anoxic marine sediments. Limnol. Oceanogr. 25, 327–337. doi:10.4319/lo.1980.25.2.0327

Lindh, M., Lagging, M., Färkkilä, M., Langeland, N., Mørch, K., Nilsson, S., Norkrans, G., Pedersen, C., Buhl, M.R., Westin, J., Hellstrand, K., 1994. Diffusion Coefficients for Hydrogen Sulfide, Carbon Dioxide, and Nitrous Oxide in Water over the Temperature Range 293-368 K. J. Chem. Eng. Data 39, 330. doi:10.1093/infdis/jir193

Mora, M., Fernández, M., Gómez, J.M., Cantero, D., Lafuente, J., Gamisans, X., Gabriel, D., 2015. Kinetic and stoichiometric characterization of anoxic sulfide oxidation by SO-NR mixed cultures from anoxic biotrickling filters. Appl. Microbiol. Biotechnol. 99, 77–87. doi:10.1007/s00253-014-5688-5

Moussa, M.S., Hooijmans, C.M., Lubberding, H.J., Gijzen, H.J., van Loosdrecht, M.C.M., 2005. Modelling nitrification, heterotrophic growth and predation in activated sludge. Water Res. 39, 5080–98. doi:10.1016/j.watres.2005.09.038

Munz, G., Gori, R., Mori, G., Lubello, C., 2009. Monitoring biological sulphide oxidation processes using combined respirometric and titrimetric techniques. Chemosphere 76, 644–650. doi:10.1016/j.chemosphere.2009.04.039

Ni, B.-J., Joss, A., Yuan, Z., 2014. Modeling nitrogen removal with partial nitritation and anammox in one floc-based sequencing batch reactor. Water Res. 67C, 321–329.

doi:10.1016/j.watres.2014.09.028

Oshiki, M., Ishii, S., Yoshida, K., Fujii, N., Ishiguro, M., Satoh, H., Okabe, S., 2013. Nitrate-dependent ferrous iron oxidation by anaerobic ammonium oxidation (anammox) bacteria. Appl. Environ. Microbiol. 79, 4087–4093. doi:10.1128/AEM.00743-13

Plattes, M., Fiorelli, D., Gillé, S., Girard, C., Henry, E., Minette, F., O'Nagy, O., Schosseler, P.M., 2007. Modelling and dynamic simulation of a moving bed bioreactor using respirometry for the estimation of kinetic parameters. Biochem. Eng. J. 33, 253–259. doi:10.1016/j.bej.2006.11.006

Rittmann, B.E., Mccarty, P.L., 2001. Environmental Biotechnology: Principles and Applications. McGraw-Hill, New York.

Russ, L., Speth, D.R., Jetten, M.S.M.M., Op den Camp, H.J.M.M., Kartal, B., 2014. Interactions between anaerobic ammonium and sulfur-oxidizing bacteria in a laboratory scale model system. Environ. Microbiol. 16, 3487–3498. doi:10.1111/1462-2920.12487

Tijhuis, L., 1994. The biofilm airlift suspension reactor biofilm formation, detachment, and heterogeneity. TU Delft.

Trapani, D. Di, Mannina, G., Torregrossa, M., Viviani, G., 2010. Quantification of kinetic parameters for heterotrophic bacteria via respirometry in a hybrid reactor. Water Sci. Technol. 61, 1757–66. doi:10.2166/wst.2010.970

van Bodegom, P., Stams, F., Mollema, L., Boeke, S., Leffelaar, P., 2001. Methane Oxidation and the Competition for Oxygen in the Rice Rhizosphere. Appl. Environ. Microbiol. 67, 3586–3597. doi:10.1128/AEM.67.8.3586

Weismann, U., 1994. Biological Nitrogen Removal from Wastewater. Adv. Biochem. Eng. Biotechnol. 51.

Witherspoon, P.A., Saraf, D.N., 1965. Diffusion of Methane, Ethane, Propane, and n-Butane in Water from 25 to 43°. J. Phys. Chem. 69, 3752–3755. doi:10.1021/j100895a017

Xu, X., Chen, C., Lee, D.-J., Wang, A., Guo, W., Zhou, X., Guo, H., Yuan, Y., Ren, N., Chang, J.-S., 2013. Sulfate-reduction, sulfide-oxidation and elemental sulfur bioreduction process: modeling and experimental validation. Bioresour. Technol. 147, 202–11. doi:10.1016/j.biortech.2013.07.113

Yu, J., Pinder, K., 1994. Effective diffusivities of volatile fatty acids in methanogenic biofilms. Bioresour. Technol. 48, 155–161.

Zeng, H., Zhang, T.C., 2005. Evaluation of kinetic parameters of a sulfur-limestone autotrophic denitrification biofilm process. Water Res. 39, 4941–52. doi:10.1016/j.watres.2005.09.034